frontiers | Research Topics

Case reports in intensive care medicine and anesthesiology

Edited by
Abanoub Riad and Yuetian Yu

Published in
Frontiers in Medicine

ISSN 1664-8714
ISBN 978-2-8325-2709-2
DOI 10.3389/978-2-8325-2709-2

About Frontiers

Frontiers is more than just an open access publisher of scholarly articles: it is a pioneering approach to the world of academia, radically improving the way scholarly research is managed. The grand vision of Frontiers is a world where all people have an equal opportunity to seek, share and generate knowledge. Frontiers provides immediate and permanent online open access to all its publications, but this alone is not enough to realize our grand goals.

Frontiers journal series

The Frontiers journal series is a multi-tier and interdisciplinary set of open-access, online journals, promising a paradigm shift from the current review, selection and dissemination processes in academic publishing. All Frontiers journals are driven by researchers for researchers; therefore, they constitute a service to the scholarly community. At the same time, the *Frontiers journal series* operates on a revolutionary invention, the tiered publishing system, initially addressing specific communities of scholars, and gradually climbing up to broader public understanding, thus serving the interests of the lay society, too.

Dedication to quality

Each Frontiers article is a landmark of the highest quality, thanks to genuinely collaborative interactions between authors and review editors, who include some of the world's best academicians. Research must be certified by peers before entering a stream of knowledge that may eventually reach the public - and shape society; therefore, Frontiers only applies the most rigorous and unbiased reviews. Frontiers revolutionizes research publishing by freely delivering the most outstanding research, evaluated with no bias from both the academic and social point of view. By applying the most advanced information technologies, Frontiers is catapulting scholarly publishing into a new generation.

What are Frontiers Research Topics?

Frontiers Research Topics are very popular trademarks of the *Frontiers journals series*: they are collections of at least ten articles, all centered on a particular subject. With their unique mix of varied contributions from Original Research to Review Articles, Frontiers Research Topics unify the most influential researchers, the latest key findings and historical advances in a hot research area.

Find out more on how to host your own Frontiers Research Topic or contribute to one as an author by contacting the Frontiers editorial office: frontiersin.org/about/contact

Case reports in intensive care medicine and anesthesiology

Topic editors

Abanoub Riad — Masaryk University, Czechia

Yuetian Yu — Shanghai Jiao Tong University, China

Citation

Riad, A., Yu, Y., eds. (2023). *Case reports in intensive care medicine and anesthesiology*. Lausanne: Frontiers Media SA. doi: 10.3389/978-2-8325-2709-2

Table of contents

frontiers | Frontiers in Medicine

CASE REPORT
published: 11 May 2022
doi: 10.3389/fmed.2022.843282

Sudden Cardiac Arrest in a Patient With COVID-19 as a Result of Severe Hyperkalemia After Administration of Succinylcholine Chloride for Reintubation. A Case Report

Mateusz Putowski[1,2], Tomasz Drygalski[2], Andrzej Morajda[2], Jarosław Woroń[2,3], Tomasz Sanak[1,2] and Jerzy Wordliczek[2,4]*

[1] Center for Innovative Medical Education, Jagiellonian University Medical College, Cracow, Poland, [2] Department of Anesthesiology and Intensive Care, University Hospital in Krakow, Krakow, Poland, [3] Department of Clinical Pharmacology, The Chair of Pharmacology, Faculty of Medicine, Jagiellonian University Collegium Medicum, Krakow, Poland, [4] Department of Intensive Interdisciplinary Therapy, Jagiellonian University Collegium Medicum, Krakow, Poland

OPEN ACCESS

Edited by:
Ata Murat Kaynar, University of Pittsburgh, United States

Reviewed by:
Edward Bittner, Massachusetts General Hospital and Harvard Medical School, United States
Jieyun Bai, Jinan University, China

***Correspondence:**
Mateusz Putowski
mateusz.putowski@uj.edu.pl

Specialty section:
This article was submitted to Intensive Care Medicine and Anesthesiology, a section of the journal Frontiers in Medicine

Received: *25 December 2021*
Accepted: *26 April 2022*
Published: *11 May 2022*

Citation:
Putowski M, Drygalski T, Morajda A, Woroń J, Sanak T and Wordliczek J (2022) Sudden Cardiac Arrest in a Patient With COVID-19 as a Result of Severe Hyperkalemia After Administration of Succinylcholine Chloride for Reintubation. A Case Report. Front. Med. 9:843282. doi: 10.3389/fmed.2022.843282

Background: We present a case study of a man with coronavirus disease 2019 (COVID-19) who developed cardiac arrest as a result of hyperkalemia following administration of chlorорsuccinylcholine during endotracheal intubation.

Case Summary: A patient with a severe course of COVID-19, hospitalized in the Intensive Care Unit, underwent reintubation on day 16. The applied scheme was rapid sequence induction and intubation with administration of chlorорsuccinylcholine. Immediately after intubation, there was a sudden cardiac arrest due to hyperkalemia (cK + 10.2 meq/L). Treatment was initiated as per guidelines, which resulted in a return to spontaneous circulation after 6 min.

Conclusion: Chlorsucynylcholine may cause life-threatening hyperkalemia. We recommend using rocuronium as a neuromuscular blocking agent in critically ill COVID-19 patients due to its more optimal safety profile.

Keywords: COVID-19, hyperkalemia, sudden cardiac arrest, rocuronium, succinylcholine

INTRODUCTION

Succinylcholine chloride is an agent commonly used to facilitate endotracheal intubation. It also remains a major drug in rapid sequence induction and intubation in many countries (1–3). Nevertheless, the British Guidelines for the management of tracheal intubation in critical ill adults recommend rocuronium as the first-line muscle relaxant for endotracheal intubation in critical condition (4). However, it is succinylcholine, as a depolarizing agent with a fast (40–60 s) and short (6–10 min) duration of action, that is more eagerly chosen in emergency conditions due to its pharmacokinetic profile compared to rocuronium, whose duration of action is about 37–72 min depending on dose (5, 6). However, it should be remembered that this drug may cause side effects such as malignant hyperthermia, rhabdomyolysis, or hyperkalemia. There are also more and more reports of sudden cardiac arrest (SCA) following the supply of succinylcholine (7, 8). Our case

report is further evidence of serious complications following the administration of this drug for endotracheal intubation in a patient with a severe course of coronavirus disease 2019 (COVID-19).

CASE REPORT

A 57-year-old patient with COVID-19 was admitted to the Anesthesiology and Intensive Care Unit after being transferred from another hospital for further treatment due to increasing respiratory failure. Patient transported by medical transport team was intubated, in critical general condition, in analgosedation, mechanically ventilated in the SIMV (*synchronized intermittent mandatory ventilation*) mode with $Fi0_2$ (*fraction of inspired oxygen*) 0.5 at PEEP (*positive end-expiratory pressure*) 14 cmH_2O. After admission, multidisciplinary and integrated treatment, empiric antibiotic therapy were implemented in accordance with the local protocol, taking into account the drug-susceptibility phenotypes of potential bacterial pathogens, antithrombotic and antiedematous prophylaxis was applied, and water-electrolyte imbalance was corrected. Mechanical ventilation mode was changed to VC/AC (Volume Control/Assist Control) with $Fi0_2$ 0.4 reduction and PEEP 15 cmH_2O. During hospitalization, the patient was placed in the prone position several times in order to improve ventilation parameters. On day 8 from admission, renal replacement therapy was administered in the mode of continuous venous-venous hemodiafiltration (CVVHDF) with an Oxiris and CytoSorb filter. On day 16, the ventilation mode was changed to pressure support ventilation and the settings were modified based on arterial blood gas test. Due to the long time since changing the previous tracheal tube, a decision was also made to reintubate the patient. Mouth opening of about 3 cm, Mallampati score III and arterial blood gas results from 2 h ago (pH 7.43, PO_2 75 mmHg, kPa, PCO_2 35 mmHg, cK + 4.5 meq/L, cLac 0.9 mmol/L, and SBE 0.0 mmol/L) were assessed. Immediately prior to intubation, the patient was under continuous infusion of noradrenaline (Levonor) and dexmedetomidine (Dexdor) and CVVHDF renal replacement therapy. The classic RSI regimen was used: fentanyl (1.5 $\mu g\ kg^{-1}$), propofol (1 $mg\ kg^{-1}$), and succinylcholine (Chlorsuccillin, 200 mg, Bausch Health Ireland Limited) at a dose of 1 $mg\ kg^{-1}$. After that, the tracheal tube was replaced using a Bougie type guide in about 20 s. Immediately after replacement of the endotracheal tube, cardiac arrhythmias in the form of bradycardia 50 bpm with wide QRS complexes and a sudden drop in invasive blood pressure were noticed on the cardiomonitor. The carotid pulse was assessed, and upon finding its absence, cardiopulmonary resuscitation was started immediately and adrenaline 1 mg was administered iv due to the non-shockable rhythm. Due to the unexpected onset of SCA in this situation, it was suspected that hyperkalemia may have occured after administration of chlorsuccinylcholine. In the next minute of CPR, arterial blood gas test was obtained and acidosis was found with severe hyperkalemia (cK + 10.2 meq/L; **Figure 1**). 10 ml of 10% calcium chloride were administered immediately, insulin (10U) with glucose (25 *g*) was infused and 60 meq of Natrium bicarbonicum 8.4% was administered. Subsequent evaluation of the rhythm, however, did not return the spontaneous circulation, and the rhythm was still non-shockable. At approximately 6 min of CPR, the spontaneous circulation was restored and the heart rate normalized to approximately 70 bpm with narrow QRS complexes. Arterial blood gas was again taken, showing a decrease in potassium ions to 4.1 meq/L (**Figure 2**). After this incident, the patient stayed in our ward for 22 days. He was discharged in a stable state, conscious in logical verbal contact, from another ward in order to continue the treatment. The co-author and supervisor of this publication is the Head Physician of our Department, who gave his written permission to describe this case.

DISCUSSION

The presented case study is further evidence of the risk of severe hyperkalemia following the administration of succinylcholine. In a review by Hovgaard et al. on suxamethonium-induced hyperkalemia and the Cochrane review regarding rocuronium versus sucinylcholine in the rapid intubation sequence not only explained the causes of the succamethonium-induced potassium upsurge, but also identified a group of patients at particular risk of this complication. Patients with severe burns, trauma, immobilized and prolonged critical illness have been shown to be at high risk of developing life-threatening hyperkalemia following administration of this drug (5, 9). It cannot be ruled out that the SARS-CoV-2 virus infection itself is another risk factor for this complication. The coronavirus infection itself can change the pharmacokinetic parameters of many drugs (10). Electrolyte disorders particularly potassium abnormalities have been repeatedly reported as common clinical manifestations of COVID-19. SARS-CoV-2 cell entry through angiotensin-converting enzyme 2 may enhance the activity of renin–angiotensin–aldosterone system classical axis and further leading to over production of aldosterone. Aldosterone is capable of enhancing the activity of epithelial sodium channels and resulting in potassium loss from epithelial cells. Damage to the renal tubules caused by ischemia and nephrotoxic effects caused by inflammation in the body is also not without significance for the disturbance of potassium homeostasis. The SARS-CoV-2 virus also influences the regulatory mechanism of the renin-angiotensin-aldosterone system. SARS-CoV-2 can lead to both decreases and increases in serum potassium levels (11).

Hyperkalemia occurs in a small subset of patients after succinylcholine (SCh) administration and can be severe and fatal. In a review of cases and the pathophysiology of succinylcholine hyperkalemia, Gerald et al. describes 2 mechanisms that lead to the disorder: upregulation of acetylcholine receptors and rhabdomyolysis. Upregulation is caused by a change in the subunit type of acetylcholine receptors and by an increase in their density as they spread over the muscle surface outside the motor endplate area. Causes of upregulation include burns, severe muscle trauma, upper or lower motor neuron denervation (e.g., stroke or spinal cord injury, respectively), and prolonged ICU care (bed rest, steroids, prolonged neuromuscular blockade).

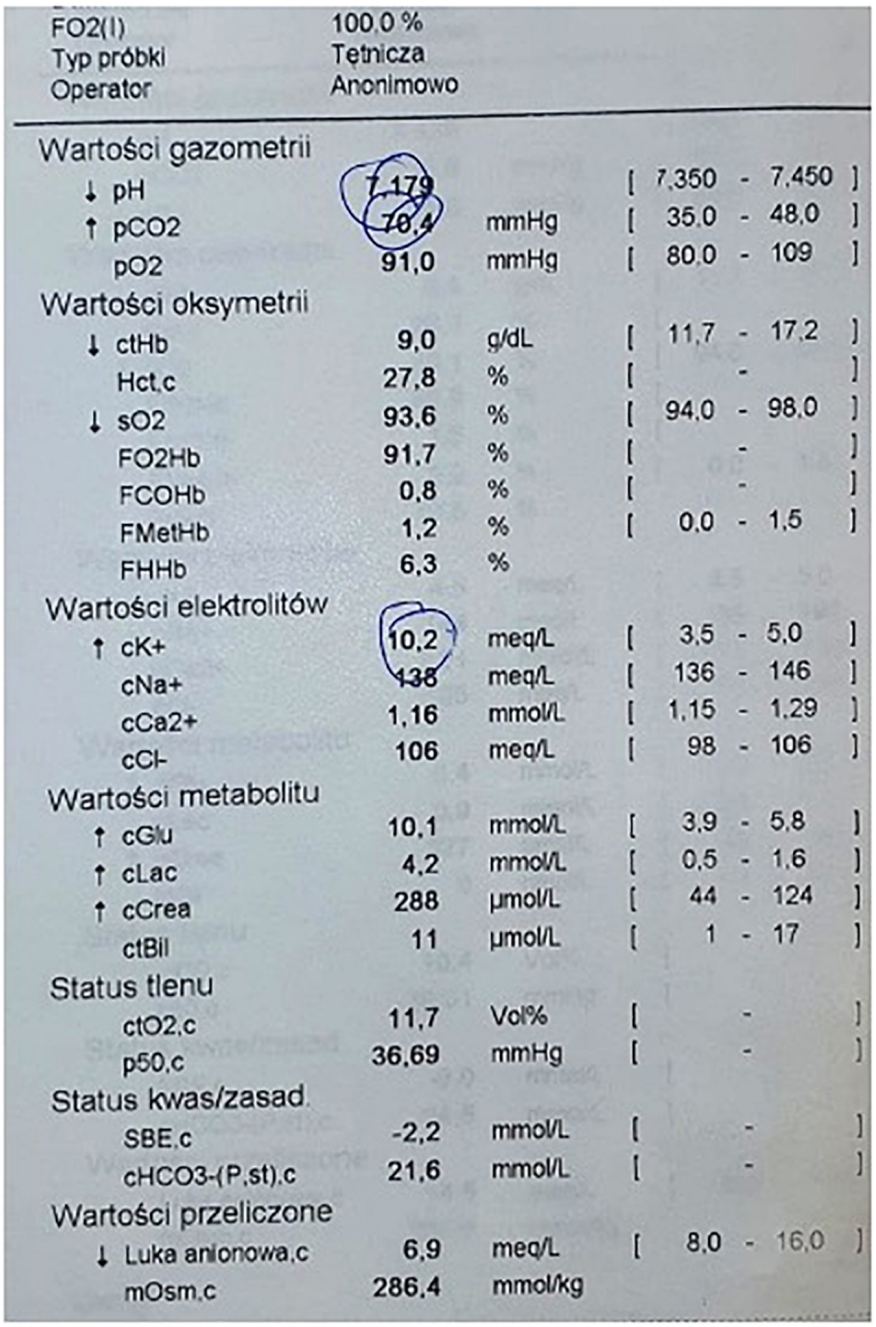

FO2(I)	100,0 %		
Typ próbki	Tętnicza		
Operator	Anonimowo		
Wartości gazometrii			
↓ pH	7,179		[7,350 - 7,450]
↑ pCO2	70,4	mmHg	[35,0 - 48,0]
pO2	91,0	mmHg	[80,0 - 109]
Wartości oksymetrii			
↓ ctHb	9,0	g/dL	[11,7 - 17,2]
Hct,c	27,8	%	[-]
↓ sO2	93,6	%	[94,0 - 98,0]
FO2Hb	91,7	%	[-]
FCOHb	0,8	%	[-]
FMetHb	1,2	%	[0,0 - 1,5]
FHHb	6,3	%	
Wartości elektrolitów			
↑ cK+	10,2	meq/L	[3,5 - 5,0]
cNa+	138	meq/L	[136 - 146]
cCa2+	1,16	mmol/L	[1,15 - 1,29]
cCl-	106	meq/L	[98 - 106]
Wartości metabolitu			
↑ cGlu	10,1	mmol/L	[3,9 - 5,8]
↑ cLac	4,2	mmol/L	[0,5 - 1,6]
↑ cCrea	288	µmol/L	[44 - 124]
ctBil	11	µmol/L	[1 - 17]
Status tlenu			
ctO2,c	11,7	Vol%	[-]
p50,c	36,69	mmHg	[-]
Status kwas/zasad.			
SBE,c	-2,2	mmol/L	[-]
cHCO3-(P,st),c	21,6	mmol/L	[-]
Wartości przeliczone			
↓ Luka anionowa,c	6,9	meq/L	[8,0 - 16,0]
mOsm,c	286,4	mmol/kg	

FIGURE 1 | Arterial blood gas obtained during cardiopulmonary resuscitation, time of the result 4:11 PM.

Both succinylcholine and acetylcholine are agonists of the acetylcholine receptor. This channel-related agonist-triggered potassium release is magnified by the number of involved muscles (12).

Unfortunately, the global disease pandemic caused by the SARS-CoV2 virus has resulted in a significant increase in people hospitalized in Intensive Care Units due to severe respiratory failure. The constant deterioration of ventilation parameters results in an urgent need for endotracheal intubation and the implementation of assisted or mechanical ventilation. Post-intubation cardiac arrest is a rare complication of intubation, but it should be noted that the number of such cases increased 1.5 times during the COVID-19 pandemic (13).

When choosing a drug regimen for RSI, one should take into account the risk of serious complications. An alternative to succinylcholine is rocuronium administered at a dose (up to RSI) of 1.2 mg/kg bw. Its main advantage is the lack of potassium ion surge, which eliminates the occurrence of hyperkalemia, but

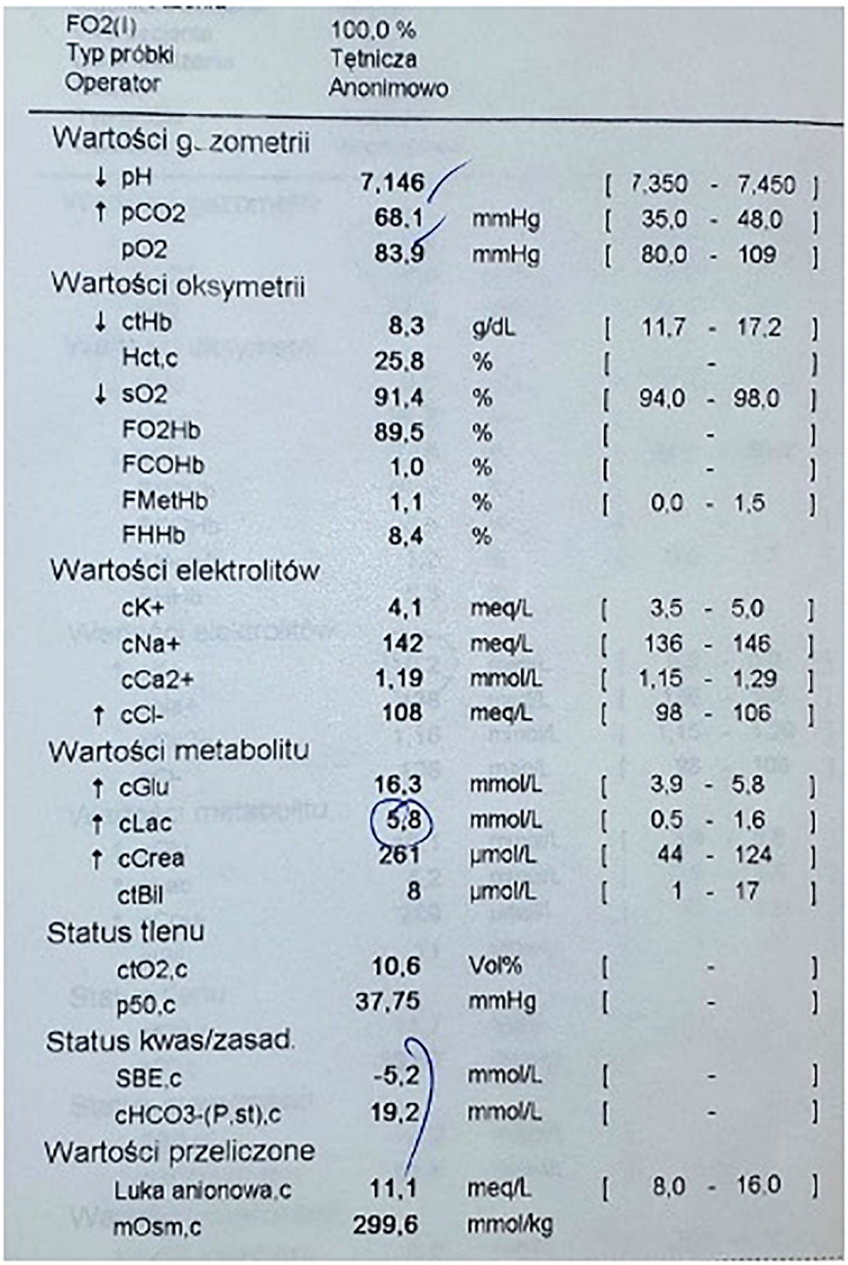

FO2(I)	100,0 %		
Typ próbki	Tętnicza		
Operator	Anonimowo		
Wartości gazometrii			
↓ pH	7,146		[7,350 - 7,450]
↑ pCO2	68,1	mmHg	[35,0 - 48,0]
pO2	83,9	mmHg	[80,0 - 109]
Wartości oksymetrii			
↓ ctHb	8,3	g/dL	[11,7 - 17,2]
Hct,c	25,8	%	[-]
↓ sO2	91,4	%	[94,0 - 98,0]
FO2Hb	89,5	%	[-]
FCOHb	1,0	%	[-]
FMetHb	1,1	%	[0,0 - 1,5]
FHHb	8,4	%	
Wartości elektrolitów			
cK+	4,1	meq/L	[3,5 - 5,0]
cNa+	142	meq/L	[136 - 146]
cCa2+	1,19	mmol/L	[1,15 - 1,29]
↑ cCl-	108	meq/L	[98 - 106]
Wartości metabolitu			
↑ cGlu	16,3	mmol/L	[3,9 - 5,8]
↑ cLac	5,8	mmol/L	[0,5 - 1,6]
↑ cCrea	261	µmol/L	[44 - 124]
ctBil	8	µmol/L	[1 - 17]
Status tlenu			
ctO2,c	10,6	Vol%	[-]
p50,c	37,75	mmHg	[-]
Status kwas/zasad.			
SBE,c	-5,2	mmol/L	[-]
cHCO3-(P,st),c	19,2	mmol/L	[-]
Wartości przeliczone			
Luka anionowa,c	11,1	meq/L	[8,0 - 16,0]
mOsm,c	299,6	mmol/kg	

FIGURE 2 | Arterial blood gas obtained after recovery of spontaneous circulation, time of the result 4:22 PM.

the duration of action is much longer, which may be a potential problem. There is indeed an antagonist for rocuronium (i.e., sugammadex), however, large doses of this drug, i.e., 16 mg/kg bw are needed to reverse the neuromuscular blockage, and the time to fully reverse the muscle blockage may take as long as 3 min (14, 15). Rocuronium also has a longer apneic window without desaturating oxygen level ("Safe Apnea Time") which allows for a change in airway management in the event of in the event unanticipated complications arise in obese patients (16).

Blanié et al. studies have shown that the risk of hyperkalemia after the administration of succinylcholine is also strongly correlated with the length of stay in the ICU. After 16 days of hospitalization, the risk of this complication is very high (17).

Sigurdsson et al. describe a similar case of cardiac arrest after administration of succinylcholine in a patient with COVID-19, but the patient showed hypoxemia and respiratory acidosis before intubation (pH 7.28, P O2 63.0 mmHg, Pco2 67.5 mmHg, and potassium 4.7 meq/L). About 60 s after drug administration, circulatory arrest occurred in a defibrillation rhythm (wide complex polymorphic ventricular tachycardia), and the hyperkalemia recorded by the authors was 6.4 meq/L of potassium (7). The patient described in our report had

no acid-base imbalance prior to intubation and additionally remained on venous-venous hemodiafiltration (CVVHDF). After administration of the drug, there was also a typical hyperkalemic arrhythmia in the form of broad QRS bradycardia, and the recorded potassium level was 10.2 meq/L (18). Another factor that should be taken into account in the case described by Sigurdsson et al. is hypercapnia. It is important to realize that during an apnea following administration of a muscle relaxant, severe acidosis may occur due to an increase in PaCO2, leading to cardiac arrest (16).

In our opinion, the supply of chlorsuccinylcholine was the main cause of cardiac arrest in this patient. We recommend that prior to selecting muscle relaxants for endotracheal intubation in the intensive care unit, one should assess not only serum potassium levels, but also hospitalization time, and use rocuronium as a neuromuscular blocking agent in critically ill patients with COVID-19 due to its more optimal safety profile.

DATA AVAILABILITY STATEMENT

The original contributions presented in the study are included in the article/supplementary material, further inquiries can be directed to the corresponding author.

AUTHOR CONTRIBUTIONS

All authors listed have made a substantial, direct, and intellectual contribution to the work, and approved it for publication.

ACKNOWLEDGMENTS

This work was performed at the University Hospital in Krakow, Poland.

REFERENCES

1. Klucka J, Kosinova M, Zacharowski K, De Hert S, Kratochvil M, Toukalkova M, et al. Rapid sequence induction: an international survey. *Eur J Anaesthesiol.* (2020) 37:435–42. doi: 10.1097/EJA.0000000000001194
2. Jensen AG, Callesen T, Hagemo JS, Hreinsson K, Lund V, Nordmark J, et al. Scandinavian clinical practice guidelines on general anaesthesia for emergency situations. *Acta Anaesthesiol Scand.* (2010) 54:922–50. doi: 10.1111/j.1399-6576.2010.02277.x
3. Quintard H, l'Her E, Pottecher J, Adnet F, Constantin JM, De Jong A, et al. Experts' guidelines of intubation and extubation of the ICU patient of French society of anaesthesia and intensive care medicine (SFAR) and French-speaking intensive care society (SRLF): in collaboration with the pediatric association of French-speaking anaesthetists and intensivists (ADARPEF), French-speaking group of intensive care and paediatric emergencies (GFRUP) and intensive care physiotherapy society (SKR). *Ann Intensive Care.* (2019) 9:13. doi: 10.1186/s13613-019-0483-1
4. Higgs A, McGrath BA, Goddard C, Rangasami J, Suntharalingam G, Gale R, et al. Guidelines for the management of tracheal intubation in critically ill adults. *Br J Anaesth.* (2018) 120:323–52. doi: 10.1016/j.bja.2017.10.021
5. Tran DTT, Newton EK, Mount VAH, Lee JS, Mansour C, Wells GA, et al. Rocuronium vs. succinylcholine for rapid sequence intubation: a Cochrane systematic review. *Anaesthesia.* (2017) 72:765–77. doi: 10.1111/anae.13903
6. Magorian T, Flannery KB, Miller RD. Comparison of rocuronium, succinylcholine, and vecuronium for rapid-sequence induction of anesthesia in adult patients. *Anesthesiology.* (1993) 79:913–8. doi: 10.1097/00000542-199311000-00007
7. Sigurdsson TS, Porvaldsson AP, Asgeirsdottir S, Sigvaldason K. Cardiac arrest in a COVID-19 patient after receiving succinylcholine for tracheal reintubation. *Br J Anaesth.* (2020) 125:e255–7. doi: 10.1016/j.bja.2020.04.073
8. Plane AF, Marsan PE, du Cheyron D, Valette X. Rapidly changing ECG in hyperkalaemia after succinylcholine. *Lancet.* (2019) 393:1983. doi: 10.1016/S0140-6736(19)30838-4
9. Hovgaard HL, Juhl-Olsen P. Suxamethonium-induced hyperkalemia: a short review of causes and recommendations for clinical applications. *Crit Care Res Pract.* (2021) 2021:6613118. doi: 10.1155/2021/6613118
10. Deb S, Arrighi S. Potential effects of COVID-19 on cytochrome P450-mediated drug metabolism and disposition in infected patients. *Eur J Drug Metab Pharmacokinet.* (2021) 46:185–203. doi: 10.1007/s13318-020-00668-8
11. Noori M, Nejadghaderi SA, Sullman MJM, Carson-Chahhoud K, Ardalan M, Kolahi AA, et al. How SARS-CoV-2 might affect potassium balance via impairing epithelial sodium channels? *Mol Biol Rep.* (2021) 48:6655–61. doi: 10.1007/s11033-021-06642-0
12. Gronert GA. Cardiac arrest after succinylcholine: mortality greater with rhabdomyolysis than receptor upregulation. *Anesthesiology.* (2001) 94:523–9. doi: 10.1097/00000542-200103000-00026
13. Kandinata N, Acharya R, Patel A, Parekh A, Santana J, Darden A, et al. Risk of post-intubation cardiac arrest with the use of high-dose rocuronium in COVID-19 patients with acute respiratory distress syndrome: a retrospective cohort study. *J Clin Transl Res.* (2021) 7:717–22.
14. Keating GM. Sugammadex: a review of neuromuscular blockade reversal. *Drugs.* (2016) 76:1041–52. doi: 10.1007/s40265-016-0604-1
15. Herring WJ, Woo T, Assaid CA, Lupinacci RJ, Lemmens HJ, Blobner M, et al. Sugammadex efficacy for reversal of rocuronium- and vecuronium-induced neuromuscular blockade: a pooled analysis of 26 studies. *J Clin Anesth.* (2017) 41:84–91. doi: 10.1016/j.jclinane.2017.06.006
16. Tang L, Li S, Huang S, Ma H, Wang Z. Desaturation following rapid sequence induction using succinylcholine vs. rocuronium in overweight patients. *Acta Anaesthesiol Scand.* (2011) 55:203–8. doi: 10.1111/j.1399-6576.2010.02365.x
17. Blanié A, Ract C, Leblanc PE, Cheisson G, Huet O, Laplace C, et al. The limits of succinylcholine for critically ill patients. *Anesth Analg.* (2012) 115:873–9. doi: 10.1213/ANE.0b013e31825f829d
18. Kim YM, Park JE, Hwang SY, Lee SU, Kim T, Yoon H, et al. Association between wide QRS pulseless electrical activity and hyperkalemia in cardiac arrest patients. *Am J Emerg Med.* (2021) 45:86–91. doi: 10.1016/j.ajem.2021.02.024

Conflict of Interest: The authors declare that the research was conducted in the absence of any commercial or financial relationships that could be construed as a potential conflict of interest.

frontiers | Frontiers in Medicine

CASE REPORT
published: 26 May 2022
doi: 10.3389/fmed.2022.919911

Neurologic Complication Due to Crystallization After Drug Interaction Between Alkalized Lidocaine and Ropivacaine: A Case Report and *in vitro* Study

Afang Zhu, Lijian Pei, Wei Liu, Wencong Cheng, Yu Zhang and Yuguang Huang*

Department of Anesthesiology, Peking Union Medical College Hospital, Chinese Academy of Medical Sciences and Peking Union Medical College, Beijing, China

Background: For pregnant women transferred to emergency cesarean section after receiving epidural labor analgesia, there is still a debate over the effective and safe means of rapidly delivering surgical anesthesia. Alkalized lidocaine is often adopted for fast onset time; however, crystallization of the anesthetic may cause severe neurologic symptoms.

Case Presentation: We report a case of a pregnant woman who underwent emergency cesarean section with satisfied analgesia but experienced severe weakness and paranaesthesia in the lower limb. After excluding lumbar disc herniation, obstetric nerve injury, and anesthesia technique causes by symptoms signs and magnetic resonance imaging, drug-related injury became the most likely cause. Our *in vitro* testing confirmed the obvious precipitation of additional anesthetic-concentrated ropivacaine (0.5–1%) with pretreated alkalized lidocaine. With trophic neurotherapy, the parturient attained prompt relief of weakness by day four, but delayed recovery of numbness, which lasted for 4 weeks.

Conclusion: To date, this is the first case reporting neurologic complication possibly due to drug crystallization in cesarean section. Our study confirmed the rapid onset of alkalized lidocaine and its safety to pretreated routine labor dose of ropivacaine (0.09%). However, additional anesthetic-concentrated ropivacaine (0.5–1%) to maintain the anesthesia and analgesia level is not suggested.

Keywords: emergency cesarean section, epidural labor analgesia, delayed neurologic recovery, alkalized lidocaine, ropivacaine crystallization

OPEN ACCESS

Edited by:
Zhongheng Zhang,
Sir Run Run Shaw Hospital, China

Reviewed by:
Tian-Long Wang,
Capital Medical University, China
Chen-Hwan Cherng,
Tri-Service General Hospital, Taiwan
Shaoqiang Huang,
Fudan University, China

****Correspondence:***
Lijian Pei
hazelbeijing@vip.163.com

Specialty section:
This article was submitted to Intensive Care Medicine and Anesthesiology, a section of the journal Frontiers in Medicine

Received: *14 April 2022*
Accepted: *06 May 2022*
Published: *26 May 2022*

Citation:
Zhu A, Pei L, Liu W, Cheng W, Zhang Y and Huang Y (2022) Neurologic Complication Due to Crystallization After Drug Interaction Between Alkalized Lidocaine and Ropivacaine: A Case Report and in vitro Study. Front. Med. 9:919911. doi: 10.3389/fmed.2022.919911

INTRODUCTION

Standard monitoring protocols for effective and safe anesthesia are important for parturients transferred for emergency cesarean section upon receiving epidural labor analgesia, even critical to the implementation of the three-child policy in China. Sodium bicarbonate was added to lidocaine mainly to adjust the pH for faster onset of action and enhance the depth of block (1, 2), which makes it an available choice for rapid anesthesia. However, the most commonly used drug in labor analgesia, ropivacaine can easily crystalize with pH elevation (3). We report a case of a pregnant

woman who experienced severe weakness and paranaesthesia post-operatively, potentially due to ropivacaine crystallization. Differential diagnosis and various mixtures of alkalized lidocaine and ropivacaine are discussed.

CASE DESCRIPTION

A 33-year-old female, 168 cm height/100 kg weight, G1P0, at 40 weeks 6 days gestational age was admitted in latent labor with an uncomplicated pregnancy. She underwent labor epidural placement at L2–3 level smoothly, and attained satisfactory analgesia with 0.09% ropivacaine and sufentanil (5 mcg/mL) at 6 mL/h for labor. For intrauterine fetal distress, decision to proceed with emergency cesarean section was undertaken 6 h after labor analgesia. With a test dose of 3 mL 2% lidocaine after 3 min, 12 mL fresh 0.83% alkalized lidocaine (L_{alk}) (15 mL 2% lidocaine plus 3 mL 5% sodium bicarbonate) was administered, followed by 7.5 mL 0.75% ropivacaine 10 min later to raise the anesthesia level from T9 to T6. Another 7.5 mL 0.75% ropivacaine was added 40 min later when closing the peritoneal. The parturient underwent cesarean section comfortably, and the epidural catheter was removed at the end of surgery. An infant with 3,990 g was delivered with right occipital transeverse position, and her Apgar score was 10 at 1, 5, and 10 min.

On the second postpartum day, the patient noted numbness and weakness in the knee when bearing weight on the right lower limb and fell when she stood, with no back or leg pain. Neurological pinprick examination identified decreased sensation in the lateral-middle lower-third of the thigh, lateral crus, and dorsum pedis, with muscle strength grade-2 and a weak knee reflex, no pathological signs elicited and negative straight leg elevation test. Magnetic resonance imaging (MRI) revealed minor expansion of the L2/L3 disc but no other abnormalities. The weakness and paresthesia improved by day three and four, respectively. She was discharged home on day five with mecobalamin and vitamin B1 for trophic neurotherapy, and the numbness persisted for 4 weeks.

Generally, the parturient received smooth labor analgesia and cesarean section, but presented with obvious weakness of the right lower limb. Although relief was observed by day four, she experienced slow recovery of numbness lasting 4 weeks, with negative magnetic resonance imaging or pathological signs.

DISCUSSION

Lumbar disc herniation often presents with low-back pain and lower limb pain; a positive straight leg elevation test and imaging performance is consistent with the symptoms. For this parturient, symptoms including weakness and numbness of the thigh seem to support herniation. However, the MRI showed no evidence of compression at the nerve root, namely herniation could not be responsible for her symptoms.

Lower extremity mononeuropathies and radiculopathies occur during delivery with an incidence as high as 0.92%, with the following nerves mostly affected: lateral femoral cutaneous nerve of the thigh, femoral, common peroneal, lumbosacral plexus, sciatic, obturator and lumbar or sacral root (4). Pregnancy-induced hormone, weight increase, articular ligament changes, and posture contribute to these. For posture, most parturients experienced trial of vaginal delivery and compression from fetal head especially during the second stage of labor. For this parturient, emergency cesarean section decision was made at three fingers-open, and she did not experience semi-Fowler lithotomy position, active force, and trial of vaginal delivery. In regard to childbirth factors, for one hand, the symptoms caused by fetal posture-related lumbosacral plexus or femoral injury are often foot drop, unable to stretch the leg or reduced knee flex, and the recovery of muscle force often takes few weeks or months. For another hand, the parturient's labor stagnated in the first stage, and her sensory and motor functions were normal before cesarean section.

Hence, factors from the parturient (herniation) and delivery (obstetric nerve injury) were not considered, and the MRI examination excluded epidural haematoma related compression. Could this abnormity be anesthetic-related? To test this hypothesis, *in vitro* testing was performed to assess the stability of the L_{alk} and ropivacaine mixture. We mixed sodium bicarbonate with lidocaine to adjust the pH for faster onset of action (∼10 min). Despite its widespread use, ropivacaine has been reported to rapidly crystallize with pH elevation (3, 5–7). To verify crystallization, we mixed various doses of 0.83% L_{alk} with 0.09% or 0.5–1% ropivacaine at 37°C. Routine ropivacaine for labor analgesia is 0.09% with 6 mL as bolus dose and 6 mL/h as maintenance dose; thus, the selected doses of ropivacaine were 6 and 12 mL. A dose of 0.83% L_{alk} is recommended for cesarean section from 10 to 20 mL; and ropivacaine for cesarean section is 0.5% with 5 or 10 mL. Therefore, we designed two tests with different concentrations of ropivacaine and various doses to detect the mixed effects. All the medicine and materials were kept in a 37°C incubator 30 min prior to use, and each mixture was prepared freshly. The pH of each medicine and mixture were recorded within 10 min, and observed with 1 h. For the short-term stability of pH-buffering (8), this test was repeated six times in all. The pH values of each medicine and mixture are presented in **Figure 1A**, and the values of L_{alk} with ropivacaine ranged from 7.03 to 7.36. Both macroscopic and microscopic visualization observed within 1 h detected no crystals in the L_{alk} −0.09% ropivacaine mixture (**Figure 1D**). However, very slight crystallization could be observed under the microscope after mixing over 1 h (**Figure 1B**). Upon increasing ropivacaine from 0.5 to 1% (routine concentration for cesarean section), larger volumes and number of rod-shaped crystals were detected; when increasing the volume of ropivacaine from 5 to 10 mL, while decreasing the volume of L_{alk} from 20 to 10 mL, the rod-shaped crystals became much larger (**Figure 1C**). The macroscopic visualization revealed more precipitation with ropivacaine increasing from 0.5 to 1%, presented as a cloudy appearance (**Figure 1E**). With higher volume of ropivacaine and smaller volume of L_{alk}, the occurrence of crystallization was easy with increase precipitation (**Figure 1E**). Collectively, we observed a ropivacaine concentration- not pH-dependent relationship precipitation. Milner et al. showed that ropivacaine (0.75 and 1%) was unsuitable for alkalization signals at pH of

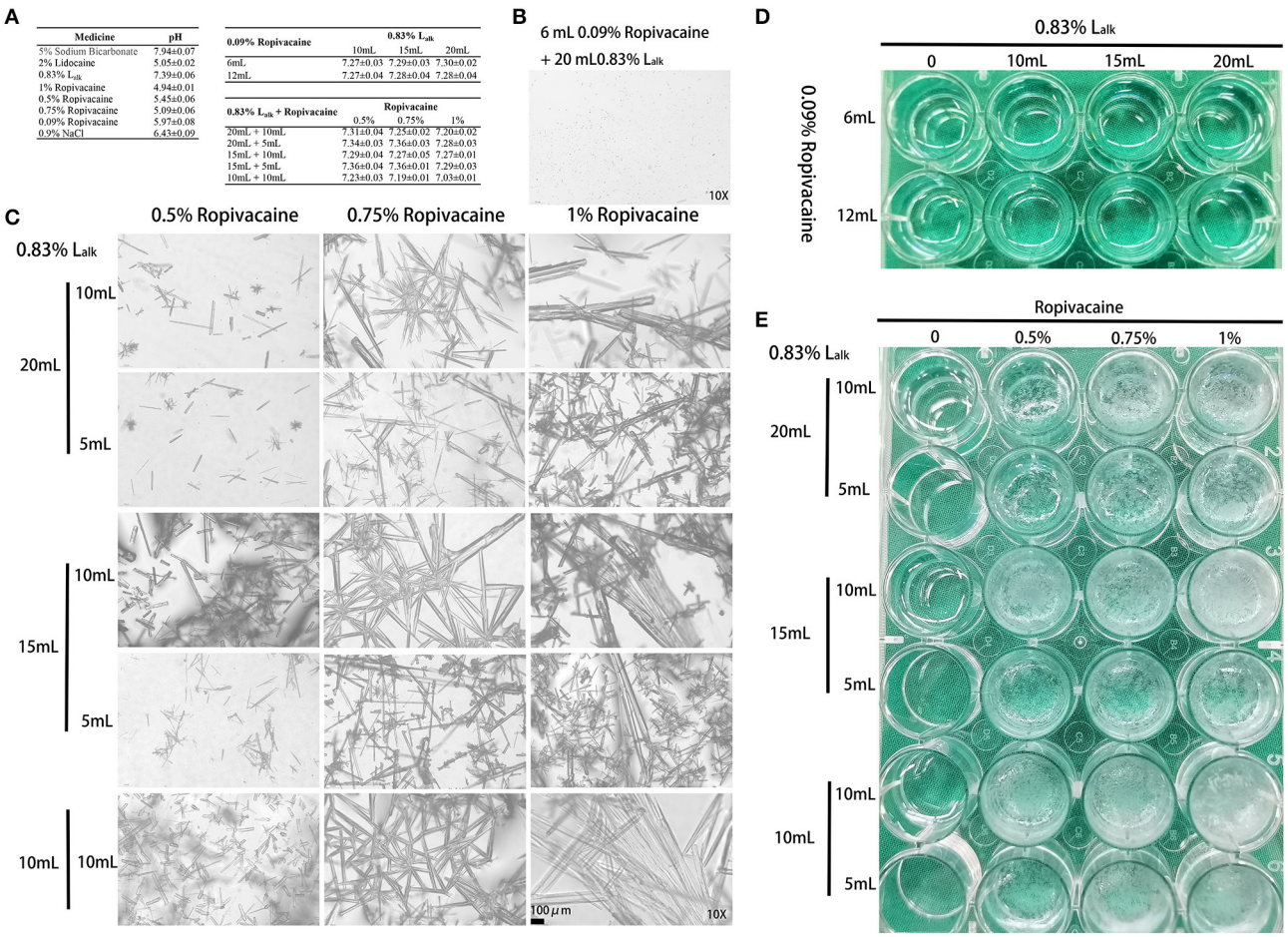

FIGURE 1 | Crystallization of medicine. **(A)** The pH values of each medicine (mean ± SEM) detected by Sartorius PB-10 within 10 min (n = 3–6). **(B)** Microscopic image (10X) of the 6 mL 0.09% ropivacaine + 20 mL 0.83% L_{alk} group after mixing over 1 h. **(C)** Microscopic image (10X) of the 0.83% L_{alk} – ropivacaine (0.5–1.0%) mixture. **(D)** Macroscopic appearance of the 0.09% ropivacaine (routine labor analgesia) – 0.83% L_{alk} (routine doses). **(E)** Macroscopic appearance of the 0.83% L_{alk} – ropivacaine (0.5–1.0%) mixture. L_{alk}, alkalized lidocaine.

6.0 (3). Actually, even at pH value of 5.8, crystals were visible under the microscope immediately in Colsoul et al.'s study who evaluated the physical stability of the mixture of ropivacaine, clonidine, and adrenaline tartrate (5). Adding corticosteroid to local anesthetics could also increase the pH of the mixture and may cause crystallization, which has been verified in Watkins et al.'s (6) and Hwang et al.'s (7) studies. Watkins et al. observed ropivacaine crystal formation when mixed with dexamethasone, and showed a positive correlation of crystallization with higher pH (7.0 vs. 6.8) and with higher concentrations of dexamethasone (10 vs. 4 mg/mL). In Hwang et al.'s study, when ropivacaine was mixed with dexamethasone or betamethasone, crystals larger than an arteriole at physiologic pH levels (7.0 and 7.5, respectively) were observed. All these studies suggested that we should pay attention to alkalized ropivacaine for its potential hazards. For this case, with factors from the parturient, delivery and anesthesia technique excluded, and the rapid and large precipitation of high concentration of ropivacaine with L_{alk} *in vitro*, the patient's paresthesia could potentially, but not certain, be explained by drug crystallization. Elimination *via* macrophage phagocytosis could help explain her symptom relief (9). However, this hypothesis warrants pathological examination for further confirmation.

In summary, adding L_{alk} to pretreated 0.09% ropivacaine (routine labor analgesia) was safe and efficient. We advise avoiding further high concentration of ropivacaine (0.5–1%) administration; additional dilution of lidocaine with low concentration and high volume may provide safe maintenance of anesthesia and analgesia. This finding also supports the pharmacological principle that a combination of drugs should be considered incompatible, until proven compatible.

DATA AVAILABILITY STATEMENT

The original contributions presented in the study are included in the article/supplementary material, further inquiries can be directed to the corresponding author/s.

ETHICS STATEMENT

Written informed consent was obtained from the individual(s) for the publication of any potentially identifiable images or data included in this article.

AUTHOR CONTRIBUTIONS

AZ drafted the manuscript and performed the *in vitro* testing. WL and WC performed the anesthesia. YZ followed up the patient. YH helped the study design. LP conceived of the study and participated in its design. All authors have read and approved the final manuscript.

FUNDING

The device, materials, and medications used in the *in vitro* testing were supported by the National Natural Science Foundation of China #81901148 (AZ) and #82071252 (YH).

REFERENCES

1. Lam DT, Ngan Kee WD, Khaw KS. Extension of epidural blockade in labour for emergency Caesarean section using 2% lidocaine with epinephrine and fentanyl, with or without alkalinisation. *Anaesthesia.* (2001) 56:790–4. doi: 10.1046/j.1365-2044.2001.02058-4.x
2. Sharawi N, Bansal P, Williams M, Spencer H, Mhyre JM. Comparison of chloroprocaine versus lidocaine with epinephrine, sodium bicarbonate, and fentanyl for epidural extension anesthesia in elective cesarean delivery: a randomized, triple-blind, noninferiority study. *Anesth Analg.* (2021) 132:666–75. doi: 10.1213/ANE.0000000000005141
3. Milner QJ, Guard BC, Allen JG. Alkalinization of amide local anaesthetics by addition of 1% sodium bicarbonate solution. *Eur J Anaesthesiol.* (2000) 17:38–42. doi: 10.1097/00003643-200001000-00007
4. Block HS, Biller J. Neurology of pregnancy. *Handb Clin Neurol.* (2014) 121:1595–622. doi: 10.1016/B978-0-7020-4088-7.00105-X
5. Colsoul ML, Lardinois B, Galanti L, Soumoy L, Hecq JD. Physical instability of an infusion containing ropivacaine, clonidine and adrenaline tartrate in syringes for pre-operative administration. *Anaesth Crit Care Pain Med.* (2019) 38:675. doi: 10.1016/j.accpm.2019.07.006
6. Watkins TW, Dupre S, Coucher JR. Ropivacaine and dexamethasone: a potentially dangerous combination for therapeutic pain injections. *J Med Imaging Radiat Oncol.* (2015) 59:571–7. doi: 10.1111/1754-9485.12333
7. Hwang H, Park J, Lee WK, Lee WH, Leigh JH, Lee JJ, et al. Crystallization of local anesthetics when mixed with corticosteroid solutions. *Ann Rehabil Med.* (2016) 40:21–7. doi: 10.5535/arm.2016.40.1.21
8. Tuleu C, Allam J, Gill H, Yentis SM. Short term stability of pH-adjusted lidocaine-adrenaline epidural solution used for emergency caesarean section. *Int J Obstet Anesth.* (2008) 17:118–22. doi: 10.1016/j.ijoa.2007.11.002
9. Chiu CC, Chuang TY, Chang KH, Wu CH, Lin PW, Hsu WY. The probability of spontaneous regression of lumbar herniated disc: a systematic review. *Clin Rehabil.* (2015) 29:184–95. doi: 10.1177/0269215514540919

Conflict of Interest: The authors declare that the research was conducted in the absence of any commercial or financial relationships that could be construed as a potential conflict of interest.

Publisher's Note: All claims expressed in this article are solely those of the authors and do not necessarily represent those of their affiliated organizations, or those of the publisher, the editors and the reviewers. Any product that may be evaluated in this article, or claim that may be made by its manufacturer, is not guaranteed or endorsed by the publisher.

frontiers | Frontiers in Medicine

CASE REPORT
published: 07 June 2022
doi: 10.3389/fmed.2022.893306

Case Report: Complex Treatment Using Vibroacoustic Therapy in a Patient With Co-Infection and COVID-19

Assema Zh. Bekniyazova[1], Assiya Kadralinova[1,2], Maiya E. Konkayeva[1], Aigerim A. Yeltayeva[1,2] and Aidos K. Konkayev[1,2]*

[1] Department of Anesthesiology and Intensive Care, Astana Medical University, Nur-Sultan, Kazakhstan, [2] Department of Anesthesiology and Intensive Care, The National Scientific Center of Traumatology and Orthopedics named after Academician N.D. Batpenov, Nur-Sultan, Kazakhstan

The present report highlights a case of successful treatment of a 59-year-old patient who experienced pain, swelling, hyperemia, the presence of a wound of the right knee joint, impaired function of the right lower limb, weakness, fatigue, and labored breathing. Sepsis was detected in the patient as a result of periprosthetic infection with concomitant severe COVID-19. The patient was admitted to the hospital for 59 days, with 57 days of treatment of the patient at the intensive care unit. A therapy of multiple organ failure involved complex treatment using antiviral and combined antibiotic therapy, taking into account the sensitivity of the pathogen to antibiotics; glucocorticoid therapy; anticoagulant therapy; the concept of non-invasive ventilation; and vibroacoustic pulmonary therapy as a method of physiotherapy as well. An integrated approach using a vibroacoustic device in the therapy of the patient with sepsis due to periprosthetic infection with concomitant coronavirus infection had a positive effect despite the lack of etiological treatment against the COVID-19.

Keywords: COVID-19, periprosthetic joint infection, vibroacoustic therapy, co-infection, case report

OPEN ACCESS

Edited by:
Yun Long,
Peking Union Medical College Hospital (CAMS), China

Reviewed by:
Elsa A. Campbell,
Caritas Association for the Karlsruhe Region, Germany
Marta Woldańska-Okońska,
Medical University of Łódź, Poland

****Correspondence:***
Assema Zh. Bekniyazova
Asemabek9@gmail.com
orcid.org/0000-0002-3117-0294

Specialty section:
This article was submitted to Intensive Care Medicine and Anesthesiology, a section of the journal Frontiers in Medicine

Received: *10 March 2022*
Accepted: *05 May 2022*
Published: *07 June 2022*

Citation:
Bekniyazova AZ, Kadralinova A, Konkayeva ME, Yeltaeva AA and Konkayev AK (2022) Case Report: Complex Treatment Using Vibroacoustic Therapy in a Patient With Co-Infection and COVID-19. Front. Med. 9:893306. doi: 10.3389/fmed.2022.893306

INTRODUCTION

During the pandemic caused by the COVID-19, humankind has faced difficulties in all areas of their lives. Particularly this pandemic situation affected workers in the field of medicine and health. For example, surgeons had to perform surgical procedures for patients with confirmed coronavirus infection who needed immediate treatment (1–3).

Periprosthetic joint infection (PJI) is a severe sequel that occurs in 1–2% of patients with primary arthroplasties. This condition is associated with a high sickness rate and requires complex therapy strategies (4, 5). Patients with the diagnosis of PJI complicated by coronavirus or bacterial co-infection in most cases face an unfavorable outcome of the treatment (6–8).

Vibroacoustic therapy (VAT) is a kind of sound treatment that implicates transiting pure low frequency sine wave vibrancies into the body using an apparatus with coupled speakers (9). VAT has been endorsed for relieving a pain, increasing a circulation and movability of a patient (10). It also has been examined in therapy of such diseases as fibromyalgia (11), cerebral palsy, and Alzheimer's disease (12).

Both, the present epidemiological situation and the high mortality due to coronavirus infection throughout the world and particularly in Kazakhstan puzzled all medical workers in search of a solution for this issue. The method of vibroacoustic lung therapy is actively used by our Center for treating many respiratory diseases. Based on the results of the treatment, this method has shown a positive effect in patients with coronavirus infection.

However, the effect of VAT in the treatment of various conditions has not been sufficiently studied (13, 14). Hence, the need for studying this method of therapy is crucial in order to get a more efficient treatment of patients with the comorbid background. The present clinical case describes the complex therapy of a patient with the PJI complicated by the COVID-19 viral infection by VAT using a vibroacoustic pulmonary device.

The clinical case deserves close attention because the patient presented in this study had been identified with coronavirus infection, with a Charlson comorbidity index of three points, which is associated with a high risk of mortality (15). Moreover, the patient was also diagnosed with sepsis, multiple organ failure, and disseminated intravascular coagulation as well, which are associated with a high risk of adverse outcomes.

CASE DESCRIPTION

Patient Information

A 59-year-old male patient was urgently admitted to the intensive care unit of the hospital. At the time of admission, the patient experienced pain, swelling, hyperemia, the presence of a wound on the right knee joint, dysfunction of the right lower limb, weakness, fatigue, as well as labored breathing at the moment of his admission to the hospital. According to the patient, his appetite was reduced with a repeated occurrence of vomiting. Heredity of the patient does not have any hereditary diseases. The patient was disabled due to a knee injury in 1990. Constantly, before the hospitalization the patient took drugs internally: acetylsalicylic acid 75 mg, bisoprolol 5 mg, clopidogrel 75 mg.

From 09.18.2020 to 09.29.2020, the patient was treated at the surgery department of a private clinic with a diagnosis of right-sided post-traumatic gonarthrosis of stage 3. Mixed contracture and pronounced pain syndrome of the right knee joint were also revealed in the patient. Moreover, the main diagnosis of the patient was complicated by hematoma of the postoperative wound of the right knee joint, and contact dermatitis. The echocardiography had indicated a minimal mitral tricuspid regurgitation.

Clinical Findings

According to the initial checkup, the patient's visible skin areas were pale gray in color with mild icteric phenomena. Pastosity of the lateral abdominal surfaces and edema of the operated limb were also observed in the patient. The patient's body temperature at the time of the examination was 38°C. Breathing of the patient was substantive, frequent (up to 24–25 per minute), shallow, and noisy. Blood pressure reached 130/90 mmHg with a pulse of 105–110 beats per minute. Furthermore, the patient's lips were dry and the tongue was covered with a brown plaque; the abdomen was not swollen and soft on palpation; peristalsis was bugged and weakened at the time of the checkup. In line with the initial checkup, the SOFA quick test was also performed on the patient that had indicated three points and focused on infection. Therefore, sepsis was not excluded from the diagnosis.

Timeline

Chronology of the patient's medical history from the moment of surgical procedure at a private clinic to the discharge from the hospital is highlighted in **Figure 1**.

Diagnostic Assessment

As a result of routine laboratory tests at the time of the patient's admission to the hospital, changes in the form of increased markers of inflammation, thrombocytosis, and anemia were revealed. The biochemical blood analysis had detected hypoproteinemia, hypokalemia, hypocalcemia, and hyperbilirubinemia. Hypocoagulation was also indicated in the analysis of the coagulogram. Blood gas analysis also showed a low oxygenation index in the patient's blood (274.8 mmHg). Additionally, the patient was diagnosed with bilateral pneumonia according to computed tomography (CT) results. Coronavirus infection was not detected by express method COVID-19 – IgM, IgG. CT picture had also indicated moderate hepatomegaly with diffuse fatty hepatosis.

At the time of the admission to the hospital, the patient was diagnosed with bilateral pneumonia, pneumosclerosis, chronic bronchitis, and pneumosclerosis as a condition after coronary artery bypass grafting (CABG; **Figure 2A**). On the 5th day, the dynamics of the X-ray had shown weakly positive changes in the condition mentioned above (**Figure 2B**). On the 12th day, X-ray dynamics on bilateral pneumonia were negative (**Figure 2C**). Furthermore, on the 26th day of the hospital stay, an X-ray picture revealed bilateral polysegmental pneumonia in the stage of incomplete resolution (**Figure 2D**) with no changes in the X-ray dynamics on the 33rd day (**Figure 2E**).

The next CT scan of the patient was performed on the 17th day after the hospitalization, and revealed focal darkening as the type of frosted glass with areas of consolidation, involving more than 75% of parenchyma. Pleural effusion had been also noted as a result of the CT. There was also a severe decline in hemodynamics and respiration of the patient, as the oxygenation index at that moment had constituted 108.6 mmHg.

The PCR test results taken from the patient for SARS-CoV-2 detection was positive. A bacteriological study of the material from the tracheostomy tube was also carried out. *Pseudomonas aeruginosa* was detected as a result of the study. Thereafter, such microorganisms as *Morganella morganii, Pseudomonas aeruginosa, Enterobacter aerogenes, Proteus vulgaris* were found in the intubation tube of the intensive care unit on different days of the patient's stay. In addition, the following types of bacteria were seeded from the area of the patient's surgical wound: *Escherichia coli* and *Staphylococcus epidermidis* which are the most common pathogens of periprosthetic infections.

Postoperative anemia of moderate severity was also detected in the patient. Sepsis was diagnosed as a condition of the

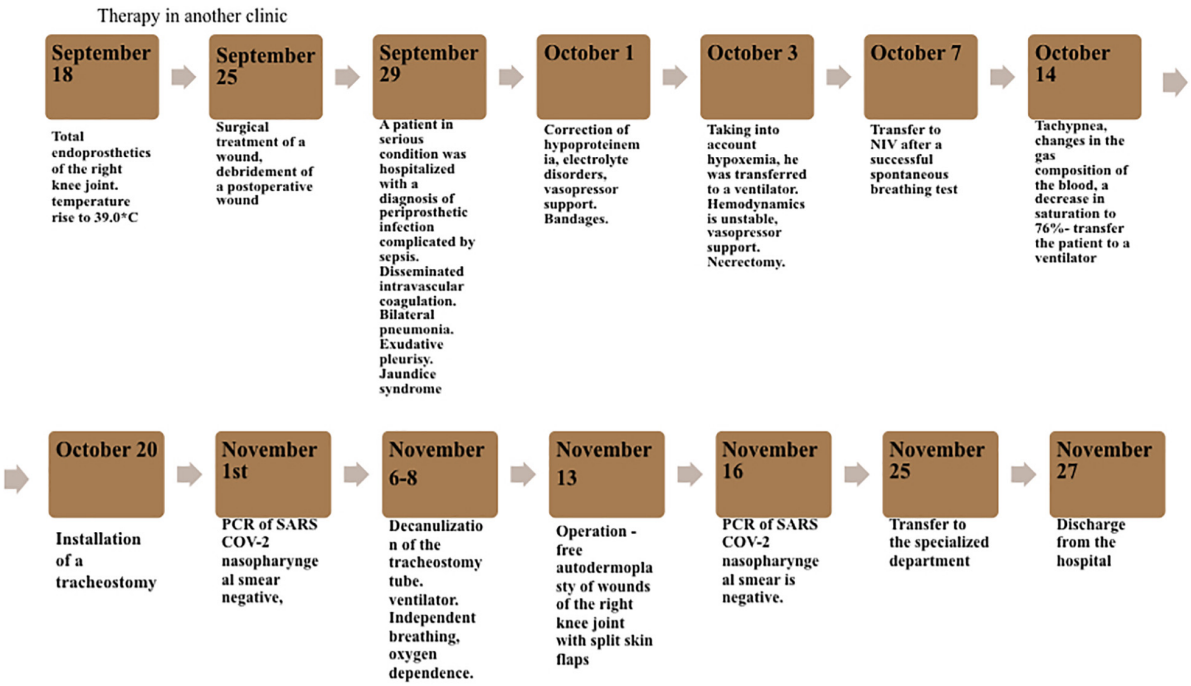

FIGURE 1 | Chronology of the patient's medical history from the moment of surgery at the private clinic to discharge from the hospital.

postoperative wound of the right knee joint. Moreover, disseminated intravascular coagulation of blood, and bilateral exudative and interstitial pleurisy was additionally revealed in the patient.

Based on the above mentioned, the preliminary diagnosis of infection and inflammatory reaction caused by endoprosthetics of the right knee joint after the total endoprosthetics of the right knee joint on 09.18.2020 and necrectomy of a postoperative wound on 09.25.2020 was made. In addition, such complications as sepsis, disseminated intravascular coagulation, bilateral pneumonia, bilateral exudative pleurisy, and anemia of moderate severity were also presented in the patient.

Except for the mentioned postoperative complications the following concomitant diseases were revealed in the patient: coronary heart disease, heart failure followed by coronary artery bypass grafting (CABG, surgical procedure was performed on 07.11.2019), as well as chronic bronchitis in remission.

Therapeutic Intervention

The surgical procedure of total endoprosthetics of the right knee joint was performed on 18.09.2020.

Surgical and postoperative treatment of the wound was carried out on 25.09.2020. The patient received a course of antibacterial therapy, including Vancomycin, hemocorrection (fresh frozen plasma), parenteral nutrition (OliClinomel), and diuretics (Spironolactone, Furosemide).

Mechanical Ventilation and Oxygen Therapy

On the 5th day of the hospitalization, the progression of hypoxemia to 58.2 mmHg was transferred to a ventilator in Biphasic positive airway pressure mode with FiO_2 – 40%, Tinsp – 1.6 s, Fr – 14 per minute, Pinsp – 18 mbar, Pasb – 8 mbar, PEEP – 8 mbar. With these parameters, Exhaled Tidal Volume was provided in 520–540 ml, minute volume – 9.7 l/min. According to the acid-base state analysis, normalization of the level of raO_2 constituted 95.8 mmHg, $raSO_2$ – 45.8 mmHg, pH – 7.403. On the 6th day, the patient was transferred to the constant positive airway pressure mode with FiO_2 – 35%.

Thereafter, the patient was transferred to non-invasive ventilation on the 8th day after a successful spontaneous breathing test, where active respiratory therapy was performed in the form of non-invasive ventilation and inhalation. Taking into account the increasing tachypnea, changes in the gas composition of the blood, and decrease in the saturation to 76%, it was decided to admit the patient to artificial lung ventilation. On the 21st day, the patient underwent a tracheostomy. Thereafter, on the 37th day, decannulation of the tracheostomy tube was performed. The patient's breathing was substantive, oxygen dependence, using NIV. Vibroacoustic pulmonary therapy was also performed on the patient every 4 h during the entire stay at the intensive care unit.

Antiviral Therapy

After positive results of the PCR test for SARS-CoV-2 detection, Remdesivir was prescribed at 100 mg on the first day of the treatment, followed by 200 mg of I/v h/w dispenser 1 time a day. Remdesivir was subsequently discontinued due to the long QT syndrome according to the electrocardiogram, as the drug's metabolism and effects are unknown.

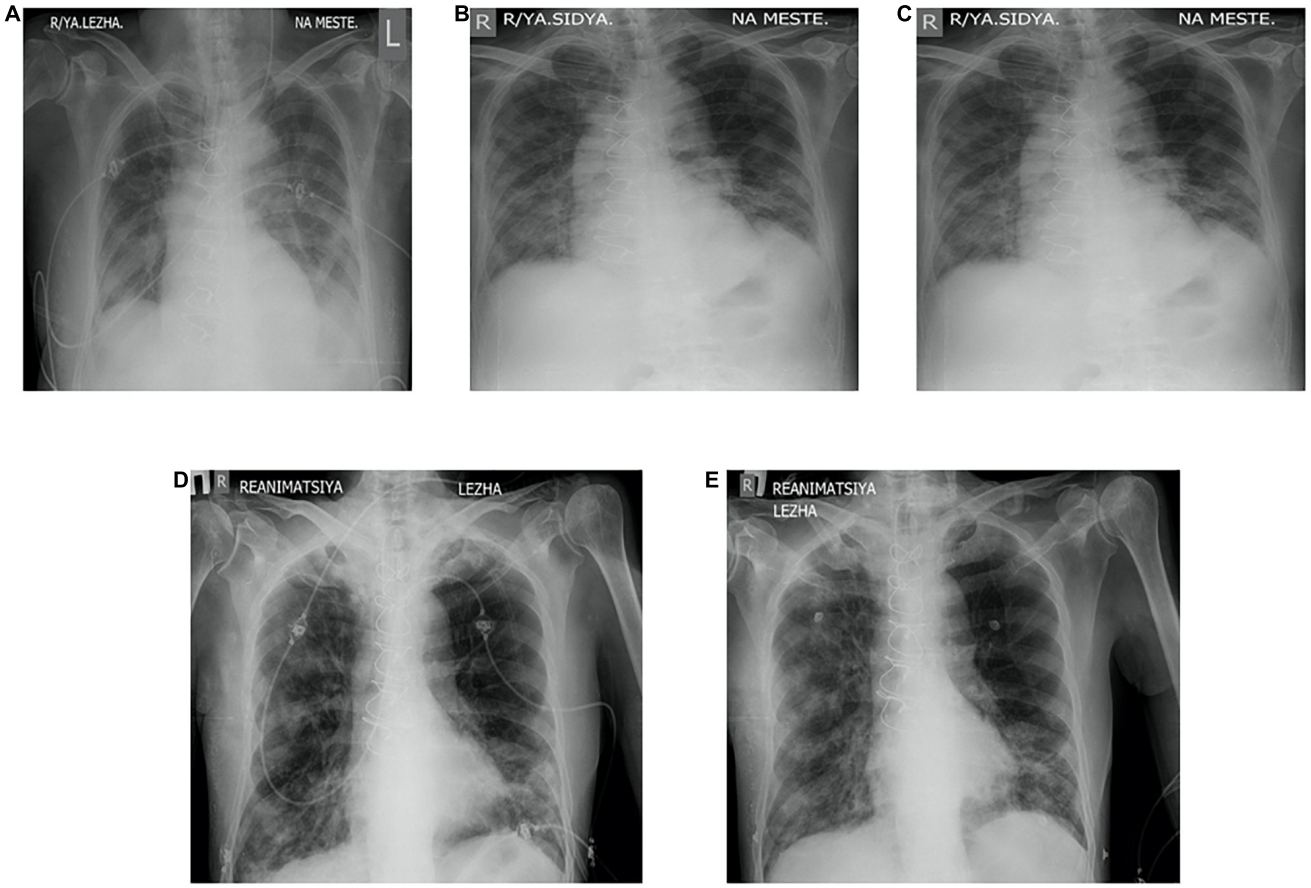

FIGURE 2 | Dynamics of X-ray after the application of VALT: CXR on the 1st day **(A)**, CXR after 18 sessions of VALT **(B)**, CXR on the 16th day (BiPAP: FiO_2 – 60%, f-18, I/E – 1/2, Pinsp – 25, PEEP – 14) **(C)**, CXR on the 25th day (BiPAP: FiO_2-40%, f-18, I/E – 1/2, Pinsp-17, PEEP-12) **(D)**, CXR on the 32nd day (BiPAP: FiO_2-40%, f-20, I/E – 1/2, Pins-20, PEEP 13) **(E)**.

Anti-infection Therapy

On the first day after the patient's admission to the hospital, the patient was empirically prescribed an intravenous drip of meropenem 1 g/v through a dispenser, and 20 ml of 0.9% sodium chloride solution at a rate of 40 ml/h, 2 times a day. The next day, this preparation was replaced with 30% lincomycin 600 mg/m intramuscularly. After receiving the results of the analysis of the microbiological study and determining the sensitivity of the isolated cultures of microorganisms, amikacin was added at the dosage of 0.5 g 2 times a day for 3 days. However, after the subsequent microbiological analyses, antibiotics were replaced in the following sequence, depending on the sensitivity of microorganisms: ciprofloxacin 1 g, 2 times a day + ceftazidime 1 g, 2 times a day; moxifloxacin 400 mg, 2 times a day + ertapenem intravenously through a dispenser 1 g, 2 times a day; cefepime intravenously 3 g, 2 times a day. Additionally, the patient received 100 mg of fluconazole daily, enterally 2 times a day.

Glucocorticoid Therapy

There also was the administration by the patient of dexamethasone at the dose of 4 mg 2 times a day with the length of administration of 17 days.

Anticoagulant Therapy

Enoxaparin at 40 mg 2 times a day and acetylsalicylic acid at 100 mg orally were also administered by the patient.

Liquid Volume Management

Transfusion with blood preparations was performed in the patient as well using fresh frozen plasma, washed erythrocytes, and albumin 10% to correct hypoproteinemia.

The assessment of the volemic status was carried out by measuring central venous pressure of the patient, and if necessary, was stimulated with furosemide intravenously at 20 mg 2 times a day. In the case of necessity, up to 100 mg of the preparation was administered using a medication dispenser during the day, under the control of central venous pressure.

Nutritional Support

The patient also received nutritional support at the rate of 25–30 kcal/kg/day, and protein provision of 1.2–1.5 g/kg/day.

Other

As additional measures, correction of metabolic and electrolyte disorders of the patient was carried out. The patient was

prescribed to receive sedation, analgesia, humanistic care, antiarrhythmic, hypotensive drugs, and adrenomimetics under control of blood pressure. Moreover, early-stage physical therapy, including vibroacoustic pulmonary therapy was performed every 4 h.

Follow-Up and Outcomes

The patient had no contraindications for the conduction of vibroacoustic pulmonary therapy, and no undesirable consequences after the procedure. The tolerance test was carried out with the help of a short application of the device for the vibroacoustic pulmonary therapy for up to 1 min, with the evaluation of parameters of hemodynamics, saturation, and the patient's sensation. The dynamics of the effect of the vibroacoustic pulmonary therapy were assessed according to the data of peripheral oximetry, blood gas composition, oxygenation index, and radiography of the chest organs. There was a short-term decrease in saturation up to 30 s, associated with active sputum discharge. Clinically, when using the apparatus, we observed an improvement in the drainage function of the bronchi. The drainage effect was also visually recorded during bronchoscopy. The positive dynamics from the treatment were assessed according to the data of peripheral oximetry, blood gas composition, oxygenation index, and radiography of the chest organs dynamics. The implementation of vibroacoustic therapy in the complex treatment of the patient contributed to faster rehabilitation and activation, and as a result, the length of the stay in the intensive care unit was significantly reduced. The dynamics of the patient's respiratory function indicators are shown in **Figure 3**. Additionally, the dynamics of tests from the moment of the admission to the hospital to the discharge of the patient are highlighted in **Figure 4**.

The patient with improved clinical and laboratory data, CT and X-ray diagnostics, negative PCR test for the COVID-19 was transferred to a specialized department in a satisfactory condition, and 2 days later, the patient was discharged from the hospital for rehabilitation treatment at the place of a residence.

DISCUSSION

As it is known, there is a tendency for unfavorable outcomes in a patient due to the presence of several disorders. Our patient had a comorbid background of the COVID-19 infection and the accompanying pathology of the cardiovascular system. Additionally, the patient had PJI, sepsis, disseminated intravascular coagulation, and multiple organ failures as well. Twenty-three days after the hospitalization, these conditions were complicated by infection with the severe infectious disease – COVID-19. We used complex treatment with vibroacoustic therapy. The treatment of coronavirus infection was carried out in accordance with the protocol "Coronavirus infection – COVID-19," 10th edition with amendments from 15.07.2020 of the Kazakhstan from 15 July 2020 Protocol No. 106.

To date, with the active spread of coronavirus infection around the world, it is crucial to be wary of the atypical course of other infections, including PJI, since the symptoms of one infection can disguise themselves as symptoms of another infectious disease. The combination of the COVID-19 and PJI has a more severe course and, accordingly, the approach to treatment becomes more complex (4). For this purpose, a multi-system approach to the treatment of this category of patients is required.

One clinical case was found by authors as a result of the literature search on the topic in the PubMed and MEDLINE databases (16). This clinical case describes a patient with comorbid background with COVID-19 infection and PJI, and its management in the operating room.

As it is known, the treatment of patients with concomitant cardiovascular pathology with the background of COVID-19 has its own complications. Pathological processes in this case have

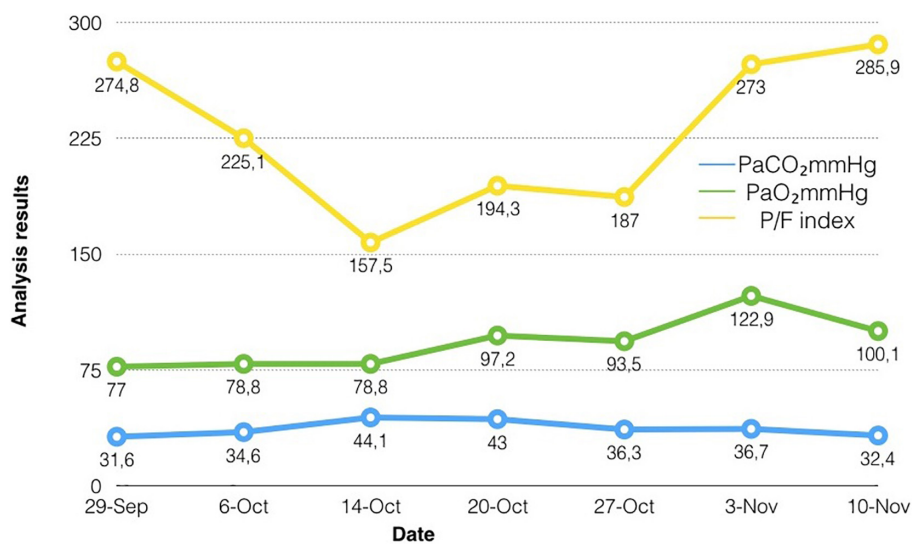

FIGURE 3 | The dynamics of the patient's respiratory function indicators.

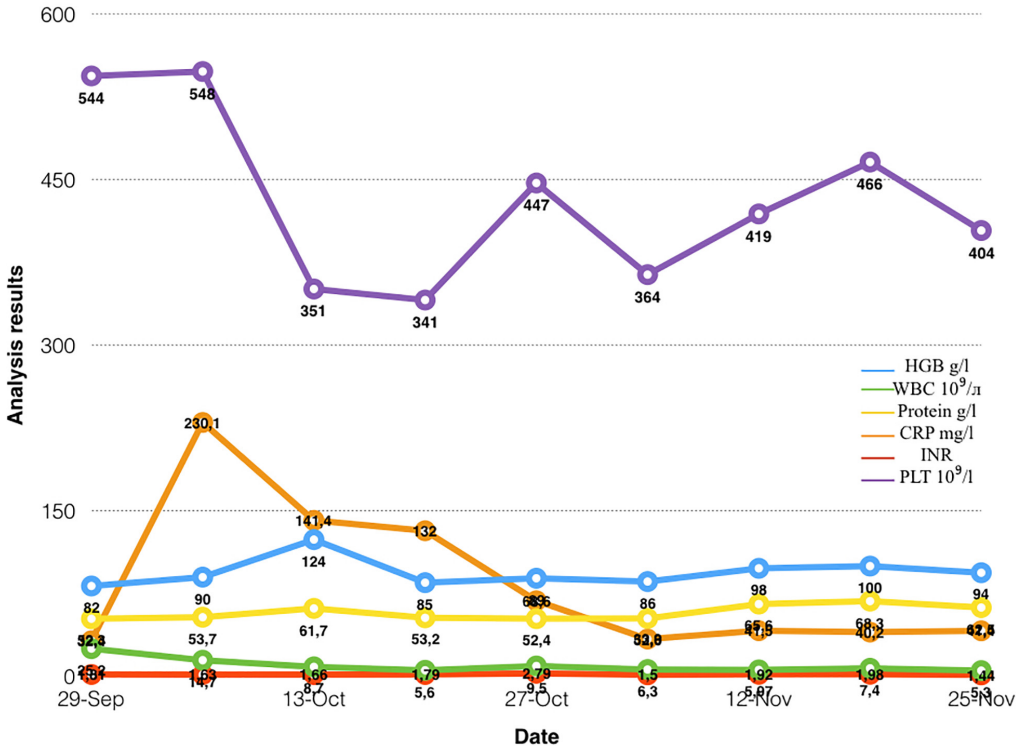

FIGURE 4 | The dynamics of tests from the moment of the patient's admission to the discharge.

a tendency of entangling one another according to the type of "vicious circle" (17).

Physiotherapy is an important and necessary stage in treating such comorbid backgrounds to improve and accelerate the outcomes of the disease (18–20). Vibroacoustic therapy, as one of the methods of physiotherapy, has a beneficial effect on vibration areas by improving blood circulation (9). The method was carried out by our department using the "VibroLUNG" device, which is specially designed for vibroacoustic "massage" of the chest. Due to the use of special emitters, intense exposure is perceived comfortably due to the large coverage area with vibroacoustic emitters. Besides, the effect is transmitted through the air due to the absence of direct contact between the movable membrane and the "irradiated" surface. The device can replace manual methods of percussion and vibration chest massage in the case of respiratory system diseases (21).

Although analysis of the literature found on vibroacoustic lung therapy had not provided extensive information on the following comorbidity, the practical application of the treatment demonstrates positive results in our patients. Conducting vibroacoustic therapy sessions every 3 h in the combination with the main treatment had had a significant effect on lung function and, as a consequence, the outcome of the disease. However, full mechanisms of action of the vibroacoustic apparatus on an organism, namely on lungs, have yet to be studied (9).

The present case shows, that an integral approach to the patient with a severe course of coronavirus infection on the background of comorbidity led to a favorable outcome. Since the COVID-19 is widespread all over the world nowadays, clinicians need to learn more about the treatment of patients with the COVID-19 along with other pathology. We hope that this clinical case will help in providing care to patients with COVID on the background of PJI.

PATIENT PERSPECTIVE

According to the patient, the hardware massage was more pleasant than the manual. Moreover, the vibroacoustic pulmonary therapy via the device had contributed to more relieving cough, and improved general condition and the health of the patient.

AUTHOR'S NOTE

The authors have read the CARE Checklist (2013), and the manuscript was prepared and revised according to the CARE Checklist (2013).

ETHICS STATEMENT

Ethical review and approval were not required for the study on human participants in accordance with the local legislation and institutional requirements. The patients/participants provided their written informed consent to participate in this study.

Written informed consent was obtained from the individual(s) for the publication of any potentially identifiable images or data included in this article.

AUTHOR CONTRIBUTIONS

AKo, MK, and AY: conceptualization and organization of the database. AKa: writing draft. AB: review and editing of the manuscript. All the authors issued final approval for the version to be submitted.

ACKNOWLEDGMENTS

We thank T. O. Zheksembiyev and V. A. Borovikov for their contribution to writing and preparing this manuscript for the publication.

REFERENCES

1. Anwarali Khan MH, Kow RY, Ramalingam S, Ho JPY, Jaya Raj J, Ganthel Annamalai K, et al. COVID-19 collateral damage: management of periprosthetic joint infection in Malaysia. *Cureus.* (2021) 13:e18820. doi: 10.7759/cureus.18820
2. Kibbe MR. Surgery and COVID-19. *JAMA.* (2020) 324:1151–2. doi: 10.1001/jama.2020.15191
3. Thaler M, Kort N, Zagra L, Hirschmann MT, Khosravi I, Liebensteiner M, et al. Prioritising of hip and knee arthroplasty procedures during the COVID-19 pan-demic: the European hip society and the European knee associates survey of members. *Knee Surg Sports Traumatol Arthrosc.* (2021) 29:3159–63. doi: 10.1007/s00167-020-06379-6
4. Mühlhofer HML, Feihl S, Suren C, Banke IGJ, Pohlig F, von Eisenhart-Rothe R. Implant-associated joint infections. *Orthopade.* (2020) 49:277–86. doi: 10.1007/s00132-020-03877-w
5. Tevell S, Christensson B, Nilsdotter-Augustinsson Å, Rydén C, Ryding U, Söderquist B, et al. Treatment of orthopedic implant-associated infections. *Lakartidningen.* (2019) 116:FR6C.
6. Goncalves Mendes Neto A, Lo KB, Wattoo A, Salacup G, Pelayo J, DeJoy R III, et al. Bacterial infections and patterns of antibiotic use in patients with COVID-19. *J Med Virol.* (2020) 93:1489–95. doi: 10.1002/jmv.26441
7. Westblade LF, Simon MS, Simon MS. Bacterial coinfections in coronavirus disease 2019. *Trends Microbiol.* (2021) 29:930–41. doi: 10.1016/j.tim.2021.03.018
8. Liu HH, Yaron D, Piraino AS, Kapelusznik L. Bacterial and fungal growth in sputum cultures from 165 COVID-19 pneumonia patients requiring intubation: evidence for antimicrobial resistance development and analysis of risk factors. *Ann Clin Microbiol Antimi-crob.* (2021) 20:69. doi: 10.1186/s12941-021-00472-5
9. Kantor J, Kantorová L, Mareèková J, Peng D, Vilímek Z. Potential of vibroacoustic therapy in persons with cerebral palsy: an advanced narrative review. *Int J Environ Res Public Health.* (2019) 16:3940. doi: 10.3390/ijerph16203940
10. Bartel LR, Chen R, Alain C, Ross B. Vibroacoustic stimulation and brain oscillation: from basic re-search to clinical application. *Music Med.* (2017) 9:153–66. doi: 10.47513/mmd.v9i3.542
11. Naghdi L, Ahonen H, Macario P, Bartel L. The effect of low-frequency sound stimulation on patients with fibromyalgia: a clinical study. *Pain Res Manag.* (2015) 20:e21–7. doi: 10.1155/2015/375174
12. McDermott B, Porter E, Hughes D, McGinley B, Lang M, O'Halloran M, et al. Gamma band neural stimulation in humans and the promise of a new modality to prevent and treat Alzhei-mer's disease". *J Alzheimers Dis.* (2018) 65:363–92. doi: 10.3233/JAD-180391
13. Bartel L, Mosabbir A. Possible mechanisms for the effects of sound vibration on human health. *Healthcare (Basel).* (2021) 9:597. doi: 10.3390/healthcare9050597
14. Cavallo F, Rovini E, Dolciotti C, Radi L, Della Ragione R, Bongioanni P. Physiological response to vibro-Acoustic stimulation in healthy subjects: a preliminary study. *Annu Int Conf IEEE Eng Med Biol Soc.* (2020) 2020:5921–4. doi: 10.1109/EMBC44109.2020.9175848
15. Tuty Kuswardhani RA, Henrina J, Pranata R, Anthonius Lim M, Lawrensia S, Suastika K. Charlson comorbidity index and a composite of poor outcomes in COVID-19 patients: a systematic review and meta-analysis. *Diabetes Metab Syndr.* (2020) 14:2103–9. doi: 10.1016/j.dsx.2020.10.022
16. Sunkin JA, Lindsey MH, Stenquist DS, Fuller BC, Chen AF, Shah VM. Surgical treatment of acute periprosthetic knee infection with concurrent presumed COVID-19. a case report. *JBJS Case Connect.* (2020) 10:e2000226. doi: 10.2106/JBJS.CC.20.00226
17. Zhang Y, Coats AJS, Zheng Z, Adamo M, Ambrosio G, Anker SD, et al. Management of heart failure patients with COVID-19: a joint position paper of the Chinese heart failure association & national heart failure committee and the heart failure association of the European society of cardiology. *Eur J Heart Fail.* (2020) 22:941–56. doi: 10.1002/ejhf.1915
18. Battaglini D, Robba C, Caiffa S, Ball L, Brunetti I, Loconte M, et al. Chest physiotherapy: an important adjuvant in critically ill mechanically ventilated patients with COVID-19. *Respir Physiol Neurobiol.* (2020) 282:103529. doi: 10.1016/j.resp.2020.103529
19. Lazzeri M, Lanza A, Bellini R, Bellofiore A, Cecchetto S, Colombo A, et al. Respiratory physiotherapy in patients with COVID-19 infection in acute setting: a position paper of the Italian association of respiratory physiotherapists (ARIR). *Monaldi Arch Chest Dis.* (2020) 90 1. doi: 10.4081/monaldi.2020.1285
20. Thomas P, Baldwin C, Bissett B, Boden I, Gosselink R, Gosselink R, et al. Physiotherapy management for COVID-19 in the acute hospital setting: clinical practice recommendations. *J Physiother.* (2020) 66:73–82. doi: 10.1016/j.jphys.2020.03.011
21. User Guide. *User Manual BARK Vibrolung.* Nur-Sultan: RP SMK (2020).

Conflict of Interest: The authors declare that the research was conducted in the absence of any commercial or financial relationships that could be construed as a potential conflict of interest.

frontiers | Frontiers in Medicine

CASE REPORT
published: 20 June 2022
doi: 10.3389/fmed.2022.915981

Case Report: Osmotic Demyelination Syndrome After Transcatheter Aortic Valve Replacement: Case Report and Review of Current Literature

*Xinhao Jin and Yonggang Wang**

Department of Critical Care Medicine, Sir Run Run Shaw Hospital, Zhejiang University School of Medicine, Hangzhou, China

Background: Osmotic demyelination syndrome (ODS) has a low incidence but is a life-threatening neurological disorder whose common cause is rapid overcorrection of chronic hyponatremia. Transcatheter aortic valve replacement (TAVR) is a new and important therapy for patients with aortic valve stenosis. In this article, we discuss the case of a 64-year-old woman who developed ODS after TAVR and provide a literature review.

Case Presentation: A 64-year-old female patient was admitted to the hospital with chest tightness, shortness of breath, and fatigue for 2 months, with worsening of symptoms for 3 days prior to presentation. Auscultation revealed crackles in the lung fields, and systolic murmurs could be easily heard in the aortic area. Echocardiography showed severe aortic stenosis. Chest X-ray showed pulmonary oedema. Laboratory examinations showed that her serum sodium was 135 mmol/L. The patient received a diuretic to relieve her symptoms but showed little benefit. Her symptoms worsened, and her blood pressure dropped. Then, she underwent emergency TAVR under extracorporeal membrane oxygenation (ECMO) support. After the operation, her urine output increased markedly, and serum sodium increased sharply from 140 to 172 mmol/L. An MRI scan showed multiple lesions in the pons suggestive of ODS.

Conclusion: To date, this is the first reported case of a patient who developed ODS after receiving TAVR. In current clinical practice, diuretics are often used in aortic stenosis patients because of pulmonary oedema. After a patient receives TAVR, kidney perfusion pressure quickly returns to normal, and with the residual effect of a high-dose diuretic, balances of fluid volume and electrolyte levels in this phase are quite fragile and must be carefully managed. If a patient has neurological symptoms/signs during this phase, ODS should be considered, and MRI might be necessary.

Keywords: **osmotic demyelination syndrome (ODS), transcatheter aortic valve replacement, case report, hyponatremia, serum sodium**

OPEN ACCESS

Edited by:
Jihad Mallat,
Cleveland Clinic Abu Dhabi,
United Arab Emirates

Reviewed by:
Hamza Rayes,
University of Cincinnati, United States
Daisy Sangroula,
University of Louisville, United States

***Correspondence:**
Yonggang Wang
3203066@zju.edu.cn

Specialty section:
This article was submitted to Intensive Care Medicine and Anesthesiology, a section of the journal Frontiers in Medicine

Received: *08 April 2022*
Accepted: *31 May 2022*
Published: *20 June 2022*

Citation:
Jin X and Wang Y (2022) Case Report: Osmotic Demyelination Syndrome After Transcatheter Aortic Valve Replacement: Case Report and Review of Current Literature. Front. Med. 9:915981. doi: 10.3389/fmed.2022.915981

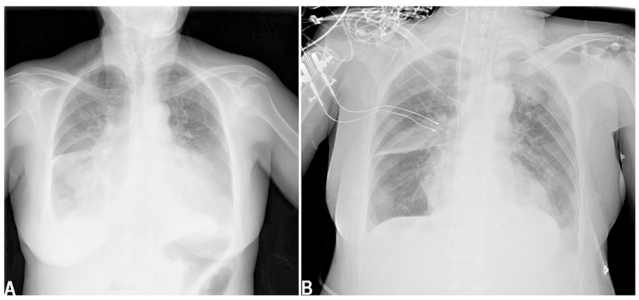

FIGURE 1 | Chest x-ray showed pulmonary oedema and bilateral pleural effusion when admission **(A)**. Chest x-ray showed pulmonary oedema and bilateral pleural effusion decreased after TAVR **(B)**.

BACKGROUND

Osmotic demyelination syndrome (ODS), which includes central pontine myelinolysis (CPM) and extrapontine myelinolysis (EPM), is defined as degeneration of myelin within the central nervous system with sharply demarcated lesions within the brain, especially the pons, and is diagnosed by magnetic resonance imaging (MRI) (1). ODS accounts for ∼0.4–0.56% of all neurological admissions to tertiary referral hospitals, and MRI-based studies describe an incidence of ODS ranging from 0.3 to 1.1% (2). Although ODS is a low-incidence disorder, it is associated with high rates of disability and mortality (3). Most published cases are related to rapid correction of hyponatremia in patients with chronic hyponatremia.

Aortic stenosis (AS) has estimated prevalence rates of 12 to 13% for all AS cases and 2 to 4% for severe AS cases in patients ≥75 years of age in the Western world (4). Severe, symptomatic aortic stenosis is fatal; if left untreated, the mortality rate is 50% at 2 years (5). In 2002, the first human transcatheter aortic valve replacement (TAVR) was performed on a 57-year-old man in Rouen (France) (6), which introduced a new interventional era. TAVR is a relatively recent revolutionary treatment that has grown exponentially over the past decade and has become the mainstay of treatment for symptomatic severe aortic stenosis.

In this article, we report a case of ODS that occurred in a patient with aortic stenosis after TAVR under extracorporeal membrane oxygenation (ECMO) support. A diuretic phase was induced by a sudden improvement of low kidney blood perfusion pressure after TAVR. Balances of fluid volume and electrolyte levels in this phase are quite fragile and must be carefully managed.

CASE DESCRIPTION

A 64-year-old female patient (140 cm/48.6 kg, BMI: 24.8) presented to the hospital with chest tightness, shortness of breath, and fatigue for 2 months, with symptom worsening for 3 days prior to presentation. The patient had no history of shortness of breath or rapid breathing. Her past surgical history included cholecystectomy 10 years prior. She was not epileptic, diabetic, or hypertensive and never smoked or drank alcohol. She and her family members had no history of kidney diseases. On admission, she had a temperature of 36.3°C, a pulse of 97 beats per minute, a blood pressure of 96/65 mmHg, and a respiratory rate of 24 cycles per minute. Her consciousness was clear, and her Glasgow Coma Scale score was 4+5+6. Auscultation revealed crackles in the lung fields, the cardiac rhythm was regular, and a systolic murmur could be easily heard in the aortic area. Both lower extremities showed mild pitting oedema. Echocardiography showed severe aortic stenosis: the aortic valve area (AVA) was 0.28 cm^2, and the ejection fraction (EF) was 23%. Color Doppler flow imaging (CDFI) showed that the blood flow of the aortic valve increased significantly, the peak velocity was 5.7 m/s, the peak gradient was 130 mmHg, and the mean gradient was 81 mmHg. The structures of the bicuspid valve and tricuspid valve were normal, but moderate regurgitation was evident in both the bicuspid and tricuspid valves. Chest X-ray showed pulmonary oedema and bilateral pleural effusion (**Figure 1A**). Lab examinations showed that her serum sodium was 135 mmol/L, AST was 396 U/L, ALT was 440 U/L, proBNP was >25,000 pg/mL, troponin I was 0.120 ng/mL, and lactic acid was 5.3 mmol/L. The patient's glomerular filtration rate was 50.5 ml/min, BUN was 12.82 mmol/L, creatinine was 76 μmol/L, serum osmolarity was 296 osmo/kg, urine osmolarity was 490 osmo/kg, urinary specific gravity was 1.014, and urine output was 950 ml/24 h. Urine glucose and urinary protein were negative.

After admission, the patient was prepared to be treated by TAVR. Before the operation, she received furosemide (20 mg p.o. qd, 1 day), spironolactone (20 mg p.o. qd, 5 days), torsemide (20 mg i.v. qd, 3 days; 20 mg i.v. bid, 2 days), and tolvaptan (7.5 mg p.o. qd, 2 days) for diuresis but showed little benefit. The patient's symptoms were worse, and her blood pressure dropped (SBP: 81–95 mmHg). Dobutamine was used immediately to maintain stable hemodynamics but failed. For unstable hemodynamics, she received emergency TAVR under the support of extracorporeal membrane oxygenation (ECMO) (venoarterial, pump rotation speed: 3,000 RPM, blood flow: 2.7 L/min). After the operation, vital signs were stable, and urine output increased markedly. On postoperative day 1, the patient's glomerular filtration rate was 45.2 ml/min, BUN was 15.45 mmol/L, creatinine was 85 μmol/L, serum osmolarity was 336 osmo/kg, urine osmolarity was 280 osmo/kg, urinary specific gravity was 1.009, and urine output was 5,720 ml/24 h (1,500 ml in the first 3 h after TAVR). Chest X-ray showed decreased pulmonary oedema and bilateral pleural effusion (**Figure 1B**), but serum sodium increased from 140 to 172 mmol/L (**Figure 2**). ECMO was discontinued on the first day after the operation. However, the patient's consciousness did not recover after the operation. CT brain scans were performed twice to look for lesions in her brain, but they did not reveal any hypodensity on CT images (**Figure 3**). Then, she underwent an MRI scan, and we found multiple lesions in the pons. We observed a symmetric low signal on T1-weighted imaging and a symmetric high signal on T2-weighted imaging and fluid attenuated inversion recovery (FLAIR) sequence imaging in the pons and medulla oblongata areas, which are called the trident sign (7) or Mercedes Benz sign (8). This classical radiological

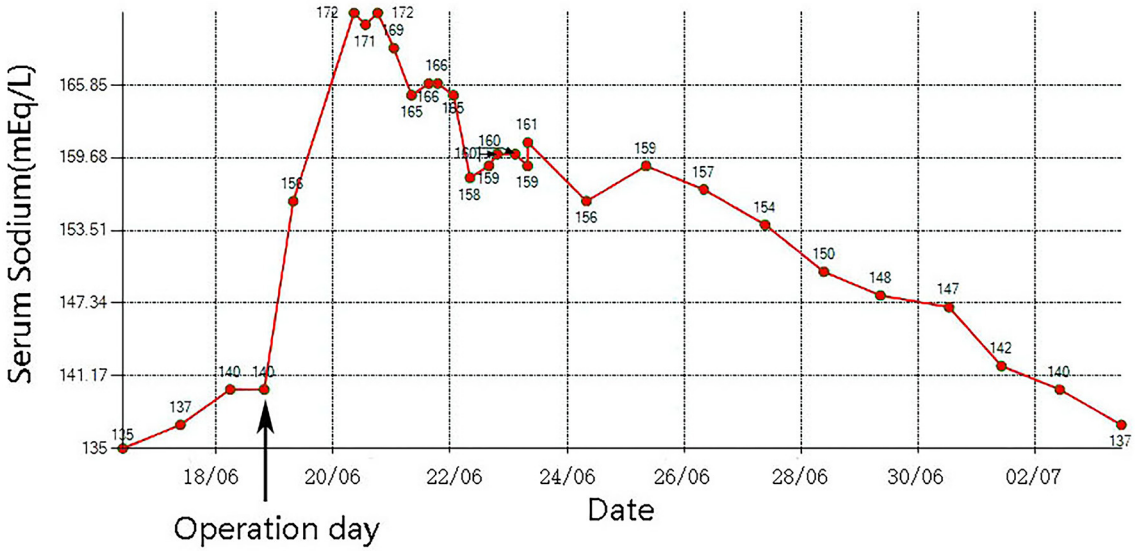

FIGURE 2 | The change of serum sodium in this case.

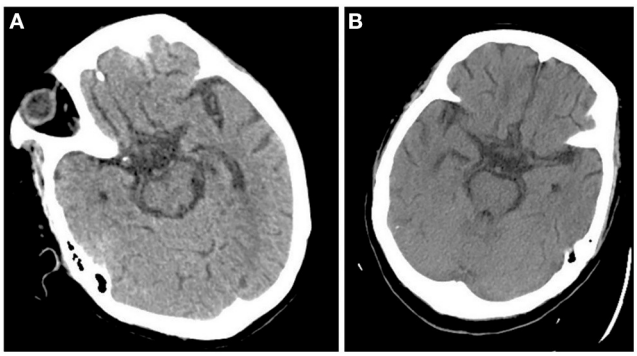

FIGURE 3 | CT scan didn't demonstrate any hypodensity in pons 1 day after the operation **(A)** and 7 days after the operation **(B)**.

picture favors a change in ODS (**Figure 4**). However, a diffusion-weighted imaging (DWI) signal change was not observed in our case.

She received corrective treatment for hypernatremia (changing all drug solvents (if applicable) from normal saline to sterile water injection or glucose injection) and was given water through a nasogastric tube (dextrose in water, n.g. 20 ml/h; electrolyte-free water n.g. 20 ml/h), and her serum sodium returned to the baseline level. She received intravenous injection of human immunoglobulin 20 g daily for 5 days and supportive care. After treatment, she regained consciousness but had dysarthria and impaired muscle power. She was discharged 1 month later with dysarthria and a muscle power of grade 2 in the left limbs and grade 5 in the right limbs. Two months later, we phoned the patient, and she told us that her phonetic function and muscle power had returned to normal.

DISCUSSION

Osmotic demyelination syndrome (ODS), which is characterized by widespread degeneration of myelin within the central nervous system (CNS), was first described by Adams et al. (9). Nearly two decades (mid-1970s) after it was described, people found that its common cause is rapid overcorrection of chronic hyponatremia. The increase in serum sodium causes an increase in serum osmolality. An increase in serum osmolality causes increased osmolality in the brain, which causes shrinkage of astrocytes and oligodendrocytes, resulting in their apoptosis and inflammation and disruption of the blood–brain barrier and thus leading to demyelination. However, in this case, the patient's serum sodium was normal when she was admitted to the hospital. After admission, she was diagnosed with severe aortic stenosis and resulting pulmonary oedema. To relieve the patient's symptoms, a massive dose of diuretic was used, but the patient's urinary output did not increase, and her symptoms worsened. In the past, patients in this situation were very difficult to manage. Fortunately, the development of TAVR and ECMO has afforded patients another chance for cure. The use of VA-ECMO as a salvage therapy in cardiogenic shock is becoming a current practice (10). The patient's hemodynamics were stable after ECMO was performed, and she underwent emergency TAVR. After the operation, the patient's urinary output increased prominently (1,500 ml in the first 3 h after TAVR), and serum sodium increased from 140 to 156 mmol/L and then to 172 mmol/L. A variety of therapies were used immediately to decrease serum sodium quickly, but the effect was not satisfactory (**Figure 2**). The patient's consciousness changed after the operation, and clinical evidence indicated that she had ODS. This case shows that ODS occurs not only in patients with chronic

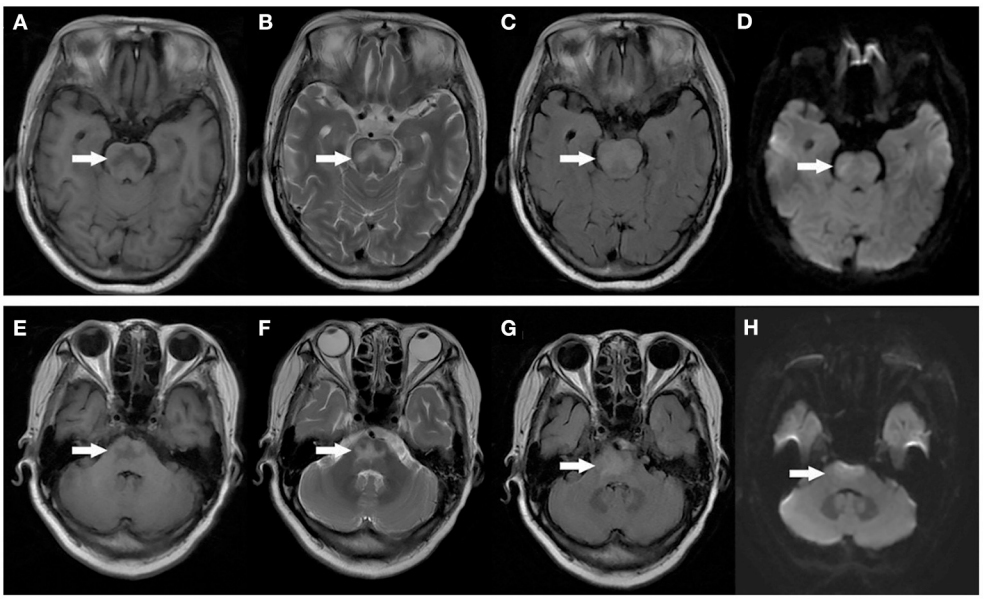

FIGURE 4 | MRI image of the patient's head: Axial T1 weighted images demonstrating symmetric low signal in the central pons **(A,E)**. Axial T2 weighted images demonstrating symmetric high signal in the central pons **(B,F)**. T2 FLAIR images demonstrate symmetric high signal in the central pons **(C,G)**. DWI images didn't show any diffusion restriction in the central pons **(D,H)**.

hyponatremia but also in patients with normal serum sodium, and that rapid sodium increases should be considered in these patients.

The frequency of symptoms and signs of heart failure (such as dyspnoea and pulmonary oedema) among patients with aortic stenosis varies depending on the stage of disease. According to the REMEDY study, the incidence of heart failure in patients with rheumatic valvular heart disease is 33.4% (11). Diuretics are often used in these patients to relieve symptoms in current clinical practice. With the development of the operation, TAVR has become a very useful therapy for patients with severe aortic stenosis. Due to blood flow disturbance from the left ventricle to the aorta in patients with severe aortic stenosis, acute prerenal kidney failure is likely caused by low kidney perfusion pressure. When aortic stenosis is relieved by TAVR, renal perfusion will improve, and renal blood flow will increase within a short time. Combined with the residual effect of a massive dose of diuretic used before surgery, the patient's urinary output will increase very quickly after the operation, and serum sodium will increase markedly, which is an important issue warranting attention. Balances of fluid volume and electrolyte levels in this phase are quite fragile. Although closely monitored and carefully managed in this case, due to systemic factors, these balances are still difficult to manage.

ODS symptoms vary, including lethargy, quadriparesis, dysarthria, ophthalmoplegia, ataxia, and even coma or death and depend on the degree of pontine involvement and the presence of extrapontine lesions (12, 13). Hildur Aegisdottir et al. analyzed 83 patients with ODS and found that 73 patients (88%) had bulbar symptoms, while 71 patients (85.5%) had dysarthria/dysphagia. Furthermore, 65 (78.3%) had limb paresis at diagnosis, and 10 (12.0%) were in a locked-in state (14). In this case, the patient's main symptoms were coma, dysarthria, and impaired muscle power, indicating injuries in the nervous system. The rate of clinical neurological events after TAVR ranges from 3 to 7% (15, 16). Patients undergoing TAVR are at an increased risk for developing acute cerebral hypoperfusion during balloon aortic-valvuloplasty/valve deployment (17). Diffusion-weighted magnetic resonance imaging (DWI) revealed new cerebral DWI lesions among >70% of patients after TAVR, regardless of the valve type or implantation strategy (18–20). In this case, when we found that the patient's consciousness had changed after TAVR, stroke was first considered. However, two CT scans did not demonstrate any hypodensity on postoperative day 1 and postoperative day 2, which did not favor stroke. After MRI was performed, a classical radiological picture was evident in the pons, which favors a change in ODS.

Early imaging evidence of changes in ODS may not appear on CT. Patients suspected of having ODS should undergo brain MRI. The typical MRI findings of ODS are a symmetric low signal on T1-weighted images and a symmetric high signal on T2-weighted and FLAIR images in the central pons or associated extrapontine structures (21, 22). The classical radiological picture is called the trident sign, butterfly sign, or Mercedes Benz sign (8). The sensitivity of DWI is still controversial. Kimberly A. Ruzek et al. found that restricted diffusion is the first imaging manifestation of CPM, which occurs within 24 h of the clinical onset of tetraplegia and before detection of abnormalities on conventional MRI images (23). However, Förster et al. analyzed eight ODS patients and found that DWI changes did not regularly precede tissue changes detectable on conventional MRI sequences (24). Therefore, Johann Lambeck believed that DWI,

T1, T2, and T2 FLAIR sequences were equivalent for detection purposes (2). These imaging changes may not be clearly visible until 1–2 weeks later (25). In our case, MRI showed a symmetric low signal on T1-weighted and a symmetric high signal on T2-weighted and FLAIR imaging in the pons and medulla oblongata areas. DWI signal changes did not occur in our case.

Apart from supportive therapy and experimental therapies, no definitive treatment has been established for ODS. Ludwig et al. reported 2 cases of ODS in which treatment with plasmapheresis and intravenous immune globulin improved long-term neurologic outcomes (26). Kengne et al. found that treatment with dexamethasone resulted in fewer neurological manifestations 24 h after correction of chronic hyponatremia in a rat model of ODS, but dexamethasone failed to reduce mortality at 5 days (27). Chemaly et al. reported a case of a 13-year-old girl diagnosed with ODS who received 0.6 mg i.v. of thyrotropin-releasing hormone (TRH) daily for 6 weeks until complete recovery (28). Haruyuki Suzukican et al. found that minocycline could protect against ODS by inhibiting the activation and accumulation of microglia at the site of demyelinative lesions in a rat model of ODS. Recently, Wijayabandara et al. reported a case in which plasmapheresis may remain effective in reversing ODS several weeks after the initial osmotic insult (29). To our knowledge, the small amount of evidence on the treatment of ODS is based purely on case reports, animal experiments or small case series (2). The treatment of patients with ODS requires further study. However, depending on disease severity, these therapeutic choices should be considered in the clinical management of ODS.

CONCLUSION

In summary, to our knowledge, this is the first reported case of ODS after TAVR. ODS occurs not only in patients with rapid overcorrection of chronic hyponatremia but also in patients with normal sodium. With the development of the operation, TAVR has become a very useful therapy for patients with severe aortic stenosis. After a patient receives TAVR, kidney perfusion pressure quickly returns to normal, and with the residual effect of a high-dose diuretic administered before surgery, balances of fluid volume and electrolyte levels in this phase are quite fragile and must be carefully managed. If a patient has neurological symptoms/signs in this phase, ODS should be considered, and MRI might be necessary.

DATA AVAILABILITY STATEMENT

The original contributions presented in the study are included in the article/supplementary material, further inquiries can be directed to the corresponding author/s.

ETHICS STATEMENT

Ethical review and approval was not required for the study on human participants in accordance with the local legislation and institutional requirements. The patients/participants provided their written informed consent to participate in this study. Written informed consent was obtained from the individual(s) for the publication of any potentially identifiable images or data included in this article.

AUTHOR CONTRIBUTIONS

XJ wrote the first draft of the manuscript and revised it. YW was involved in the conception and design of the work and revised the manuscript. All authors contributed to the article and approved the submitted version.

REFERENCES

1. Nelson NR, Tompkins MG, Thompson BM. Plasma exchange as treatment for osmotic demyelination syndrome: case report and review of current literature. *Transfus Apher Sci.* (2019) 58:102663. doi: 10.1016/j.transci.2019.10.005
2. Lambeck J, Hieber M, Dressing A, Niesen WD. Central pontine myelinosis and osmotic demyelination syndrome. *Dtsch Arztebl Int.* (2019) 116:600–6. doi: 10.3238/arztebl.2019.0600
3. Herraiz L, Cuesta M, Runkle I. Osmotic demyelination syndrome in a patient with uncontrolled hyperglycemia. *Med Clin (Barc).* (2017) 149:370–1. doi: 10.1016/j.medcle.2017.09.008
4. Osnabrugge RL, Mylotte D, Head SJ, Van Mieghem NM, Nkomo VT, LeReun CM, et al. Aortic stenosis in the elderly: disease prevalence and number of candidates for transcatheter aortic valve replacement: a meta-analysis and modeling study. *J Am Coll Cardiol.* (2013) 62:1002–12. doi: 10.1016/j.jacc.2013.05.015
5. Varadarajan P, Kapoor N, Bansal RC, Pai RG. Survival in elderly patients with severe aortic stenosis is dramatically improved by aortic valve replacement: results from a cohort of 277 patients aged > or =80 years. *Eur J Cardiothorac Surg.* (2006) 30:722–7. doi: 10.1016/j.ejcts.2006.07.028
6. Cribier A, Eltchaninoff H, Bash A, Borenstein N, Tron C, Bauer F, et al. Percutaneous transcatheter implantation of an aortic valve prosthesis for calcific aortic stenosis: first human case description. *Circulation.* (2002) 106:3006–8. doi: 10.1161/01.CIR.0000047200.36165.B8
7. Balcerac A, Nichelli L, Demeret S, Le Guennec L. The piglet and the trident sign in osmotic demyelination syndrome. *Intensive Care Med.* (2021) 47:476–7. doi: 10.1007/s00134-021-06354-w
8. Kumar AS, Naheed D, Balaini N, Mehta S, Lal V. "Mercedes benz sign: osmotic demyelination syndrome. *Neurol India.* (2021). 69:777–8. doi: 10.4103/0028-3886.319223
9. Adams RD, Victor M, Mancall EL. Central pontine myelinolysis: a hitherto undescribed disease occurring in alcoholic and malnourished patients. *AMA Arch Neurol Psychiatry*. (1959). 81:154–72. doi: 10.1001/archneurpsyc.1959.02340140020004
10. Le Gall A, Follin A, Cholley B, Mantz J, Aissaoui N, Pirracchio R. Veno-arterial-ECMO in the intensive care unit: from technical aspects to clinical practice. *Anaesth Crit Care Pain Med.* (2018) 37:259–68. doi: 10.1016/j.accpm.2017.08.007
11. Zuhlke L, Engel ME, Karthikeyan G, Rangarajan S, Mackie P, Cupido B, et al. Characteristics, complications, and gaps in evidence-based interventions in rheumatic heart disease: the global rheumatic heart disease registry (the REMEDY study). *Eur Heart J.* (2015) 36:1115–22.
12. Mohammed AS, Boddu P, Yazdani DF. Clinical evolution of central pontine myelinolysis in a patient with alcohol withdrawal: a blurred clinical horizon. *Case Rep Med.* (2016) 2016:6065259. doi: 10.1155/2016/6065259
13. Singh TD, Fugate JE, Rabinstein AA. Central pontine and extrapontine myelinolysis: a systematic review. *Eur J Neurol.* (2014) 21:1443–50. doi: 10.1111/ene.12571

14. Aegisdottir H, Cooray C, Wirdefeldt K, Piehl F, Sveinsson O. Incidence of osmotic demyelination syndrome in Sweden: a nationwide study. *Acta Neurol Scand.* (2019) 140:342–9. doi: 10.1111/ane.13150
15. Adams DH, Popma JJ, Reardon MJ, Yakubov SJ, Coselli JS, Deeb GM, et al. Transcatheter aortic-valve replacement with a self-expanding prosthesis. *N Engl J Med.* (2014) 370:1790–8. doi: 10.1056/NEJMoa1400590
16. Miller DC, Blackstone EH, Mack MJ, Svensson LG, Kodali SK, Kapadia S, et al. Transcatheter (TAVR) vs. surgical (AVR) aortic valve replacement: occurrence, hazard, risk factors, and consequences of neurologic events in the PARTNER trial. *J Thorac Cardiovasc Surg.* (2012) 143:832–43. doi: 10.1016/j.jtcvs.2012.01.055
17. Abawi M, de Vries R, Stella PR, Agostoni P, Boelens D, van Jaarsveld RC, et al. Evaluation of cognitive function following transcatheter aortic valve replacement. *HEART LUNG CIRC.* (2018) 27:1454–61. doi: 10.1016/j.hlc.2017.10.006
18. Rodes-Cabau J, Kahlert P, Neumann FJ, Schymik G, Webb JG, Amarenco P, et al. Feasibility and exploratory efficacy evaluation of the Embrella Embolic Deflector system for the prevention of cerebral emboli in patients undergoing transcatheter aortic valve replacement: the PROTAVI-C pilot study. *JACC Cardiovasc Interv.* (2014) 7:1146–55. doi: 10.1016/j.jcin.2014.04.019
19. Auffret V, Regueiro A, Del TM, Abdul-Jawad AO, Campelo-Parada F, Chiche O, et al. Predictors of early cerebrovascular events in patients with aortic stenosis undergoing transcatheter aortic valve replacement. *J Am Coll Cardiol.* (2016) 68:673–84. doi: 10.1016/j.jacc.2016.05.065
20. Pagnesi M, Martino EA, Chiarito M, Mangieri A, Jabbour RJ, Van Mieghem NM, et al. Silent cerebral injury after transcatheter aortic valve implantation and the preventive role of embolic protection devices: a systematic review and meta-analysis. *Int J Cardiol.* (2016) 221:97–106. doi: 10.1016/j.ijcard.2016.06.143
21. Lee KB, Hong BY, Kim JS, Son DB, Choi SI, Lim SH. The effect of white matter integrity on functional outcome in central pontine demyelination. *J Phys Ther Sci.* (2019) 31:698–701. doi: 10.1589/jpts.31.698
22. Chong A, Ha JM, Chung JY, Kim H, Cho YS. Follow-up of brain single-photon emission computed tomography (spect) and magnetic resonance imaging (mri) in a case of seizure caused by osmotic demyelination syndrome. *Am J Case Rep.* (2020) 21:e923406. doi: 10.12659/AJCR.923406
23. Ruzek KA, Campeau NG, Miller GM. Early diagnosis of central pontine myelinolysis with diffusion-weighted imaging. *Am J Neuroradiol.* (2004) 25:210–3. Available online at: http://www.ajnr.org/content/25/2/210.long
24. Förster A, Nolte I, Wenz H, Al-Zghloul M, Kerl HU, Brockmann C, et al. Value of diffusion-weighted imaging in central pontine and extrapontine myelinolysis. *Neuroradiology.* (2013) 55:49–56. doi: 10.1007/s00234-012-1083-z
25. Jahan M, Sharma S, Rehmani R. Osmotic demyelination syndrome despite appropriate hyponatremia correction. *Cureus.* (2020) 12:e8209. doi: 10.7759/cureus.8209
26. Ludwig KP, Thiesset HF, Gayowski TJ, Schwartz JJ. Plasmapheresis and intravenous immune globulin improve neurologic outcome of central pontine myelinolysis occurring post orthotopic liver transplant. *Ann Pharmacother.* (2011) 45:e10. doi: 10.1345/aph.1P371
27. Kengne FG, Soupart A, Pochet R, Brion JP, Decaux G. Re-induction of hyponatremia after rapid overcorrection of hyponatremia reduces mortality in rats. *Kidney Int.* (2009) 76:614–21. doi: 10.1038/ki.2009.254
28. Chemaly R, Halaby G, Mohasseb G, Medlej R, Tamraz J, El-Koussa S. [Extrapontine myelinolysis: treatment with TRH]. *Rev Neurol (Paris).* (1998) 154:163–5.
29. Wijayabandara M, Appuhamy S, Weerathunga P, Chang T. Effective treatment of osmotic demyelination syndrome with plasmapheresis: a case report and review of the literature. *J Med Case Rep.* (2021) 15:6. doi: 10.1186/s13256-020-02573-9

Conflict of Interest: The authors declare that the research was conducted in the absence of any commercial or financial relationships that could be construed as a potential conflict of interest.

frontiers | Frontiers in Medicine

TYPE Case Report
PUBLISHED 11 August 2022
DOI 10.3389/fmed.2022.970239

OPEN ACCESS

EDITED BY
Yuetian Yu,
Shanghai Jiao Tong University, China

REVIEWED BY
Qinghe Meng,
Upstate Medical University,
United States
Alessandro Boscarelli,
Institute for Maternal and Child Health
Burlo Garofolo (IRCCS), Italy
Bassam Redwan,
Klinikum Westfalen - Klinik am Park,
Germany

*CORRESPONDENCE
Hiroyuki Yamamoto
hyamamoto19700908@gmail.com

SPECIALTY SECTION
This article was submitted to
Intensive Care Medicine
and Anesthesiology,
a section of the journal
Frontiers in Medicine

RECEIVED 15 June 2022
ACCEPTED 28 July 2022
PUBLISHED 11 August 2022

CITATION
Konagaya K, Yamamoto H, Nishida T, Morita T, Suda T, Isogai J, Murayama H and Ogino H (2022) Negative-pressure wound therapy to treat thoracic empyema with COVID-19-related persistent air leaks: A case report. *Front. Med.* 9:970239. doi: 10.3389/fmed.2022.970239

Negative-pressure wound therapy to treat thoracic empyema with COVID-19-related persistent air leaks: A case report

Kensuke Konagaya[1], Hiroyuki Yamamoto[2]*, Tomoki Nishida[3], Tomotaka Morita[4], Tomoyuki Suda[1,5], Jun Isogai[6], Hiroyuki Murayama[1] and Hidemitsu Ogino[1]

[1]Department of Surgery, Narita-Tomisato Tokushukai Hospital, Chiba, Japan, [2]Department of Cardiovascular Medicine, Narita-Tomisato Tokushukai Hospital, Chiba, Japan, [3]Department of General Thoracic Surgery, Shonan Kamakura General Hospital, Kanagawa, Japan, [4]Department of Anesthesiology, Narita-Tomisato Tokushukai Hospital, Chiba, Japan, [5]Department of General Surgery, Shonan Kamakura General Hospital, Kanagawa, Japan, [6]Department of Radiology, Asahi General Hospital, Asahi, Japan

The novel coronavirus disease (COVID-19) has resulted in a global pandemic. Recently, COVID-19-related pneumothorax has gained attention because of the associated prolonged hospital stay and high mortality. While most cases of pneumothorax respond well to conservative and supportive care, some cases of refractory pneumothorax with persistent air leaks (PALs) do not respond to conventional therapies. There is a lack of evidence-based management strategies to this regard. We describe the case of a 73-year-old man with COVID-19-related acute respiratory distress syndrome (ARDS) who developed delayed tension pneumothorax with PALs caused by alveolopleural fistulas. Despite chest tube drainage, autologous blood pleurodesis, and endoscopic procedures, the PALs could not be closed, and were complicated by thoracic empyema. Subsequent minimally invasive open-window thoracostomy (OWT) with vacuum-assisted closure (VAC) therapy helped successfully control the refractory PALs. Serial chest computed tomography monitoring was useful for the early detection of the pneumothorax and understanding of its temporal relationship with air-filled lung cysts. Our case provides a new perspective to the underlying cause of refractory pneumothorax with PALs, secondary to COVID-19-related ARDS, and underscores the potential of OWT with VAC therapy as a therapeutic alternative in such cases.

KEYWORDS

COVID-19, pneumothorax, persistent air leaks, empyema, open-window thoracostomy, negative-pressure wound therapy

Introduction

Coronavirus disease (COVID-19) caused by severe acute respiratory syndrome coronavirus 2 (SARS-CoV-2) has resulted in a global pandemic. Though it can affect all organs, it has a predilection for the respiratory system, where it easily progresses to acute respiratory distress syndrome (ARDS) in severe cases. While the management of the acute and critical phase of COVID-19 has advanced rapidly, the treatment of its sequelae remains a challenge.

Pneumothorax is defined as the presence of air in the pleural space with subsequent impairment of oxygen supply and ventilation. It is a known sequela of COVID-19. The association between COVID-19 and pneumothorax development has recently gained attention because of the latter's association with prolonged hospitalization and increased in-hospital mortality (1). Pneumothorax is a common complication strongly associated with barotrauma during invasive mechanical ventilation (IMV) (2). However, COVID-19-related pneumothorax can develop in both spontaneous breathing and mechanical ventilation settings (3). It can also develop irrespective of body weight, pre-existing lung disease, or smoking status, which are well-known risk factors for pneumothorax (3). The exact mechanism underlying COVID-19-related pneumothorax therefore remains poorly understood. SARS-CoV-2 infection complicated by pneumothorax is managed by either general supportive care or removal of air from the pleural space through chest tube thoracostomy. Among such cases, the management of refractory cases with persistent air leaks (PALs) remains challenging, owing to its complex diagnosis and lack of evidence-based treatment strategies.

Case description

A 73-year-old man was admitted to our hospital for general fatigue, presenting with symptoms of productive cough and fever for 4 days. He was a former smoker who had smoked 20 cigarettes a day for 20 years but had no pre-existing lung disease. His vital signs were as follows: blood pressure, 115/80 mmHg; heart rate, 110 beats/min; blood temperature, 36.2°C; respiratory rate, 24 breaths/min; and oxygen saturation, 90% on ambient air. Hematological examination revealed the following: white blood cell count, 2,600 cells/μL; differential count, 65.5% neutrophils, and elevated levels of C-reactive protein, 5.13 mg/dL (normal < 0.14 mg/dL); D-dimer, 10.1 μg/mL (normal < 1.0 μg/mL); LDH, 384 U/L (normal range, 124–222 U/L); and serum ferritin, 1,776 ng/mL (normal range, 20–200 ng/mL). SARS-CoV-2 infection was confirmed through reverse-transcriptase polymerase chain reaction (RT-PCR). Chest computed tomography (CT) on admission revealed patchy ground-glass opacities in both peripheral lungs, indicative of interstitial pneumonia (**Figure 1A**). A monoclonal antibody therapy directed against the spike protein of SARS-CoV-2 (casirivimab–imdevimab, 600/600 mg as a single intravenous dose) was initiated for moderate COVID-19 pneumonia; however, it was ineffective. On day 3, the patient continued to worsen clinically with progressive ground-glass opacities observed on the follow-up chest CT (**Figure 1B**). Thus, oxygen was administered with a high-flow nasal cannula (HFNC) at 40 L/min, with FiO_2 titrated for oxygenation. In addition, we used a combination of oral dexamethasone (6 mg daily for 10 day) and IV remdesivir (200 mg, followed by 100 mg daily for 5 day), together with tocilizumab infusion (480 mg daily for 1 day). The chest CT on day 7 of admission revealed extensive ground-glass opacities, and diffuse consolidation with air bronchogram showing anteroposterior gradient in both the lungs, consistent with that of ARDS (**Figures 1C,D**). The patient developed severe hypoxemia of SpO_2 80%, despite HFNC oxygen therapy (FiO_2 1.0, 40 L/min), requiring intubation for respiratory insufficiency and IMV in the intensive care unit. The PaO_2/FiO_2 ratio was 120, suggestive of moderate ARDS. The IMV in the prone position was applied at a tidal volume of 6.6 mL/kg, positive end-expiratory pressure of 15 cm H_2O, plateau pressure of 14 cm H_2O, and respiratory frequency of 28/min. On day 15, a catheter-related bloodstream infection caused by *Enterobacter aerogenes* led to bacterial septic shock, consequent acute kidney injury and disseminated intravascular coagulation, requiring vasopressors, continuous renal replacement therapy, steroid infusion (Solu-Medrol 40 mg, daily for 16 day), and heparin infusion for 7 day. In addition, broad-spectrum antimicrobial treatment with meropenem (1 g/day IV for 10 day) was initiated, followed by antimicrobial de-escalation based on antimicrobial susceptibility test results (ceftriaxone, 4 g/day IV for 12 day). The chest CT on day 22 of admission revealed several lung cysts related to diffuse alveolar damage, predominantly on the right lung. Note the air-filled cystic lesion communicating to the segmental bronchus, was suspicious of a bronchopleural fistula (BPF) (**Figure 2A**). Follow-up RT-PCR confirmed SARS-CoV-2 negativity. On day 26, since the patient's clinical status gradually improved, he was weaned off the IMV and extubated. The patient's clinical condition remained stable thereafter; however, consecutive chest CT scans revealed progressive increase in size and number of lung cysts

Abbreviations: ABP, autologous blood pleurodesis; AKI, acute kidney injury; APF, alveolopleural fistula; ARDS, acute respiratory distress syndrome; BPF, bronchopleural fistula; COVID-19, coronavirus infections 2019; CT, computed tomography; DEX, dexamethasone; DIC, disseminated intravascular coagulation; EWS, endobronchial Watanabe spigot; HFNC, high-flow nasal cannula; IMV, invasive mechanical ventilation; mAb, monoclonal antibody; NWPT, negative-pressure wound therapy; OWT, open-window thoracostomy; PALs, persistent air leaks; P-SILI, patient self-inflicted lung injury; RDV, remdesivir; RT-PCR, reverse-transcriptase-polymerase chain reaction; SARS-CoV-2, severe acute respiratory syndrome coronavirus type 2; TCZ, tocilizumab; VAC, vacuum-assisted closure.

with a tendency to fuse with each other (Figure 2B). Two days later, the patient presented with dyspnea and severe chest pain. His vital signs were as follows: blood pressure, 90/70 mmHg; heart rate, 124 beats/min; respiratory rate, 38 breaths/min; and oxygen saturation, 83% on ambient air. The breath sounds were significantly diminished on the right side. Chest CT revealed a large right pneumothorax due to collapsed cysts with mediastinal shift, strongly suggestive of tension pneumothorax (Figure 2C). Air leaks had persisted despite two consecutive 20-Fr chest drain insertions (Figure 2D). On day 53, autologous blood pleurodesis (ABP) procedure was performed (100 mL, twice), but PALs were still observed. Moreover, collected material from chest cavity drainage tube was purulent, and CT findings on day 70 of admission were consistent with those of empyema (Figure 3A). On day 76, we attempted to facilitate healing of the PALs by inserting an Endobronchial Watanabe Spigot (EWS), a type of silicone bronchial blocker. Leak isolation performed *via* sequential balloon occlusion of the segmental bronchus using a bronchoscope revealed that the main source of the PALs was located in the right B8b segment, which was confirmed by an immediate reduction in air leaks on deploying a medium-sized EWS (Novatech, La Ciotat, France), and the procedure was completed (Figure 3B). Although air leaks recurred after an hour, bronchoscopy did not show any displacement of the implanted EWS, suggesting that the PALs were presumably due to myriad alveolopleural fistulas (APFs). Subsequent thoracoscopy revealed that the empyema cavity was too narrow for thoracoscopic manipulation. Therefore, minimally invasive open-window thoracostomy (OWT) using a wound edge protector was performed to eliminate PALs (Figure 3C and Supplementary Figure 1A). The incision length was 7 cm and surgical time was 105 min. Nine days after a dressing change, we clinically confirmed the cessation of air leaks. On day 90, negative-pressure wound therapy (NPWT) with a vacuum-assisted closure (VAC) device (KCI Medical Products, Winborne, Dorset, United Kingdom) was performed (Figure 3D). The pleural cavity was filled with GranuFoam (VAC Granufoam; KCI Medical, San Antonio, TX, United States), and covered with semipermeable films. Continuous suction was initially started at a negative pressure of 50 mmHg, and then maintained at a maximum negative pressure of 125 mmHg, alongside careful monitoring of the lung tissue damage. The dressings were changed twice per week. The patient well-tolerated these serial procedures, and experienced relief from dyspnea. NPWT for 28 days allowed re-expansion of the collapsed lung and enhanced wound granulation, resulting in closure of the thoracic cavity without the need for muscular flaps (Figures 3E,F and Supplementary Figures 1B-E). The postoperative course was uneventful. However, on day 110, the patient developed an extrapulmonary complication of a subcortical hemorrhage of the right parietal lobe, for which endoscopic hematoma evacuation was performed on day 125. Eventually, the patient was transferred to another hospital for further rehabilitation on day 158. At the 1-year follow-up, no recurrence of pneumothorax was observed. We present a timeline of the case in Figure 4.

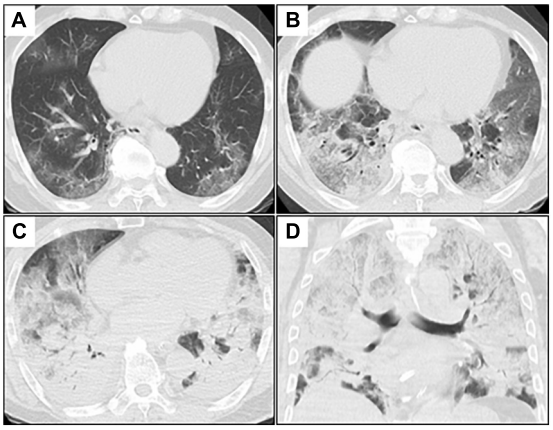

FIGURE 1
Serial chest CT images after admission. **(A–C)**, axial images; **(D)**, coronal image. **(A)** Initial chest CT shows patchy GGOs in bilateral peripheral lungs. **(B)** Chest CT on day 3 (day 3 of admission) shows extensive and diffuse GGOs with patchy consolidation. **(C,D)** Chest CT on day 7 shows diffuse consolidations worsening from GGOs with air bronchogram in both the lungs. CT, computed tomography; GGOs, ground-glass opacities.

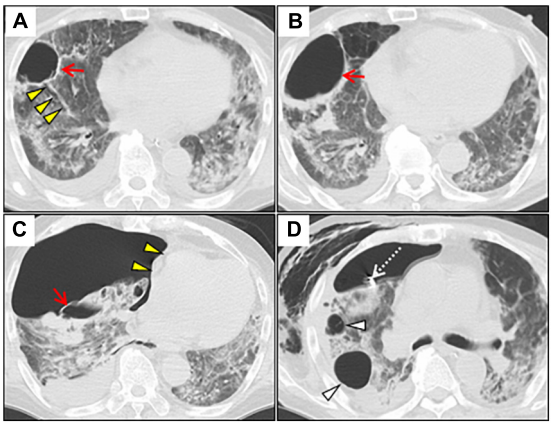

FIGURE 2
Serial chest CT images after induction of the invasive mechanical ventilation. **(A)** Axial chest CT on day 22 shows a lung cyst formation (red arrow) at the right S8 segment. Note the segmental bronchus connecting to the lung cyst (yellow arrowheads). **(B)** Chest CT on day 41 shows the gradually expanded cyst with air-fluid level, and wall thickening secondary to lung suppuration (red arrow). **(C)** Chest CT on day 43 shows a huge right-sided pneumothorax with mediastinal shift (yellow arrowheads). Note the collapsed cyst in the right segment 8 (red arrow). **(D)** Chest CT on day 51 shows residual air leaks after chest tube drainage (white dotted arrow), extending massive subcutaneous emphysema, and further enlargement of other lung cysts (white arrowheads). CT, computed tomography.

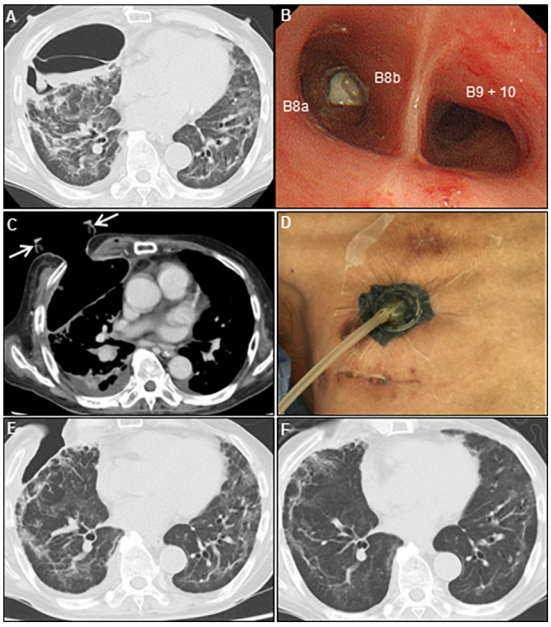

FIGURE 3
Multidisciplinary approach for persistent air leaks. **(A)** Chest CT on day 70 shows empyema and dense pleural thickening with air-fluid level. **(B)** Bronchoscope shows an endobronchial valve deployment inserted into the right B8b segment. **(C)** Post-minimally invasive OWT using a wound retractor (white arrows). **(D)** VAC system. Chest CT on day 97 **(E)** and 143 **(F)** show re-expansion of the collapsed lung parenchyma, and a repair of the chest wall after VAC therapy. CT, computed tomography; OWT, open-window thoracostomy; VAC, vacuum-assisted closure.

Discussion

The association between COVID-19 pneumonia and pneumothorax development has received increasing attention in the recent years. Previous retrospective and observational studies have shown that the incidence of pneumothorax is 1% in patients with COVID-19 pneumonia who need hospitalization, 2% in those who need intensive care treatment, and 5.9–15% in those receiving IMV (3–5). In a recent retrospective review examining 1,595 patients with COVID-19, pneumothorax occurred in 7% of patients, among whom IMV-related pneumothorax was diagnosed in 80% (1). Another retrospective study that examined 601 patients with COVID-19 pneumonia requiring IMV also supported the above epidemiological findings (4). Among patients requiring IMV, the frequency of barotrauma in the group with COVID-19 pneumonia was significantly higher than in the non-COVID-19 group (15 vs. 0.5%, $p < 0.001$), and in those with ARDS prior to the COVID-19 pandemic (15 vs. 10%, $p < 0.001$). Interestingly, pneumothorax occurs spontaneously in patients with COVID-19 pneumonia even in the absence of pre-existing lung disease or the need for IMV (6). Approximately 20% of patients with COVID-19 develop ARDS, which requires IMV (1). Given the high incidence rate of pneumothorax complicated by COVID-19-related ARDS, early detection and management of COVID-19-related pneumothorax is essential. While most cases of COVID-19-related pneumothorax resolve spontaneously or require chest tube drainage (1), some cases of refractory pneumothorax with PALs, secondary to COVID-19, eventually required thoracic surgery (7–9). However, COVID-19-related PALs pose diagnostic and therapeutic challenges.

Here, we described a refractory case of delayed tension pneumothorax in a patient with COVID-19-related PALs, that developed after IMV treatment for ARDS. This case provides the following two instructive clinical lessons.

Firstly, OWT-VAC therapy helped successfully control thoracic empyema with COVID-19-related PALs in our case.

A retrospective single-center study reported the details of the management and outcomes of COVID-19 complicated by pneumothorax (1). Patients having COVID-19 combined with pneumothorax were significantly associated with higher rates of in-hospital mortality than those without pneumothorax (58 vs. 13%, $p < 0.001$). Most patients having COVID-19 combined with pneumothorax (78%) required chest tube thoracostomy drainage for a median of 15 days (range, 2–86 days) with a median of one chest tube (range, 1–5 tubes). Large-bore chest tubes ($\geq$ 20 F) were recommended over small-bore chest tubes ($\leq$ 14 F) due to fewer tube-related complications. Approximately 5% of patients with pneumothorax ultimately required surgical intervention for PALs following tube thoracostomy drainage for a median of 47 days. PAL, defined as an air leak lasting for more than 5 days, can be caused by APF, BPF, or both. Although no solid guidelines exist for the management of COVID-19-related PALs, varied approaches have been documented in limited case reports and series. The surgical intervention techniques can be classified into two types depending on whether air leaks are identified. In cases of COVID-19 combined with refractory pneumothorax where air leaks can be identified anatomically, successful salvage lobectomy, surgical stapling, surgical resection of pneumatoceles, and thoracoscopic resection of blebs have been successfully performed to control PALs (1, 7–9). For patients with contraindications for surgery (advanced cancer, hemodynamic instability, severe hypoxemia, or very poor performance status), less invasive bronchoscopic interventions, such as use of endotracheal valves to seal BPFs or APFs, are indicated (10). Besides, a unique approach using endobronchial stents combined with occlusive materials for BPF closure has been reported. A combination of EWS with n-butyl-2-cyanoacrylate was successfully used to treat COVID-19-related BPFs in both elderly patients with a poor general condition complicated by multiple respiratory infections and middle-aged patients with alcoholic liver disease presenting with respiratory failure (11). In cases of COVID-19 with

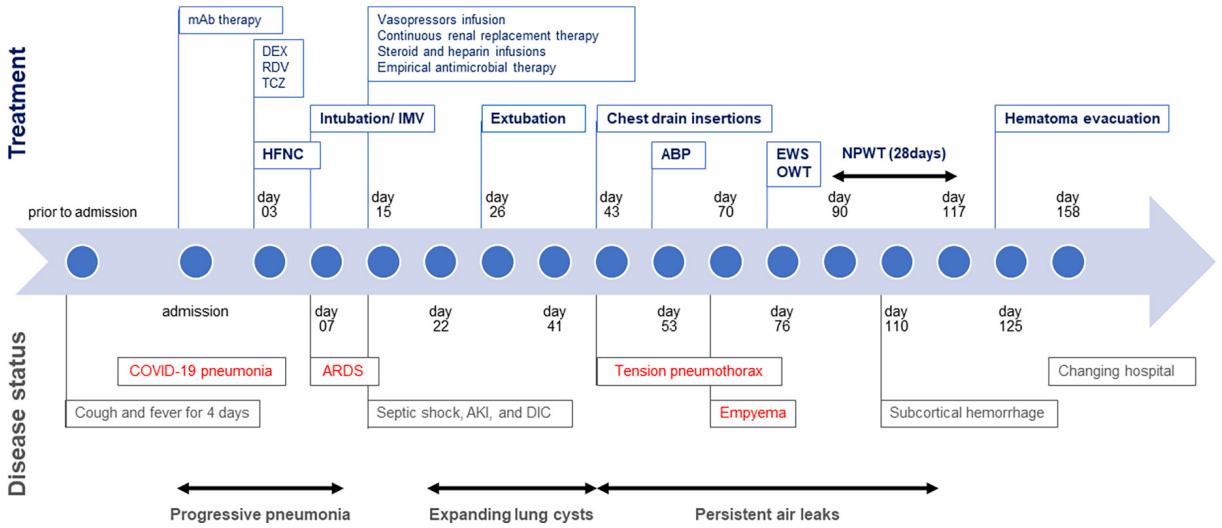

FIGURE 4
Timeline of case presentation.

refractory pneumothorax where anatomical identification of air leaks is not possible, ABP is a non-surgical alternative to control COVID-19-related PALs. ABP is reportedly effective for the treatment of persistent pneumothorax with PALs in elderly patients with COVID-19 at high risk for surgery and anesthesia (12). ABP is a preferred, safe, and simple procedure for controlling PALs, with an overall success rate of approximately 92% (13). The proposed mode of action includes direct sealing of air leaks and induction of pleural inflammation, resulting in subsequent pleurodesis. However, serious complications, including tension pneumothorax caused by chest tube obstruction or empyema, may occur in $< 10\%$ of the cases (14).

In our case, adequate chest tube drainage and ABP failed to control COVID-19-related PALs, which were complicated by empyema, presumably due to procedure-related contamination or prolonged chest tube placement. Considering that the PALs persisted after endobronchial blockade in this case, the presence of residual APFs was strongly suspected. Therefore, we switched to OWT-VAC therapy, which is an ideal treatment option for empyema, eventually leading to a successful control of PALs. While conventional OWT, being minimally invasive, and allowing the direct drainage of empyema through the chest wall, effectively resolves the infections, the procedure requires resection of the ribs and intercostal muscles to permit repeated drainage and dressing of the cavity (15). Therefore, a delay in thoracostomy closure remains a concern, and a few cases warrant additional surgery. However, when combined with a VAC device, NPWT can facilitate drainage of the empyema and thoracic cavity closure, thereby shortening the length of hospital stay. NPWT is preferred over conventional therapies, owing to its advantage of faster wound healing. The following potentially beneficial effects have been considered (16): (1) a decrease in bacterial colonization of the affected tissue owing to increased clearance of infections and waste products; (2) increased circulation and oxygenation in damaged tissues owing to enhanced rapid angiogenesis; (3) reduction in interstitial edema; and (4) promotion of wound granulation, thus facilitating flap survival. Recently, NPWT has been extended to thoracic surgery. A cohort study that examined 19 patients with recurrent empyema revealed that NPWT more effectively reduced the empyema cavity, with the concurrent re-expansion of the residual lung tissue, leading to an early cure (17): The average duration of the OWT for patients undergoing VAC treatment ($n = 11$) was 39 ± 17 days versus 933 ± 1422 days for those not receiving VAC treatment ($n = 8$). Theoretically, NPWT carries the risk of aggravating BPFs and causing excessive negative-pressure-induced organ damage through the fistula, and hence, should be avoided. However, in patients with small-sized BPFs of ≤ 1 mm, NPWT is considered safe and effective for both empyema and BPF closure, under a negative pressure of 125 mmHg or less (18), by maximizing blood flow and not causing tissue damage, as proven in animal studies (19). Similarly, NPWT was safely performed in our patient with PALs caused by APFs. In addition, minimally invasive OWT using a wound retractor (XS size; Applied Medical, Rancho Santa Margarita, CA, United States) allowed minimal stoma and rib resection, maintained wound patency, and permitted daily dressing changes (20). Moreover, the combination with the VAC device induced re-expansion of the residual lung tissue and contributed to the closure of the APFs by presumably contacting the chest wall and adjacent lung lobes, thus controlling PALs. Therefore, this case highlights the potential

of OWT-VAC therapy as a promising therapeutic alternative to control COVID-19-related PALs, refractory to multiple surgical interventions.

This approach has the following four possible limitations. First, as described above, NPWT is originally not indicated for treating BPFs due to the risk of negative pressure-related organ damage through the fistula (17). However, several successful cases of BPF with NPWT have been reported: NPWT performed at a negative pressure of 75–125 mmHg was effective for a 1-mm BPF but not for an 8-mm BPF (18). Therefore, in cases of large BPFs, the fistula should be controlled by either bronchoscopic or surgical interventions before NPWT. Second, for patients with poor performance status and long-term hospitalization, OWT with rib resection may have further reduced the activities of daily living due to pain. Third, there may be a residual risk of uncontrollable APFs even after OWT-VAC therapy as it does not involve radical closure of APFs. A final limitation is that additional invasive thoracoplasty may be necessary to reduce the thoracic cavity volume in case of residual free space in the thoracic cavity even after the thoracic empyema has healed. Therefore, further investigation of the efficacy of OWT-VAC therapy in refractory pneumothorax with PALs is warranted.

Secondly, serial CT monitoring facilitated the detection of pneumothorax secondary to COVID-19-related ARDS and for understanding its pathogenesis in our case.

The pathogenesis of COVID-19-related pneumothorax remains poorly understood and is considered multifactorial. It involves barotrauma, a type of ventilator-induced lung injury (21), and radiological cystic features of the lungs, which may be attributable to adverse lung processes caused by severe SARS-CoV-2 infection (22). However, the latter remains controversial due to the spontaneous resolution of cystic features in some cases while pneumothorax may occur, without accompanying cystic changes (12, 23). In addition, a patient's self-inflicted lung injury (P-SILI) or steroids can influence pneumothorax development (24, 25). Considering that the lung cysts that developed during IMV rapidly expanded after extubation and consequently ruptured, it is highly likely that lung cysts with barotrauma-induced APFs maintained their sizes during IMV, under a lung-protective strategy. However, after IMV, they acutely progressed to rupture owing to P-SILI, which increased the volume and negative intrathoracic pressure during spontaneous single-lung ventilation, resulting in a delayed pneumothorax in this case. In addition, prolonged steroid treatment may have contributed to the lung fragility, rendering them prone to cystic degeneration. A systematic review of air leaks in COVID-19 patients showed that the average time from symptom onset to diagnosis of pneumothorax was 11.63 days (range, 1–30 days), except for a single patient (26) who developed pneumothorax after 56 days. Furthermore, several cases of recently resolved COVID-19 pneumonia have been reported for readmission with tension pneumothorax, approximately 3 weeks after symptom onset (27, 28). Our patient developed delayed tension pneumothorax 47 days after symptom onset, and 15 days after IMV withdrawal, which is the second latest manifestation of COVID-19, and rare to the best of our knowledge. Therefore, this case illustrates the significance of considering tension pneumothorax in patients showing rapid hemodynamic instability despite the resolution of COVID-19-related ARDS.

In conclusion, we reported a case of COVID-19-related PALs with delayed tension pneumothorax after IMV for ARDS. The PALs caused by APFs were refractory to multiple surgical interventions and complicated by empyema, which was eventually cured with minimally invasive OWT-VAC treatment. To the best of our knowledge, this is the first case report to describe this unique technique. Further evidence is warranted to validate OWT-VAC therapy for empyema with COVID-19-related PALs. Clinicians should be fully aware of the possibility of serious sequelae of pneumothorax in COVID-19 patients, even after associated ARDS resolution. Close CT monitoring in severe cases of COVID-19 pneumonia can be beneficial, and lung cysts should be monitored carefully for its susceptibility to secondary pneumothorax.

Data availability statement

The original contributions presented in this study are included in the article/**Supplementary material**, further inquiries can be directed to the corresponding author.

Ethics statement

A written consent was obtained from the patient. Furthermore, the authorization for waiver of consent was approved by the Institutional Review Board (IRB) of Narita-Tomisato Tokushukai Hospital with the permission of the director, HO. All images in the current case are entirely unidentifiable, and patient anonymity is completely preserved. The head of the IRB was responsible for anonymizing the patient.

Author contributions

HY was responsible for the clinical study design and conceptualization of the study. KK, TN, TM, TS, HM, and HO were involved in the acquisition of clinical data. HY, TN, and JI analyzed and interpreted the data. HY and JI drafted the manuscript. All authors discussed, read, and approved the submission of this manuscript for publication.

Conflict of interest

The authors declare that the research was conducted in the absence of any commercial or financial relationships that could be construed as a potential conflict of interest.

Publisher's note

All claims expressed in this article are solely those of the authors and do not necessarily represent those of their affiliated organizations, or those of the publisher, the editors and the reviewers. Any product that may be evaluated in this article, or claim that may be made by its manufacturer, is not guaranteed or endorsed by the publisher.

Supplementary material

The Supplementary Material for this article can be found online at: https://www.frontiersin.org/articles/10.3389/fmed.2022.970239/full#supplementary-material

References

1. Geraci TC, Williams D, Chen S, Grossi E, Chang S, Cerfolio RJ, et al. Incidence, management, and outcomes of patients with COVID-19 and pneumothorax. *Ann Thorac Surg.* (2021) 114:401–7. doi: 10.1016/j.athoracsur.2021.07.097

2. Torosyan Y, Hu Y, Hoffman S, Luo Q, Carleton B, Marinac-Dabic D. An in silico framework for integrating epidemiologic and genetic evidence with health care applications: ventilation-related pneumothorax as a case illustration. *J Am Med Inform Assoc.* (2016) 23:711–20. doi: 10.1093/jamia/ocw031

3. Martinelli AW, Ingle T, Newman J, Nadeem I, Jackson K, Lane ND, et al. COVID-19 and pneumothorax: a multicentre retrospective case series. *Eur Respir J.* (2020) 56:2002697. doi: 10.1183/13993003.02697-2020

4. McGuinness G, Zhan C, Rosenberg N, Azour L, Wickstrom M, Mason DM, et al. Increased incidence of barotrauma in patients with COVID-19 on invasive mechanical ventilation. *Radiology.* (2020) 297:E252–62. doi: 10.1148/radiol.2020202352

5. Yao W, Wang T, Jiang B, Gao F, Wang L, Zheng H, et al. Emergency tracheal intubation in 202 patients with COVID-19 in Wuhan, China: lessons learnt and international expert recommendations. *Br J Anaesth.* (2020) 125:e28–37. doi: 10.1016/j.bja.2020.03.026

6. Agrafiotis AC, Rummens P, Lardinois I. Pneumothorax in otherwise healthy non-intubated patients suffering from COVID-19 pneumonia: a systematic review. *J Thorac Dis.* (2021) 13:4519–29. doi: 10.21037/jtd-21-208

7. Geraci TC, Narula N, Smith DE, Moreira AL, Kon ZN, Chang SH. Lobectomy for hemorrhagic lobar infarction in a patient with COVID-19. *Ann Thorac Surg.* (2021) 111:e183–4. doi: 10.1016/j.athoracsur.2020.08.003

8. Castiglioni M, Pelosi G, Meroni A, Tagliabue M, Uslenghi E, Salaris D, et al. Surgical resections of superinfected pneumatoceles in a COVID-19 patient. *Ann Thorac Surg.* (2021) 111:e23–5. doi: 10.1016/j.athoracsur.2020.06.008

9. Aiolfi A, Biraghi T, Montisci A, Bonitta G, Micheletto G, Donatelli F, et al. Management of persistent pneumothorax with thoracoscopy and bleb resection in COVID-19 patients. *Ann Thorac Surg.* (2020) 110:e413–5. doi: 10.1016/j.athoracsur.2020.04.011

10. Talon A, Arif MZ, Mohamed H, Khokar A, Saeed AI. Bronchopleural fistula as a complication in a COVID-19 patient managed with endobronchial valves. *J Investig Med High Impact Case Rep.* (2021) 9:23247096211013215. doi: 10.1177/23247096211013215

11. Morita C, Kitamura A, Okafuji K, Ro S, Imai R, Shirasaki K, et al. Combined treatment with endobronchial Watanabe spigot and *N*-butyl-2-cyanoacrylate for refractory pneumothorax in COVID-19. *Respirol Case Rep.* (2022) 10:e0923. doi: 10.1002/rcr2.923

12. S Rashid Ali MR. The first reported use of autologous blood pleurodesis for treatment of prolonged air leak in COVID-19-related spontaneous pneumomediastinum and pneumothorax: a case report. *Respirol Case Rep.* (2021) 9:e0840. doi: 10.1002/rcr2.840

13. Chambers A, Routledge T, Billè A, Scarci M. Is blood pleurodesis effective for determining the cessation of persistent air leak?. *Interact Cardiovasc Thorac Surg.* (2010) 11:468–72. doi: 10.1510/icvts.2010.234559

14. Manley K, Coonar A, Wells F, Scarci M. Blood patch for persistent air leak: a review of the current literature. *Curr Opin Pulm Med.* (2012) 18:333–8. doi: 10.1097/MCP.0b013e32835358ca

15. Smolle-Jüttner F, Beuster W, Pinter H, Pierer G, Pongratz M, Friehs G. Open-window thoracostomy in pleural empyema. *Eur J Cardiothorac Surg.* (1992) 6:635–8. doi: 10.1016/1010-7940(92)90186-2

16. Sinha K, Chauhan VD, Maheshwari R, Chauhan N, Rajan M, Agrawal A. Vacuum assisted closure therapy versus standard wound therapy for open musculoskeletal injuries. *Adv Orthop.* (2013) 2013:245940. doi: 10.1155/2013/245940

17. Palmen M, van Breugel HN, Geskes GG, van Belle A, Swennen JM, Drijkoningen AH, et al. Open window thoracostomy treatment of empyema is accelerated by vacuum-assisted closure. *Ann Thorac Surg.* (2009) 88:1131–6. doi: 10.1016/j.athoracsur.2009.06.030

18. Sziklavari Z, Grosser C, Neu R, Schemm R, Kortner A, Szöke T, et al. Complex pleural empyema can be safely treated with vacuum-assisted closure. *J Cardiothorac Surg.* (2011) 6:130. doi: 10.1186/1749-8090-6-130

19. Morykwas MJ, Argenta LC, Shelton-Brown EI, McGuirt W. Vacuum-assisted closure: a new method for wound control and treatment: animal studies and basic foundation. *Ann Plast Surg.* (1997) 38:553–62. doi: 10.1097/00000637-199706000-00001

20. Shimizu K, Ohtaki Y, Nakazawa S, Obayashi K, Nagashima T, Yajima T, et al. Minimally invasive open-window thoracostomy using wound edge protectors. *Ann Thorac Surg.* (2019) 107:e371–3. doi: 10.1016/j.athoracsur.2018.10.064

21. Gajic O, Dara SI, Mendez JL, Adesanya AO, Festic E, Caples SM, et al. Ventilator-associated lung injury in patients without acute lung injury at the onset of mechanical ventilation. *Crit Care Med.* (2004) 32:1817–24. doi: 10.1097/01.ccm.0000133019.52531.30

22. Shi H, Han X, Jiang N, Cao Y, Alwalid O, Gu J, et al. Radiological findings from 81 patients with COVID-19 pneumonia in Wuhan, China: a descriptive study. *Lancet Infect Dis.* (2020) 20:425–34. doi: 10.1016/S1473-3099(20)30086-4

23. Kunadharaju R, Monegro A. COVID-19 presenting as pneumatoceles and spontaneous cavitary lesion as a late complication. *BMJ Case Rep.* (2021) 14:e246516. doi: 10.1136/bcr-2021-246516

24. Gattioni L, Chiumello D, Caironi P, Busana M, Romitti F, Brazzi L, et al. COVID-19 pneumonia: different respiratory treatments for different phenotypes?. *Intensive Care Med.* (2020) 46:1099–102. doi: 10.1007/s00134-020-06033-2

25. Palumbo D, Campochiaro C, Belletti A, Marinosci A, Dagna L, Zangrillo A, et al. COVID-BioB study group. Pneumothorax/pneumomediastinum in non-intubated COVID-19 patients: differences between first and second Italian pandemic wave. *Eur J Intern Med.* (2021) 88:144–6. doi: 10.1016/j.ejim.2021.03.018

26. Singh A, Singh Y, Pangasa N, Khanna P, Trikha A. Risk factors, clinical characteristics, and outcome of air leak syndrome in COVID-19: a systematic review. *Indian J Crit Care Med.* (2021) 25:1434–45. doi: 10.5005/jp-journals-10071-24053

27. Vahidirad A, Jangjoo A, Ghelichli M, Arian Nia A, Zandbaf T. Tension pneumothorax in patient with COVID-19 infection. *Radiol Case Rep.* (2021) 16:358–60. doi: 10.1016/j.radcr.2020.11.044

28. Tirimanna R, Myerson J, Okorie M, Dorman E. Diagnosis of spontaneous secondary tension pneumothorax following apparent recovery from coronavirus disease 2019 pneumonitis: a case report. *J Med Case Rep.* (2022) 16:88. doi: 10.1186/s13256-022-03313-x

frontiers | Frontiers in Medicine

TYPE Case Report
PUBLISHED 26 September 2022
DOI 10.3389/fmed.2022.955955

OPEN ACCESS

EDITED BY
Yuetian Yu,
Shanghai Jiao Tong University, China

REVIEWED BY
Patrick Jon Biggs,
Massey University, New Zealand
Chaitanya Tellapragada,
Karolinska Institutet (KI), Sweden

*CORRESPONDENCE
Jin-Min Peng
pjm731@hotmail.com

†These authors have contributed equally to this work

SPECIALTY SECTION
This article was submitted to Intensive Care Medicine and Anesthesiology, a section of the journal Frontiers in Medicine

RECEIVED 29 May 2022
ACCEPTED 09 September 2022
PUBLISHED 26 September 2022

CITATION
Li S, Jiang W, Wang C-Y, Weng L, Du B and Peng J-M (2022) A case of disseminated Legionnaires' disease: The value of metagenome next-generation sequencing in the diagnosis of Legionnaires. *Front. Med.* 9:955955. doi: 10.3389/fmed.2022.955955

A case of disseminated Legionnaires' disease: The value of metagenome next-generation sequencing in the diagnosis of Legionnaires

Shan Li†, Wei Jiang†, Chun-Yao Wang, Li Weng, Bin Du and Jin-Min Peng*

Medical Intensive Care Unit, Peking Union Medical College Hospital, Chinese Academy of Medical Sciences, Beijing, China

Background: *Legionella* rarely causes hospital-acquired pneumonia (HAP), although it is one of the most common pathogens of community-acquired pneumonia. Hospital-acquired Legionnaires' disease, mainly occurring in immunocompromised patients, is often delayed in diagnosis with high mortality. The use of the metagenome Next-Generation Sequencing (mNGS) method, which is fast and unbiased, allows for the early detection and identification of microorganisms using a culture-independent strategy.

Case report: A 52-year-old male, with a past medical history of Goods syndrome, was admitted due to nephrotic syndrome. The patient developed severe pneumonia, rhabdomyolysis, and soft tissue infection after receiving immunosuppressive therapy. He did not respond well to empiric antibiotics and was eventually transferred to the medical intensive care unit because of an acute respiratory failure and septic shock. The patient then underwent a comprehensive conventional microbiological screening in bronchoalveolar lavage fluid (BALF) and blood, and the results were all negative. As a last resort, mNGS of blood was performed. Extracellular cell-free and intracellular DNA fragments of *Legionella* were detected in plasma and blood cell layer by mNGS, respectively. Subsequent positive results of polymerase chain reaction for *Legionella* in BALF and soft tissue specimens confirmed the diagnosis of disseminated Legionnaires' disease involving the lungs, soft tissue, and blood stream. The patient's condition improved promptly after a combination therapy of azithromycin and moxifloxacin. He was soon extubated and discharged from ICU with good recovery.

Conclusion: Early recognition and diagnosis of disseminated Legionnaires' disease is challenging. The emergence and innovation of mNGS of blood has the potential to address this difficult clinical issue.

KEYWORDS

disseminated Legionnaires' disease, metagenome next-generation sequencing, hospital-acquired pneumonia, immunocompromised adult, blood

Background

Legionella are recognized as a common cause of community-acquired pneumonia, while a rare pathogen of hospital-acquired pneumonia (HAP). Old age, underlying debilitating conditions, and immunocompromised status are risk factors for Legionnaires' disease. *Legionella* species are best known for causing pneumonia and can also cause a wide range of extra-pulmonary manifestations, which is known as disseminated Legionnaires' disease (DLD). Life-threatening multiple organ dysfunction can occur in severe cases (1). The diagnosis of DLD can be challenging due to the rarity of the infection and the fastidious growth in unbiased-culture based testing (2). Metagenomic next-generation sequencing (mNGS) is a nucleic acid sequencing technique with high-throughput capacity for the detection of pathogens in a single assay. A chief advantage of mNGS is unbiased sampling, which enables broad identification of known as well as unexpected pathogens or even the discovery of new organisms (3). Here, we present a case of disseminated Legionnaires' disease in a patient with immunodeficiency disease and treated with immunosuppressive therapy, whose conventional microbiologic testing were all negative and finally achieved the correct diagnosis by mNGS of blood. This is the first case of DLD diagnosed by mNGS to our knowledge. This case warrants the attention of Legionnaires' disease in hospitalized patients and highlights the value of mNGS technology in diagnosing the disease.

Case report

A 52-year-old male was admitted to the department of nephrology in our hospital presenting with edema of the eyelids and bilateral lower extremities for 1 month. Laboratory findings upon admission revealed a large amount of proteinuria, hypoalbuminemia, and hyperlipidemia, which suggested the diagnosis of nephrotic syndrome. The patient then received oral methylprednisolone 60 mg daily. Meanwhile, he was diagnosed with Good's syndrome for concurrent thymoma and significant hypogammaglobulinemia. Two weeks later, the patient developed high fever, productive cough with non-purulent sputum. Pneumonia was confirmed by chest CT, and he received empirical ceftazidime, imipenem, and intravenous immunoglobulin without good clinical response. He also complained of myalgia and muscle swelling in his left lower extremity. Twenty-two days after admission, the patient was transferred into the medical intensive care unit (MICU) because of the aggravating respiratory failure. The patient was a non-smoker and had no history of diabetes or alcoholism. He did not recall any exposure to potentially contaminated water or animals.

On admission to MICU (day 0), he was drowsy and distressful. His vital signs were as follows: body temperature 38.0°C, pulse rate 125 beats/min, respiratory rate 38 breaths/min, blood pressure 116/74 mmHg, and pulse oxygen saturation 97% with a non-rebreather mask. Diminished breath sounds in the right lower lung were heard on auscultation. There was no audible cardiac murmur. His abdomen was soft and non-tender without hepatosplenomegaly. Shifting dullness was positive, along with moderate pitting edema of the limbs and lumbosacral area. The skin over his left calf was congestive and swollen with tenderness (**Figure 1A**). Laboratory findings upon admission revealed a white blood cell count of 2.67×10^9/L with an elevated neutrophil ratio of 96.3%, hemoglobin of 120 g/L, and platelet count of 62×10^9/L. The serum biochemistry panel was remarkable for striking elevation of muscle enzyme spectrum on MICU day 0, including creatine kinase increased from 10,759 to 13,514 U/L, myoglobin from 2,820 to 93,484 μg/L, alanine aminotransferase 131 U/L, aspartate aminotransferase 254 U/L and lactic dehydrogenase 1,489 U/L. The serum creatinine was 226 μmol/L with hyperkalemia. The concentration of C-reactive protein and procalcitonin was 271.33 and 100 ng/mL. Cytomegalovirus (CMV) DNA in peripheral blood was 300,000 copies/ml detected by polymerase reaction (PCR). Chest CT revealed patchy shadows and consolidations in both lungs and pleural effusion bilaterally. Presumed abscess in the right lower lobe and cavitation in the left upper lobe were noted as well (**Figure 2**).

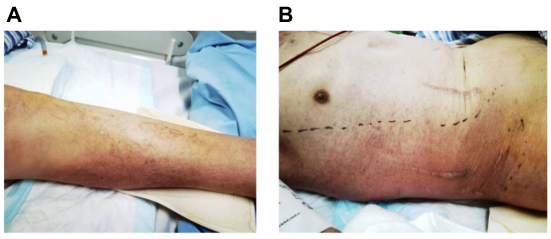

FIGURE 1
Skin congestion and swelling on the left calf **(A)** on admission, and right chest wall **(B)** 5 days after admission.

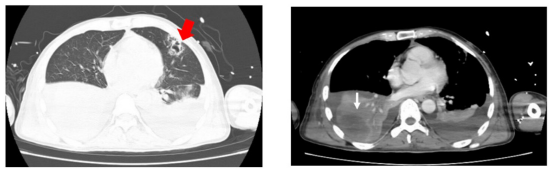

FIGURE 2
Chest CT on admission revealed patchy shadows and consolidations in both lungs and pleural effusion bilaterally. Presumed abscess in the right lower lobe (white fine arrow) and cavitation in the left upper lobe (red thick arrow) were noted.

After MICU admission, intravenous vancomycin and ganciclovir were added for the presumed skin and soft tissue infections and cytomegalovirus viremia, respectively. However, the patient's condition kept deteriorating with persistent fever, skin lesion expanding (**Figure 1B**), rhabdomyolysis and subsequently acute respiratory distress syndrome. The patient was intubated and on invasive mechanical ventilation on MICU day 1, and continuous renal replacement therapy was initiated on MICU day 2.

Tracheal aspiration was found to be non-purulent after intubation. The patient underwent a standard of care microbiologic diagnostics for bacteria, viruses, and fungi, including staining and culture, multiplex PCR, and serologic testing. Unfortunately, any clinical relevant pathogens were undetected. Although no pathogen was identified through comprehensive conventional microbiologic workup, infection was still highly suspected, and thus, blood and the skin specimen were sent for mNGS assay on MICU day 3. We performed mNGS on the Illumina platform by using DNA extracted from the peripheral blood and the skin specimen. In terms of blood mNGS, nucleic acids were extracted from the plasma and blood cell layer, respectively, corresponding to cell-free DNA (cfDNA) and intracellular DNA (iDNA). The total numbers of sequencing reads were 27 million, 12.5 million, and 51 million sequences for the libraries of mNGS on the plasma, blood cell layer, and skin sample, respectively. PathoXtract Nucleic Acid Kit (*WYXM03001S, Willingmed Corp., Beijing, China*) was used to extract DNA. Sequencing data were processed using Pathogen Identification Sequencing (PIseq) Metagenomic Sequencing Data Management System V2.0 (*Willingmed Corp.*) automatically. The high-quality sequencing data were compared with the human reference genome GRCH37 (hg19) by alignment software to remove the human host sequence and obtain clean data for use in the subsequent identification of pathogenic microorganisms. The clean data were aligned with the established reference database of pathogenic microorganisms to perform the annotation of pathogenic microorganism species, complete the final analysis, and obtain results on microorganism identification. We got the detection report the next day, revealing cell-free DNA (cfDNA) of *Legionella pneumophila* as high as 84,930 reads per Million (RPM) in the plasma layer, and intracellular DNA (iDNA) of the same pathogen as 6,470 RPM in the blood cell layer. mNGS of the skin specimen of left lower limb identified *Legionella pneumophila* with 349 RPM. The test also revealed low to moderate levels of CMV in both plasma and blood cell layer. Meanwhile, low level of *Pseudomonas aeruginosa* was also detected in plasma, which was 30 RPM. Further pertinent investigation revealed positive serum IgM, IgG antibodies of *Legionella*. PCR of *Legionella pneumophila* on BALF was also positive. Specific DNA sequences of *Legionella pneumophila* were identified by PCR in the skin specimen as well. On MICU day 5, azithromycin and moxifloxacin were used instead of imipenem according to the diagnosis of disseminated *Legionella* infection. The patient's fever subsided soon afterward, along with skin alleviation of congestion and tenderness. After another 1 week of treatment, his condition improved dramatically with muscle enzymes dropping into the normal range and with the recovery of renal function. He was extubated on MICU day 9 and was transferred to general ward on MICU day 12 (**Figure 3**). The patient was in good condition during the follow-up. After rehabilitation exercises, the patient could take care of himself, with normal body temperature and no need of any oxygen support before he was discharged from the hospital.

Discussion

We here reported a rare case of hospital-acquired disseminated Legionnaires' disease in an immunocompromised patient, who had a history of Good's syndrome and nephrotic syndrome and received immunosuppressive therapy due to nephrotic syndrome. Clinical and imaging examination demonstrated evidences of severe pneumonia, rhabdomyolysis, and local skin infection. All conventional microbiologic tests were negative, and the causative pathogen (*Legionella pneumophila*) was finally identified by mNGS.

Generally, *Legionella* was not considered on the list of candidate pathogens of HAP, therefore the diagnosis and treatment of hospital-acquired Legionnaires' disease is often delayed. Disseminated Legionnaires' disease is even more difficult to diagnose for its rarity and lack of efficient testing methods. There are some differences between hospital-acquired and community-acquired Legionnaires' disease. Community-acquired Legionnaires' disease is often caused by *Legionella pneumophila* (Lp), which often occurs in people with competent immunity, presenting non-specific clinical manifestations (1). Hospital-acquired Legionnaires' disease is more likely to be caused by other *Legionella* species and often occurs in patients with immunodeficiency (4). Severe cases are more common in hospital acquired cases, with prone pulmonary cavities, extrapulmonary presentations such as skin eruption, myositis, pericarditis, and myocarditis, thus with a higher mortality rate (5, 6). Skin presentations are uncommon in Legionnaires' disease and hard to diagnose, erythema, nodules, and blisters can be seen locally, while skin pathology lacks specificity (2, 7). Dagan et al. found that the mortality of HAP caused by *Legionella* is higher than CAP caused by the same pathogen, which may be attributed to the former's delayed diagnosis and treatment as was also seen in this case (8). In the present case, the nucleic acid of *Legionella* in peripheral blood was firstly detected by mNGS. Thereafter, the detection of nucleic acid of *Legionella* in both BALF and skin by PCR further confirmed the diagnosis. Serum IgM and IgG antibodies of *Legionella* were also positive. The etiologic diagnosis of disseminated Legionnaires'

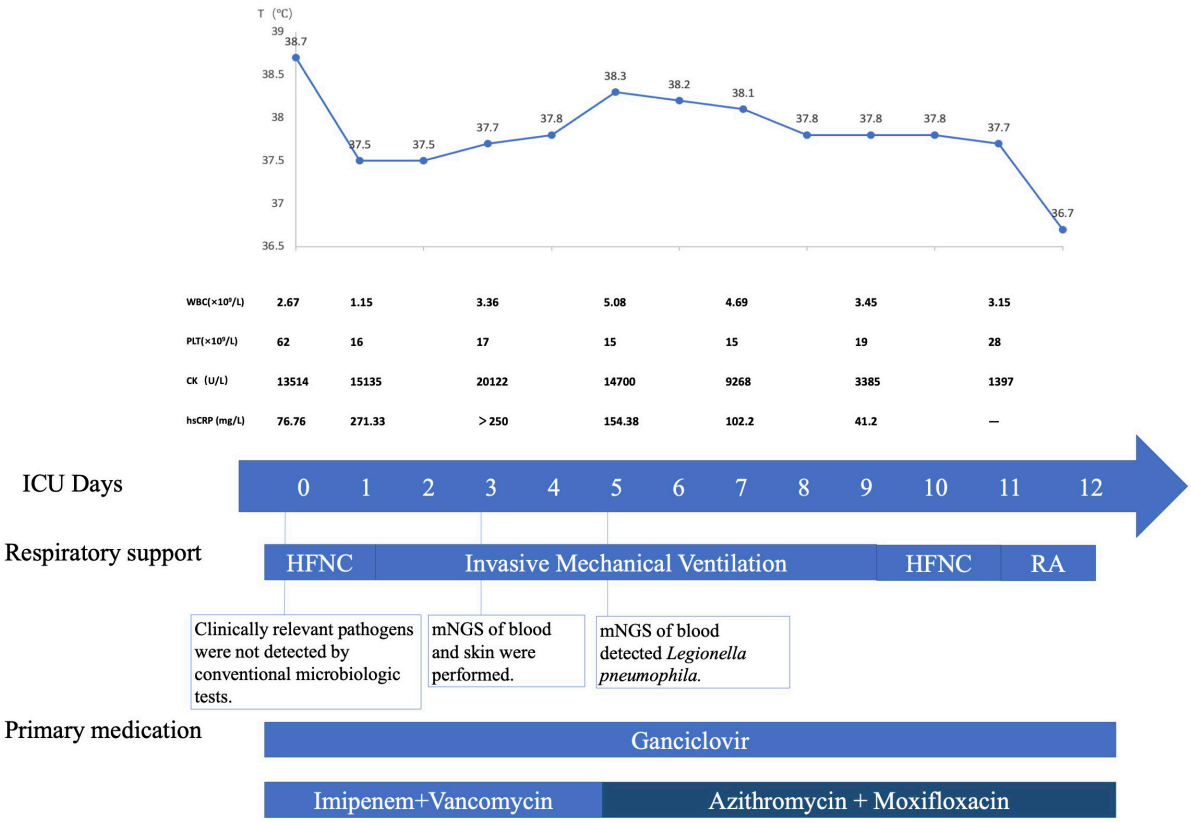

FIGURE 3
Timeline of the patient with disseminated Legionnaires' disease. The patient was transferred into MICU on May 12, 2021, which was ICU Day 0. Major events during the course of the patient's illness are indicated in the graph. The upper graph shows the body-temperature curve (blue line). Laboratory values obtained and primary medications administered during the patient's ICU hospitalization are shown below. HFNC denotes high-flow nasal cannula, MICU medical intensive care unit, RA room air, mNGS metagenome Next-Generation Sequencing.

disease was made according to above clinical data in 5 days. This patient had a significantly large area of consolidation in the right lung combined with rhabdomyolysis and skin lesions in the early stage, which all resolved after azithromycin and moxifloxacin treatments specific to *Legionella*. Early diagnosis played a tremendous role in the successful treatment.

The mNGS results in this case is a turning point in the diagnosis of DLD. mNGS is a nucleic acid sequencing technique with high-throughput capacity and un-biased pathogen detection in a single assay. It has been increasingly applied in kinds of infectious diseases for its ability to discover new or unexpected organisms (3). For suspected pneumonia in critically ill immunocompromised patients, BALF mNGS and conventional microbiological tests had comparable diagnostic accuracy for bacterial and viral infections (9). For septic patients in ICU, plasma mNGS was more sensitive than blood culture in detecting bacterial infections and allowed for simultaneous detection of viral pathogens (10). mNGS show more priority in areas where conventional diagnostic approaches have limitations. At present, missed diagnosis of *Legionella* infection is still common due to limited detection methods such as gram stain and immunofluorescence stain. As for other methods, the urine antigen of *Legionella* is limited to the Lp1 serotype, and it is difficult to make the diagnosis of acute infection based on positive serum antibodies. The blood culture of *Legionella* is not sensitive because strict bacterial growth conditions are needed (1). The emergence of mNGS has the potential to facilitate the early recognition and diagnosis of *Legionella* disease, which is approved again by this case. Fast and unbiased, the technical advantages of mNGS prevent rare but lethal pathogens such as *Legionella* from being omitted in the diagnostic process and thus benefit critically ill patients. In conclusion, mNGS performs well in detecting uncommon, novel, and co-infecting pathogens without the need for *a priori* knowledge, thus providing new diagnostic clues for difficult-to-diagnose infections in critically ill or immunocompromised patients. However, it is worth noting that mNGS has some potential drawbacks and unresolved issues in clinical practice. First, mNGS is not standardized between laboratories, and interlaboratory variability makes results not comparable between laboratories. Secondly, it is challenging to discriminate causative pathogens from others (normal microbes

and environmental contaminants) due to the lack of a unified approach to interpreting the result of mNGS (3). Last, as with all nucleic acid assays, the identification of microbes in mNGS does not directly confirm the presence of viable, live organisms. The clinical significance of organisms should be determined by a combination of the clinical manifestation, conventional testing, and the application of antibiotics.

Nowadays, plasma mNGS assay for identifying microbial cfDNA sequencing to predict bloodstream infection is increasingly used in critical patients. It has many limitations though, such as interference by both human nucleic acid signal and background microbial signals (11, 12). The detection of circulating microbial cfDNA in plasma presents either true bloodstream infection or circulating microbial DNA in the bloodstream derived from other local infection sources. By limiting detection to plasma, intact or intracellular microorganisms might also be missed (13). With the maturation of human-derived host nucleic acid removal technology in peripheral blood samples by PathoXtract Nucleic Acid Kit (*WYXM03001S, Willingmed Corp., Beijing, China*), the derived mNGS technology can detect DNA sequences in both plasma (cfDNA) and blood cells (intracellular DNA, iDNA). The cfDNA contains information about cells that are lysed hours or days previously, while the iDNA essentially indicates the existence of potentially alive or intact bacteria (14). Technically speaking, the detection of microbial iDNA in the blood cell layer might indicate true bloodstream infection, rather than local infection sources. Intracellular pathogens, such as *Legionella* and *Listeria monocytogenes*, can also be detected from microbial iDNA sequencing. *Legionella* sequences were detected in both plasma and blood cell layer in our patient, which suggested that *Legionella* was disseminated by the bloodstream.

Azithromycin, doxycycline, or levofloxacin can be considered as first-line therapy. β-lactams and aminoglycosides are ineffective. The combination of azithromycin and fluoroquinolones has been used in mostly severe unresponsive disease. However, there is no convincing evidence of its effectiveness (1). Early adequate therapy can reduce mortality (15). Immunocompromised patients with Legionnaires' disease are at risk for both severe infection and relapse. In addition, extrapulmonary infections often occur in immunocompromised patients. An extended course for more than 14 days is recommended for patients with immunosuppression. The total course should be adjusted based on clinical response. Because of the risk of relapse, we also consider reducing immunosuppression when possible. If prolonged and high levels of immunosuppression are required, a suppressive course of therapy (e.g., 3–6 months) can be given (16). Our patient received 10 days combination of azithromycin and levofloxacin, reducing to azithromycin alone for 2 months. He responded promptly to treatment and has not relapsed.

Hospital-acquired Legionnaires' disease mainly occurs in immunosuppressed patients, which results in high morbidity and mortality. This unique case indicates that mNGS is a promising unbiased diagnostic technique for early detection of *Legionella* and other unexpected pathogens. Early adequate therapy can improve outcomes of critically ill patients with DLD.

Data availability statement

The raw data supporting the conclusions of this article will be made available by the authors, without undue reservation.

Ethics statement

Written informed consent was obtained from the individual(s) for the publication of any potentially identifiable images or data included in this article.

Author contributions

SL and WJ carried out the literature search and drafted the first draft of the manuscript. LW and C-YW treated the patient and gave advices. J-MP and BD were responsible for designing and revised the draft. All authors read and approved the final manuscript.

Funding

This work was partially supported by the National Key R&D Program of China (2021YFC2500801) and Postdoctoral Science Foundation of China (2020M670006ZX).

Conflict of interest

The authors declare that the research was conducted in the absence of any commercial or financial relationships that could be construed as a potential conflict of interest.

Publisher's note

References

1. Cunha BA, Burillo A, Bouza E. Legionnaires' disease. *Lancet.* (2016) 387:376–85. doi: 10.1016/S0140-6736(15)60078-2

2. Padrnos LJ, Blair JE, Kusne S, DiCaudo DJ, Mikhael JR. Cutaneous legionellosis: case report and review of the medical literature. *Transpl Infect Dis.* (2014) 16:307–14. doi: 10.1111/tid.12201

3. Gu W, Miller S, Chiu CY. Clinical metagenomic next-generation sequencing for pathogen detection. *Annu Rev Pathol.* (2019) 14:319–38. doi: 10.1146/annurev-pathmechdis-012418-012751

4. Chambers ST, Slow S, Scott-Thomas A, Murdoch DR. Legionellosis caused by non-*Legionella pneumophila* species, with a focus on *Legionella longbeachae*. *Microorganisms.* (2021) 9:291. doi: 10.3390/microorganisms9020291

5. Joseph CA, Watson JM, Harrison TG, Bartlett CL. Nosocomial legionnaires' disease in England and Wales, 1980-92. *Epidemiol Infect.* (1994) 112:329–45. doi: 10.1017/s0950268800057745

6. Guy SD, Worth LJ, Thursky KA, Francis PA, Slavin MA. *Legionella pneumophila* lung abscess associated with immune suppression. *Intern Med J.* (2011) 41:715–21. doi: 10.1111/j.1445-5994.2011.02508.x

7. Chitasombat MN, Ratchatanawin N, Visessiri Y. Disseminated extrapulmonary *Legionella pneumophila* infection presenting with panniculitis: case report and literature review. *BMC Infect Dis.* (2018) 18:467. doi: 10.1186/s12879-018-3378-0

8. Dagan A, Epstein D, Mahagneh A, Nashashibi J, Geffen Y, Neuberger A, et al. Community-acquired versus nosocomial *Legionella pneumonia*: factors associated with *Legionella*-related mortality. *Eur J Clin Microbiol Infect Dis.* (2021) 40:1419–26. doi: 10.1007/s10096-021-04172-y

9. Peng JM, Du B, Qin HY, Wang Q, Shi Y. Metagenomic next-generation sequencing for the diagnosis of suspected pneumonia in immunocompromised patients. *J Infect.* (2021) 82:22–7. doi: 10.1016/j.jinf.2021.01.029

10. Jing Q, Leung CHC, Wu AR. Cell-Free DNA as biomarker for sepsis by integration of microbial and host information. *Clin Chem.* (2022) 68:1184–95. doi: 10.1093/clinchem/hvac097

11. Peri AM, Stewart A, Hume A, Irwin A, Harris PNA. New microbiological techniques for the diagnosis of bacterial infections and sepsis in ICU including point of care. *Curr Infect Dis Rep.* (2021) 23:12. doi: 10.1007/s11908-021-00755-0

12. Grumaz S, Grumaz C, Vainshtein Y, Stevens P, Glanz K, Decker SO, et al. Enhanced performance of next-generation sequencing diagnostics compared with standard of care microbiological diagnostics in patients suffering from septic shock. *Crit Care Med.* (2019) 47:e394–402. doi: 10.1097/CCM.0000000000003658

13. Greninger AL, Naccache SN. Metagenomics to assist in the diagnosis of bloodstream infection. *J Appl Lab Med.* (2019) 3:643–53. doi: 10.1373/jalm.2018.026120

14. Nagler M, Podmirseg SM, Mayr M, Ascher-Jenull J, Insam H. The masking effect of extracellular DNA and robustness of intracellular DNA in anaerobic digester NGS studies: a discriminatory study of the total DNA pool. *Mol Ecol.* (2021) 30:438–50. doi: 10.1111/mec.15740

15. Gudiol C, Verdaguer R, Angeles Domínguez M, Fernández-Sevilla A, Carratalà J. Outbreak of Legionnaires' disease in immunosuppressed patients at a cancer centre: usefulness of universal urine antigen testing and early levofloxacin therapy. *Clin Microbiol Infect.* (2007) 13:1125–8. doi: 10.1111/j.1469-0691.2007.01805.x

16. Htwe TH, Khardori NM. Legionnaire's disease and immunosuppressive drugs. *Infect Dis Clin North Am.* (2017) 31:29–42. doi: 10.1016/j.idc.2016.10.003

frontiers | Frontiers in Medicine

TYPE Case Report
PUBLISHED 04 October 2022
DOI 10.3389/fmed.2022.991182

OPEN ACCESS

EDITED BY
Yuetian Yu,
Shanghai Jiao Tong University, China

REVIEWED BY
Chun Pan,
Southeast University, China
Zhongheng Zhang,
Sir Run Run Shaw Hospital, China

*CORRESPONDENCE
Linhao Ma
macro118@139.com

†These authors have contributed equally to this work

SPECIALTY SECTION
This article was submitted to Intensive Care Medicine and Anesthesiology, a section of the journal Frontiers in Medicine

RECEIVED 11 July 2022
ACCEPTED 02 September 2022
PUBLISHED 04 October 2022

CITATION
Zhang B, Duan L, Ma L, Cai Q, Wu H, Chang L, Li W and Lin Z (2022) Rapidly progressive Guillain–Barré syndrome following amitriptyline overdose and severe *Klebsiella pneumoniae* infection: A case report and literature review. *Front. Med.* 9:991182. doi: 10.3389/fmed.2022.991182

Rapidly progressive Guillain–Barré syndrome following amitriptyline overdose and severe *Klebsiella pneumoniae* infection: A case report and literature review

Boyu Zhang[1†], Liwei Duan[2†], Linhao Ma[1*], Qingqing Cai[3], Hao Wu[1], Liang Chang[1], Wenfang Li[1] and Zhaofen Lin[1]

[1]Department of Emergency and Critical Care Medicine, Changzheng Hospital, Naval Medical University, Shanghai, China, [2]Department of Emergency Medicine, Shanghai Fourth People's Hospital Affiliated to Tongji University School of Medicine, Shanghai, China, [3]Genoxor Medical & Science Technology Inc., Shanghai, China

Guillain–Barré syndrome (GBS) is a potentially life-threatening post-infectious autoimmune disease characterized by rapidly progressive symmetrical weakness of the extremities. Herein, we report a case of GBS associated with drug poisoning complicated by *Klebsiella pneumoniae* infection. A 38-year-old woman was admitted to the intensive care unit after taking an overdose of amitriptyline and was later diagnosed with coma, *Klebsiella pneumoniae* infection, and septic shock. Thirteen days after admission, she was diagnosed with GBS based on acute muscle pain, flaccid paralysis, hyporeflexia, reduced amplitude of compound muscle action potential, and albuminocytologic dissociation in the cerebrospinal fluid. GBS rarely occurs after a drug overdose and septic shock, and this is the first report of a rapidly progressive GBS following amitriptyline overdose and severe *Klebsiella pneumoniae* infection.

KEYWORDS

Guillain–Barré syndrome (GBS), *Klebsiella pneumoniae* infection, amitriptyline overdose, bilateral weakness, case report

Introduction

Guillain–Barré syndrome (GBS) is an acute, generalized polyradiculoneuropathy that can cause rapidly progressive flaccid weakness (1). Although its pathogenesis is not fully understood, most experts believe that it might be due to the recognition of antigens in the body by the immune system, which causes the autoimmune cells and antibodies to attack the peripheral nerves and cause peripheral nerve demyelination (2). Herein, we present a case of amitriptyline overdose complicated by *Klebsiella pneumoniae* infection-induced pneumonia and secondary GBS.

Case description

A 38-year-old woman, known to have had depression for over half a year, presented to the emergency department 6 h after taking an overdose of amitriptyline (about 100 tablets). On examination, she had a heart rate of 134 beats/min, a blood pressure of 110/66 mmHg, a respiratory rate of 21 breaths/min, a body temperature of 36.2°C, an oxygen saturation level of 98%, a Glasgow Coma Scale score of five, and a sequential organ failure assessment score of nine. Chest computed tomography (CT) (Figure 1) revealed inflammation in both the lungs, especially in the right lung, which was considered to be due to aspiration pneumonia, local bronchiectasis in the middle lobe of the right lung, and interstitial pulmonary edema in the upper lobe of both lungs. In addition, we were informed that the patient was allergic to penicillin and had no other significant medical or family genetic history.

On admission, the patient was immediately scheduled for emergency treatment. After gastric lavage, endotracheal intubation, and blood pressure control with vasoactive drugs, the patient was admitted to the intensive care unit (ICU). The remaining drugs were removed by hemoperfusion combined with hemofiltration adsorption. Meanwhile, moxifloxacin and biapenem were used to treat the infection and for organ support. After 2 days, the concentration of amitriptyline in the patient's blood decreased significantly (Table 1).

However, 72 h after admission, her body temperature rose to 39.8°C, while her blood pressure and oxygen saturation continued to decline. The invasive hemodynamic assessment was performed by measuring pulse index continuous cardiac output, and the patient was diagnosed with septic shock in addition to amitriptyline overdose. Chest CT (Figure 1) showed progression of pneumonia, and skull CT (Figure 2) showed brain edema due to hypoperfusion. Metagenomic next-generation sequencing (mNGS) of the bronchoscope lavage fluid revealed the abundance of *Klebsiella pneumoniae* sequence, and the pathogen *Klebsiella pneumoniae* was confirmed by quantitative polymerase chain reaction (qPCR) (Figure 3). Imipenem and tigecycline were used as anti-infective agents, considering the possibility of septic shock caused by aspiration pneumonia. At the same time, other symptomatic treatments were administered, such as acid suppression, liver protection, phlegm resolution, white protein supplementation, diuresis, rehydration, and potassium supplementation through micro-pumps, fluid infusion, and nutritional support. On the second day of treatment, the patient showed substantial clinical improvement. The blood gas analysis results were satisfactory after endotracheal intubation was removed, and the patient was transferred out of the ICU after 5 days.

Unfortunately, the patient gradually developed symmetrical limb weakness, which continued to worsen and was primarily diagnosed as ICU-acquired weakness. The patient could neither move her limbs nor eat independently for 4 days despite being transferred out of the ICU. Physical examination showed that the limb muscle strength level was within the range of grade 0–1, muscle tone was decreased, expectoration could not be produced, and sputum was abundant and viscous. Ceftazidime–avibactam sodium was administered as an anti-infective treatment (2.5 g q8h). Cerebrospinal fluid was collected through a lumbar puncture on the fifth day for laboratory examination and diagnosis. The results confirmed protein cell separation; cerebrospinal fluid protein levels were 1,104 mg/L, and cerebrospinal fluid leukocytes were 3×10^6/L. The nerve conduction study test showed severely slowed conduction velocities with disappeared compound motor action potential and absent H-reflexes and F-waves, thus suggesting demyelination of nerves. The antibodies in cerebrospinal fluid against autoimmune peripheral neuropathy and myasthenia gravis were absent. Therefore, these symptoms could not be explained by ICU-acquired weakness and sepsis secondary to multiple myopathies, which have normal findings on the nerve conduction study tests. Based on the results of these tests and consultation with neurology experts, the patient was diagnosed with secondary GBS.

Afterward, human immunoglobulin was administered at 0.4 g/kg body weight/day (daily dose, 20 g; calculated according to her body weight) for 5 days, with close monitoring of the patient's respiratory status and supplementation by symptomatic support treatment. After 5 days, the patient's mental state improved. Her voice was louder, and she could move her fingers and toes slightly. Furthermore, the infection index and chest CT (Figure 1) showed significant clinical improvement. She was subsequently transferred to a rehabilitation hospital for maintenance therapy 2 weeks later. Four weeks after she was discharged, the muscle strength of the distal extremities was within the range of grade 1–2, and the symptoms gradually resolved. The timeline of the patient's clinical course described above is presented in Figure 4.

Discussion

Pathogen infection might be a crucial essential factor causing GBS

Two-thirds of patients with GBS have prior respiratory or gastrointestinal symptoms. Usually, an abnormal autoimmune response is induced in the peripheral nerve and the spinal cord root due to infection or other immune stimulation, which leads to the development of GBS (1, 2). Infection with severe acute respiratory syndrome coronavirus 2 (SARS-CoV-2), *Campylobacter jejuni*, cytomegalovirus, Epstein–Barr virus, *Haemophilus influenzae*, *Mycoplasma pneumoniae*, herpes simplex virus, and *Borrelia burgdorferi* (Lyme disease) are

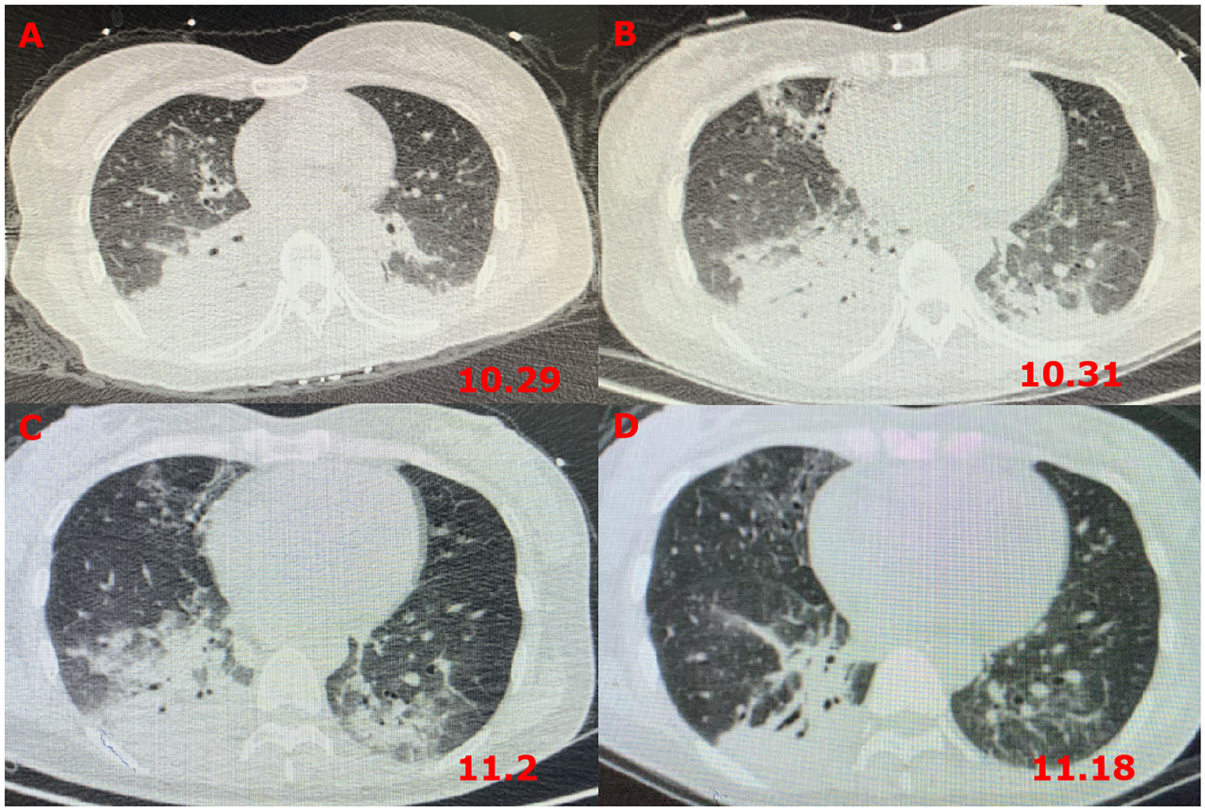

FIGURE 1
Chest CT images revealing pneumonia. **(A)** CT scans on the first day after admission; **(B)** CT scans at 72 h after admission; **(C)** CT scans on the fourth day after transferring out of the ICU; and **(D)** CT scans after GBS diagnosis and treatment for 5 days.

TABLE 1 Concentrations of amitriptyline in the patient's blood.

	10.29 (Before adsorbent)	10.29 (After adsorbent)	10.31	11.1
Amitriptyline	1.4 μg/ml	1.2 μg/ml	0.6 μg/ml	0.5 μg/ml
Olanzapine	14 ng/ml	15 ng/ml	5 ng/ml	4 ng/ml

reportedly associated with the pathogenesis of GBS (3). GBS has also been reported to occur following SARS-CoV-2 vaccination (4). In this case, we believe that the coma after drug poisoning caused aspiration pneumonia by *Klebsiella pneumoniae*. According to the findings of this case of severe respiratory tract infection caused by *Klebsiella pneumoniae*, the diagnosis of GBS should be considered if the patient shows clinical symptoms such as symmetrical limb weakness.

Clinical classification and diagnostic criteria for GBS

GBS is characterized by rapid progression and symmetrical limb weakness with hyporeflexia or the disappearance of reflexes but has not been reported to be caused by inhalation infection after drug poisoning. Its clinical causes, sensory symptoms, muscle weakness, ataxia, pain, and autonomic nerve dysfunction are highly variable (5). According to its clinical signs and electrophysiological diagnostic characteristics, GBS can be divided into four subtypes: acute motor axonal neuropathy, acute motor and sensory axonal neuropathy (AMSAN) with both motor and sensory involvement, acute inflammatory demyelinating polyneuropathy characterized by demyelinating lesions and sensory disorders, and Miller Fisher syndrome dominated by facial paralysis (2, 3). BS diagnosis depends mainly on clinical symptoms, followed by cerebrospinal fluid evaluation and electromyography. Different subtypes have different clinical manifestations, electrophysiology, and histopathology. For typical GBS, rapid progressive bilateral limb

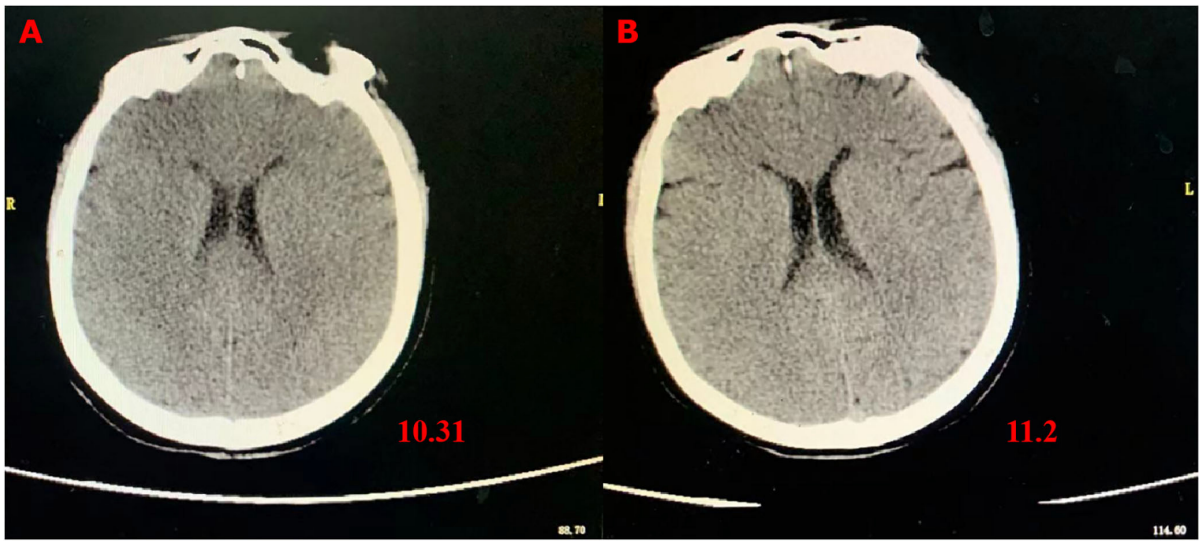

FIGURE 2
Skull CT images showing brain edema. **(A)** CT scans at 72 h after admission; **(B)** CT scans on the fourth day after transferring out of the ICU.

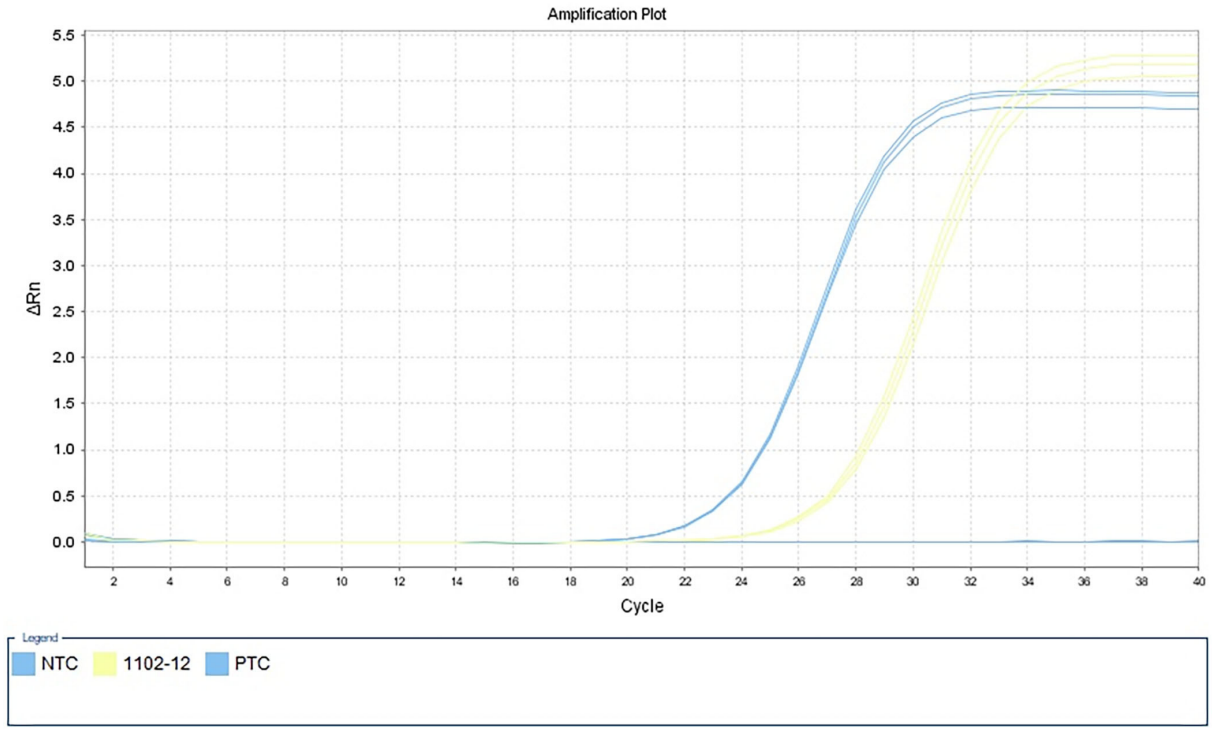

FIGURE 3
Detection of *Klebsiella pneumoniae* by qPCR in alveolar lavage fluid samples. NTC, negative control; 1102–12, alveolar lavage fluid sample; PTC, positive control.

weakness is the main symptom. In other subtypes, patients show cranial nerve function defects, especially bilateral facial muscle weakness, dysphagia, or extraocular muscle dyskinesia. Some patients experience respiratory failure or severe autonomic nerve dysfunction. A slight increase in leukocyte count may be found in cerebrospinal fluid analysis. However, due to

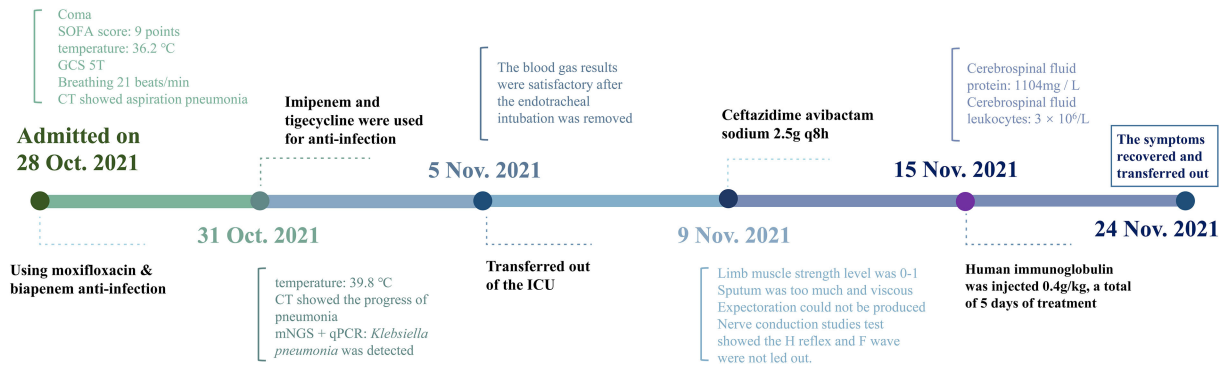

FIGURE 4
Diagnosis and treatment timeline of the case.

the dissociation of albumin cells, the protein count in the cerebrospinal fluid remains very high (2, 6). In this study, despite actively controlling the condition, symmetrical weakness of the limbs gradually increased, resulting in the patient being unable to move her limbs or eat independently. The limb muscle strength level of the distal extremities was within the range of grade 0–1, the muscle tone was decreased, and she could not expectorate, which was consistent with the symptoms of AMSAN (2, 7). Her diagnosis of GBS is a diagnosis of exclusion, as the primary attempt of our in-depth workup was to exclude all other likely diagnoses that would explain her clinical presentation. Demyelination was detected upon nerve conduction study, and this could be used to distinguish GBS from ICU-acquired weakness. The antibodies in cerebrospinal fluid against autoimmune peripheral neuropathy and myasthenia gravis were absent, so multiple myopathies were excluded from the diagnosis. After the GBS diagnosis was confirmed, and intravenous immunoglobulin was administered, the patient showed noticeable improvement (8).

Immunomodulatory therapy is the primary clinical treatment

Multidisciplinary cooperation and immunotherapy are often used to treat GBS, with plasma exchange (PE) therapy and intravenous immunoglobulin being the effective methods (7). PE therapy within the first 4 weeks of onset has been reported as a proven effective treatment method for GBS. As intravenous immunoglobulin is also easier to administer and is more widely available than plasma exchange, it is usually the treatment of choice (8–10). PE acts by reducing or removing specific antibody components in the blood, thereby reducing immune cross-reactions. Usually, in patients with GBS, PE therapy is performed three to five times every other day for 7–14 days, and the PE rate is 120–200 ml/kg (40–50 ml/kg/day) (11). Similarly, intravenous injection of high-dose immunoglobulin (in the present case, the dose administered was 0.4 g/kg body weight/day for 5 days) can reduce the concentration of specific antibodies in the patient's blood by increasing the amount of immunoglobulin and reducing the antibody response to pathogenic antigens (12). Its curative effect was reported to be similar to that of PE therapy (13, 14). Intravenous injection of gamma globulin usually begins within 2 weeks of GBS onset. Early initiation of intravenous immunoglobulin or PE is beneficial and crucial, especially in patients with rapidly progressive weakness (11, 15). Previous studies showed that following the progression stage of the disease is the plateau stage, which usually lasts for 2 days−6 months (average, 7 days), after which the patient starts to recover (2, 3, 7). In the present case, because of the timely diagnosis, a 5 day human immunoglobulin dose of 0.4 g/kg body weight/day was administered. We significantly controlled the development of the disease and, thus, had adequate time for follow-up rehabilitation.

Conclusion

We reported a case of amitriptyline overdose complicated by severe pneumonia caused by *Klebsiella pneumoniae* infection and rapidly progressive GBS. It is necessary to distinguish cases of the unexplained decline of limb muscle strength or abnormal sensations from easily confused conditions, such as ICU-acquired weakness and multiple myopathies, and be alert to possible GBS. Careful medical history, examination of systemic nervous function, cerebrospinal fluid examination, detection of pathogenic microbes by mNGS, magnetic resonance imaging of the head and the neck, electromyography, and autoantibody spectrum of autoimmune peripheral neuropathy should be considered for precise diagnosis. In addition, predictive biomarkers need to be developed to achieve better results for faster identification and to guide diagnosis and treatment.

Data availability statement

The original contributions presented in the study are included in the article/supplementary material, further inquiries can be directed to the corresponding author.

Ethics statement

Written informed consent was obtained from the patient for the publication of any potentially identifiable images or data included in this article.

Author contributions

BZ collected clinical data and wrote the manuscript. QC guided mNGS, qPCR experiments, and data analysis. LD, HW, LC, WL, and ZL participated in the clinical care of the patient and collected a large body of literature to support this diagnosis. WL and ZL assisted in interpreting the results from a clinical perspective and provided suggestions for later revision of the article. LM designed the study and critically revised the manuscript for intellectual content. All authors have read and approved the final manuscript.

Acknowledgments

We thank the efforts and contributions of the reported patient and clinical staff in this study.

Conflict of interest

Author QC is employed by Genoxor Medical & Science Technology Inc., Shanghai, China.

The remaining authors declare that the research was conducted in the absence of any commercial or financial relationships that could be construed as a potential conflict of interest.

Publisher's note

References

1. Hahn AF. Guillain-Barré syndrome. *Lancet.* (1998) 352:635–41. doi: 10.1016/S0140-6736(97)12308-X

2. Willison HJ, Jacobs BC, van Doorn PA. Guillain-Barré syndrome. *Lancet.* (2016) 388:717–27. doi: 10.1016/S0140-6736(16)00339-1

3. Pelea T, Reuter U, Schmidt C, Laubinger R, Siegmund R, Walther BW. SARS-CoV-2 associated Guillain-Barré syndrome. *J Neurol.* (2021) 268:1191–4. doi: 10.1007/s00415-020-10133-w

4. Bijoy George T, Kainat A, Pachika PS, Arnold J. Rare occurrence of Guillain-Barré syndrome after moderna vaccine. *BMJ Case Rep.* (2022) 15:e249749. doi: 10.1136/bcr-2022-249749

5. van den Berg B, Walgaard C, Drenthen J, Fokke C, Jacobs BC, van Doorn PA. Guillain-Barré syndrome: pathogenesis, diagnosis, treatment and prognosis. *Nat Rev Neurol.* (2014) 10:469–82. doi: 10.1038/nrneurol.2014.121

6. Lleixà C, Martín-Aguilar L, Pascual-Goñi E, Franco T, Caballero M, de Luna N, et al. Autoantibody screening in Guillain-Barré syndrome. *J Neuroinflammation.* (2021) 18:251. doi: 10.1186/s12974-021-02301-0

7. Nguyen TP, Taylor RS. *Guillain Barre Syndrome.* Treasure Island, FL: StatPearls (2021).

8. Leonhard SE, Mandarakas MR, Gondim FAA, Bateman K, Ferreira MLB, Cornblath DR, et al. Diagnosis and management of Guillain-Barré syndrome in ten steps. *Nat Rev Neurol.* (2019) 15:671–83. doi: 10.1038/s41582-019-0250-9

9. Van Koningsveld R, Van Doorn PA, Schmitz PI, Ang CW, Van der Meché FG. Mild forms of Guillain-Barré syndrome in an epidemiologic survey in The Netherlands. *Neurology.* (2000) 54:620–5. doi: 10.1212/WNL.54.3.620

10. Rajabally YA. Immunoglobulin and monoclonal antibody therapies in Guillain-Barré syndrome. *Neurotherapeutics.* (2022) 19:885–96. doi: 10.1007/s13311-022-01253-4

11. Verboon C, van Doorn PA, Jacobs BC. Treatment dilemmas in Guillain-Barré syndrome. *J Neurol Neurosurg Psychiatry.* (2017) 88:346–52. doi: 10.1136/jnnp-2016-314862

12. Chevret S, Hughes RA, Annane D. Plasma exchange for Guillain-Barré syndrome. *Cochrane Database Syst Rev.* (2017) 2:CD001798. doi: 10.1002/14651858.CD001798.pub3

13. Hughes RA, Wijdicks EF, Barohn R, Benson E, Cornblath DR, Hahn AF, et al. Practice parameter: immunotherapy for Guillain-Barré syndrome: report of the quality standards subcommittee of the American academy of neurology. *Neurology.* (2003) 61:736–40. doi: 10.1212/WNL.61.6.736

14. van der Meché FG, Schmitz PI. A randomized trial comparing intravenous immune globulin and plasma exchange in Guillain-Barré syndrome. Dutch Guillain-Barré study group. *N Engl J Med.* (1992) 326:1123–9. doi: 10.1056/NEJM199204233261705

15. Hund EF, Borel CO, Cornblath DR, Hanley DF, McKhann GM. Intensive management and treatment of severe Guillain-Barré syndrome. *Crit Care Med.* (1993) 21:433–46. doi: 10.1097/00003246-199303000-00023

frontiers | Frontiers in Medicine

TYPE Case Report
PUBLISHED 08 November 2022
DOI 10.3389/fmed.2022.1051468

OPEN ACCESS

EDITED BY
Yuetian Yu,
Shanghai Jiao Tong University, China

REVIEWED BY
Marko Sallisalmi,
Karolinska University Hospital, Sweden
Warwick Wolf Butt,
Royal Children's Hospital, Australia

*CORRESPONDENCE
Brendan Gill
Gill-Brendan@cooperhealth.edu

SPECIALTY SECTION
This article was submitted to Intensive Care Medicine and Anesthesiology, a section of the journal Frontiers in Medicine

RECEIVED 22 September 2022
ACCEPTED 19 October 2022
PUBLISHED 08 November 2022

CITATION
Gill B, Bartock JL, Damuth E, Puri N and Green A (2022) Case report: Isoflurane therapy in a case of status asthmaticus requiring extracorporeal membrane oxygenation. *Front. Med.* 9:1051468. doi: 10.3389/fmed.2022.1051468

Case report: Isoflurane therapy in a case of status asthmaticus requiring extracorporeal membrane oxygenation

Brendan Gill*, Jason L. Bartock, Emily Damuth, Nitin Puri and Adam Green

Department of Critical Care Medicine, Cooper University Health Care, Camden, NJ, United States

Volatile anesthetics have been described as a rescue therapy for patients with refractory status asthmaticus (SA), and the use of isoflurane for this indication has been reported since the 1980s. Much of the literature reports good outcomes when inhaled isoflurane is used as a rescue therapy for patients for refractory SA. Venovenous (VV) extracorporeal membrane oxygenation (ECMO) is a mode of mechanical circulatory support that is usually employed as a potentially lifesaving intervention in patients who have high risk of mortality, primarily for underlying pulmonary pathology. VV ECMO is usually only considered in cases where patients gas exchange cannot be satisfactorily maintained by conventional therapy and mechanical ventilation strategies. We report the novel use of isoflurane delivered systemically as treatment for severe refractory SA in a patient on VV ECMO. A 51-year-old male with a history of asthma was transferred from another institution for management of severe SA. He was intubated at the referring hospital after failing non-invasive ventilation. Initial arterial blood gas (ABG) showed pH 7.21, partial pressure of carbon dioxide (PCO_2) >95 mmHg, and partial pressure of oxygen (PaO_2) 60 mmHg. VV ECMO was initiated on hospital day (HD) 1 due to refractory respiratory acidosis. After ECMO initiation, acid-base status improved, however, severe bronchospasm persisted and intrinsic positive end expiratory pressure (PEEP) was measured at 18 cm H_2O. Systemic paralysis was employed, respiratory rate (RR) was reduced to 4 breaths per minute. This degree of bronchospasm did not allow for ECMO weaning. On HD 5, the patient received systemic isoflurane *via* the ECMO circuit for 20 h. The following morning, intrinsic PEEP was 4 cm H_2O, and wheezing improved. He was decannulated from VV ECMO on HD 10 and extubated on HD 17. Inhaled isoflurane therapy in patients on VV ECMO for refractory SA has shown good results, but requires delivery of the medication *via* anesthesia ventilators. Our case highlights an effective alternative, systemic delivery of anesthetic *via* the ECMO circuit, as it is often difficult and dangerous to transport these patients to the operating room (OR) or have an intensive care unit (ICU) room adjusted to accommodate an anesthesia ventilator.

KEYWORDS

ECMO–extracorporeal membrane oxygenation, status asthmaticus, isoflurane, venovenous ECMO, asthma, respiratory acidosis, bronchospasm, anesthetics: volatile: halothane sevoflurane

Introduction

Status asthmaticus overview

Status asthmaticus (SA) is defined as the condition of a patient in progressive respiratory failure due to asthma, in whom conventional forms of therapy have failed (1). Approximately 10% of the world's population suffers from asthma, and there is a 15% disease burden in the United States over the last two decades (2). It is estimated that 3–16% of hospitalized adult patients with asthma progress to respiratory failure requiring ventilator support. Mortality is reported at approximately 10% in ICU patients admitted with SA (3), and reported to be as high as 21% in intubated patients (4).

Therapeutic approach to status asthmaticus

The standard approach to treating severe asthma exacerbations include the use of short-acting inhaled beta-agonists with a preference for albuterol due to higher beta-2 selectivity (5) along with systemic corticosteroids such as methylprednisolone (6). Other adjunctive pharmacotherapy include inhaled anticholinergics (ipratropium) and intravenous magnesium (7).

Ventilator management in status asthmaticus

A small percentage (2–4%) of those with SA will require mechanical ventilation due to encephalopathy, inability to oxygenate or ventilate, or muscle fatigue (8, 9). The decision to intubate should be made clinically, and should be considered in patients with increasing lethargy, use of accessory muscles, change in posture or speech, and/or decreasing rate and depth of respiration (10). After initiation of mechanical ventilation, it is important to monitor airway resistance and pulmonary hyperinflation, titrate FiO_2 to maintain a SpO_2 90–92% and adjust minute ventilation to maintain a pH >7.25. To avoid intrinsic PEEP, a strategy of permissive hypercapnia is employed by reducing tidal volumes (5–7 mL/kg), lowering respiratory rate (10–12 breaths per min) and extending expiratory time through adjustment of I:E ratio (I:E 1:3–1:4) (11).

Volume-controlled modes are recommended due to the delivery of constant flow, which can help decrease peak airway pressures. Pressure-controlled modes allow for control of peak airway pressures, however, in asthma the high peak airway pressure is due to airway resistance rather than reduced compliance. In the absence of intrinsic PEEP, plateau pressure should only be mildly elevated, as it provides the best estimate of alveolar distending pressure when esophageal pressure monitoring is unavailable. Elevation of plateau pressure >25 cm H20 should raise concern for severe dynamic hyperinflation, which can cause life-threatening hemodynamic instability and barotrauma. Minimal PEEP should be utilized to prevent intrinsic PEEP and not contribute to hyperinflation.

Patients who are intubated for status asthmaticus should be deeply sedated, and paralyzed if necessary, to prevent any patient-ventilator dyssynchrony.

Advanced therapies for status asthmaticus

VV ECMO is a form of mechanical circulatory support reserved for those with respiratory failure refractory to conventional treatment (12). Large cannulas are peripherally placed in central veins allowing for the removal and return of venous blood as it is passed through a membrane serving to oxygenate and remove carbon dioxide through centrifugal forces. The use of VV ECMO in status asthmaticus is rare and only reserved for those who have inadequate gas exchange with mechanical ventilation or unsafe airway pressures. Unlike in acute respiratory distress syndrome (ARDS), the criteria for cannulation are less concrete. This is mostly due to the significantly fewer cases. However, those who require ECMO support tend to have favorable outcomes with a survival reported at 84% (13). While selection criteria vary from center to center, common exclusion criteria include age, presence of chronic comorbidities or concern for neurological injury. Potential complications include major bleeding, thromboses, infection, renal failure, pulmonary and CNS hemorrhage among many others. The use of ECMO in asthma patients allows the lungs to rest, thus providing time for bronchiolar relaxation until the bronchospasm has subsided. While imposing risk, ECMO has been used successfully as an early adjunct to therapy in patients whose gas exchange cannot otherwise be satisfactorily maintained by conventional therapy and ventilation strategies (14).

Inhaled volatile anesthetics have been cited as a rescue therapy for severe refractory status asthmaticus (15–18). There are multiple postulated mechanisms regarding how these agents work, including direct relaxation of bronchial smooth muscle, inhibition of the release of inflammatory mediators, beta adrenergic receptor stimulation, reduction of vagal tone and vagal-mediated reflexes and antagonism of the effects of histamine and methacholine (19–21). The use of inhaled anesthetics in patients requiring ECMO has been reported more recently, both in severe refractory SA and acute respiratory distress syndrome (ARDS) (19, 22); however, the literature is limited. In previously reported cases of utilization of inhaled volatile anesthetics for severe SA, the anesthetics were delivered *via* the inhalational route utilizing an anesthesia ventilator (19,

23). In the case presented here, isoflurane was administered systemically *via* the ECMO circuit. To our knowledge, this is the first case in the literature to describe this route of isoflurane delivery.

Case

A 51-year-old male with no baseline functional limitations and a medical history of asthma and tobacco use disorder initially presented to an outside hospital (OSH) with an acute asthma exacerbation. His outpatient asthma regimen consisted of tiotropium, montelukast, an albuterol inhaler as needed, and prednisone 10 mg daily. He was started on non-invasive positive pressure ventilation at the referring hospital, but required endotracheal intubation for worsening respiratory distress. Post intubation, there was significant difficulty with ventilation due to severe bronchospasm. Despite neuromuscular blockade and attempts at using a variety of mechanical ventilation modes, there was little improvement in his respiratory acidosis. Pharmacological treatment included systemic steroids, bronchodilators, ketamine, intramuscular epinephrine, and racemic epinephrine. The patient was transferred for escalation of care and consideration for VV ECMO.

On arrival to our institution, the patient was noted to have diffuse wheezing. He required continued deep sedation and paralysis for ventilator dyssynchrony. His initial arterial blood gas revealed a pH of 7.21, PCO_2 > 95 mmHg and a PaO_2 60 mmHg on an FiO2 of 40% on pressure control ventilation with an inspiratory pressure of 30 cmH_2O and a PEEP of 5 cm H_2O. Due to high intrinsic PEEP (18 cm H_2O), he was changed to pressure regulated volume control with a tidal volume of 500 mL, respiratory rate of 12 and PEEP of 5 improving his intrinsic PEEP to 12 cm H_2O.

His respiratory acidosis worsened requiring initiation of VV ECMO on hospital day 1.

VV ECMO criteria used for cannulation included refractory respiratory acidosis with a PCO2 > 60 mmHg despite optimal ventilator management. He was cannulated with a 25 french drainage cannula in the right femoral vein, and a 20 french return cannula in the right internal jugular vein. In order to avoid over correction of his PCO_2, as this has been linked to poor neurological outcomes (24), the initial sweep gas flow was set at 2 L/min with ventilator settings of PRVC set to a TV 350 mL (4.7 cc/kg IBW), RR 8 breaths per minute and a PEEP of 5 cm H_2O. Post cannulation ABG demonstrated a pH of 7.32, PcO_2 86 mmHg and a PaO_2 135 mmHg.

The patient continued to have evidence of severe bronchospasm with wheezing and poor air movement throughout all lung fields and ongoing intrinsic PEEP despite excessive expiratory time. A brief trial of Heliox was utilized but was stopped after no clinical improvement. He was continued on short-acting bronchodilators, systemic and inhaled corticosteroids, montelukast along with chest physiotherapy to avoid atelectasis. The sedation approach included a combination of propofol, ketamine, midazolam, and fentanyl along with periods of neuromuscular blockade. There was improvement in his intrinsic PEEP, but he continued to not tolerate increases in native minute ventilation *via* mechanical ventilation in an attempt to wean sweep gas flow. Given overall lack of significant clinical improvement, a multi-disciplinary team including anesthesia, critical care, perfusion, and pulmonary medicine met to discuss the role of inhaled anesthetics (isoflurane). The patient was initiated on isoflurane *via* the ECMO circuit on hospital day 5.

An isoflurane vaporizer was attached to the ECMO circuit and a line was run from the vaporizer to the ECMO oxygenator. A separate waste anesthesia gas line was run from the circuit to the waste chamber. A separate port at the bottom of the membrane oxygenator served as an open vent to draw air into the oxygenator and not allow air or waste anesthesia gas to escape into the atmosphere, risking staff exposure. Vaporized isoflurane was instilled into the ECMO circuit at an initial concentration of 0.8%, and incrementally increased to 1.2%, and did not go above this (due to safety concerns for patient and providers). This medication was continued for 20 h.

On the morning after initiation, there was clinical improvement in air movement and markedly reduced airway resistance. The intrinsic PEEP was noted to be 3–4 cm H_2O, see Figure 1. Two days after isoflurane therapy, the patient's tidal volume (500 mL) and respiratory rate (20 bpm) were able to be increased without development of elevated airway pressures or intrinsic PEEP, allowing for weaning of ECMO support. He was decannulated from ECMO on hospital day 10, and extubated hospital day 17, see Table 1.

Although during the admission he only met 2 of the primary criteria for allergic bronchopulmonary aspergillosis, the patient was started on a prolonged course of isovuconazole as he grew aspergillus in his sputum, had tree-in-bud opacities in left lower lobe on CT of the chest, and was having intermittent fevers. His IgE level was normal at 109 kU/L, but it was noted that patient had been on high-dose systemic steroids since admission. He was discharged to an acute rehabilitation facility on Isovuconazole therapy, with plans to continue this for 12 weeks, and follow up with the infectious disease specialists in the outpatient setting with interval imaging as well.

Discussion

This case illustrates the successful use of isoflurance delivered systemically through the ECMO circuit in a patient with status asthmaticus. Previous reports describe administration of isoflurane solely to the bronchiolar system *via* inhalation. This alternative route of delivery was chosen due to the inability to utilize inhaled anesthetics in the intensive care

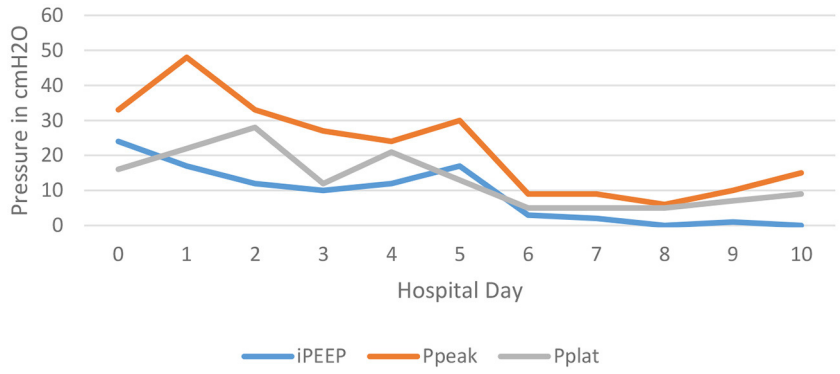

FIGURE 1
This depicts the trend of the patient's intrinsic PEEP, peak airway pressures, and plateau pressures over the first 10 days of the hospitalization. Notice the significant decrease in all three pressures after day 5; the day that isoflurane was administered.

TABLE 1 Laboratory values at the time of admission, immediately prior to and after ECMO cannulation, mid-ECMO run, day of decannulation from ECMO, day of extubation, and day of discharge.

	Admission	Pre-cannulation	Post cannulation	Mid-ECMO Run	Decannulation	Extubation	Discharge
WBC count	19.8	23.07	18.76	15.7	17.5	9.5	6.93
Hemoglobin	13.4	13.8	10.6	9.4	8.4	8.0	11.0
BUN	29	31	46	36	28	20	6
Creatinine	1.19	1.42	1.24	0.64	0.46	0.41	0.45
pH	7.17	7.17	7.35	7.41	7.40		
pCO_2	>95	>95	77	69	49		
pO_2	77	81	272	81	88		

WBC count measured in $10^*3/\mu L$, Hemoglobin is measured in g/dL, BUN and Creatinine are measured in mg/dL, pCO_2 and pO_2 are measured in mmHg. WBC, White Blood Cell; BUN, Blood Urea Nitrogen; pCO_2, Partial pressure of arterial carbon dioxide; pO_2, Partial pressure of arterial oxygen.

unit (safety concerns) and the inability to transport the patient to the operating room for delivery the anesthetic (resource limitation). Systemic delivery of volatile anesthetics could still lead to gas exposure to the room from the ventilator exhaust, it likely would be minimal and significantly less than previously describes delivery routes.

According to the Extracorporeal Life Support Organization (ELSO) Registry, a total of 272 patients were placed on ECMO for management of life-threatening asthma from March 1992 to March 2016. In this group, the weaning success rate was 86.7%, and the rate to survival to hospital discharge was 83.5% (25). A small case series (24 patients) sites mortality of roughly 16% for patients requiring VV-ECMO for SA (13). Commonly encountered complications include major bleeding (due to coagulopathy or the utilization of systemic anticoagulation to prevent thromboses), thrombosis, infection, renal failure, pulmonary and CNS hemorrhage (13).

Volatile anesthetics cause relaxation through direct action on bronchiole smooth muscle and through systemic uptake (19). They have also shown immune modulatory and anti-inflammatory actions (26). The use of volatile anesthetics in management of refractory status asthmaticus has been described since the 1980's. In most cases, these agents are delivered *via* inhalation, solely to the bronchiolar system. In fact, to our knowledge, we report the first case of isoflurane delivered systemically *via* the ECMO circuit as rescue therapy for severe refractory status asthmaticus. There is a higher risk for hypotension due to dose-dependent reduction in systemic vascular resistance and cardiac arrhythmias when used intravenously. This was not witnessed in the case of our patient.

The coordination of care in this case was complex, and the time spent by multiple providers, both in consultation with each other and individually, would likely limit the possibility of isoflurane delivery becoming a common practice. Anesthetic delivery systems that administer volatile anesthetics directly into endotracheal tubes have been developed and are being researched for the delivery of anesthetics to invasively ventilated patients (22). In a retrospective study of 74 patients, Grasselli et al. found that inhaled volatile anesthetic (isoflurane) delivered *via* the inhalation route using one of these anesthetic delivery systems can be a safe alternative to continuous IV sedation

in patients on VV ECMO for ARDS. While systemic delivery is novel, there are limitations that should be mentioned. The amount of systemic absorption is unknown and dependent on the size of the gas used as well as the oxygenator components (the type of plastic used and how porous it is). The long-term use of these gases in the treatment of status asthmaticus is also unknown. Larger scale studies and more case reports are necessary to further evaluate the use of inhaled volatile anesthetics in patients on VV ECMO, and for management of severe refractory status asthmaticus in adults.

Data availability statement

The original contributions presented in the study are included in the article/Supplementary material, further inquiries can be directed to the corresponding author.

Ethics statement

Ethical review and approval was not required for the study on human participants in accordance with the local legislation and institutional requirements. Written informed consent from the (patients/participants OR patients/participants legal guardian/next of kin) was not required to participate in this study in accordance with the national legislation and the institutional requirements. Written informed consent was obtained from the patient for the publication of any potentially identifiable images or data included in this article.

Author contributions

BG wrote the manuscript, developed the tables and figures, and researched the relevant information. AG contributed to the manuscript, made several revisions, and revised figures and tables. JB, ED, and NP revised the manuscript and contributed to writing. All authors contributed to the article and approved the submitted version.

Conflict of interest

The authors declare that the research was conducted in the absence of any commercial or financial relationships that could be construed as a potential conflict of interest.

Publisher's note

All claims expressed in this article are solely those of the authors and do not necessarily represent those of their affiliated organizations, or those of the publisher, the editors and the reviewers. Any product that may be evaluated in this article, or claim that may be made by its manufacturer, is not guaranteed or endorsed by the publisher.

Supplementary material

The Supplementary Material for this article can be found online at: https://www.frontiersin.org/articles/10.3389/fmed.2022.1051468/full#supplementary-material

References

1. Cohen NH, Eigen H, Shaughnessy TE. Status asthmaticus. *Crit Care Clin.* (1997) 13:459–76. doi: 10.1016/S0749-0704(05)70324-9

2. Papiris S, Kotanidou A, Malagari K, Roussos C. Clinical review: severe asthma. *Crit Care.* (2002) 6:30–44. doi: 10.1186/cc1451

3. Afessa B, Morales I, Cury JD. Clinical course and outcome of patients admitted to an ICU for status asthmaticus. *Chest.* (2001) 120:1616–21. doi: 10.1378/chest.120.5.1616

4. Shapiro JM. Intensive care management of status asthmaticus. *CHEST J.* (2001) 120:1439–41. doi: 10.1378/chest.120.5.1439

5. National Asthma Education and Prevention Program. Expert Panel Report 3 (EPR-3): guidelines for the diagnosis and management of asthma-summary report 2007. *J Allergy Clin Immunol.* (2007) 120 (5 Suppl):S94–138. doi: 10.1016/j.jaci.2007.09.029

6. Edmonds ML, Milan SJ, Camargo CA, Pollack CV, Rowe BH. Early use of inhaled corticosteroids in the emergency department treatment of acute asthma. *Cochrane Database Syst Rev.* (2012) 12:CD002308. doi: 10.1002/14651858.CD002308.pub2

7. Griffiths B, Kew KM, Normansell R. Intravenous magnesium sulfate for treating children with acute asthma in the emergency department. *Paediatr Respir Rev.* (2016) 20:45–7. doi: 10.1016/j.prrv.2016.07.001

8. Pendergraft TB, Stanford RH, Beasley R, Stempel DA, Roberts C, McLaughlin T. Rates and characteristics of intensive care unit admissions and intubations among asthma-related hospitalizations. *Ann Allergy Asthma Immunol.* (2004) 93:29–35. doi: 10.1016/S1081-1206(10)61444-5

9. Leatherman J. Mechanical ventilation for severe asthma. *Chest.* (2015) 147:1671–80. doi: 10.1378/chest.14-1733

10. Meduri GU, Cook TR, Turner RE, Cohen M, Leeper KV. Noninvasive positive pressure ventilation in status asthmaticus. *Chest.* (1996) 110:767–74. doi: 10.1378/chest.110.3.767

11. Yartsev A. *Ventilation strategies for Status Asthmaticus.* (2015). Deranged Physiology. Available online at: https://derangedphysiology.com/main/required-reading/respiratory-medicine-and-ventilation/Chapter%20611/ventilation-strategies-status-asthmaticus-0 (accessed September 3, 2022).

12. Gorman D, Green A, Puri N, Dellinger RP. Severe ARDS secondary to *Legionella* pneumonia requiring VV ECMO in the setting of newly diagnosed hairy cell leukemia. *J Investig Med High Impact Case Rep.* (2022) 10:1–8. doi: 10.1177/23247096211065618

13. Mikkelsen ME, Woo YJ, Sager JS, Fuchs BD, Christie JD. Outcomes using extracorporeal life support for adult respiratory failure due to status asthmaticus. *ASAIO J.* (2009) 55:47–52. doi: 10.1097/MAT.0b013e3181901ea5

14. Di Lascio G, Prifti E, Messai E, Peris A, Harmelin G, Xhaxho R, et al. Extracorporeal membrane oxygenation support for life-threatening acute severe status asthmaticus. *Perfusion*. (2017) 32:157–63. doi: 10.1177/0267659116670481

15. Fuchs AM. The interruption of the asthmatic crisis by tribromethanol (avertin). *J Allergy*. (1937) 8:340–6. doi: 10.1016/S0021-8707(37)90143-6

16. Meyer NE, Schotz S. The relief of severe intractable bronchial asthma with cyclopropane anesthesia. *J Allergy*. (1939) 10:239–40. doi: 10.1016/S0021-8707(39)90472-7

17. Bierman MI, Brown M, Muren O, Keenan RL, Glauser FL. Prolonged isoflurane anesthesia in status asthmaticus. *Crit Care Med*. (1986) 14:832–3. doi: 10.1097/00003246-198609000-00017

18. Johnston RG, Noseworthy TW, Friesen EG, Yule HA, Shustack A. Isoflurane therapy for status asthmaticus in children and adults. *Chest*. (1990) 97:698–701. doi: 10.1378/chest.97.3.698

19. LaGrew JE, Olsen KR, Frantz A. Volatile anesthetic for treatment of respiratory failure from status asthmaticus requiring extracorporeal membrane oxygenation. *BMJ Case Rep*. (2020) 13:e231507. doi: 10.1136/bcr-2019-231507

20. Hirshman CA, Edelstein G, Peetz S, Wayne R, Downes H. Mechanism of action of inhalational anesthesia on airways. *Anesthesiology*. (1982) 56:107–11. doi: 10.1097/00000542-198202000-00005

21. Warner DO, Vettermann J, Brichant JF, Rehder K. Direct and neurally mediated effects of halothane on pulmonary resistance *in vivo*. *Anesthesiology*. (1990) 72:1057–63. doi: 10.1097/00000542-199006000-00017

22. Grasselli G, Giani M, Scaravilli V, Fumagalli B, Mariani C, Redaelli S, et al. Volatile Sedation for Acute Respiratory Distress Syndrome patients on venovenous extracorporeal membrane oxygenation and ultraprotective ventilation. *Crit Care Explor*. (2021) 3:e0310. doi: 10.1097/CCE.0000000000000310

23. Raff LA, Schneider AB, Charles AG, Gallaher JR. Treatment of acute severe asthma exacerbation with extracorporeal membrane oxygenation and inhaled volatile anesthestic. *Am Surg*. (2021) 1—3. doi: 10.1177/00031348211047489

24. Cannizzaro G, Garbin L, Clivati A, Pesce LI. Correction of hypoxia and hypercapnia in COPD patients: effects on cerebrovascular flow. *Monaldi Arch Chest Dis*. (1997) 52:9–12.

25. Yeo HJ, Kim D, Jeon D, Kim YS, Rycus P, Cho WH. Extracorporeal memebrane oxygenation for life-threatening asthma refractory to mechanical ventilation: analysis of the Extracorporeal Life Support Organization registry. *Crit Care*. (2017) 1–9. doi: 10.1186/s13054-017-1886-8

26. Verkoyen K, Schildhauer TA, Strauch JT, Swol J. The effects of propofol and isoflurane sedation on the outcomes of surgical patients receiving extracorporeal membrane oxygenation. *ASAIO J*. (2017) 63:174–8. doi: 10.1097/MAT.0000000000000466

frontiers | Frontiers in Medicine

TYPE Case Report
PUBLISHED 21 November 2022
DOI 10.3389/fmed.2022.1053012

OPEN ACCESS

EDITED BY
Yuetian Yu,
Shanghai Jiao Tong University, China

REVIEWED BY
Julie Talano,
Medical College of Wisconsin, United States
Kassem Hammoud,
University of Kansas Hospital, United States
Qihan Li,
Institute of Medical Biology, China
Hannamari Välimaa,
University of Helsinki, Finland

*CORRESPONDENCE
Elvio Mazzotta
Elvio.Mazzotta@osumc.edu

SPECIALTY SECTION
This article was submitted to Intensive Care Medicine and Anesthesiology, a section of the journal Frontiers in Medicine

RECEIVED 24 September 2022
ACCEPTED 02 November 2022
PUBLISHED 21 November 2022

CITATION
Mazzotta E, Fiorda Diaz J, Echeverria-Villalobos M, Eisinger G, Sprauer S, Singha A and Lyaker MR (2022) Case report: Disseminated herpes simplex virus 1 infection and hemophagocytic lymphohistiocytosis after immunomodulatory therapy in a patient with coronavirus disease 2019. *Front. Med.* 9:1053012. doi: 10.3389/fmed.2022.1053012

Case report: Disseminated herpes simplex virus 1 infection and hemophagocytic lymphohistiocytosis after immunomodulatory therapy in a patient with coronavirus disease 2019

Elvio Mazzotta[1]*, Juan Fiorda Diaz[1], Marco Echeverria-Villalobos[1], Gregory Eisinger[2], Sarah Sprauer[2], Arindam Singha[2] and Michael R. Lyaker[1]

[1]Department of Anesthesiology, The Ohio State University Wexner Medical Center, Columbus, OH, United States, [2]Division of Pulmonary, Critical Care, and Sleep Medicine, Department of Internal Medicine and Emergency Medicine, The Ohio State University Wexner Medical Center, Columbus, OH, United States

Corticosteroids and immunomodulatory therapies are widely used to treat patients with severe coronavirus disease 2019 (COVID-19). Janus kinase (JAK) inhibitors such as tofacitinib have been recently studied as adjuvants in the treatment of COVID-19. Although immunomodulatory therapies may be linked to decreased mortality rates in the acute phase, subsequent severe infectious complications may result from them. We describe a case of a multiorgan system failure secondary to disseminated primary herpes simplex virus 1 (HSV-1) infection and hemophagocytic lymphohistiocytosis (HLH) following treatment with tofacitinib and high-dose dexamethasone therapy for severe COVID-19. Early diagnosis and treatment of these life-threatening conditions may have a significant impact on COVID-19 patients' outcomes.

KEYWORDS

human herpes simplex virus 1, COVID-19, liver failure, hemophagocytic lymphohistiocytosis, tofacitinib

Introduction

The hallmark of severe coronavirus disease 2019 (COVID-19) is an aggressive pro-inflammatory response known as "cytokine storm" (1). Studies have shown that immune system dysregulation and hyperinflammation are associated with increased mortality in severely ill patients (1, 2). Multiple studies suggest that glucocorticoids, Janus kinase (JAK) inhibitors, and interleukin 6 (IL-6) inhibitors may be associated with decreased mortality in critically ill COVID-19 patients (3, 4). However, the immunosuppressive state induced by these agents may increase the

risk of secondary infections (5, 6). Herpes simplex virus (HSV) reactivation is a widely known complication in critically ill patients in the intensive care unit (ICU) (7). Nevertheless, disseminated HSV infection and subsequent potentially lethal complications such as hemophagocytic lymphohistiocytosis (HLH) are very uncommon (8, 9).

Hemophagocytic lymphohistiocytosis is a rare and life-threatening condition characterized by an uncontrolled hyper-inflammatory response with hyperactivation of histiocytes leading to hemophagocytosis. Diagnostic criteria include fever, organomegaly, cytopenia, hypertriglyceridemia, and extremely high ferritin (10). Risk factors include, but are not limited to, genetic mutations, immunodeficiency, infections, and malignancy (11). Published literature on HLH treatment and outcomes is limited considering its low incidence. We report a case of disseminated HSV-1 associated with HLH in a patient recently treated with steroids and tofacitinib for COVID 19.

Case presentation

A 58-year-old Caucasian female without significant past medical history presented to an outside emergency department with a complaint of abdominal pain. She had been recently admitted with respiratory failure secondary to COVID-19 pneumonia. During her hospital course, she was treated with 15 L/min of oxygen by high flow nasal cannula and tofacitinib (10 mg twice daily for 10 days), remdesivir (200 mg on day 1 follow by 100 mg for 5 days), and dexamethasone (6 mg/daily). After 10 days of a relatively uneventful admission, she was discharged home on 3 L of oxygen.

Five days after discharge, the patient presented to an outside hospital emergency department with severe abdominal pain that steadily worsened. Initial laboratory results (**Table 1**) were notable for pancytopenia, severe acute liver injury, and elevation of inflammatory makers including lactate dehydrogenase (LDH) and ferritin. Her hepatitis panel (including serology for hepatitis A, B, C, cytomegalovirus, and Epstein-Barr virus), and reverse transcriptase polymerase chain reaction (RT-PCR) for severe acute respiratory syndrome coronavirus 2 (SARS-CoV-2) were negative. Computerized tomography (CT) of abdomen and pelvis showed hepatic steatosis without others abdominopelvic findings. Alcohol abuse and acetaminophen ingestion were ruled out. Consequently, the patient was admitted with acute liver injury of unknown origin and concomitant oliguric acute kidney injury (AKI) that subsequently resulted in transfer to our institution for higher level of care.

TABLE 1 Initial laboratory results.

Laboratory test (normal ranges, units)	Results
WBC count (3.99–11.19 K/μL)	3.00
RBC count (3.91–5.04 M/μL)	3.76
Hemoglobin (11.4–15.2 g/dL)	11.1
Hematocrit (34.9–44.3%)	33.2
Platelet count (150–393 K/μL)	42
PT (11.9–14.2 s)	32.1
INR (0.9–1.1)	3.2
PTT (24.0–34.3 s)	66.2
Creatinine (0.50–1.20 mg/dL)	5.45
Bilirubin direct (<0.3 mg/dL)	1.2
Bilirubin total (<1.5 mg/dL)	2.1
ALP (32–126 U/L)	181
ALT (9–48 U/L)	7,750
AST (10–39 U/L)	13,680
Ferritin (10.0–291.0 ng/mL)	98,821
LDH total (100–190 U/L)	16,190
Triglycerides (<150 mg/dL)	126

WBC, white blood cells; RBC, red blood cells; PT, prothrombin time; INR, international normalized ratio; PTT, partial thromboplastin time; ALP, alkaline phosphatase; ALT, alanine transaminase; AST, aspartate transaminase; LDH, lactate dehydrogenase.

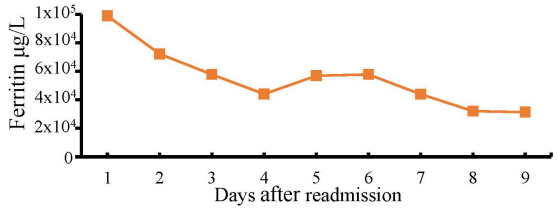

FIGURE 1
Down-trending ferritin levels after hospital admission.

Shortly after transfer to our institution, the patient developed a rapidly progressive encephalopathy with respiratory distress and septic shock requiring ICU admission, mechanical ventilation, and hemodynamic support. Vancomycin resistant enterococcus (VRE) bacteremia was diagnosed, and the patient was started on daptomycin (10 mg/kg/daily). HLH was initially suspected due to the extremely high ferritin levels. However, a moderate predictive score with normal triglycerides and down-trending ferritin levels delayed the definitive diagnosis (**Figure 1**) (12).

Furthermore, a rash involving her inguinal area was noted. Both, lesion swab and serum PCR, were positive for herpes simplex virus 1 (HSV-1). Primary infection was confirmed with a positive HSV-1 I gM and negative IgG. In addition, chest CT showed bilateral multifocal pneumonia, that had progressed from her prior imaging during COVID admission

Abbreviations: COVID-19, coronavirus disease 2019; HSV, herpes simplex virus; ICU, intensive care unit; HLH, hemophagocytic lymphohistiocytosis; LDH, lactate dehydrogenase; PCR, polymerase chain reaction; RT- PCR, reverse transcriptase polymerase chain reaction; SARS-CoV-2, severe acute respiratory syndrome coronavirus 2; CT, computerized tomography; AKI, acute kidney injury; VRE, Vancomycin resistant enterococcus; BID, twice daily; CRRT, continuous renal replacement therapy.

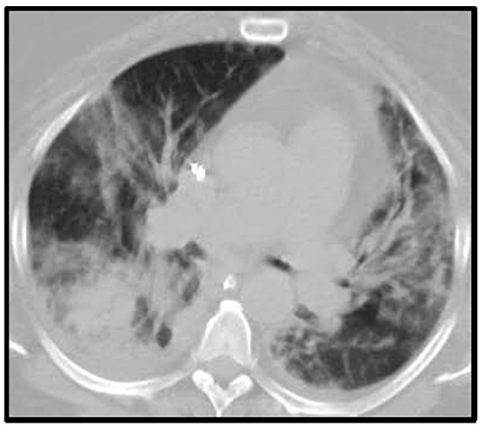

FIGURE 2
Chest CT after ICU admission. Description: Bilateral multifocal irregular patchy and confluent ground glass and consolidative opacities with associated predominantly bilateral lower lobe irregular reticulations. Small **(right)** and trace **(left)** pleural effusion. CT, computerized tomography; ICU, intensive care unit.

(Figure 2). Bronchoscopy was performed and notable for diffusely erythematous friable bronchial mucosa. Cytopathology of the bronchial lavage fluid was notable for multinucleated cells with glassy chromatin suggestive of HSV-1 viral pneumonitis (13).

Central nervous system (CNS) involvement of HSV-1 infection was strongly suspected, but lumbar puncture was deferred due to worsening coagulopathy. However, the patient was empirically treated with meningitis dosing of acyclovir (10 mg/kg twice daily).

On admission day 7, increased triglyceride levels and an updated H-score (used for diagnosis of HLH) indicated more than 99% chances of HLH this time (fever 101.1-102.9, Pancytopenia 3 lineages, ferritin >6,000 ng/mL, triglyceride 500 mg/dL, fibrinogen 110 mg/dL, AST 5,470 U/L) (14).

Bone marrow biopsy was not performed due to clinical instability, coagulopathy, and very high pretest probability for HLH. In consultation with hematology, empiric immunosuppressive therapy with intravenous dexamethasone (40 mg/day) was started.

On admission day 10, the patient's clinical condition continued to deteriorate with worsening shock, AKI requiring continuous renal replacement therapy (CRRT), refractory metabolic acidosis, escalating ventilator requirements, and loss of brain stem reflexes. Head CT showed a trace of right frontal convexity subarachnoid hemorrhage and Abdomen/Pelvis CT displayed iliopsoas hematoma. Given the poor prognosis, the family made the decision to transition to comfort measures and on hospital day 11, patient expired (Figure 3).

Discussion

We described a case of a disseminated primary HSV-1 infection complicated by HLH in a patient treated with tofacitinib and dexamethasone for COVID-19. While treatment with corticosteroids is supported by high quality evidence (4) and has become standard of care for patient with respiratory failure secondary to COVID-19, the role of other adjunctive immunomodulatory agents in patients with a hyperinflammatory profile remains controversial (12). Of concern, reduced immune response induced by immunomodulators may be associated with an increased risk of secondary bacterial, viral, and fungal infections in COVID-19 patients (6).

Our patient was treated with tofacitinib, a specific JAK inhibitor widely used for treatment of rheumatoid arthritis

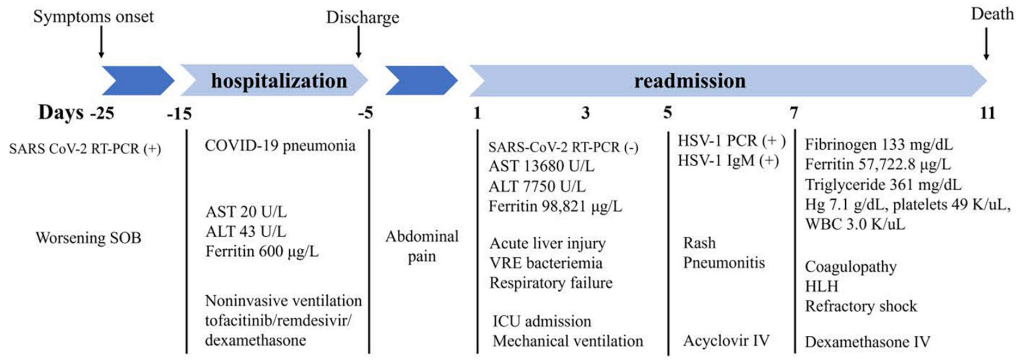

FIGURE 3
Flow chart of significant clinical events and outcomes. SARS, severe acute respiratory syndrome; COVID-19, coronavirus disease 2019; RT-PCR, reverse transcriptase polymerase chain reaction; SOB, shortness of breath; AST, aspartate transaminase; ALT, alanine transaminase; VRE, vancomycin resistant enterococcus; ICU, intensive care unit; HSV-1, herpes simplex virus 1; IV, intravenous; Hg, hemoglobin; WBC, white blood cells; HLH, hemophagocytic lymphohistiocytosis.

and a common alternative to tocilizumab and baricitinib. In a randomized clinical trial including 289 patients admitted with COVID-19 pneumonia, tofacitinib significantly reduced the cumulative incidence of death or respiratory failure at 28 days when compared with placebo (RR 0.63; 95% confidence interval [CI], 0.41 to 0.97; $p = 0.04$) (15). The risk of severe infections was not greater in the tofacitinib group in comparison with placebo; however, a significant increase in transaminase levels was reported in the tofacitinib group (15). Moreover, suppressed lymphocyte activation and proliferation induced by this drug may result in a higher susceptibility to HSV-1 infection (16–19). The fulminant disease course may be entirely or partly due to use of JAK inhibitor and its risk of severe secondary infection. However, the patient also had several major risk factors for severe disease and poor outcome of COVID-19.

Herpes simplex virus reactivation is a well-known complication in critically ill patients in the ICU; however, disseminated HSV-1 infection with concomitant hepatitis and pneumonitis is an uncommon clinical entity linked to high mortality rates (8). Fatal cases of disseminated HSV-1 infection have been reported elsewhere in cases of COVID-19 infection. Busani et al. recently described acute liver failure and HSV-1 infection in two male patients who received tocilizumab and corticosteroids as part of their therapy for COVID-19 (5). The authors reported refractory metabolic acidosis, irreversible shock, and impaired liver function as the main causes of death in both patients. Both patients received similar therapies including hydroxychloroquine, azithromycin, tocilizumab, and methylprednisolone. Recognition of disseminated HSV-1 was delayed in both patients, with diagnosis on days 15 and 33 of admission, respectively (5).

To confirm the diagnosis of disseminated HSV, invasive procedures such as liver biopsy and spinal puncture can be considered. However, these procedures carry an increased risk of bleeding. Therefore, it is crucial to weight risks and benefits in a coagulopathic patient.

In adults, the most common triggers for HLH are infection or alteration in immune homeostasis like autoimmune diseases and cancer (10). Primary viral infections or reactivation have been commonly identified as the main causes of HLH, being Epstein-Barr virus the most commonly reported followed by herpes simplex virus and cytomegalovirus (10, 20). Growing evidence suggests an increased incidence of HLH in patients with severe COVID-19. However, most of these cases are clinically diagnosed and lack confirmatory testing (i.e., bone marrow biopsy) due to patients' instability (21). The cornerstone of HLH management includes the treatment of the triggering condition, aggressive immunosuppression, and corticosteroids (10, 22). In our patient, the course of events of the COVID-19 and HLH diagnoses did not overlap, making the disseminated primary HSV its most likely trigger. Extremely high ferritin level with pancytopenia raised primary concerns for secondary HLH. However, down-trending ferritin could have delayed this diagnosis. Additionally, the risks and benefits of instituting aggressive immunosuppression for the treatment of HLH were challenging to weigh in a patient with disseminated HSV-1 and enterococcal bacteremia. It is unknown whether earlier steroid treatment would have improved the outcome or worsened the infectious processes.

Conclusion

To the best of our knowledge, our case report may be the first case reporting a patient with a disseminated HSV-1 infection associated with HLH after treatment for COVID-19. Immunomodulatory therapies for moderate-to-severe COVID-19 may place patients at higher risk of severe secondary infections. Disseminated HSV-1 and acute liver failure are associated with high mortality rates. Future research on immunomodulatory therapies for COVID-19 management may elucidate the associated risks and benefits in patients with potential predisposing factors for severe systemic diseases.

Data availability statement

The original contributions presented in this study are included in the article/supplementary material, further inquiries can be directed to the corresponding author.

Ethics statement

Ethical review and approval was not required for the study on human participants in accordance with the local legislation and institutional requirements. The patients/participants provided their written informed consent to participate in this study. Written informed consent was obtained from the individual(s) for the publication of any potentially identifiable images or data included in this article.

Author contributions

All authors listed have made a substantial, direct, and intellectual contribution to the work, and approved it for publication.

Conflict of interest

The authors declare that the research was conducted in the absence of any commercial or financial relationships that could be construed as a potential conflict of interest.

Publisher's note

References

1. Gustine JN, Jones D. Immunopathology of hyperinflammation in COVID-19. *Am J Pathol.* (2021) 191:4–17. doi: 10.1016/j.ajpath.2020.08.009

2. Ruan Q, Yang K, Wang W, Jiang L, Song J. Clinical predictors of mortality due to COVID-19 based on an analysis of data of 150 patients from Wuhan, China. *Intensive Care Med.* (2020) 46:846–8. doi: 10.1007/s00134-020-05991-x

3. Hermine O, Mariette X, Tharaux P-L, Resche-Rigon M, Porcher R, Ravaud P, et al. Effect of tocilizumab vs. usual care in adults hospitalized with COVID-19 and moderate or severe pneumonia: a randomized clinical trial. *JAMA Intern Med.* (2021) 181:32–40. doi: 10.1001/jamainternmed.2021.2209

4. World Health Organization [WHO]. *Corticosteroids for COVID-19: Living guidance, 2 September 2020*. Geneva: World Health Organization (2020).

5. Busani S, Bedini A, Biagioni E, Serio L, Tonelli R, Meschiari M, et al. Two fatal cases of acute liver failure due to HSV-1 infection in COVID-19 patients following immunomodulatory therapies. *Clin Infect Dis.* (2021) 73:e252–5. doi: 10.1093/cid/ciaa1246

6. Ritchie AI, Singanayagam A. Immunosuppression for hyperinflammation in COVID-19: a double-edged sword?. *Lancet.* (2020) 395:1111. doi: 10.1016/S0140-6736(20)30691-7

7. Cantan B, Luyt C-E, Martin-Loeches I. Influenza infections and emergent viral infections in intensive care unit. *Semin Respir Crit Care Med.* (2019) 40:488–97. doi: 10.1055/s-0039-1693497

8. Taplitz RA, Jordan MC. Pneumonia caused by herpesviruses in recipients of hematopoietic cell transplants. *Semin Respir Infect.* (2002) 17:121–9. doi: 10.1053/srin.2002.33447

9. Drori A, Ribak Y, van Heerden PV, Meir K, Wolf D, Safadi R. Hemophagocytic lymphohistiocytosis due to acute primary herpes simplex virus 1 infection. *J Clin Virol.* (2015) 68:6–10. doi: 10.1016/j.jcv.2015.04.013

10. Ramos-Casals M, Brito-Zerón P, López-Guillermo A, Khamashta MA, Bosch X. Adult haemophagocytic syndrome. *Lancet.* (2014) 383:1503–16. doi: 10.1016/S0140-6736(13)61048-X

11. Filipovich A, McClain K, Grom A. Histiocytic disorders: recent insights into pathophysiology and practical guidelines. *Biol Blood Marrow Transplant.* (2010) 16:S82–9. doi: 10.1016/j.bbmt.2009.11.014

12. Stone JH, Frigault MJ, Serling-Boyd NJ, Fernandes AD, Harvey L, Foulkes AS, et al. Efficacy of tocilizumab in patients hospitalized with Covid-19. *N Engl J Med.* (2020) 383:2333–44. doi: 10.1056/NEJMoa2028836

13. Cunha BA, Eisenstein LE, Dillard T, Krol V. Herpes simplex virus (HSV) pneumonia in a heart transplant: diagnosis and therapy. *Heart Lung.* (2007) 36:72–8. doi: 10.1016/j.hrtlng.2006.07.005

14. Jordan MB, Allen CE, Weitzman S, Filipovich AH, McClain KL. How I treat hemophagocytic lymphohistiocytosis. *Blood.* (2011) 118:4041–52. doi: 10.1182/blood-2011-03-278127

15. Guimarães PO, Quirk D, Furtado RH, Maia LN, Saraiva JF, Antunes MO, et al. Tofacitinib in patients hospitalized with Covid-19 pneumonia. *N Engl J Med.* (2021) 385:406–15. doi: 10.1056/NEJMoa2101643

16. Strand V, Ahadieh S, French J, Geier J, Krishnaswami S, Menon S, et al. Systematic review and meta-analysis of serious infections with tofacitinib and biologic disease-modifying antirheumatic drug treatment in rheumatoid arthritis clinical trials. *Arthritis Res Ther.* (2015) 17:362. doi: 10.1186/s13075-015-0880-2

17. Winthrop KL. The emerging safety profile of JAK inhibitors in rheumatic disease. *Nat Rev Rheumatol.* (2017) 13:234–43. doi: 10.1038/nrrheum.2017.23

18. Curtis JR, Xie F, Yun H, Bernatsky S, Winthrop KL. Real-world comparative risks of herpes virus infections in tofacitinib and biologic-treated patients with rheumatoid arthritis. *Ann Rheumat Dis.* (2016) 75:1843–7. doi: 10.1136/annrheumdis-2016-209131

19. Krzyzowska M, Jarneborn A, Thorn K, Eriksson K, Jin T. Tofacitinib treatment in primary herpes simplex encephalitis interferes with anti-viral response. *J Infect Dis.* (2022) 225:1545–53. doi: 10.1093/infdis/jiac040

20. Freytag MR, Jørgensen SE, Thomsen MM, Al-Mousawi A, Hait AS, Olagnier D, et al. Postpartum disseminated HSV-1 infection with hemophagocytic lymphohistiocytosis and fulminant neonatal herpes infection. *J Infect Dis.* (2021) 225:157–62. doi: 10.1093/infdis/jiab290

21. Retamozo S, Brito-Zerón P, Sisó-Almirall A, Flores-Chávez A, Soto-Cárdenas M-J, Ramos-Casals M. Haemophagocytic syndrome and COVID-19. *Clin Rheumatol.* (2021) 40:1233–44. doi: 10.1007/s10067-020-05569-4

22. Sandler RD, Tattersall RS, Schoemans H, Greco R, Badoglio M, Labopin M, et al. Diagnosis and management of secondary HLH/MAS following HSCT and CAR-T cell therapy in adults; a review of the literature and a survey of practice within EBMT centres on behalf of the autoimmune diseases working party (ADWP) and transplant complications working party (TCWP). *Front Immunol.* (2020) 11:524. doi: 10.3389/fimmu.2020.00524

frontiers | Frontiers in Medicine

TYPE Case Report
PUBLISHED 25 November 2022
DOI 10.3389/fmed.2022.1057591

OPEN ACCESS

EDITED BY
Yuetian Yu,
Shanghai Jiao Tong University, China

REVIEWED BY
Chuan Huang,
Reproductive & Genetic Hospital of Citic-Xiangya, China
Tsuneaki Kenzaka,
Kobe University, Japan

*CORRESPONDENCE
Eunice J. Y. Kok
eunicekokjy@gmail.com

SPECIALTY SECTION
This article was submitted to Intensive Care Medicine and Anesthesiology, a section of the journal Frontiers in Medicine

RECEIVED 29 September 2022
ACCEPTED 08 November 2022
PUBLISHED 25 November 2022

CITATION
Kok EJY and Lee YL (2022) *Ureaplasma urealyticum* infection presenting as altered mental status in a post-chemotherapy patient: Case report and literature review. *Front. Med.* 9:1057591. doi: 10.3389/fmed.2022.1057591

Ureaplasma urealyticum infection presenting as altered mental status in a post-chemotherapy patient: Case report and literature review

Eunice J. Y. Kok* and Y. L. Lee

Division of Anesthesiology, Singapore General Hospital, Singapore, Singapore

Hyperammonemia due to Ureaplasma infection is rare but often fatal, largely due to the delayed recognition, diagnosis, and treatment of the condition. It has mostly been described in solid organ transplant patients in the literature. This case presents the diagnostic challenge of an immunocompromised patient with previous resected pancreatic head adenocarcinoma and chemotherapy, presenting with altered mental status due to hyperammonemia from Ureaplasma infection. It is imperative to consider this condition in unexplained hyperammonemia, especially in immunocompromised patients. Timely diagnosis of this condition can help to reduce complications from encephalopathy such as cerebral edema and seizures.

KEYWORDS

***Ureaplasma urealyticum*, hyperammonemia, altered mental status (AMS), immunocompromised, chemotherapy, cancer**

Introduction

Ureaplasma infection is a rare cause of non-cirrhotic hyperammonemia. The literature surrounding this topic is largely limited to case reports and series. It has been traditionally described in solid organ transplant recipients, but there has been increasing numbers of reports on this in immunocompromised, non-transplant patients (1–3). Here, we describe the diagnostic challenge of a case of hyperammonemia syndrome due to Ureaplasma infection in a post-chemotherapy patient, discuss our approach to altered mental status (AMS), and review the available literature on hyperammonemia syndrome due to Ureaplasma infections. Written consent has been obtained from the patient's relative in accordance with Singapore's research ethics guidelines.

Case description

The case is a 67-year-old female with hypertension, hyperlipidemia, and left breast cancer for which she underwent a mastectomy and adjuvant chemotherapy from 2016 to 2017. In July 2020, she was diagnosed with a second malignancy—locally advanced pancreatic head adenocarcinoma, received neoadjuvant chemotherapy from August 2020 to January 2021, surgical resection (total pancreatectomy, extended right hemicolectomy and portal vein resection) in May 2021, and adjuvant chemotherapy from 18 October 2021 to 31 October 2021.

In December 2021, she attended a routine clinic review and was found to be significantly malnourished—she had extremely poor oral intake, wasting of muscle bulk, a body mass index of 18.9, and severe hypoalbuminemia (albumin 15 g/L; reference range 40–50 g/L). Her vital signs were stable—temperature of 36.2 degrees Celsius, blood pressure was 103/67 mmHg, heart rate of 91 beats per minute, and SpO2 96% on room air. She was admitted for inpatient enteral nutrition support. She remained well for a week before developing acute AMS. Clinical examination revealed a gradual decline of her Glasgow Coma Scale (GCS) from 15 to 11 over several days, but was otherwise unremarkable with no focal neurological deficits.

An extensive biochemistry panel revealed hyperammonemia (with an initial ammonia level of 144 umol/L; reference range 16–53 umol/L), hypophosphatemia (0.57 mmol/L; reference range 0.94–1.50 mmol/L), and micronutrient (zinc, copper, selenium, vitamin A, vitamin D2, vitamin D3, vitamin E) deficiencies. There was suspicion of an acute coronary syndrome in view of new anterolateral ST segment elevations on her electrocardiogram and raised troponin levels, but this was ruled out with a negative coronary angiogram and attributed to stress cardiomyopathy with a depressed ejection fraction of 25%. Neuroimaging (computed tomography and magnetic resonance imaging of brain, magnetic resonance angiogram of brain) was normal. An electroencephalogram showed severe diffuse encephalopathy with generalized triphasic waves suggestive of metabolic encephalopathy. Basic microbiological investigations including aerobic and anaerobic blood cultures, she was initially managed for metabolic encephalopathy, likely contributed by constipation, hyperammonemia, electrolyte imbalance, and stress cardiomyopathy. Her mental status improved to normal with regular opening of bowels and electrolytes correction.

However, her neurological status gradually deteriorated from a GCS of 15 to 3 over the next 2 weeks, associated with multiple episodes of hypoglycemia. There was no improvement to her mental status after correction of hypoglycemia. Thus, a repeat workup including neuroimaging, electroencephalogram and lumbar puncture was performed. A comprehensive panel of microbiological investigations—including aerobic and anaerobic bacterial blood cultures, fungal blood cultures, viral serology panel,[1] sputum cultures, urine cultures, cerebrospinal fluid (CSF) cultures, CSF meningoencephalitis panel,[2] tests for syphilis infection and tuberculosis infection—was also sent. The investigations were significant for hyperammonemia (234 umol/L), positive urine cultures for *Escherichia coli*, and positive sputum cultures for *Klebsiella pneumoniae* and *Stenotrophomonas maltophilia*. She was started on intravenous (IV) Meropenem and Minocycline to cover for these organisms, and concomitantly worked up for the underlying etiology of hyperammonemia.

A liver duplex ultrasound revealed possible right portal vein thrombosis. Hence, she underwent a percutaneous transhepatic biliary drainage, portal vein angioplasty and stenting. Her ammonia levels improved transiently to 74 umol/L but rose back up again after several days post-procedure with no improvement in neurology. Her blood and endotracheal aspirates were sent for Ureaplasma and Mycoplasma cultures. She had earlier been commenced on a course of Minocycline (IV Minocycline 200 mg loading dose, followed by 100 mg every 12 h for a week) to cover for the Stenotrophomonas pulmonary infection, as well as for empirical coverage of possible Ureaplasma infection. The blood culture eventually returned positive for *Ureaplasma urealyticum*. By this time, she had completed a week of Minocycline, and was continued on another week of Azithromycin (Oral Azithromycin 500 mg once daily). A repeat Ureaplasma blood culture thereafter was negative. The patient had undergone chemotherapy with *TS-One* (Tegafur, Gemeracil, Oteracil) in October 2021. However, her medical oncologist felt that the time frame (*TS-One* was given more than 6 weeks before her presentation of hyperammonemia) was not compatible with *TS-One* as the cause of her current encephalopathy or hyperammonemia. Finally, a metabolic panel for urea cycle disorders was sent and returned negative.

Simultaneously, supportive treatment was initiated to promote ammonia clearance with lactulose, rifaximin, sodium benzoate, and hemodialysis, as well as to reduce ammonia production through dietary protein restriction.

Retrospectively, we found that her mentation improved most dramatically with a combination of: (1) lowering her ammonia levels with dialysis, (2) treatment of Ureaplasma infection with the appropriate anti-microbials, (3) treatment with high dose thiamine for presumed thiamine deficiency, and (4) nutritional replacement for micronutrient deficiencies. The final diagnosis was metabolic encephalopathy contributed by thiamine deficiency (causing a Wernicke-like state), exacerbated by hyperammonemia from Ureaplasma infection,

1 The viral serology panel included evaluation for the following organisms: Hepatitis B, Hepatitis C, HIV, JC virus, Cytomegalovirus, Herpes Simplex virus, Varicella-Zoster virus.

2 The CSF meningoencephalitis panel included evaluation for the following organisms: *Escherichia coli*, *Hemophilus influenzae*, *Listeria monocytogenes*, *Neisseria meningitidis*, *Streptococcus agalactiae*, *Streptococcus pneumoniae*.

and micronutrient deficiencies related to a post-pancreatectomy state. Subsequently, with the appropriate treatment and normalization of ammonia levels, she recovered to full neurology and was able to follow instructions. However, her protracted intensive care unit (ICU) stay was complicated by critical illness myopathy. She was discharged from ICU after 41 days but eventually succumbed to nosocomial infections and passed on day 83 of her hospital stay.

Table 1 shows the timeline of events that occurred.

TABLE 1 Timeline of events.

Date	Events
December 23, 2021	• Found to be significantly malnourished at a routine clinic review • Admitted for inpatient enteral nutrition support
January 1, 2022	• Developed altered mental status • Biochemistry panel sent for evaluation of altered mental status ⇒ Hyperammonemia (144 umol/L), hypophosphatemia, micronutrient deficiencies ⇒ Coronary angiogram done in view of new anterolateral ST segment elevations on ECG and raised troponin levels • Coronary angiogram negative for significant coronary vessel occlusion ⇒ Diagnosed with stress cardiomyopathy with a depressed ejection fraction of 25%
January 13, 2022	• GCS gradually dropped from 15 to E3V5M3 • Hypoglycemia (capillary blood glucose 2.0 mmol/L) detected and corrected, but no improvement in mental status
January 14, 2022	• CT brain performed for altered mental status and worsening GCS—normal • Developed hospital-acquired pneumonia and urinary tract infection, started on broad-spectrum IV antibiotics
January 18, 2022	• GCS dropped further to 3 • EEG performed for altered mental status and worsening GCS—severe diffuse encephalopathy with generalized triphasic waves suggestive of metabolic encephalopathy
January 19, 2022	• MRI brain performed for altered mental status and worsening GCS—normal
January 21, 2022	• Developed type 2 respiratory failure from severe hospital-acquired pneumonia ⇒ Intubated and sent to ICU • Initial impression was septic encephalopathy secondary to bilateral hospital-acquired pneumonia • Worsening hyperammonemia—peak 234 umol/L • Started on hemodialysis for ammonia clearance
January 22–30, 2022	• No improvement in mental status despite adequate treatment of hospital-acquired pneumonia • Ureaplasma blood culture sent on January 27, 2022, started on empirical Minocycline
January 31, 2022	• Repeat biochemistry panel, EEG and neuroimaging done—significant for hyperammonemia and severe diffuse encephalopathy likely from metabolic causes • Metabolic panel for urea cycle disorders sent—normal • Liver duplex ultrasound performed for evaluation of possible shunt as a cause of hyperammonemia—possible right portal vein thrombosis
February 1, 2022	• Underwent a percutaneous transhepatic biliary drainage (PTBD) and portal vein angioplasty and stenting for possible portal vein thrombosis • Ammonia levels improved transiently to 74 umol/L after the procedure, but rose back up again • No improvement in mental status

(Continued)

Discussion

This case demonstrated the diagnostic challenge of a patient with a background resected pancreatic head adenocarcinoma and previous chemotherapy, presenting with AMS. After an extensive evaluation, she was found to have hyperammonemia syndrome secondary to Ureaplasma infection. To our knowledge, this is first reported case of hyperammonemia syndrome due to Ureaplasma infection presenting in a post-chemotherapy patient (the only other similar case being a patient undergoing chemotherapy). This case adds to the growing amount of literature and interest in this topic, especially in non-transplant patients, and emphasizes the post-chemotherapy, immunocompromised state as a plausible risk factor for disseminated Ureaplasma infections. Certainly, this will require further reports of similar cases and a more rigorous study methodology to test the conceivability and validity of this hypothesis.

Evaluation of altered mental status

Altered mental status is a broad presentation with a myriad of differential diagnoses. The first step (shown in Table 2) is to differentiate between an acute or subacute disease, and chronic cognitive decline. Here, we endeavor to create our systematic approach to this clinical presentation with a focus on the acute and subacute etiologies (refer to Figure 1).

History taking is often limited from patients with AMS, hence it is prudent to obtain collaborative history from the patient's relatives and caregivers. A detailed drug chart including over-the-counter medications, traditional medications and other possible use of illicit substances is also essential. Physical examination begins with an assessment of the patient's airway, breathing, and circulation, followed by a full neurological examination to check for focal neurological deficits. Additionally, an assessment of the perfusion status, looking for signs of a prior trauma, localizing signs of infection, and signs of organ failures can provide relevant and valuable information.

Point-of-care testing is simple, convenient, and very useful in the evaluation. This includes a fingerstick test for capillary

TABLE 1 (Continued)

Date	Events
February 4, 2022	• Lumbar puncture performed—CSF biochemistry panel normal, CSF cultures normal, syphilis screen negative, autoimmune encephalitis panel normal, paraneoplastic panel normal • Mental status started to improve
February 8, 2022	• First Ureaplasma blood culture sent on January 27, 2022 returned as positive • 1 week of Minocycline completed • Second Ureaplasma blood culture sent • Started on Azithromycin
February 9–March 14, 2022	• Mental status continued to improve, gradually returned to her normal baseline • Suffered a series of nosocomial and opportunistic infections—intra-abdominal sepsis from PTBD leak and cytomegalovirus colitis, catheter-associated urinary tract infection, candidemia
March 15, 2022	• Developed acute respiratory failure with hemodynamic instability from new severe pneumonia and fluid overload • Passed on day 83 of hospital stay

blood glucose to check for hypoglycemia, and an arterial blood gas to check for respiratory failure and metabolic derangements.

The choice of laboratory and radiological investigations should be guided by the clinical picture obtained from history taking and physical examination. **Table 3** shows a non-exhaustive list of investigations.

Hyperammonemia in Ureaplasma infections

Ureaplasma species is commonly found as a urogenital commensal and typically has low pathogenicity (4). However, two specific organisms *Ureaplasma urealyticum* and *Ureaplasma parvum* have been increasingly reported to cause disease, most commonly in the form of hyperammonemia syndrome. Hyperammonemia syndrome is characterized by high serum ammonia concentrations [there is no defined level but some suggest an upper limit of 200 umol/L (5)] with new onset or progressive neurological dysfunction (1, 5).

TABLE 2 Step 1 in the approach to altered mental status (AMS)—acute or subacute disease vs. chronic cognitive decline.

	Delirium	Dementia	Depression
Onset	Acute, hours to days	Insidious, chronic, months to years	Variable
Course/ Progression	Fluctuating	Progressive	Variable
	Sun-downing	Sun-downing	
Orientation	Disoriented	Oriented until later stages	Usually oriented
Attention	Inattentive	Attentive	Inattentive
Speech and language	Incoherent, illogical	Aphasia, anomia	Normal
Affect/Mood	Dysphoric, labile	Depressed, abulic	Depressed
Sleep	Disturbed sleep-wake cycle	Reversed sleep-wake cycle	Early morning awakening

Ureaplasma contains urease, an enzyme which hydrolyzes urea to ammonia and carbon dioxide. This hydrolysis reaction provides a potential gradient to generate energy for the organism in the form of adenosine triphosphate (6). Simultaneously, the ammonia product from the hydrolysis reaction becomes a substrate for the synthesis of more urea, thereby perpetuating this cycle and the growth of the Ureaplasma organism (7). It is widely postulated that the eventual build-up of ammonia to supernormal levels causes neurological dysfunction from metabolic encephalopathy due to hyperammonemia, which can lead to fatal complications such as cerebral edema and brain herniation (1).

While hyperammonemia syndrome was described almost three decades ago by Davies et al. (8) it was not until Bharat et al.'s landmark paper (7) in 2015 that there was a postulated link between Ureaplasma infection and hyperammonemia. In a case series in lung transplant patients, Bharat described several patients who had unexplained, fatal hyperammonemia syndrome. This was eventually attributed to Ureaplasma infection, after Ureaplasma organisms were isolated in the bronchoalveolar lavage cultures and blood cultures of both the donors of the affected recipients, and the affected recipients. Since then, there have been several other case reports on hyperammonemia from Ureaplasma infections. A systematic review and meta-analysis on hyperammonemia syndrome associated with Ureaplasma spp. infections in immunocompromised patients and transplant recipients suggested that there was a higher incidence of hyperammonemia syndrome in Ureaplasma-positive lung transplant recipients (41.67%) as compared to Ureaplasma-negative recipients (2.84%) (1). The affected population is mostly solid organ transplant recipients (lung and kidney), with a few reported cases on immunocompromised patients such as those with hematological malignancies (9, 10), those undergoing hematopoietic stem cell transplant (3) and those undergoing chemotherapy (11).

The clinical presentation of hyperammonemia from Ureaplasma infection is usually neurological dysfunction—it may present as AMS, agitation, disorientation, lethargy, confusion, drowsiness, and a drop in the GCS, or seizures (3). Laboratory investigations are often unremarkable apart from hyperammonemia with normal neuroimaging. Electroencephalograms may show diffuse encephalopathy typical of metabolic encephalopathy.

Hyperammonemia from Ureaplasma infections has been described in several reports to be fatal without prompt recognition, diagnosis and treatment with a mortality rate

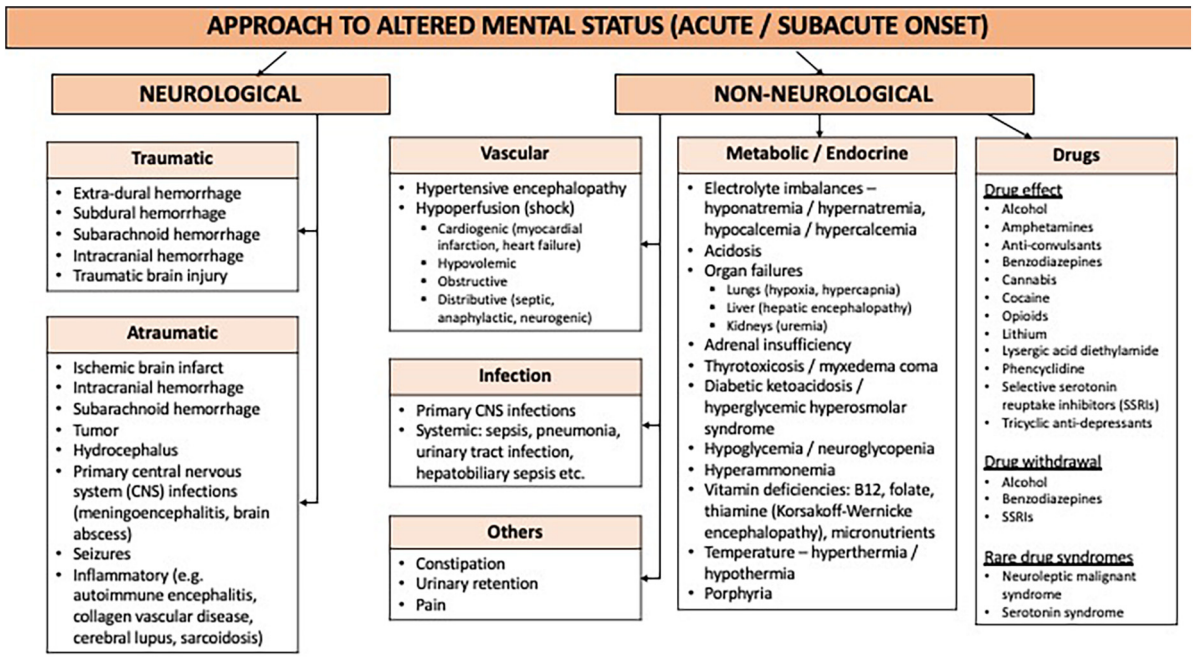

FIGURE 1
Approach to altered mental status (AMS) (acute and subacute onset).

in immunocompromised and post-transplant patients of 42–75% (12). Hence, there should be a high index of suspicion for Ureaplasma infection this subgroup of patients and investigation performed. Hyperammonemia from Ureaplasma infections is notorious for not responding well to usual ammonia-lowering strategies without the appropriate anti-microbial treatment for the Ureaplasma infection (13). As Ureaplasma species lack a cell wall, they are unable to be visualized with gram stain nor cultured in conventional medium (13), and hence require a special culture medium for growth and identification. This may take several days to a week to be out and so empirical use of antibiotics to cover for Ureaplasma have been recommended so as not to delay treatment which could result in major morbidity and mortality (11, 13). Some centers offer molecular testing for Ureaplasma species in the form of polymerase chain reaction (PCR) assays. There are two types of PCR assays—gel-based conventional PCR assays which use targeted sequences of 16s ribosomal ribonucleic acid found in Ureaplasma species, and real-time PCR assays which identify urease genes and their subunits (14). These PCR assays have a turnaround time of a few hours—significantly faster than that for the Ureaplasma culture.

There are two main tenets in the management of this syndrome. First, treat the underlying cause (Ureaplasma infection) with the appropriate anti-microbials. As Ureaplasma species lack a cell wall, they do not respond well to beta-lactams. As such, antibiotics such as macrolides, tetracyclines, and fluoroquinolones are recommended (6, 15). There is some debate about whether a single agent or combination therapy (with more than one agent from different classes) is a better option for treatment—no high-quality, conclusive evidence has been presented thus far. In our patient, a single agent

TABLE 3 Investigations for the workup of altered mental status (AMS).

Laboratory	Radiological
• Full blood count • Biochemistry panel—electrolytes (sodium, potassium, calcium, phosphate), glucose, urea, creatinine, bicarbonate • Liver function test • Arterial blood gas • Thyroid function test • Ammonia • Thiamine • Serum B12 and folate • Micronutrients (zinc, copper, selenium, vitamin A, vitamin D2, vitamin D3, vitamin E) • Syphilis panel • Blood and urine toxicology • Urinalysis • Lumbar puncture (opening pressure, CSF glucose and protein, CSF white blood cells and red blood cells, gram stain and culture, acid fast bacilli smear and culture, fungal microscopy, meningitis multiplex/tetraplex panels, cytology, oligoclonal band) • Autoimmune encephalitis panel • Serum paraneoplastic panel	Neuroimaging • CT brain • MRI brain and angiogram Systemic infection • Chest X-ray • CT thorax, abdomen, pelvis **Others** • Electroencephalogram • Electrocardiogram

(Minocycline) seemed to have been sufficient for eradication of the Ureaplasma bacteremia. The second agent (Azithromycin) was started after the second Ureaplasma blood culture was taken, with the intent of not delaying treatment should the culture return as positive for Ureaplasma a week later. The second Ureaplasma blood culture turned out to be negative. If there are infected collections, surgical drainage should be considered for source control, in addition to anti-microbial treatment (15).

Second, lowering the serum ammonia with strategies to promote ammonia clearance and to reduce ammonia production. Lactulose acidifies the gut, and causes ammonia to be ionized into ammonium, which reduces the absorption and increases the excretion of ammonia from the gastrointestinal tract (16). Rifampicin is an anti-microbial used to reduce ammonia-producing bacteria (17, 18). Dietary modifications can be made to reduce the protein load so as to reduce the substrate for ammonia production (16). In our patient, the protein content in her diet was restricted to 0.8 g/kg/day, and was gradually increased back to 1.2–1.5 g/kg/day with improving ammonia levels. Nitrogen scavengers such as sodium benzoate and sodium phenylbutyrate promote the diversion of nitrogen away from the urea cycle, to other metabolic pathways (18). Finally, hemodialysis may be indicated for hyperammonemia that is refractory to medical therapy. Ammonia is a small molecule, water soluble and not highly protein bound—these intrinsic qualities allow it to be efficiently cleared by hemodialysis. Higher efficiency dialysis (with higher blood flow rate, higher dialysate flow rate, and larger dialyzer membrane surface area) results in better ammonia clearance (19), and has been associated with increased survival in post-lung transplantation patients with hyperammonemia syndrome (20).

Conclusion

Ureaplasma species infections should be considered in patients with unexplained hyperammonemia, and particularly in immunocompromised patients (such as patients who are undergoing or have undergone systemic chemotherapy) who are more susceptible to disseminated infections. Given the high mortality of untreated hyperammonemia syndrome from Ureaplasma infections, prompt recognition, diagnosis and treatment are the cornerstones in the management of this condition. It is important to consider empirical antibiotics for Ureaplasma infections before the Ureaplasma culture or PCR results are out. The increasing awareness about this condition in the medical and scientific community is encouraging and a big step forward in reducing major morbidity and mortality from this treatable condition.

Data availability statement

The original contributions presented in this study are included in the article/supplementary material, further inquiries can be directed to the corresponding author.

Author contributions

EK helped to conceptualize and write the manuscript. YL helped to conceptualize and review the manuscript. Both authors contributed to the article and approved the submitted version.

Conflict of interest

The authors declare that the research was conducted in the absence of any commercial or financial relationships that could be construed as a potential conflict of interest.

Publisher's note

References

1. Tantengco OAG, De Jesus FCC II, Gampoy EFS, Ornos EDB, Vidal MS Jr., Abad CLR. Hyperammonemia syndrome associated with *Ureaplasma* spp. Infections in immunocompromised patients and transplant recipients: a systematic review and meta-analysis. *Clin Transplant.* (2021) 35:e14334. doi: 10.1111/ctr.14334

2. Tawfik P, Arndt P. Lethal hyperammonemia in a CAR-T cell recipient due to *Ureaplasma* pneumonia: a case report of a unique severe complication. *BMJ Case Rep.* (2021) 14:e242513. doi: 10.1136/bcr-2021-242513

3. Graetz R, Meyer R, Shehab K, Katsanis E. Successful resolution of hyperammonemia following hematopoietic cell transplantation with directed treatment of *Ureaplasma parvum* infection. *Transpl Infect Dis.* (2018) 20:e12839. doi: 10.1111/tid.12839

4. Paparoupa M, Barten MJ, de Heer J, Giessen HS, Frings D, Kluge S. Hyperammonemia by *Ureaplasma urealyticum* pneumonia after lung transplantation. *Respir Med Case Rep.* (2020) 30:101080. doi: 10.1016/j.rmcr.2020.101080

5. Roberts SC, Bharat A, Kuhihara C, Tomic R, Ison MG. Impact of screening and treatment of *Ureaplasma* species on hyperammonemia syndrome in lung transplant recipients: a single center experience. *Clin Infect Dis.* (2021) 73:e2531–7. doi: 10.1093/cid/ciaa1570

6. Matson KM, Sonetti DA. Successful treatment of *Ureaplasma*-induced hyperammonemia syndrome post-lung transplant. *Transpl Infect Dis.* (2019) 21:e13022. doi: 10.1111/tid.13022

7. Bharat A, Cunningham SA, Scott Budinger GS, Kreisel D, DeWet CJ, Gelman AE, et al. Disseminated *Ureaplasma* infection as a cause of fatal hyperammonemia in humans. *Sci Transl Med.* (2015) 7:284re3. doi: 10.1126/scitranslmed.aaa8419

8. Davies SM, Szabo E, Wagner JE, Ramsay NK, Weisdorf DJ. Idiopathic hyperammonemia: a frequently lethal complication of bone marrow transplantation. *Bone Marrow Transplant.* (1996) 17:1119–25.

9. Placone N, Kao RL, Kempert P, Ruiz ME, Casillas JN, Okada M, et al. Hyperammonemia from *Ureaplasma* infection in an immunocompromised child. *J Pediatr Hematol Oncol.* (2019) 42:e114–6. doi: 10.1097/MPH.0000000000001414

10. Smith M, Crews JD, Cheek N, Srivastava R, Appachi E. Hyperammonemic encephalopathy due to *Ureaplasma parvum* infection in an immunocompromised child. *Pediatrics.* (2019) 144:e20190601. doi: 10.1542/peds.2019-0601

11. Nowbakht C, Edwards AR, Rodriguez-Buritica DF, Luce AM, Doshi PB, De Golovine A, et al. Two cases of fatal hyperammonemia syndrome due to *Mycoplasma hominis* and *Ureaplasma urealyticum* in immunocompromised patients outside lung transplant recipients. *Open Forum Infect Dis.* (2019) 6:ofz033. doi: 10.1093/ofid/ofz033

12. Chen C, Bain KB, Iuppa JA, Yusen RD, Byers DE, Patterson GA, et al. Hyperammonemia syndrome after lung transplantation: a single center experience. *Transplantation.* (2016) 100:678–84. doi: 10.1097/TP.0000000000000868

13. Higgins AB, Farmakiotis D, Rogers R, Osband AJ, Seo A, Chen B, et al. Hyperammonemia syndrome due to *Ureaplasma urealyticum* in a kidney transplant recipient: a case of disseminated disease from a fluoroquinolone-resistant isolate. *Transpl Infect Dis.* (2020) 22:e13328. doi: 10.1111/tid.13328

14. Waites KB, Xiao L, Paralanov V, Viscardi RM, Glass JI. Molecular methods for the detection of *Mycoplasma* and *Ureaplasma* infections in humans. *J Mol Diagn.* (2012) 14:437–50. doi: 10.1016/j.jmoldx.2012.06.001

15. Cannon CA, Corcorran MA, Shaw KW, Montenovo M, Sibulesky L, Reyes JD, et al. Hyperammonemia syndrome due to *Ureaplasma* infection after liver-kidney transplant. *Transpl Infect Dis.* (2020) 22:e13298. doi: 10.1111/tid.13298

16. Leger RF, Silverman MS, Hauck ES, Guvakova KD. Hyperammonemia post lung transplantation: a review. *Clin Med Insights Circ Respir Pulm Med.* (2020) 14:1179548420966234. doi: 10.1177/1179548420966234

17. Buzo BF, Preiksaitis JK, Halloran K, Nagendran J, Townsend DR, Zelyas N, et al. Association between *Mycoplasma* and *Ureaplasma* airway positivity, ammonia levels, and outcomes post-lung transplantation: a prospective surveillance study. *Am J Transplant.* (2021) 21:2123–31. doi: 10.1111/ajt.16394

18. McLaughlin DC, Mallea JM, Ng LK. Hyperammonemia presenting as refractory status epilepticus after lung transplant in a patient positive for *Ureaplasma parvum*. *Indian J Crit Care Med.* (2018) 22:463–5. doi: 10.4103/ijccm.IJCCM_356_17

19. Fenves AZ, Schwartz JC, Rees L. *Intermittent Dialysis and Continuous Modalities for Patients with Hyperammonemia. UpToDate*. (2021). Available online at: https://www.uptodate.com/contents/intermittent-dialysis-and-continuous-modalities-for-patients-with-hyperammonemia?search=hyperammonemia&source=search_result&selectedTitle=1~{}130&usage_type=default&display_rank=1#H2552795378 (accessed July 13, 2022).

20. Anwar S, Gupta D, Ashraf MA, Khalid SA, Rizvi SM, Miller BW, et al. Symptomatic hyperammonemia after lung transplantation: lessons learnt. *Hemodial Int.* (2014) 18:185–91. doi: 10.1111/hdi.12088

frontiers | Frontiers in Medicine

TYPE Case Report
PUBLISHED 08 December 2022
DOI 10.3389/fmed.2022.1058121

OPEN ACCESS

EDITED BY
Yuetian Yu,
Shanghai Jiao Tong University, China

REVIEWED BY
Gefei Wang,
Jinling Hospital, China
Marta Fogolari,
Campus Bio-Medico University, Italy

*CORRESPONDENCE
Mohammad Nizam Mokhtar
drnizam@ukm.edu.my

†These authors have contributed equally to this work and share senior authorship

SPECIALTY SECTION
This article was submitted to Intensive Care Medicine and Anesthesiology, a section of the journal Frontiers in Medicine

RECEIVED 30 September 2022
ACCEPTED 22 November 2022
PUBLISHED 08 December 2022

CITATION
Mokhtar MN, Azaharuddin I, Abdullah FH, Izaham A and Abdul Rahman R (2022) A rare case of *Pseudomonas putida* ventriculitis in intensive care unit: A case report. *Front. Med.* 9:1058121. doi: 10.3389/fmed.2022.1058121

A rare case of *Pseudomonas putida* ventriculitis in intensive care unit: A case report

Mohammad Nizam Mokhtar*, Izzuddin Azaharuddin, Farah Hanim Abdullah, Azarinah Izaham† and Raha Abdul Rahman†

Department of Anaesthesiology and Intensive Care, Faculty of Medicine, Universiti Kebangsaan Malaysia, Kuala Lumpur, Malaysia

Pseudomonas putida is a rare pathogen leading to nosocomial and central nervous system infections. Despite having a low virulence and being a rare organism to cause bacteremia, it can evolve into a multidrug-resistant organism and lead to mortality and morbidity in the intensive care setting. A 64-year-old male gardener was presented with extensive acute subarachnoid hemorrhage with intraventricular extension causing hydrocephalus requiring embolization and coiling following a cerebral angiogram, which showed bilateral posterior circulation aneurysm and left anterior circulation aneurysm. External ventricular drain (EVD) was inserted given the worsening hydrocephalus. During his stay in the intensive care unit (ICU), he was becoming more septic and a full septic workup including a cerebral spinal fluid culture taken from the indwelling catheter of the EVD and was found to be positive for a ceftazidime-sensitive strain of *P. putida*. Following the treatment with intravenous ceftazidime for 1 week and a revision of the EVD on day 32 of admission, he continued to recover well and showed an improvement in his Glasgow Coma Scale (GCS) and septic parameters. Eventually, he was able to wean off mechanical ventilation. He was discharged from ICU care to the neurosurgical ward with supplemental oxygen on day 42 of admission. It is necessary to be aware of the possibility of nosocomial *P. putida* infection, especially in patients with indwelling catheters, and to consider the early initiation of appropriate antibiotic regimens once detected as well as strict precautions in hygiene during the management of these patients to avoid further development of multi-drug resistant (MDR) strains.

KEYWORDS

***Pseudomonas putida*, ventriculitis, meningitis, nosocomial infection, external ventricular drain (EVD)**

Introduction

Pseudomonas putida is a member of the fluorescent group of pseudomonas (1). *P. putida* is a Gram-negative rod-shaped bacterium that is seen in soil, water, and moist environments. It may colonize the skin and may lead to opportunistic infections in immunocompromised patients. *P. putida* is a rare pathogen leading to nosocomial infections (2). Despite its low virulence, it can evolve into multi-drug resistant (MDR) organisms and lead to mortality and morbidity in the intensive care setting (2). In our local setting, we have encountered only three cases of *P. putida* infection in the past 5 years, two of which were bacteremia in immunocompromised patients, therefore, the prevalence of *P. putida* in our intensive care was found to be less than 0.1% of all Gram-negative infections. We report a case of ventriculitis with *P. putida* occurring in an immunocompetent host following a neurosurgical procedure.

Case presentation

A 64-year-old male gardener presented to the emergency department with hypertensive emergency and reduced consciousness. Computed Tomography (CT) brain upon admission revealed extensive acute subarachnoid hemorrhage with intraventricular extension causing hydrocephalus (**Figures 1**, **2**). He was admitted into our intensive care unit (ICU) following an external ventricular drain (EVD) insertion procedure to treat the hydrocephalus (**Figure 3**). The following day, he underwent cerebral aneurysm embolization and coiling following a cerebral angiogram, which showed a bilateral posterior circulation aneurysm and left anterior circulation aneurysm. Upon ICU admission, cerebral resuscitation was initiated and multiple attempts of weaning and extubation throughout a period of 2 weeks were done. Despite that, he had poor Glasgow Coma Scale (GCS) recovery, following which a tracheostomy was performed on day 21 of admission.

Subsequently, he became more septic with worsening hemodynamics requiring intravenous noradrenaline infusion to achieve a mean arterial pressure (MAP) of 80 mmHg and the increasing ventilatory requirement to maintain adequate oxygenation. He was treated for ventilator-associated pneumonia (VAP) evidenced by *Acinetobacter* sp. isolated from the tracheal aspirates. Despite the resolution of pneumonia following a 1-week course of high dose intravenous Unasyn® (ampicillin sodium/sulbactam sodium) evidenced by negative cultures from the tracheal aspirates and blood cultures, he

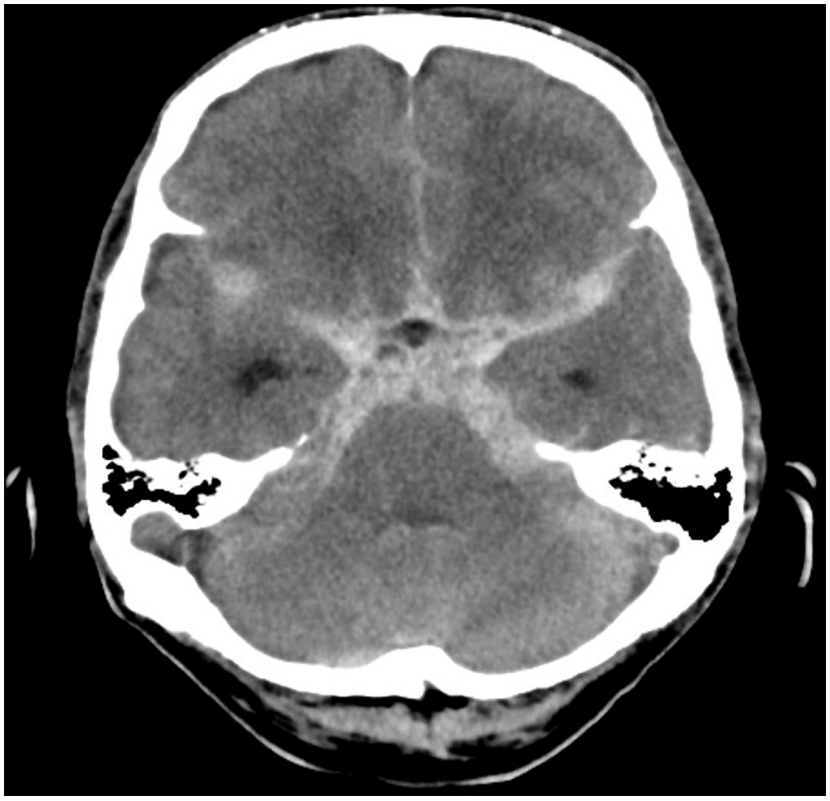

FIGURE 1
Computed tomography brain showing extensive acute subarachnoid hemorrhage.

FIGURE 2
Computed tomography brain showing intraventricular extension leading to hydrocephalus.

continued to be clinically septic with multiple spikes of the temperature of above 39.5°C. However, it was found the serum lactate was persistently within the range of 2.0–4.3 mmol/L, suggestive of ongoing sepsis; furthermore, other septic parameters such as procalcitonin and C-reactive protein (CRP) did not improve despite antibiotics (**Table 1**). The consciousness level also worsened during this episode of sepsis with a fluctuating GCS between 7 and 10. A full septic workup including a cerebral spinal fluid (CSF) culture was taken from the indwelling catheter of the EVD and was found to be positive for a *P. putida,* sensitive to ceftazidime with a minimum inhibitory concentration (MIC) of 1.5.

Following treatment with intravenous ceftazidime for 1 week and a revision of the EVD on day 32 of admission, his clinical condition improved with a GCS of 14 and was able to be weaned off from mechanical ventilation. A repeated CT brain excluded further complications or any new infections originating from the central nervous system (CNS). Infective markers including white cell count, CRP, and procalcitonin level showed significant reduction (**Table 1**). He was shifted from ICU care to the neurosurgical ward with supplemental oxygen on day 42 of admission for further rehabilitation.

Discussion

Ventriculitis often complicates external shunts and catheters involving the CNS which includes the commonly used EVD system in many neurosurgical cases with infection being one of the most common complications of this procedure where infection rates vary between 3.9 and 19% (3). The common pathogens that cause ventriculitis identified are coagulase-negative staphylococcus (62%) followed by *Enterococcus* sp. (19%) (4). Scheithauer et al. (5) reported that coagulase-negative staphylococci were the main pathogen (56%) responsible for meningitis, followed by *Staphylococcus aureus* (25%). A recent larger study done in 2021 states that the main pathogens were streptococci (44.9%), Gram-negative bacilli (27.6%), and staphylococci (15.3%) (6). Gram-negative ventriculitis is associated with a worse outcome in comparison with Gram-positive ventriculitis with mortality rates from 8 to 70% in more severe cases (7).

In our intensive care setting, *P. putida* is found in the environment together with other Gram-negative bacteria which include *Acinetobacter* sp. and *Stenotrophomonas* sp.

FIGURE 3
Computed tomography brain with EVD traversing through the right lateral ventricle with reduction of hydrocephalus.

TABLE 1 Range of infective markers during ICU stay.

Parameters	Day 1	Day 7	Day 14	Day 21	Day 28	Day 35	Day 42
White blood cell count ($\times 10^9$/L)	7.2	3.9	17.3	15.0	21.7	19.1	8.7
C-reactive protein (mg/dl)	0.91	19.27	25.56	28.11	33.78	25.71	2.33
Procalcitonin (ng/ml)	0.14	0.22	0.43	1.55	2.23	1.15	0.23
Lactate (mmol/L)	1.1	2.3	2.7	1.9	4.3	3.1	0.9

It can lead to nosocomial infections, especially in patients who are immunocompromised as well as those with invasive catheter placement and medical devices such as EVD (2, 8). Despite clinical data regarding *P. putida* infection being scarce given the low virulence of this organism, it is important to highlight its potential to cause nosocomial infection in our ICU settings and can develop MDR strains to most beta-lactam antibiotics. *P. putida* infection may also occur in immunocompetent patients, thus a high index of suspicion is very important for the diagnosis. Furthermore, CSF biochemistry can be indistinguishable from other forms of meningitis or ventriculitis. Therefore, CSF Gram staining and culturing are crucial in all patients with a suspected diagnosis of CNS infections.

Compared to *Pseudomonas aeruginosa* isolates, *P. putida* isolates were generally considered to have a low level of virulence and to be of little clinical significance. A series of cases of *P. putida* bacteremia was described by Yoshino et al. (8) in 2011 over 4 years with a total of 28 reports. It is typically associated with an indwelling device (61.9%) or immunocompromised state (85.7%). However, the prognosis of *P. putida* bacteremia is excellent following a targeted course of antibiotics with 92.9% cured with appropriate antimicrobial therapy and good source control which is the removal or exchange of the indwelling catheter (2, 8).

Pseudomonas putida is recognized as a rare pathogen of meningitis in adult patients and is usually associated with

indwelling CNS catheters. The presence of a solid tumor was the most common underlying disease related to the *P. putida* infection (n = 8, 44%), followed by traumatic intracranial hemorrhage (n = 2, 11%). A total of 44% of patients underwent surgery prior to diagnosis and 11% had an immunocompromised state with 89% of patients having exposure to antibiotics 1 month prior to infection. Most cases were related to indwelling catheters (2). Following this, the strategy that one could apply to prevent *P. putida* infection would be a strict aseptic technique when handling indwelling catheters. Cohort nursing is also important especially in the ICU setting to prevent cross infection between patients. Unnecessary peripheral lines or catheters should be removed promptly as it is a source of infection. If a *P. putida* infection has been isolated, a discussion with a clinical microbiologist for early commencement of appropriate antibiotics would be beneficial to prevent further complications.

Conclusion

Thus, it is necessary to be aware of the possibility of nosocomial *P. putida* infection, especially in patients with indwelling catheters, and to consider the early initiation of appropriate antibiotic regimens once detected as well as strict precautions in hygiene during the management of these patients to avoid further development of MDR strains.

Data availability statement

The raw data supporting the conclusions of this article will be made available by the authors, without undue reservation.

Ethics statement

Ethical review and approval was not required for the study on human participants in accordance with the local legislation and institutional requirements. The patients/participants provided their written informed consent to participate in this study. Written informed consent was obtained from the individual(s) for the publication of any potentially identifiable images or data included in this article.

Author contributions

MM, IA, and FA contributed in acquisition of data, relevant investigations, getting informed consent from the patient, and helping out in writing up the manuscript. RA and AI edited, critically revised, and proofread the manuscript. All authors contributed to the article and approved the submitted version.

Conflict of interest

The authors declare that the research was conducted in the absence of any commercial or financial relationships that could be construed as a potential conflict of interest.

Publisher's note

References

1. Hsueh PR, Teng LJ, Pan HJ, Chen YC, Sun CC, Ho SW, et al. Outbreak of *Pseudomonas fluorescens* bacteremia among oncology patients. *J Clin Microbiol.* (1998) 36:2914–7. doi: 10.1128/JCM.36.10.2914-2917.1998

2. Kim SE, Park SH, Park HB, Park KH, Kim SH, Jung SI, et al. Nosocomial *Pseudomonas putida* Bacteremia: high rates of carbapenem resistance and mortality. *Chonnam Med J.* (2012) 48:91–5. doi: 10.4068/cmj.2012.48.2.91

3. Yuen J, Selbi W, Muquit S, Berei T. Complication rates of external ventricular drain insertion by surgeons of different experience. *Ann R Coll Surg Engl.* (2018) 100:221–5. doi: 10.1308/rcsann.2017.0221

4. Hagel S, Bruns T, Pletz MW, Engel C, Kalff R, Ewald C. External ventricular drain infections: risk factors and outcome. *Interdiscip Perspect Infect Dis.* (2014) 2014:708531.

5. Scheithauer S, Bürgel U, Ryang YM, Haase G, Schiefer J, Koch S, et al. Prospective surveillance of drain associated meningitis/ventriculitis in a neurosurgery and neurological intensive care unit. *J Neurol Neurosurg Psychiatry.* (2009) 80:1381–5. doi: 10.1136/jnnp.2008.165357

6. Luque-Paz D, Revest M, Eugène F, Boukthir S, Dejoies L, Tattevin P, et al. Ventriculitis: a severe complication of central nervous system infections. *Open Forum Infect Dis.* (2021) 8:ofab216.

7. Tängdén T, Enblad P, Ullberg M, Sjölin J. Neurosurgical gram-negative bacillary ventriculitis and meningitis: a retrospective study evaluating the efficacy of intraventricular gentamicin therapy in 31 consecutive cases. *Clin Infect Dis.* (2011) 52:1310–6. doi: 10.1093/cid/cir197

8. Yoshino Y, Kitazawa T, Kamimura M, Tatsuno K, Ota Y, Yotsuyanagi H. *Pseudomonas putida* bacteremia in adult patients: five case reports and a review of the literature. *J Infect Chemother.* (2011) 17:278–82. doi: 10.1007/s10156-010-0114-0

frontiers | Frontiers in Medicine

TYPE Case Report
PUBLISHED 08 December 2022
DOI 10.3389/fmed.2022.1058824

OPEN ACCESS

EDITED BY
Yuetian Yu,
Shanghai Jiao Tong University, China

REVIEWED BY
Kazuo Yamashiro,
Juntendo University Urayasu Hospital, Japan
Jagadeesh Kalavakunta,
Michigan State University, United States

*CORRESPONDENCE
L. A. S. den Otter
ldenotter@spaarnegasthuis.nl

SPECIALTY SECTION
This article was submitted to Intensive Care Medicine and Anesthesiology, a section of the journal Frontiers in Medicine

RECEIVED 30 September 2022
ACCEPTED 19 October 2022
PUBLISHED 08 December 2022

CITATION
Otter LASd, Vermin B and Goeijenbier M (2022) Fat embolism syndrome in a patient that sustained a femoral neck fracture: A case report. *Front. Med.* 9:1058824. doi: 10.3389/fmed.2022.1058824

Fat embolism syndrome in a patient that sustained a femoral neck fracture: A case report

L. A. S. den Otter[1]*, B. Vermin[1] and M. Goeijenbier[1,2]

[1]Department of Intensive Care Medicine, Spaarne Gasthuis, Haarlem, Netherlands, [2]Department of Intensive Care Medicine, Erasmus Medical Center, Rotterdam, Netherlands

Background: We present a case of a patient with a femoral neck fracture that shows neurological impairment and respiratory distress 1 day after trauma, caused by the Fat Embolism Syndrome with the presence of Cerebral Fat Embolisms.

Case summary: A 75 year old female remained unresponsive after a hemi arthroplasty was performed because of a 1 day old femoral neck fracture. She rapidly developed respiratory insufficiency and an obstructive shock with right ventricle dilatation on transthoracic echocardiography. The diffusion-weighted MRI brain images showed the "Starfield" pattern, a radiologic phenomenon typical for FES. During 3 weeks of ICU admission the neurologic state slowly ameliorated.

Conclusion: The rare FES is a clinical diagnosis with mainly respiratory, neurologic and dermatologic symptoms in the setting of a trauma patient. Fat embolisms are able to reach the brain without the presence of a patent foramen ovale to cause neurological symptoms. Diagnosing FES remains challenging but the distinctive "Starfield" pattern on MRI scans is promising.

KEYWORDS

fat embolisms, fat embolism syndrome, cerebral fat embolisms, "Starfield" pattern, patent foramen ovale (PFO)

Introduction

Fat embolisms (FE) are defined as the presence of fat particles in the blood circulation and Fat Embolism Syndrome (FES) is a rare condition that occurs when FE result in symptoms and/or organ failure. FE seem to be common after trauma, with prospective studies and autopsy reports showing high incidences of FE (41–94%). Only a few of these patients however develop FES (recent reported incidence ranges from 1–11%) and even less patients are diagnosed with CFE (1–6). The pathophysiology of FES remains speculative and diagnosing FES challenging. Our case report illustrates the unpredictable clinical course of FES and the challenges when diagnosing FES.

Case report

A 75 year old female presented to the emergency room with a dislocated femoral neck fracture after a fall off her electrical bike on the left hip. She had a history of

chronic obstructive pulmonary disease gold (COPD)III, hypertension with stage III renal failure and an abdominal aortic aneurysm, for which an endovascular aortic repair was performed ('16) and later on an aortic bifurcation graft was inserted ('18). Since it was an isolated fall on her hip and the neurological exam was normal, a computed tomography (CT) scan of the brain was not performed. She was admitted to the surgical ward with systemic opioids and a femoral nerve catheter with bupivacaine 0.25% as analgesia and surgical fixation by a hemi arthroplasty was performed the next day. Anesthesia consisted of a spinal block with bupivacaine 0.5% and midazolam (2mg) was administered as part of sedation. After surgery she remained unresponsive with a Glasgow Coma Scale (GSC) of 4 (E2M1V1) and on examination the patient appeared to be sweating and showed an impaired breathing pattern. Her vital signs showed a mild tachycardia (110/min) with normal blood pressure. Arterial blood gas analysis showed a mild hypercapnia (pCO2 7.2 kPa). Other important lab values contained a hemoglobin level of 7.1 mmol/l, a leukocyte count of 26.4 $\times$ 10^9/l, a C-reactive protein level of 103 mg/l and a blood glucose level of 6.5 mmol/l. Naloxone was administered as an antidote for the opioids and Flumazenil as an antidote for midazolam, both without clinical effect. Fysostigmine was administered to treat a possible central anticholinergic syndrome, also without any clinical effect.

The patient was admitted to the Intensive Care Unit (ICU) with non-invasive ventilation for further diagnostics and treatment. The neurologist was consulted to exclude neurologic pathology for the impaired consciousness. Neurologic examination showed an impaired consciousness with a GCS of 4 (E2M1V1), no signs of lateralisation, pupils normal in size, shape and responsive to light, normotone muscle state and symmetrical hyporeflexia with indifferent Babinski reflexes. Within 1 hour her consciousness improved to a GCS of 7 (E2M4V1). A CT brain was not performed because of an improvement in consciousness and vital signs that were not typical for a neurologic origin of an impaired consciousness.

A few hours later, her clinical status deteriorated with an acute drop in blood pressure and hypoxia which made us decide to intubate and start mechanical ventilation. Subsequently a central venous line for vasopressors was placed. A chest X-ray was performed which showed no abnormalities. Bedside transthoracic echocardiography (TTE) of the heart showed a remarkable dilatation of the right ventricle with multiple hyperechoic particles (Figure 1). This made us think of Fat Embolism Syndrome (FES) as a cause for her neurologic, respiratory and hemodynamic symptoms. Her electrocardiogram (ECG) showed a sinus tachycardia without signs of acute ischemia.

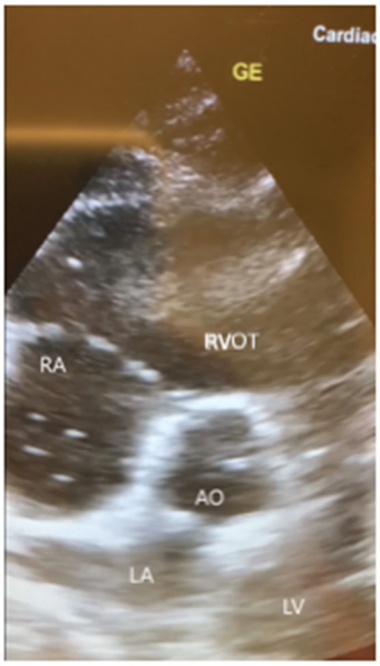

FIGURE 1
Images of bedside transthoracic echocardiography (subcostal 5-chamber view, short axis) of our patient showing a remarkable dilated right ventricle with multiple hyperechoic floating dots. RA, right atrium; RVOT, right ventricle outflow tract; LA, left atrium; LV, left ventricle; AO, aorta; GE, ultrasound marker.

A CT of the brain without contrast was performed and showed no abnormalities. A CT with contrast (arterial phase) of the thorax was performed which excluded pulmonary embolisms, but did confirm a widened right ventricle. On the third day of admission both a transthoracic and transesophageal ultrasound of the heart were performed which showed a dilatation of the right ventricle, no signs of ischemia and moreover no patent foramen ovale (PFO) or other intracardiac shunt. Having excluded other more common causes for the symptoms, we suspected FES as cause for the obstructive shock. Furthermore, we suspected cerebral fat embolisms (CFE) as a possible cause for the impaired consciousness. As recommended, we continued with "best supportive care", which mainly included mechanical ventilation for respiratory insufficiency and inotropic and vasopressor medication for an obstructive shock.

On day 4 of admission a CT scan of the brain with venous contrast was performed to exclude a basilar artery occlusion and did not show any abnormalities. On day 6 a magnetic resonance imaging (MRI) scan of the brain was performed which showed diffuse small foci of reduced diffusion and edema on the diffusion-weighted scan (Figure 2) as well

Abbreviations: CFE, Cerebral Fat Embolisms; FE, Fat embolisms; FES, Fat Embolism Syndrome; GSC, Glasgow Coma Scale; PFO, Patent foramen ovale; TTE, Transthoracic echocardiography; TEE, Transesophageal echocardiography.

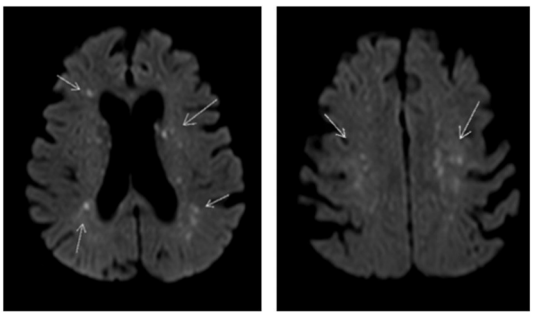

FIGURE 2
Diffusion weighted MRI scan of the brain of our patient showing multiple small foci of reduced diffusion and edema. Arrow shows small foci of reduced diffusion and edema.

as petechial hemorrhage on the T2-weighted scan. These lesions are described in literature as the "Starfield" pattern, a radiographic phenomenon suggestive for CFE. Patient remained hemodynamically stable after recovery and with the use of a tracheostoma she was weaned of mechanical ventilation. In light of her COPD gold III, we chose rapid weaning of mechanical ventilation using early tracheostomy to minimize muscle loss. During 3 weeks of ICU admission the neurologic state slowly ameliorated to a maximal EMV score with a partial recovery of verbal communication and an improving critical illness polyneuropathy.

Discussion

FES has mainly been reported to develop after traumatic fractures and sometimes after other traumatic events like burns and soft tissue injury (7). In rare cases, FES has been described after non-traumatic events like pancreatitis, sickle cell disease, corticosteroid therapy and lipid infusions (8). Risk factors for the development of FES include long-bone (mainly femur- and tibial shaft) and pelvic fractures, the presence of bilateral/multiple fractures and late fixation of the fractures (9). FES has been diagnosed in the adult and pediatric population and is mostly seen in males under the age of 30 years, probably because of the high incidence of trauma in this age group.

Symptoms of FES typically appear 24 to 48 h after sustaining the fracture and predominantly include a triad of respiratory, neurological and dermatological symptoms. Respiratory symptoms like tachypnea and dyspnea are the most common and respiratory signs can include hypoxemia, pulmonary edema and acute respiratory distress syndrome (ARDS). Although the severity of respiratory distress varies, fulminant respiratory failure which requires mechanical ventilation has been reported in 44% of FES cases (10). Massive FE can even lead to obstructive shock and can progress to acute right heart failure (11). Neurological features are reported in >50% of cases and can include confusion, an altered consciousness, seizures and/or focal neurological deficits (1). Again, the extent of these neurological impairment varies from mild confusion to refractory status epilepticus and brain death. Next to respiratory and neurologic symptoms and -signs, a petechial rash is the third most reported sign of FES that is mainly seen at the axillae, trunk and sclera. In our case, symptoms developed approximately 26–28 h after trauma and consisted of neurological impairment and respiratory failure. We did not observe a petechial rash.

The pathophysiology behind FES remains unknown but several theories have been proposed to clarify its pathogenesis. The mechanical theory suggests that bone marrow derived fat droplets enter the venous circulation as a result of increased medullary pressure caused by the fracture. These will at some point lead to occlusion, presumably in the pulmonary arterial circulation (7, 12). Activation of the clotting cascade by thromboplastin may play a role in this process, since FE in lung tissue appear to be surrounded by platelet aggregations. This "coagulation theory" will lead to expansion of the fat droplets in size, making it more likely to occlude a vessel (13). These mechanisms however do not account for the delay between the traumatic events and the symptoms.

The biochemical theory states that tissue lipases, products of a systemic inflammatory response induced by a stress state after trauma, break down fat particles into free fatty acids. These free fatty acids are toxic for and injure the endothelium, making it more susceptible for obstruction. This two-hit theory can explain the delay between the traumatic event and symptoms of FES and can also account for the non-traumatic cases of FES (14, 15).

FE can enter the arterial circulation by an intra-cardiac shunt like a PFO or through the lung capillary bed as micro-emboli to disseminate in the systemic (micro)circulation (16, 17). The latter being the suspected route to the brain in our patient since she did not seem to have a PFO.

Diagnosing FES is challenging since at this moment, there is no diagnostic tool that can diagnose FES. Diagnosis is often established at autopsy when FE are shown in organ systems which correlates with premortal clinical symptoms fitting for FES. Since FES is a rare disorder, more common causes of the respiratory or neurological symptoms must be excluded. Laboratory results and radiologic tests are all non-specific for FES. The most common lab findings include anemia (or a drop in hemoglobin) and thrombocytopenia.

A X ray or CT scan of the chest can show no abnormalities like in our case report or show non-specifics abnormalities like bilateral diffuse infiltrates and pulmonary oedema (18). Transoesophageal and transthoracic ultrasound of the heart have been used to detect fat emboli (16, 19). Our ultrasound images (Figure 1) are very similar to the images shown in case reports (20, 21).

A CT scan of the brain will mainly be used to exclude more common causes of neurological symptoms like cerebral

strokes and like our case, usually shows no abnormalities in FES patients. Remarkable is a typical pattern seen on the diffusion weighted MRI images of brains of patients with CFE. This so-called "Starfield" pattern consists of bilateral widely spread hyper intense foci of restricted diffusion and edema in both white and gray matter and at this point seems to be the most distinctive feature to FES (22–24). This "Starfield" pattern is easily recognized on diffusion weighted MRI images of our patient. Petechial hemorrhages can be seen in subacute stages op T2 MRI images, which was also seen on MRI images our patient (25). Repeating the MRI scan has shown complete resolution of these lesions in patients that clinically recovered from FES, suggesting MRI images correlate with the extent of neurological impairment (26, 27). Unfortunately, we do not have a repeated MRI scan of the brain.

The lack of a diagnostic tool makes FES a clinical diagnosis. Although no diagnostic scoring system has been validated, the most commonly used diagnostic criteria include the Gurd and Wilson criteria, consisting of major and minor criteria. Major criteria contain the triad of respiratory distress, cerebral symptoms (without the presence of head injury) and a petechial rash. Minor criteria include tachycardia, a fever, renal or retinal involvement, jaundice and lab results (thrombocytopenia, a descending hemoglobin level, an elevated erythrocyte sedimentation rate and fat macroglobulinemia). Diagnosis requires either two major criteria or one major and four minor criteria (28). The patient in our case met two major criteria (respiratory and cerebral involvement) and at least three minor criteria (tachycardia, thrombocytopenia, a drop in hemoglobin level) and according to Gurd and Wilson's criteria would suggest the presence of FES.

Treatment options are limited and at this moment. Heparin has been proposed as a therapeutic agent because it stimulates lipase enzyme activity which lowers intravascular lipid concentrations. Since the FES mainly occurs in trauma patients, the concomitant risk of bleeding makes the use of heparin controversial. With the biochemical theory in mind, corticosteroids were thought to be beneficial in treating and even preventing FES. Conflicting results of studies combined with a high rate of infectious complications are the main reason corticosteroids are not recommended as standard treatment for FES (29).

Due to the lack of therapeutic options, best supportive care to optimize oxygenation, ventilation and circulation is the only recommended treatment. Literature states a mortality rate with best supportive care lower than 10% and a full recovery of symptoms in most patients within days to 1 week (30). In a smaller subset of patients, FES sets a fulminant course and leads to death, with the main causes being respiratory failure, shock, and/or braindead.

Preventative measures have not been thoroughly researched yet and mainly focus on timing of surgery and surgical techniques. Early fixation of fractures has been suggested to reduce the incidence of FES by retrospective and prospective studies (31–33). For instance, using techniques to lower the intramedullary pressure during surgery (for instance using reamer systems with vacuum or venting options or applying intraoperative medullary cavity suction and/or irrigation) reduces the presence of FE (visualized by intraoperative TEE) (34, 35).

Conclusion

Whereas the presence of FE is common, FES is a rare disorder. Knowledge of the typical triad of respiratory, neurologic and dermatologic symptoms in the setting of a trauma patient is important to recognize FES. Diagnosing FES remains a challenge since there is no validated laboratory test or imaging modality that can diagnose FES. It remains a diagnosis of exclusion but distinctive patterns on MRI scans are promising and have potential to become the gold standard in diagnosing FES. Echocardiography should be used as a tool since it is easy to perform, non-invasive and might help raise suspicion for FES, like in our case. It is important to realize that even without the presence of a PFO, FE are able to reach the brain and cause neurological symptoms. Due to a lack of treatment options, best supportive care is the current therapeutic management with relatively good prognostic outcomes. However, in a minority of patients a fulminant FES is observed with potentially fatal outcomes. Patience is key in treating FES, as our case illustrates. This case report illustrates the turbulent clinical course and the remarkable recovery potential of FES and emphasizes the importance of a high suspicion of FES in trauma patients.

Data availability statement

The original contributions presented in the study are included in the article/supplementary material, further inquiries can be directed to the corresponding author/s.

Author contributions

LO study of literature and writing first draft. BV and MG reviewing and editing the first draft. All authors listed issued final approval of the version that is submitted.

Conflict of interest

The authors declare that the research was conducted in the absence of any commercial or financial relationships that could be construed as a potential conflict of interest.

Publisher's note

References

1. Bulger EM, Smith DG, Maier RV, Jurkovich GJ. Fat embolism syndrome. A 10-year review. *Arch Surg.* (1997) 132:435–9. doi: 10.1001/archsurg.1997.01430280109019

2. Tsai IT, Hsu CJ, Chen YH, Fong YC, Hsu HC, Tsai CH. Fat embolism syndrome in long bone fracture–clinical experience in a tertiary referral center in Taiwan. *J Chin Med Assoc.* (2010) 73:407–10. doi: 10.1016/S1726-4901(10)70088-5

3. Emson HE. Fat embolism studied in 100 patients dying after injury. *J Clin Pathol.* (1958) 11:28–35. doi: 10.1136/jcp.11.1.28

4. Timon C, Keady C, Murphy CG. Fat embolism syndrome - a qualitative review of its incidence, presentation, pathogenesis and management. *Malays Orthop J.* (2021) 15:1–11. doi: 10.5704/MOJ.2103.001

5. Talbot M, Schemitsch EH. Fat embolism syndrome: history, definition, epidemiology. *Injury.* (2006) 37:S3–7. doi: 10.1016/j.injury.2006.08.035

6. Milroy CM, Parai JL. Fat embolism, fat embolism syndrome and the autopsy. *Acad Forensic Pathol.* (2019) 9:136–54. doi: 10.1177/1925362119896351

7. Gossling HR, Pellegrini VD. Fat embolism syndrome: a review of the pathophysiology and physiological basis of treatment. *Clin Orthop Relat Res.* (1982) (165):68–82. doi: 10.1097/00003086-198205000-00011

8. Vichinsky E, Williams R, Das M, Earles AN, Lewis N, Adler A, et al. Pulmonary fat embolism: a distinct cause of severe acute chest syndrome in sickle cell anemia. *Blood.* (1994) 83:3107–12. doi: 10.1182/blood.V83.11.3107.bloodjournal83113107

9. Robert JH, Hoffmeyer P, Broquet PE, Cerutti P, Vasey H. Fat embolism syndrome. *Orthop Rev.* (1993) 22:567–71.

10. Lindeque BG, Schoeman HS, Dommisse GF, Boeyens MC, Vlok AL. Fat embolism and the fat embolism syndrome. A double-blind therapeutic study. *J Bone Joint Surg Br.* (1987) 69:128–31. doi: 10.1302/0301-620X.69B1.3818718

11. Peltier LF. Fat embolism. A perspective. *Clin Orthop Relat Res.* (1988) (232):263–70. doi: 10.1097/00003086-198807000-00033

12. Gauss H. The pathology of fat embolism. *Arch surgery.* (1924) 9:605. doi: 10.1001/archsurg.1924.01120090110007

13. Wenda K, Runkel M, Degreif J, Ritter G. Pathogenesis and clinical relevance of bone marrow embolism in medullary nailing–demonstrated by intraoperative echocardiography. *Injury.* (1993) 24:S73–81. doi: 10.1016/0020-1383(93)90011-T

14. Baker PL, Pazell JA, Peltier LF. Free fatty acids, catecholamines, and arterial hypoxia in patients with fat embolism. *J Trauma.* (1971) 11:1026–30. doi: 10.1097/00005373-197112000-00006

15. Kellogg RG, Fontes RB, Lopes DK. Massive cerebral involvement in fat embolism syndrome and intracranial pressure management. *J Neurosurg.* (2013) 119:1263–70. doi: 10.3171/2013.7.JNS13363

16. Pell AC, Christie J, Keating JF, Sutherland GR. The detection of fat embolism by transoesophageal echocardiography during reamed intramedullary nailing. A study of 24 patients with femoral and tibial fractures. *J Bone Joint Surg Br.* (1993) 75:921–5. doi: 10.1302/0301-620X.75B6.8245083

17. Vetrugno L, Bignami E, Deana C, Bassi F, Vargas M, Orsaria M, et al. Cerebral fat embolism after traumatic bone fractures: a structured literature review and analysis of published case reports. *Scand J Trauma Resusc Emerg Med.* (2021) 29:47. doi: 10.1186/s13049-021-00861-x

18. Erdem E, Namer IJ, Saribas O, Aras T, Tan E, Bekdik C, et al. Cerebral fat embolism studied with MRI and SPECT. *Neuroradiology.* (1993) 35:199–201. doi: 10.1007/BF00588493

19. Maghrebi S, Cheikhrouhou H, Triki Z, Karoui A. Transthoracic echocardiography in fat embolism: a real-time diagnostic tool. *J Cardiothorac Vasc Anesth.* (2017) 31:e47–8. doi: 10.1053/j.jvca.2017.01.008

20. Yonezaki S, Nagasaki K, Kobayashi H. Ultrasonographic findings in fat embolism syndrome. *Clin Pract Cases Emerg Med.* (2021) 5:263–4. doi: 10.5811/cpcem.2021.2.51270

21. Takahashi S, Kitagawa H, Ishii T. Intraoperative pulmonary embolism during spinal instrumentation surgery. A prospective study using transoesophageal echocardiography. *J Bone Joint Surg Br.* (2003) 85:90–4. doi: 10.1302/0301-620X.85B1.13172

22. Parizel PM, Demey HE, Veeckmans G, Verstreken F, Cras P, Jorens PG, et al. Early diagnosis of cerebral fat embolism syndrome by diffusion-weighted MRI (starfield pattern). *Stroke.* (2001) 32:2942–4. doi: 10.1161/str.32.12.2942

23. Bollineni VR, Gelin G, Van Cauter S. Cerebral fat embolism syndrome. *J Belg Soc Radiol.* (2019) 103:20. doi: 10.5334/jbsr.1781

24. Scarpino M, Lanzo G, Lolli F, Grippo A. From the diagnosis to the therapeutic management: cerebral fat embolism, a clinical challenge. *Int J Gen Med.* (2019) 12:39–48. doi: 10.2147/IJGM.S177407

25. Kuo KH, Pan YJ, Lai YJ, Cheung WK, Chang FC, Jarosz J. Dynamic MR imaging patterns of cerebral fat embolism: a systematic review with illustrative cases. *AJNR Am J Neuroradiol.* (2014) 35:1052–7. doi: 10.3174/ajnr.A3605

26. Hoiland RL, Griesdale DE, Gooderham P, Sekhon MS. Intraparenchymal neuromonitoring of cerebral fat embolism syndrome. *Crit Care Explor.* (2021) 3:e0396. doi: 10.1097/CCE.0000000000000396

27. Takahashi M, Suzuki R, Osakabe Y, Asai JI, Miyo T, Nagashima G, et al. Magnetic resonance imaging findings in cerebral fat embolism: correlation with clinical manifestations. *J Trauma.* (1999) 46:324–7. doi: 10.1097/00005373-199902000-00021

28. Gurd AR, Wilson RI. The fat embolism syndrome. *J Bone Joint Surg Br.* (1974) 56B:408–16. doi: 10.1302/0301-620X.56B3.408

29. Cavallazzi R, Cavallazzi AC. The effect of corticosteroids on the prevention of fat embolism syndrome after long bone fracture of the lower limbs: a systematic review and meta-analysis. *J Bras Pneumol.* (2008) 34:34–41. doi: 10.1590/S1806-37132008000100007

30. Gupta A, Reilly CS. Fat embolism. *BJA Education.* (2007) 7:148–51. doi: 10.1093/bjaceaccp/mkm027

31. White T, Petrisor BA, Bhandari M. Prevention of fat embolism syndrome. *Injury.* (2006) 37:S59–67. doi: 10.1016/j.injury.2006.08.041

32. Bone LB, Johnson KD, Weigelt J, Scheinberg R. Early versus delayed stabilization of femoral fractures. A prospective randomized study. *J Bone Joint Surg Am.* (1989) 71:336–40. doi: 10.2106/00004623-198971030-00004

33. Riska EB, von Bonsdorff H, Hakkinen S, Jaroma H, Kiviluoto O, Paavilainen T. Prevention of fat embolism by early internal fixation of fractures in patients with multiple injuries. *Injury.* (1976) 8:110–6. doi: 10.1016/0020-1383(76)90043-7

34. Pitto RP, Koessler M, Kuehle JW. Comparison of fixation of the femoral component without cement and fixation with use of a bone-vacuum cementing technique for the prevention of fat embolism during total hip arthroplasty. A prospective, randomized clinical trial. *J Bone Joint Surg Am.* (1999) 81:831–43. doi: 10.2106/00004623-199906000-00010

35. Hall JA, McKee MD, Vicente MR, Morison ZA, Dehghan N, Schemitsch CE, et al. Prospective randomized clinical trial investigating the effect of the reamer-irrigator-aspirator on the volume of embolic load and respiratory function during intramedullary nailing of femoral shaft fractures. *J Orthop Trauma.* (2017) 31:200–4. doi: 10.1097/BOT.0000000000000744

frontiers | Frontiers in Medicine

TYPE Case Report
PUBLISHED 12 December 2022
DOI 10.3389/fmed.2022.1065319

OPEN ACCESS

EDITED BY
Yuetian Yu,
Shanghai Jiao Tong University, China

REVIEWED BY
Tommaso Mauri,
University of Milan, Italy
Pedja Kovacevic,
University Clinical Center of Republika Srpska, Bosnia and Herzegovina
Changsheng Zhang,
First Medical Center of Chinese PLA General Hospital, China

*CORRESPONDENCE
Na Cui
pumchcn@163.com

SPECIALTY SECTION
This article was submitted to Intensive Care Medicine and Anesthesiology, a section of the journal Frontiers in Medicine

RECEIVED 09 October 2022
ACCEPTED 28 November 2022
PUBLISHED 12 December 2022

CITATION
Liu W, Ding X, He H, Long Y and Cui N (2022) Screening for the causes of refractory hypoxemia in critically ill patients: A case report. *Front. Med.* 9:1065319. doi: 10.3389/fmed.2022.1065319

Screening for the causes of refractory hypoxemia in critically ill patients: A case report

Wanglin Liu, Xin Ding, Huaiwu He, Yun Long and Na Cui*

Department of Critical Care Medicine, Peking Union Medical College Hospital, Chinese Academy of Medical Science and Peking Union Medical College, Beijing, China

Hypoxemia was a very common symptom in critical patients and should be treated immediately before resulting in permanent organ failure. Rapid diagnosis of the etiology of hypoxemia could be achieved by combining the use of various bedside and radiation-free techniques such as lung ultrasound, electrical impedance tomography and echocardiography. By presenting a case of serious acute refractory hypoxemia, we proposed an efficient protocol for diagnosing and treating hypoxemia in a safe and fast way.

KEYWORDS

hypoxeima, causes, lung ultrasound, echocardiography, electrical impedance tomography

Introduction

Hypoxemia is defined as a low oxygen level in the blood. It is most commonly seen in critically ill patients and is a very common reason for admitting to intensive care unit (ICU). Hypoxemia could cause tissue hypoxia and lead to organ failure and life-threatening conditions (1). There are various causes of hypoxemia including hypoventilation, lung ventilation/perfusion mismatch, right-to-left shunt, diffusion impairment, and low inspired partial pressure of oxygen (2). Identifying the right cause and correcting hypoxemia in time is crucially important for critical patients. The authors present a case of middle-aged patient who developed unusual acute and severe hypoxemia after receiving a congenital atrial defect repair surgery. A series of assessments were performed for this patient to identify and treat the severe hypoxemia.

Case report

A 41-year-old man diagnosed with congenital atrial septal defect was admitted to our surgical ICU after an atrial defect repair surgery through right lateral thoracotomy approach. He had received jejunal stromal tumor surgery 1 year ago, when the congenital atrial defect was found by routine echocardiography. The patient had no other notable past medical history. He was asymptomatic before the cardiac surgery. At admission to the cardiac surgery ward before surgery, he showed a pulse oxyhemoglobin saturation (SpO2) of 96.6%, arterial partial pressure of oxygen (PaO2) of 79 mmHg by arterial blood gas (ABG) analysis. Preoperative transthoracic echocardiography (TTE) showed an atrial septal defect size of 36 mm near the inferior vena cava with left to right shunt flow and estimated systolic pulmonary artery pressure of 38 mmHg.

The operation lasted about 8 h. ABG drawn before intubation and mechanical ventilation showed: pH 7.37, arterial partial pressure of carbon dioxide (PaCO2) 35.6 mmHg, PaO2 115 mmHg, base excess (BE) −3.6 mmol/L, lactate 0.9 mmol/L. The ventilation strategy used during the surgery was as follows: volume control, tidal volume (VT) of 450 ml, respiratory frequency (f) of 13 breaths/min, fraction of inspired oxygen (FiO2) of 100%, positive end-expiratory pressure (PEEP) of 5 cmH2O. ABG drawn at the end of the operation showed: pH 7.32, PaCO2 50.1 mmHg, PaO2 91.7 mmHg, BE −0.8 mmol/L, lactate 1.3 mmol/L. Routine intraoperative TEE conducted by the anesthetist at the end of the surgery did not reveal significant abnormal structure cardiac defect. The cardiac surgeon who performed the surgery claimed the operation successful. The patient was transferred from the operation room to ICU at midnight under sedation and intubation for post-cardiac surgery care. He presented with a hear rate (HR) of 100 b.p.m, blood pressure (BP) of 150/93 mmHg, SpO2 of 93% (mechanical ventilation, volume control, FiO2 of 50%, VT of 450 ml, PEEP of 8 cmH2O, f of 15 breaths/min). ABG showed a PaO2 of 58 mmHg, arterial partial pressure of carbon dioxide (PaCO2) of 47 mmHg. After adjusting the ventilator settings (volume control, FiO2 100%, VT 500 ml, PEEP 8 cmH2O, f 18 breaths/min), ABG was drawn again and showed a PaO2 of 81 mmHg, PaCO2 of 31 mmHg. The patient was severely hypoxic with a P/F ratio <100 mmHg. In order to figure out and correct the cause of hypoxemia, we performed a series of examinations in terms of airway, lung ventilation, lung perfusion, and ventilation/perfusion (V/Q) mismatch.

Airway check

Firstly, there was no obstruction in the airway, as we made sure that there was neither mucus plugging nor airway stenosis. There was no air leak in the artificial airway and the breathing circuit. Hypoventilation was ruled out since the PaCO2 returned to normal after adjusting the ventilator, with minute ventilation volume about 9 L/min. Thus, airway related etiologies of hypoxemia were ruled out in the first place.

Lung ultrasound and electrical impedance tomography ventilation

Was lung collapse or inhomogeneous ventilation the cause of hypoxemia in this patient? We performed a quick bedside lung ultrasound using a twelve-zone scanning protocol (3) to figure out whether lung consolidation or pleural effusion existed. The result showed tissue-like signs, which indicated lung consolidation, in the regions of R6, L5, and L6 (Figure 1), while lung sliding and A-lines were observed in the other regions. Pulmonary edema was also not supported by lung ultrasound findings. The chest X ray was not remarkable except for decreased transparency in the right lower lung field. To improve hypoxemia that could be caused by the consolidation in the dorsal regions of bilateral lungs, lung recruitment maneuver with PEEP of 20 cmH2O and peak airy way pressure of 40 cmH2O for 2 min was performed, but little effect was achieved. To check for regional ventilation distribution, we then conducted bedside electrical impedance tomography (EIT) (4). EIT measurements were performed with PulmoVista 500 (Dräger Medical, Lübeck, Germany). A silicone EIT belt with 16 surface electrodes was placed around the patient's thorax at the fourth intercostal space level. EIT measurements were continuously recorded at 20 Hz when the patients were at relative stable condition after medical treatment (5). The EIT ventilation image of our patient showed decreased ventilation distribution in the right lung (Figure 2A), which was probably related with the right lateral thoracotomy surgical approach. Decreased right lung ventilation might contributed partly to hypoxemia in this patient. But the main cause still remained to be detected.

EIT Perfusion

Was V/Q mismatch the main cause of hypoxemia in this patient? We reviewed the past medical history and found that lung V/Q mismatch related comorbidities including interstitial lung disease and chronic obstructive pulmonary disease were not present in our patient. And preoperative TTE showed that pulmonary hypertension was not significantly increased. However, newly developed disease conditions such as lung atelectasis and vascular embolism could also lead to V/Q mismatch. Thus, we decided to assess lung V/Q match by EIT. After obtaining informed consent, 10 ml of hypertonic saline (10%) bolus infusion was performed at bedside to assess the regional pulmonary ventilation and perfusion mismatch (5–7). EIT data were recorded throughout the PEEP titration in the supine position. During this period, the patient was fully sedated using continuous infusion of midazolam, propofol and fentanyl to prevent any spontaneous breathing (5). The data of V/Q match were analyzed offline using customized software programmed with MATLAB R2015 (the MathWorks Inc., Natick, MA) (5). Perfusion of the right lung was markedly low. The dead space of the whole lung was 24.4%, and the shunt was 10.29% (Figures 2B,C).

CTPA

Our previous study found a cutoff value of 30.37% dead space was related to pulmonary embolism (PE). However, the relatively high dead space ventilation together with a history of jejunal stromal tumor might be indicative of potential

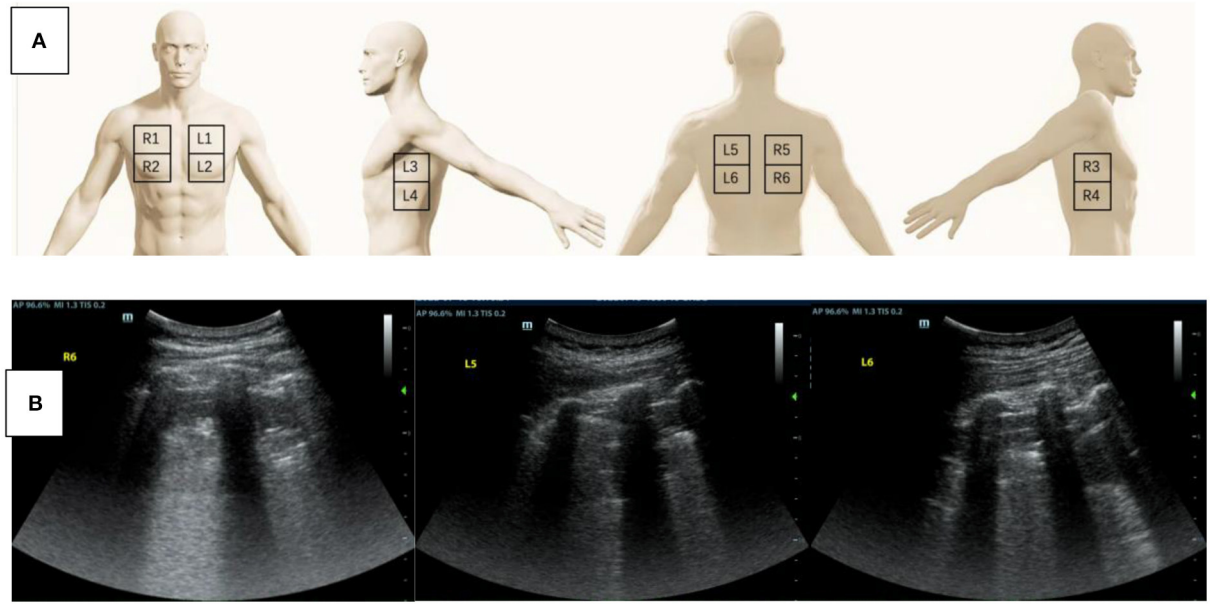

FIGURE 1
(A) A schematic diagram of the twelve-zone scanning lung ultrasound protocol. **(B)** Lung ultrasound was performed to assess the cause of hypoxemia. Tissue-like signs were found in the region of R6, L5, and L6.

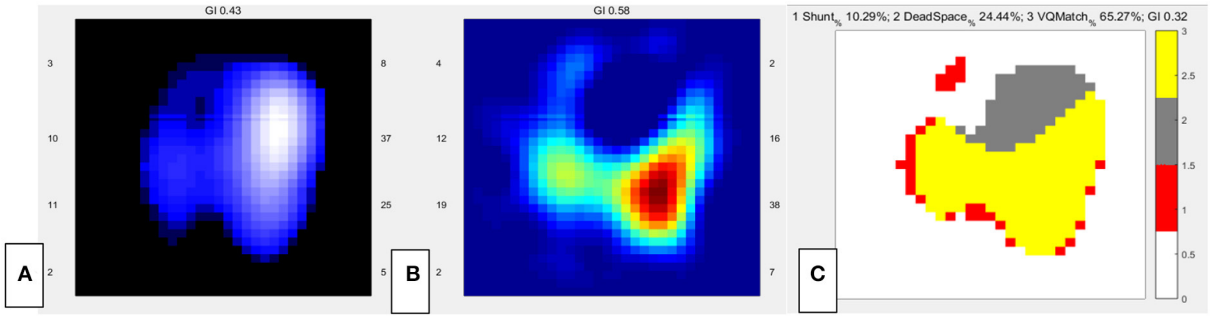

FIGURE 2
EIT images of the functional ventilation distribution **(A)** (dark blue areas indicated low ventilated regions and white areas indicated high ventilated regions), functional perfusion distribution **(B)** (red areas indicated high-perfusion regions and blue areas indicated low-perfusion regions), and distribution of the regional ventilation/perfusion ratios **(C)** (Ventilated regions were defined as pixels with impedance changes higher than 20% of the maximum tidal impedance variation in the functional ventilation image. Perfused regions were defined as pixels higher than 20% of the maximum bolus-related impedance change in the functional perfusion image. Gray areas indicated regions with high ventilation and low perfusion. Red areas indicated low ventilation and high perfusion regions. Yellow areas indicated good ventilation-perfusion matching).

pulmonary embolism in this case. But bedside ultrasound examination did not find venous thrombosis in bilateral lower extremities. With the aim to exclude pulmonary embolism, we transferred the patient for a computed tomography pulmonary angiography (CTPA) in the following morning. CTPA revealed small embolism in the superior lobar branch of the right pulmonary artery (Figure 3). The main pulmonary trunk was markedly widened, but not significantly changed compared with the preoperative CT scan. There was mild atelectasis in the inferior lobes of bilateral lungs and a small amount of operation related pneumothorax as showed in the CTPA. The poor perfusion of the right lung by EIT was consistent with the result of CTPA. However, neither the mild atelectasis nor the small embolism in the superior lobar branch of right pulmonary artery were able to explain the severity of refractory hypoxemia in this patient in our experience.

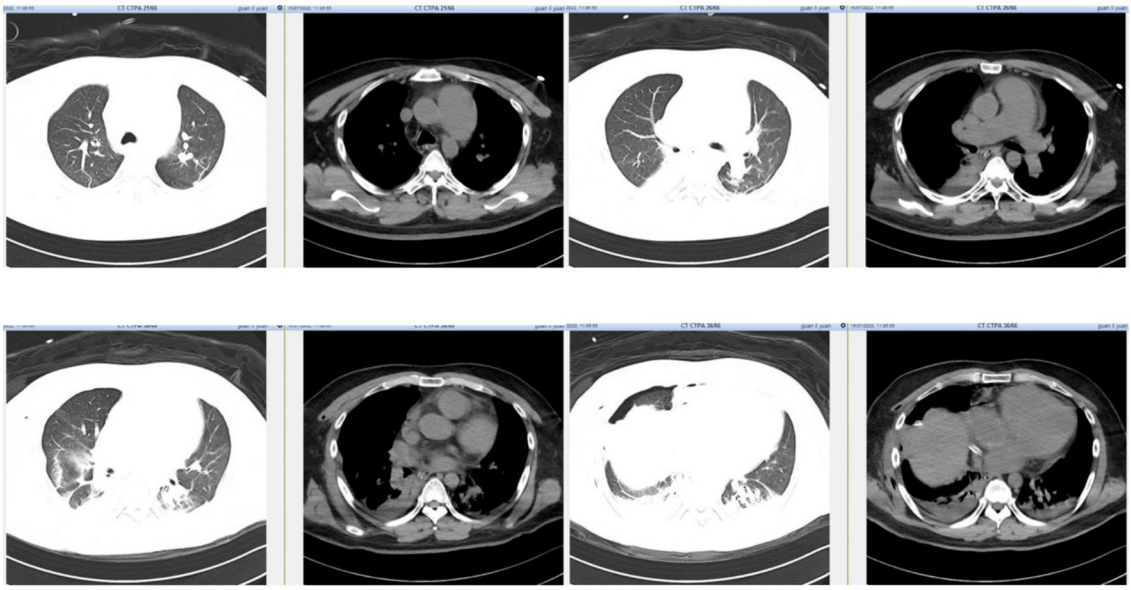

FIGURE 3
CTPA demonstrated mild atelectasis in the inferior lobes of bilateral lungs and a small amount of operation related pneumothorax. The small embolism in the superior lobar branch of right pulmonary artery was not shown in the picture.

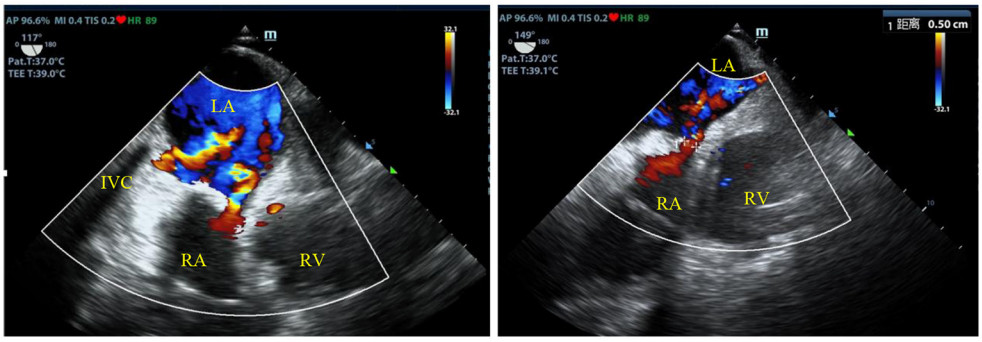

FIGURE 4
TEE showed a residual atrial septal defect with a size of 5 mm and bidirectional multicolored shunt flow signal. And an IVC-left atrium shunt was also found soon after the repair. TEE, transesophageal echocardiography; LA, left atrium; RA, right atrium; RV, right ventricle; IVC, inferior vena cava.

Transesophageal echocardiography

The cardiac structure and function were urgently to be examined, since the main cause of hypoxemia still remained unclear in our patient. Pulmonary arteriovenous malformation or potential right to left intracardiac shunt resulted by abnormal cardiac structure might be the last cause of severe hypoxemia in this case. Hypoxemia caused by intracardiac shunt usually responded poorly to increase of inspired oxygen concentration, as in the case with our patient. TTE image was not clear because of the influence of surgical operation. We thus conducted bedside transesophageal echocardiography (TEE). Finally, we found a residual atrial septal defect with a size of 5 mm by TEE. Bidirectional multicolored shunt flow signal was detected through this atrial defect (Figure 4). In addition, TEE revealed a second shunt flow signal through a defect possibly between the inferior vena cava (IVC) and the left atrium. After all, the intracardiac shunt found by TEE seemed to be able to explain the refractory hypoxemia in this patient.

Treatment and outcome

After the above examinations, we concluded that the residual right-left atrial shunt and the IVC-left atrial shunt most likely had the biggest impact on this patient's severe hypoxemia. The cardiac surgeon scheduled a repair of the surgery. During the patient's waiting period for a second surgery, we conducted intermittent prone positioning to improve ventilation distribution of the dependent-dorsal lung regions. EIT has been used in perioperative patients for individual optimization of ventilator settings (8). For post-operative patients who underwent a long operation, the risk of developing acute respiratory disease syndrome was high. The patient presented mild atelectasis in the inferior lobes of bilateral lungs showed by lung ultrasound and CTPA. Thus, we titrated PEEP by EIT with the crossing method, which is routinely conducted by us in our department (6). During the process of PEEP titration using EIT, we closely monitored the patient's hemodynamics to avoid severe adverse hemodynamic effect. The patient was hemodynamically stable without any vasoactive agents during the process. Thus, we set an optimal PEEP of 9 cmH2O based on the result of EIT PEEP titration for better gas distribution in the lungs. Esophageal pressure and other respiratory mechanics were monitored to avoid patient self-inflicted lung injury (P-SILI). However, hypoxemia progressively deteriorated to PaO2 of 47 mmHg at ventilator FiO2 of 100% (P/F ratio = 47 mmHg) on the third day after the first surgery, when a second surgery was scheduled. The surgeons confirmed the residual IVC-left atrium and the atrial septal defect during the second open-heart surgery through the midline sternotomy approach. They removed the originally mis-sutured patch and re-patched the defect. Hypoxemia was greatly improved on the first night after the second surgery, with a PaO2 of 134 mmHg at ventilator FiO2 of 60% (P/F ratio = 223 mmHg). With pulmonary physical therapy and negative fluid balance, the P/F ratio further improved (P/F ratio = 322 mmHg) at the third day after the second surgery. The patient was off the ventilator and extubated successfully 3 days later. He was transferred back to the general ward the day after extubation and subsequently discharged from the hospital.

Discussion

Post-operative hypoxemia is very common in ICU patients who had underwent thoracic or cardiac surgery. Various etiologies including interstitial lung disease, COPD, pulmonary hypertension, pulmonary embolism, pulmonary edema, pneumonia, atelectasis, mucus plugging, pulmonary arteriovenous malformation, and right to left intracardiac shunt could be the cause. These etiologies cause hypoxemia through mainly three mechanisms: impaired diffusion, V/Q mismatch and shunt. In our case, the patient developed severe hypoxemia soon after cardiac surgery. Through rapid bedside evaluation, we ruled out airway obstruction, hypoventilation, pulmonary edema, and extreme lung V/Q mismatch. The small PE revealed by CTPA could also not explain the severe hypoxemia in our case. Finally, intracardiac shunt found by TEE was confirmed to be the main cause of hypoxemia in this patient. A second repair surgery successfully corrected the cause and cured the patient.

Treating the patient with acute life-threatening hypoxemia during mechanical ventilation should begin with a quick and safe approach, with the goal of improving oxygenation and minimizing the harmful effects. There are various assessments to investigate the causes of hypoxemia in clinical practice. For non-ICU patients, CT or CTPA when necessary is most often conducted. For ICU patients who are in critical conditions, transferring to a CT machine for a scan is risky and may even be life-threatening. The development of new techniques including lung ultrasound and EIT enabled quick and convenient diagnosis of hypoxemia at bedside without the risk of transferring a critical patient. EIT is a non-invasive technique that provides dynamic tidal images of gas distribution (9). EIT has been widely used for lung recruitment, positive end-expiratory pressure (PEEP) adjustment, lung volume estimation, and homogeneity of gas distribution during mechanical ventilation (9). The combination of these new techniques (EIT, lung ultrasound) and the traditional imaging methods (chest X-ray, CTPA) could provide quicker, better and more accurate diagnostic power for identifying causes of hypoxemia. Undoubtedly, this could lead to better outcome for the critical patients.

Lung ultrasound can be performed conveniently and repeatedly at bedside (10), allowing immediate diagnosis of different lung pathologies including lung consolidation, interstitial disease, pneumothorax, and pleural effusion at any emergent conditions and free of radiations. Lung sliding and A-lines were normal dynamic and static signs by lung ultrasound. The quad or sinusoid sign by lung ultrasound indicated pleural effusion. Tissue like sign and the shred sign indicated alveolar consolidation. B-lines by lung ultrasound were indicative of interstitial syndrome caused either by hemodynamic or inflammatory pulmonary edema (10). By combining the use of lung ultrasound and echocardiography, hemodynamic pulmonary edema could be diagnosed and treated timely. Pneumothorax could be detected as lung point sign or absence of lung sliding by lung ultrasound before confirming by chest X-ray. Lung consolidation or atelectasis can be detected by lung ultrasound and further verified by decreased ventilation of the dorsal lung in functional EIT ventilation image.

EIT could provide both lung ventilation and perfusion image (4, 11). Pneumothorax could also present as decreased regional ventilation and could be supported by lung point sign in lung ultrasound. Ventilation defect of gravity dependent area detected by EIT could be caused by lung consolidation,

which presented as tissue like or shred sign in lung ultrasound. The ventilation/perfusion match image by EIT would reveal increased shunt flow when lung consolidation was the main cause of hypoxemia. Both ventilation and perfusion of the right lung was decreased by EIT in our patient. As a result, the shunt was relatively low (10.29%). Hypoxic pulmonary vasoconstriction might have contributed to decreased perfusion by compensatory mechanism. And the small embolism in the superior lobar branch of the right pulmonary artery might also have contributed to decreased perfusion. Further experimental research is warranted to validate these mechanisms. Increased dead space by EIT indicated pulmonary vascular dysfunction, among which PE was the most common etiology. Increased dead space by EIT enhanced the indication for performing CTPA and might decrease unnecessary risk for transferring the critical patient.

In our case, we have ruled out all common causes of hypoxemia after clearing airway and breathing circuit and completing lung ultrasound, EIT and CTPA in the early stage. there was one rare but non-negligible cause, intracardiac shunt, remained to be examined. The patient developed newly unexplained refractory hypoxemia soon after atrial defect repair surgery, which might imply cardiac causes of hypoxemia. Echocardiography (TEE or TTE) was the right assessment for cardiac causes. The residual right-left atrial shunt and the IVC-left atrial shunt revealed by the TEE proved to be the prime cause of refractory hypoxemia in our case, confirmed by the second open-heart surgery. Previous literature reported complication of hypoxemia soon after the repair surgery of inferior sinus venosus defects, which is a rare type of interatrial communication involving lower part of the atrial septum derived from the sinus venosus. Preoperative diagnosis of this type of atrial defect is difficult and challenging (12). The lower edge of the defect has no residual atrial septal tissue thus the orifice of IVC strides over the atrial septum. Giant residual Eustachian valve in some patients may be mistaken as the lower edge of the defect, leading to mis-suture in the surgery and resulting in residual IVC- left atrial shunt. The patient in our case fell into this situation. TEE proves to be better than

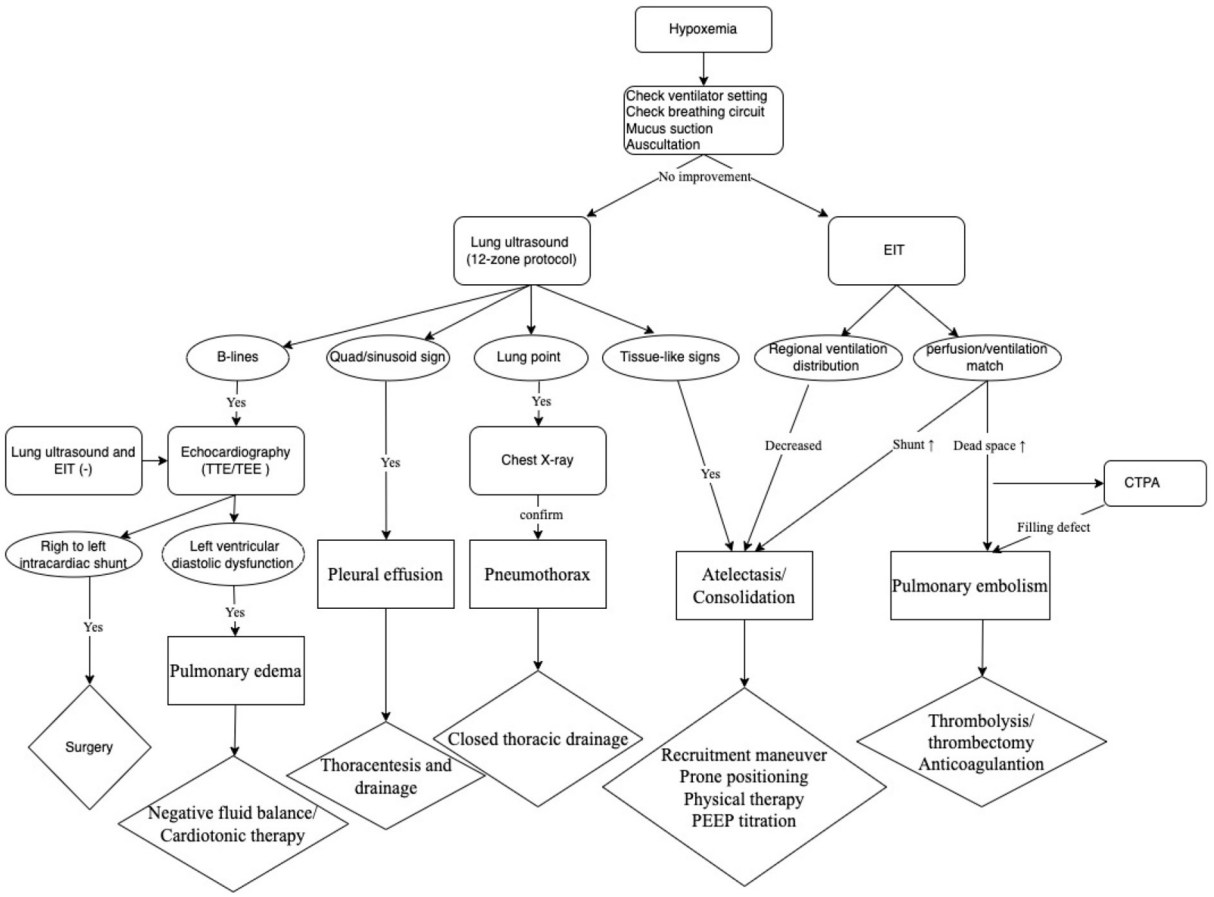

FIGURE 5
The protocol for assessments of hypoxemia in ICU critical patients.

TTE in accurately diagnosing this type of defect because of close proximity of atrial septum to TEE transducer. TEE is the diagnostic procedure of choice and should be suggested when atrial defect near IVC was identified before operation or at any time. However, diagnosing inferior sinus venosus defects by TTE can still be difficult in adult patients with congenital heart disease. Contrast echocardiography with microbubbles provides accurate detection of cardiovascular shunts. However, it fails to reveal detailed information about anatomical and functional characterizations. Cardiac MRI can also be used to precisely determine ventricular volumes, degree of left-to-right shunts, as well as anatomical vascular and cardiac abnormalities. Contrast-enhanced CT scan is another valuable method for detection of the defect. But this method leads to exposure to ionizing radiation and may reveal insufficient information (13). Furthermore, intraoperative injection of agitated saline contrast *via* intravenous cannulation in a lower extremity can allow for detection and correction of residual defects during the operation. Careful intraoperative examination of the posterior-inferior portion of the interatrial septum should be done in patients with isolated interatrial shunts and in patients with concomitant congenital heart defects (14). Accurate preoperative diagnosis is critical for post-operative recover of the patient. Careful preoperative planning and intraoperative examination could significantly reduce the incidence of residual defects and free the patient from reoperation (14).

Bedside technologies including lung ultrasound, EIT ventilation and perfusion image, and echocardiography were combinedly used in our patient. Based on the clinical practice, we developed a protocol, which consisted of a bundle of assessments, to screen for etiology and treat newly developed acute hypoxemia in critical patients in our ICU (Figure 5). In our protocol, all potential causes for hypoxemia could be detected.

Conclusion

In conclusion, we developed a protocol of assessments for rapidly identifying etiologies of hypoxemia. Thus, safe and timely treatment was expected to be achieved by our protocol in ICU critically ill patients. The protocol combined various methods and technologies, mainly lung ultrasound, echocardiography and EIT, which could be conveniently conducted at bedside, reducing medical risk by shortening the time to diagnosis and free of transportation in patients with life-threatening conditions. This protocol could assist intensivist to better diagnose and treat hypoxic critical patients.

Data availability statement

The studies involving human participants were reviewed and approved by Peking Union Medical College Hospital.

Ethics statement

Written informed consent was obtained from the next of kin of the patient for the publication of any potentially identifiable images or data included in this article.

Author contributions

WL and XD: collected data and drafted the manuscript. NC, HH, and YL: revised the manuscript. All authors have read and approved the final version of the manuscript.

Funding

The work was supported by National Natural Science Foundation of China (No. 82072226), National Key R&D Program of China 2022YFC2009803 from Ministry of Science and Technology of the People's Republic of China, Beijing Municipal Science and Technology Commission (No. Z201100005520049), CAMS Innovation Fund for Medical Sciences (CIFMS) 2021-I2M-1-062 from Chinese Academy of Medical Sciences.

Conflict of interest

The authors declare that the research was conducted in the absence of any commercial or financial relationships that could be construed as a potential conflict of interest.

Publisher's note

References

1. Maca J, Kanova M, Kula R, Sevcik P. Hypoxemia/hypoxia and new concepts of oxygen therapy in intensive care. *Vnitr Lek.* (2020) 66:63–70. doi: 10.36290/vnl.2020.038

2. Sarkar M, Niranjan N, Banyal PK. Mechanisms of hypoxemia. *Lung India.* (2017) 34:47–60. doi: 10.4103/0970-2113.197116

3. Levy Adatto N, Preisler Y, Shetrit A, Shepshelovich D, Hershkoviz R, Isakov O. Rapid 8-zone lung ultrasound protocol is comparable to a full 12-zone protocol for outcome prediction in hospitalized COVID-19 patients. *J Ultrasound Med.* (2022) 41:1677–87. doi: 10.1002/jum.15849

4. Frerichs I, Amato MBP, Van Kaam AH, Tingay DG, Zhao Z, Grychtol B, et al. Chest electrical impedance tomography examination, data analysis, terminology, clinical use and recommendations: consensus statement of the TRanslational EIT developmeNt stuDy group. *Thorax.* (2017) 72:83–93. doi: 10.1136/thoraxjnl-2016-208357

5. He H, Chi Y, Long Y, Yuan S, Zhao Z. Three broad classifications of acute respiratory failure etiologies based on regional ventilation and perfusion by electrical impedance tomography: a hypothesis-generating study. *Ann Intensive Care.* (2021) 11:1–2. doi: 10.1186/s13613-021-00921-6

6. He H, Chi Y, Yang Y, Yuan S, Zhao Z. Early individualized positive end-expiratory pressure guided by electrical impedance tomography in acute respiratory distress syndrome: a randomized controlled clinical trial. *Critical care.* (2021) 25:230. doi: 10.1186/s13054-021-03645-y

7. He H, Chi Y, Long Y, Yuan S, Zhang R, Frerichs I, et al. Bedside evaluation of pulmonary embolism by saline contrast electrical impedance tomography method: a prospective observational study. *Am J Respir Crit Care Med.* (2020) 202:1464–8. doi: 10.1164/rccm.202005-1780LE

8. Spinelli E, Mauri T, Fogagnolo A, Scaramuzzo G, Rundo A, Grieco DL, et al. Electrical impedance tomography in perioperative medicine: careful respiratory monitoring for tailored interventions. *BMC Anesthesiol.* (2019) 19:1471–2253. doi: 10.1186/s12871-019-0814-7

9. Shono A, Kotani T. Clinical implication of monitoring regional ventilation using electrical impedance tomography. *J Intensive Care.* (2019) 7:4. doi: 10.1186/s40560-019-0358-4

10. Lichtenstein DA. Lung ultrasound in the critically ill. *Ann Intensive Care.* (2014) 4:1–12. doi: 10.1186/2110-5820-4-1

11. Ball L, Scaramuzzo G, Herrmann J, Cereda M. Lung aeration, ventilation, and perfusion imaging. *Curr Opin Crit Care.* (2022) 28:302–7. doi: 10.1097/MCC.0000000000000942

12. Lin F, Tang H, Xiao X. Surgical repair of inferior sinus venosus defects: a novel approach with unsnared inferior vena cava. *J Cardiothorac Surg.* (2015) 10:1–3. doi: 10.1186/s13019-015-0359-x

13. Ghaemian A, Nabati M, Shokri M. Undiagnosed inferior vena cava type of sinus venosus atrial septal defect in a middle-aged woman: a rare case report. *J Clin Ultrasound.* (2020) 48:56–8. doi: 10.1002/jcu.22767

14. Banka P, Bacha E, Powell AJ, Benavidez OJ, Geva T. Outcomes of inferior sinus venosus defect repair. *J Thorac Cardiovasc Surg.* (2011) 142:517–22. doi: 10.1016/j.jtcvs.2011.01.031

frontiers | Frontiers in Medicine

TYPE Case Report
PUBLISHED 12 December 2022
DOI 10.3389/fmed.2022.1096900

OPEN ACCESS

EDITED BY
Yuetian Yu,
Shanghai Jiao Tong University, China

REVIEWED BY
Hongbo Chen,
Huazhong University of Science and Technology, China
Igor Dumic,
Mayo Clinic, United States

*CORRESPONDENCE
Maarten A. J. De Smet
maa.desmet@gmail.com

SPECIALTY SECTION
This article was submitted to Intensive Care Medicine and Anesthesiology, a section of the journal Frontiers in Medicine

RECEIVED 12 November 2022
ACCEPTED 28 November 2022
PUBLISHED 12 December 2022

CITATION
De Smet MAJ, Bogaert S, Schauwvlieghe A, Dendooven A, Depuydt P and Druwé P (2022) Case report: Hemorrhagic fever with renal syndrome presenting as hemophagocytic lymphohistiocytosis. *Front. Med.* 9:1096900. doi: 10.3389/fmed.2022.1096900

Case report: Hemorrhagic fever with renal syndrome presenting as hemophagocytic lymphohistiocytosis

Maarten A. J. De Smet[1]*, Simon Bogaert[1], Alexander Schauwvlieghe[2], Amélie Dendooven[3], Pieter Depuydt[1] and Patrick Druwé[1]

[1]Department of Intensive Care Medicine, Ghent University Hospital, Ghent, Belgium, [2]Department of Hematology, Ghent University Hospital, Ghent, Belgium, [3]Department of Pathology, Ghent University Hospital, Ghent, Belgium

Hemophagocytic lymphohistiocytosis may occur in patients with genetic predisposition and in sporadic cases due to malignancy or infection. We describe a 49-year old man with hemorrhagic fever, type 1 respiratory insufficiency and acute kidney injury. Diagnostic work up showed a hyperinflammatory syndrome, hypertriglyceridemia, hemophagocytosis, very high ferritin and significantly elevated sCD25. The findings were compatible with hemophagocytic lymphohistiocytosis based on the HLH-2004 criteria. Serological testing indentified *Puumala virus* as the causal pathogen. The patient was successfully treated with pulse corticosteroids, intravenous immunoglobins and supportive therapy.

KEYWORDS

hemophagocytic lymphohistiocytosis, hemorrhagic fever with renal syndrome, hantavirus, critical care, communicable diseases *Puumala virus*-associated hemophagocytosis

Introduction

Hemophagocytic lymphohistiocytosis (HLH) is a rare syndrome, characterized by an aberrant hyperinflammatory and hyperferritinemic immune response that is driven by T cells and excessive proliferation of activated histiocytes. HLH occurs as a primary genetic form or secondary to malignancy, infections, immunodeficiency and rheumatological

or auto-immune disorders (1). Infection-associated HLH may be caused by viral, bacterial, parasitic or fungal pathogens. Viral infections, such as Epstein-Barr virus, cytomegalovirus, herpes simplex virus, varicella zoster virus, influenza, SARS-CoV-2, and HIV, are known to trigger HLH. Rarely, HLH is associated with hemorrhagic fever with renal syndrome (HFRS) caused by *Hantaan, Seoul, Dobrava/Belgrade, or Puumala virus*. Six case reports have been described with only one identifying *Puumala virus* as the causal pathogen (2–7). Here, we describe a case of HLH secondary to HFRS caused by *Puumala virus*.

Case report

A 49-year old man presented to the emergency department following a week of night sweats and fever up to 39°C. He complained of right upper quadrant pain, dyspnea, headache, photophobia, and diplopia. The patient was a metal worker and kept guinea pigs, hamsters and rabbits. No other animal contact was reported. Two weeks before presentation, he received a second dose of the BNT162b2 mRNA COVID-19 vaccine. There was no history of recent or travel to endemic areas. He smoked actively, drank alcohol sporadically and used no drugs. There were no known allergies and the family history, including active or recent infections, was negative. On examination, heart rate was 83 beats per minute, blood pressure 118/81 mmHg, respiratory rate 18 per minute, oxygen saturation 98% without supplemental oxygen and temperature 38°C. Lung auscultation revealed bibasal inspiratory crepitations. The right upper quadrant was painful upon palpation without signs of hepatosplenomegaly or peritonitis. No other significant abnormalities were present. Hemoglobin was 11.1 g/dL, platelet count 27 × 10^3/μL, white blood cell count 20.4 × 10^3/μL with neutrophilia, serum creatinine 4.3 mg/dL, aspartate aminotransferase 87 U/L, alanine aminotransferase 59 U/L, gamma-glutamyl transferase 72 U/L, alkaline phosphatase 102 U/L, lactate dehydrogenase (LDH) 538 U/L, CRP 78 mg/L, ferritin 10631 μg/L, triglycerides 518 mg/dL, albumin 24 g/L, fibrinogen 360 mg/dL (**Table 1**). Computed tomography of head, chest and abdomen revealed ascites without other abnormalities. Blood and urine cultures were incubated. A SARS-CoV-2 PCR was negative.

The patient was started on ceftriaxone and vancomycin because of suspected meningoencephalitis. After 2 days, persistently high inflammation prompted a switch of vancomycin to doxycycline. Blood and urine cultures were repeated and remained sterile.

The patient was transferred to the ICU because of type 1 respiratory failure due to pulmonary edema and bilateral pleural effusions requiring High Flow Nasal Oxygen (HFNO). In addition, he developed nephrotic syndrome as documented by arterial hypertension, microscopic hematuria and proteinuria (5.2 g protein/g creatinine). Because of suspected HLH, intravenous immunoglobins (IVIGs, 1 g/kg daily for 3 days) and pulse corticosteroids (dexamethasone 20 mg on the first day, followed by 10 mg daily) were started.

Further workup showed NT-proBNP of 5466 pg/mL with normal cardiac structure and function on transthoracic echocardiography. A lumbar puncture was acellular and showed LDH of 47 U/L and total protein of 224 mg/dL without monoclonality. Cerebrospinal fluid culture and viral PCRs for *herpes simplex virus, varicella-zoster virus, enterovirus, Epstein-Barr virus and cytomegalovirus* remained negative. Serum and urinary protein electrophoresis did not show monoclonality. Bone marrow aspiration showed reactive changes without evidence of malignancy. Bone marrow biopsy revealed hemophagocytosis (**Figure 1**). Kidney biopsy showed slight acute tubular damage. Soluble CD25 (sCD25) was 3602 pg/mL. Natural Killer cell function was normal without perforin deficit.

Hemophagocytic lymphohistiocytosis was diagnosed because of a suggestive clinical phenotype in combination with a hyperinflammatory syndrome, fever, hypertriglyceridemia, hemophagocytosis, very high ferritin and significantly elevated sCD25 (1). *Puumala virus* serology was positive on hospital day 3 and 10 (**Table 1**), confirming HFRS. *Hantavirus* PCR was negative on blood and urine. Serology for other relevant infections and auto-immune disorders was negative (**Supplementary Table 1**). Exome sequencing could not reveal mutations at HLH foci or for immunodeficiency syndromes. Additional lab work did not uncover any immunocompromising factors.

Two days after the start of IVIGs and corticosteroids, serum creatinine improved and the patient could be weaned off HFNO therapy. Dexamethasone was tapered over 3 months. Currently, the patient is asymptomatic, with normal kidney function and without inflammation.

Discussion

Hemophagocytic lymphohistiocytosis is a rare syndrome, characterized by an aberrant hyperinflammatory and hyperferritinemic immune response that is driven by T cells and excessive proliferation of activated histiocytes. HLH may occur as a primary genetic form or secondary to infections, malignancy, immunodeficiency and rheumatological or auto-immune disorders. While variations in HLH-associated genes may also play a role in adult-onset HLH, primary HLH occurs mostly in children. Secondary HLH is most common in adolescents and adults as a result of acquired immune dysfunction in response to infections, malignancies, and immune disorders (1).

10.3389/fmed.2022.1096900

TABLE 1 Results of laboratory testing.

	Admission	Day 3	Day 5	Day 10	Discharge	1 Month	3 Months
Blood							
ESR (mm/h) (<15)	2	15					
CRP (mg/L) (<5)	57	78.2	34.5	4	3.1	<1	<1
Ferritin (μg/L) (20–280)	10631	6999	4947	1453		634	313
D-dimer (ng/mL) (<500)	2420	4680					
Fibrinogen (mg/dL) (200–400)		360	287	199		190	197
Erythrocytes (10^6/μL) (4.4–5.8)	3.45	3.8	3.45	3.74	3.47	3.62	3.67
Hb (g/dL) (13.5–17)	11.1	12.6	11.1	12.2	11.4	12	12.5
Hct (%) (39.9–51)	32	35.3	32	35.2	33.9	37.9	36.4
PLC (10^3/μL) (143–325)	27	76	129	381	324	332	408
Citrate PLC (10^3/μL) (143–325)	20	70					
WBC (10^3/μL) (4.3–9.6)	20.4	17.6	14.35	20.72	17.19	16.78	7.64
Neutrophils (10^3/μL) (1.9–5.9)	15.2	11			12.59		
Lymphocytes (10^3/μL) (1.2–3.4)	2.1	3.6					
Monocytes (10^3/μL) (0.3–0.8)	1	2.2					
Eosinophils (10^3/μL) (0.03–0.4)	0.4	0.3					
Basophils (10^3/μL) (0.02–0.1)	0.1	0.1					
Creatinin (mg/dL) (0.7–1.2)	1.2	4.3	3.74	1.02	0.84	0.74	0.78
Total bilirubin (mg/dL) (0.2–1.3)	0.6	0.4	0.4	0.6	0.6	0.4	0.5
Total protein (g/L) (64–83)		47	64	65	58		
Albumin (g/L) (35–52)		24	25	29			
AST (U/L) (<37)	87	68	114	35	43	23	18
ALT (U/L) (7–40)	59	48	77	107	111	39	16
γGT (U/L) (<64)	72	51	203	174	171	75	19
AP (U/L (30–120)	102	90	114	110	110	76	68
LDH (U/L) (105–250)	500	538	467	302	286	269	193
NT-proBNP (pg/mL) (<125)		5466					
Triglycerides (mg/dL) (58–327)		518	287	395			
sCD25 (U/mL) (458–1997)		3602					
NK cells (/μL) (90–600)		129.5					
NK perforin (%)		86.9					
NK cell function (degranulation test)		Normal					
Leptospira antibodies		Negative					
Puumala IgG (<0.8)		3.1		3.5			
Puumala IgM (<0.8)		8.8		7.2			
Puumala PCR		Negative					
Panhantavirus PCR		Negative					
Urine							
Puumala PCR		Negative					
Panhantavirus PCR		Negative					

ESR, erythrocyte sedimentation rate; CRP, C-reactive protein; Hb, hemoglobin; Hct, hematocrit; PLC, platelet count; WBC, white blood cells count; AST, aspartate aminotransferase; ALT, alanine aminotransferase; γGT, gamma-glutamyl transferase; AP, alkaline phosphatase; LDH, lactate dehydrogenase; NT-proBNP, N-terminal prohormone of brain natriuretic peptide; sCD25, soluble CD25; NK, natural killer; PCR, polymerase chain reaction.

Infection-associated HLH may be caused by viral, bacterial, fungal or parasitic pathogens. Viral infections, such as Epstein-Barr virus, cytomegalovirus, influenza, SARS-CoV-2, and HIV, are known to trigger HLH (8, 9). Rarely, HLH is associated with hemorrhagic fever with renal syndrome (HFRS) (2–7). HFRS is a zoonotic viral disease caused by Old World hantaviruses, occurring in Asia and Europe, such as *Hantaan, Seoul, Dobrava/Belgrade or Puumala virus*. In contrast, New

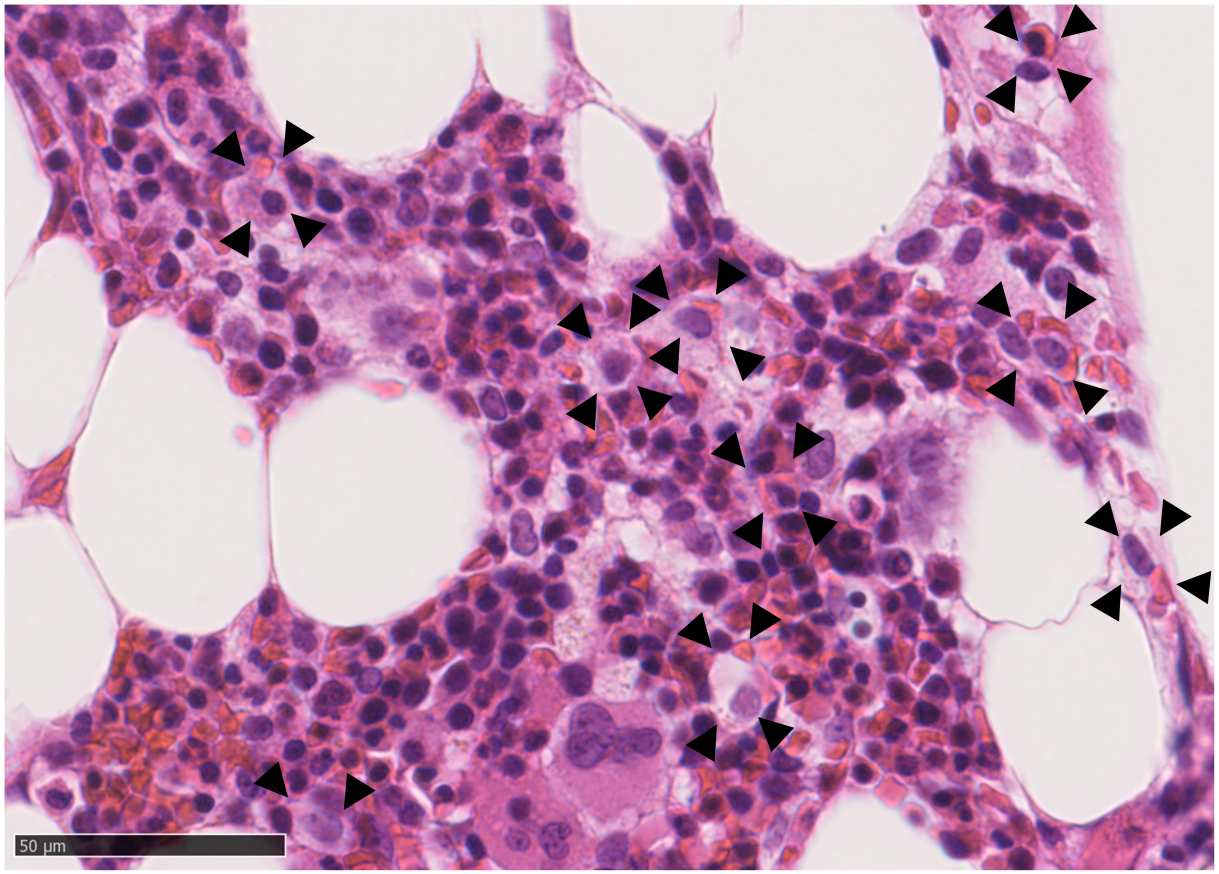

FIGURE 1
Bone marrow biopsy (Hematoxylin and Eosin stained, 400×) showing histiocytes (arrows) engulfing red blood elements compatible with hemophagocytosis.

World hantaviruses, occurring in the Americas, may cause hantavirus pulmonary syndrome (HPS). To our knowledge, no reports of HLH in HPS have been described in the literature. Transmission occurs through contact with saliva from bites or inhalation of aerosolized excrements of asymptomatically infected rodents. Clinical presentation varies from subclinical to fatal. After an incubation period of 2–4 weeks, patients may show non-specific symptoms such as fever, chills, headache, abdominal pain, nausea, and vomiting. After the initial period, hemorrhagic complications as well as renal dysfunction may occur that are associated with mortality. The diagnosis of hantavirus infection is generally confirmed by serological testing since viral RNA usually disappears from the circulation a few days after symptoms start. Six case reports have described HLH secondary to hantavirus infection with only one identifying *Puumala virus* as the causal pathogen (2–7). The bank vole is the reservoir for *Puumala*. However, here, clinical history suggests transmission through domesticated rodents. Experimental research shows hamsters may be subclinically infected with *Puumala*, but naturally occurring transmission has not been previously described (10). To the best of our knowledge, this is the first report describing such a possibility of transmission for *Puumala virus*.

Hemophagocytic lymphohistiocytosis is diagnosed based on the HLH-2004 criteria (**Supplementary Box 1**) (1). Firstly, heterozygosity for HLH-associated mutations or gene defects of other immune regulatory genes together with clinical findings associated with HLH may diagnose the syndrome. Alternatively, five of the following findings must be present for the diagnosis of HLH: fever $\geq$ 38.5°C, splenomegaly, peripheral blood cytopenia (at least two of the following: hemoglobin <9 g/dL, platelets < 100,000/µL, absolute neutrophil count < 1000/µL), hypertriglyceridemia $\geq$265 mg/dL and/or hypofibrinogenemia $\leq$ 150 mg/dL, evidence of hemophagocytosis, low or absent NK cell activity, ferritin $\geq$ 500 ng/mL and elevated sCD25 $\geq$ 2400 U/mL. In this case, HLH diagnosis could be confirmed based on five criteria: fever, hypertriglyceridemia, hemophagocytosis, very high ferritin and significantly elevated sCD25. Additionally,

functional and genetic testing did not reveal pathogenic variants associated with HLH or primary cytotoxicity defects, suggesting secondary HLH.

Given the coagulation abnormalities in this case, disseminated intravascular coagulation (DIC) has to be considered as a complication. Signs of DIC are common in hantavirus infection. In *Puumala virus* infections, 28% of patients may be diagnosed with DIC. DIC was also associated with more severe disease and may also complicate HLH (11).

The previously mentioned diagnostic criteria do not always need to be met in order to initiate treatment. Early suspicion is important to initiate HLH-specific therapy in critically ill or deteriorating patients. The HScore may be used to assess the probability of HLH (**Supplementary Box 2**) (1). This score incorporates points for immunosuppression, fever, hepatosplenomegaly, triglyceride level, ferritin, AST and fibrinogen, cytopenias and presence of hemophagocytosis on bone marrow aspiration. An HScore $\geq$ 250 confers a 99% probability of HLH, whereas a score of $\leq$90 confers a $<$ 1% probability of HLH. In this case, HScore was 196 with a probability of having HLH of 85% based on fever, thrombycytopenia, very high ferritin, triglycerides $>$350 mg/dL, fibrinogen $\leq$ 250 mg/dL and AST $\geq$ 30 U/L. When hemophagocytosis was additionally shown to be present, HScore increased to 231 with an HLH probability of 98%.

Hemophagocytic lymphohistiocytosis-specific therapy may consist of pulse corticosteroids, IVIGs, etoposide, cyclosporin A and/or biologics such as the interleukin-1 antagonist anakinra or the interleukin-6 antagonist tocilizumab (1). In patients with central nervous system involvement, methotrexate may be added (1). The HLH-94 protocol suppresses activated T cells and inflammatory cytokine production. It is the mainstay treatment in children up to 18 years of age, where genetic causes of HLH are enriched. The HLH-94 protocol consists of corticosteroids, cyclosporin A and etoposide. Additional intrathecal therapy is suggested in case of progressive neurological symptoms or persistent abnormal cerebrospinal fluid after 2 weeks of therapy.

The heterogeneity of adult HLH prohibits a single uniform protocol. Accordingly, treatment in adults cannot be standardized and needs tailoring according to the underlying condition and HLH-initiating trigger (infection, malignancy, auto-immune/auto-inflammatory conditions, drug-induced, other causes) (1). The treatment experience of HFRS-induced HLH is very limited. Successful results have been reported with supportive therapy, IVIGs, corticosteroids and etoposide (2–7). Additionally, in infection-associated HLH, the causal pathogen should be identified rapidly and empiric or directed therapy should be initiated. In this case and supplementary to HLH-specific therapy, the patient was treated with broad-spectrum antibiotics, on a suspicion of sepsis. Antibiotic treatment was stopped when cultures remained negative.

Conclusion

Hemophagocytic lymphohistiocytosis may be associated with HFRS caused by *Puumala virus* infection and may be successfully treated with supportive therapy, IVIGs and pulse corticosteroids.

Data availability statement

The original contributions presented in this study are included in this article/**Supplementary material**, further inquiries can be directed to the corresponding author.

Ethics statement

Ethical review and approval was not required for the study on human participants in accordance with the local legislation and institutional requirements. The patients/participants provided their written informed consent to participate in this study.

Author contributions

All authors listed have made a substantial, direct, and intellectual contribution to the work, and approved it for publication.

Conflict of interest

The authors declare that the research was conducted in the absence of any commercial or financial relationships that could be construed as a potential conflict of interest.

Publisher's note

Supplementary material

The Supplementary Material for this article can be found online at: https://www.frontiersin.org/articles/10.3389/fmed.2022.1096900/full#supplementary-material

References

1. La Rosée P, Horne A, Hines M, von Bahr Greenwood T, Machowicz R, Berliner N, et al. Recommendations for the management of hemophagocytic lymphohistiocytosis in adults. *Blood.* (2019) 133:2465–77. doi: 10.1182/blood.2018894618

2. Baty V, Schuhmacher H, Bourgoin C, Latger V, Buisine J, May T, et al. Hemophagocytic syndrome and hemorrhagic fever with renal syndrome. *Presse Med.* (1998) 27:1577.

3. Lee J, Chung I, Shin D, Cho S, Cho D, Ryang D, et al. Hemorrhagic fever with renal syndrome presenting with hemophagocytic lymphohistiocytosis. *Emerg Infect Dis.* (2002) 8:209–10. doi: 10.3201/eid0802.010299

4. Tian M, Li J, Lei W, Shu X. A hidden cause of MERS and HLH in a girl: unusual presentation of hantaviruses infection. *Neuropediatrics.* (2019) 50:202–3. doi: 10.1055/s-0038-1675630

5. Shastri B, Kofman A, Hennenfent A, Klena J, Nicol S, Graziano J, et al. Domestically acquired seoul virus causing hemophagocytic lymphohistiocytosis-Washington, DC, 2018. *Open forum Infect Dis.* (2019) 6:ofz404. doi: 10.1093/ofid/ofz404

6. Yang X, Wang C, Wu L, Jiang X, Zhang S, Jing F. Hemorrhagic fever with renal syndrome with secondary hemophagocytic lymphohistiocytosis in West China: a case report. *BMC Infect Dis.* (2019) 19:492. doi: 10.1186/s12879-019-4122-0

7. Rao Q, Luo L, Gao L, Xiong W, Nie Q, Wu D. Hemorrhagic fever with renal syndrome presenting as leukemoid reaction and hemophagocytic lymphohistiocytosis. *J Med Virol.* (2022) 94:433–5. doi: 10.1002/jmv.27323

8. George M. Hemophagocytic lymphohistiocytosis: review of etiologies and management. *J Blood Med.* (2014) 5:69–86. doi: 10.2147/JBM.S46255

9. Mehta P, McAuley D, Brown M, Sanchez E, Tattersall R, Manson JJ, et al. COVID-19: consider cytokine storm syndromes and immunosuppression. *Lancet.* (2020) 395:1033–4. doi: 10.1016/S0140-6736(20)30628-0

10. Safronetz D, Ebihara H, Feldmann H, Hooper JW. The Syrian hamster model of hantavirus pulmonary syndrome. *Antiviral Res.* (2012) 95:282. doi: 10.1016/j.antiviral.2012.06.002

11. Ling L, Huang X, Liu C, Liao J, Zhou J. Monitoring coagulation-fibrinolysis activation prompted timely diagnosis of hemophagocytic lymphohistiocytosis-related disseminated intravascular coagulation. *Thrombosis J.* (2021) 19:82. doi: 10.1186/s12959-021-00338-y

frontiers | Frontiers in Medicine

TYPE Case Report
PUBLISHED 06 January 2023
DOI 10.3389/fmed.2022.1038455

OPEN ACCESS

EDITED BY
Abanoub Riad,
Masaryk University, Czechia

REVIEWED BY
Angelo Naselli,
MultiMedica Holding SpA (IRCCS), Italy
Tuan Thanh Nguyen,
School of Medicine (UC), Irvine,
United States

*CORRESPONDENCE
Zhihui Li
✉ lizhihui@zcmu.edu.cn

SPECIALTY SECTION
This article was submitted to Intensive Care Medicine and Anesthesiology, a section of the journal Frontiers in Medicine

RECEIVED 07 September 2022
ACCEPTED 05 December 2022
PUBLISHED 06 January 2023

CITATION
Yang Z and Li Z (2023) Sepsis caused by emphysematous pyelonephritis: A case report. *Front. Med.* 9:1038455. doi: 10.3389/fmed.2022.1038455

Sepsis caused by emphysematous pyelonephritis: A case report

Zheng Yang and Zhihui Li*

Department of Intensive Care Unit, Hangzhou Red Cross Hospital, Hangzhou, Zhejiang, China

Purpose: Emphysematous pyelonephritis (EPN) is a rare, life-threatening necrotizing renal parenchymal infection. It is most commonly reported in patients with poor glycemic control.

Patient concerns: We report the case of a 64-year-old woman who presented to the emergency room with fever and weakness over the last few days.

Diagnosis: After a series of tests in the diagnostic workup, the patient was diagnosed with emphysematous pyelonephritis and sepsis.

Intervention and outcome: She received conservative treatment with meropenem and symptomatic treatment, and the symptoms improved significantly.

Lessons: EPN can be reliably diagnosed using non-contrast abdominal CT imaging. The infection is most commonly caused by the *Escherichia coli* species, and a good curative effect can be achieved with early diagnosis and appropriate and timely treatment.

KEYWORDS

case report, sepsis, infection, diabetes, emphysematous pyelonephritis (EPN)

1. Introduction

Emphysematous pyelonephritis (EPN) is an acute, severe necrotizing infection resulting in gas in the renal parenchyma, collecting system, or perinephric tissue. EPN is uncommon due to its rare characteristics. Literature on the most effective treatment approach for EPN is scarce. Recently, after reviewing the literature, the researchers emphasized that the symptoms of this illness demonstrate unique pathology and point to microbiological and epidemiological causes (1). The condition was prolonged in this case and was carefully managed with good clinical effects.

We report a case of EPN in a 64-year-old female patient with type 2 diabetes mellitus, which was confirmed using computed tomography (CT) and laboratory evaluations.

2. Case report

A 64-year-old woman presented to the emergency room with fever and weakness over the last few days. The patient was feeling agitated during the physical examination. She also complained of left loin pain. Her medical history included poorly controlled type II diabetes mellitus and chronic renal failure. Laboratory results demonstrated that her

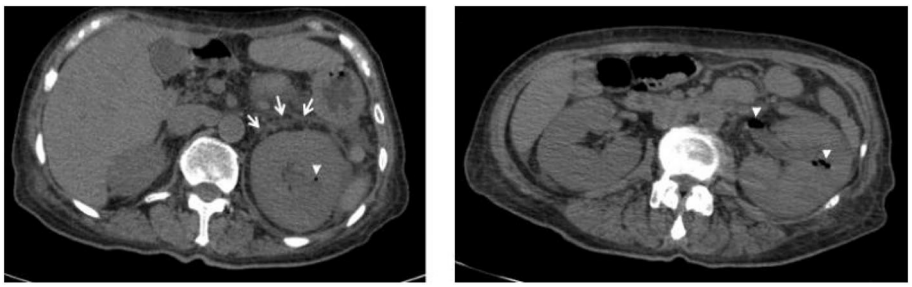

FIGURE 1
CT scan revealed gas collection in the parenchyma and renal pelvis (arrowheads) and perirenal fascia thickening (arrows) of the left kidney.

white cell count was 27,700 cells per cubic millimeter (the normal range: 3,500 to 9,500). The C-reactive protein level was 32.873 mg per deciliter, the blood urea nitrogen level was 20.70 mmol per liter, and the creatinine level was 312.7 μmol per liter. Urinalysis showed an elevated leukocyte count and bacteriuria. A CT scan in horizontal plane sectioning showed that the left kidney was significantly enlarged with thickened perirenal fascia, which was related to the presence of gas in the renal parenchyma and the kidney pelvis (Figure 1). She was transferred to the intensive care unit and treated with meropenem and broad-spectrum empirical antibiotics.

On admission to the ICU (day 0), she was drowsy. Her vital signs were as follows: body temperature, 37.5°C; pulse rate, 102 beats/min; respiratory rate, 28 breaths/min; blood pressure, 122/54 mmHg (noradrenaline 0.5 microg/kg per min); and pulse oxygen saturation, 98% with high flow oxygen therapy. Diminished breath sounds in the right lower lung were heard on auscultation. There was no audible cardiac murmur. Her abdomen was soft but she failed to cooperate with the abdominal tenderness examination, along with mild pitting edema of both lower limbs. The patient was diagnosed with emphysematous pyelonephritis and septic shock, possibly caused by a gas-producing uropathogenic infection. Unfortunately, according to the RIFLE criteria (2), the patient developed acute renal failure and was treated with continuous renal replacement therapy. However, after active treatment, the clinical effect was remarkable. Her clinical symptoms and serum inflammatory indicators (Figures 2A–C) improved gradually, and she stopped using norepinephrine (day 3). Her renal function (day 3) also recovered (Figures 2D, E), and she was successfully weaned with continuous renal replacement therapy. On the third day, both blood and urine cultures reported extended-spectrum beta-lactamase (ESBL)-producing *E. coli*. The patient's condition continued to improve, and she no longer needed to be treated in the ICU on the 6th day. The patient's abdominal CT scan (day 12) revealed that the gas collection in the pelvis and calyces had disappeared. Finally, the patient was discharged.

Abbreviations: EPN, emphysematous pyelonephritis; CT, computed tomography; ESBL, extended-spectrum beta-lactamase.

3. Discussion

After admission, the patient's EPN was diagnosed according to clinical manifestations, laboratory examinations, and abdominal CT scan results. Septic shock and acute renal failure occurred. We empirically gave anti-infection treatment, and the patient received appropriate supportive treatment while controlling the blood sugar at the appropriate level.

Currently, an abdominal CT scan is the preferred radiographic method for diagnosing EPN and staging its severity, which is related to its treatment plan (3). Huang et al. classified EPN into four classes: Class 1 indicates gas confined to the collecting system; Class 2 indicates gas confined to the renal parenchyma without extension to the extrarenal space; Class 3A indicates extension of gas or abscess to the perinephric space; Class 3B pertains to extension of the gas or abscess to the pararenal space; and Class 4 refers to bilateral EPN or a solitary kidney with EPN (4). Our patient was judged to have a Class 3A EPN.

A recent meta-analysis found that the mortality rate among patients with EPN disease was 13%, with a significantly decreasing trend in mortality rates from 1985 to 2020 (5). EPN was first defined by Schultz and Klorfein (6), and they opposed open surgical drainage of multiple cortical abscesses. The doctors' constant supervision revealed compelling results. Compared with conservative treatment, patients with diabetes mellitus who underwent surgical drainage or nephrectomy had lower mortality (7). Since then, open surgery has played a central role in the management of EPN, and the results from statistics from Shah's study showed that open surgery was associated with high mortality (8). A report published 10 years later by Chen et al. recommended different procedures. Antibiotic therapy combined with CT-guided percutaneous drainage for the treatment of emphysematous pyelonephritis is an appropriate alternative to antibiotic therapy with surgical intervention (9).

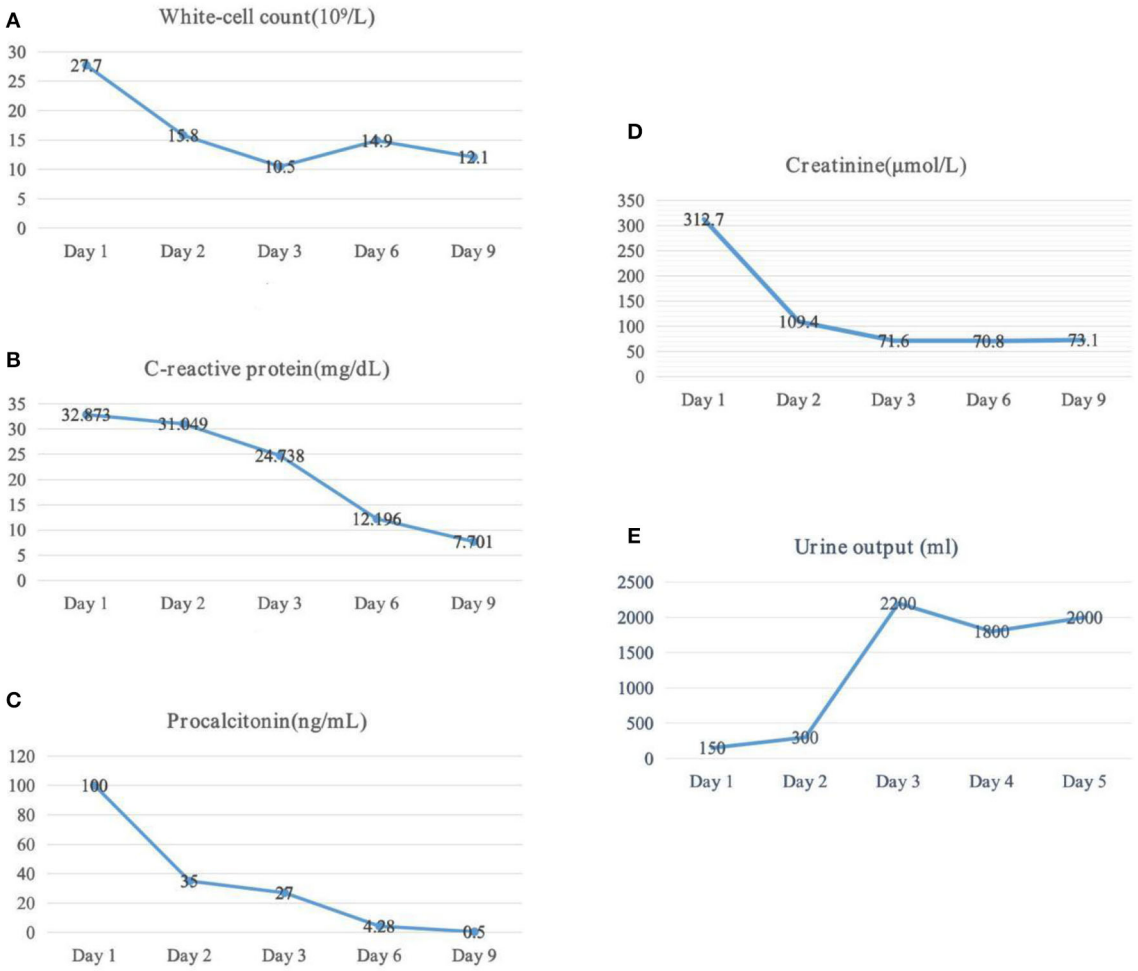

FIGURE 2
Laboratory tests and urine output dynamic change. **(A)** Changes of white-cell, **(B)** changes of c-reactive protein, **(C)** changes of procalcitonin, **(D)** changes of serum creatinine, and **(E)** changes of urine output.

With the advent of modern imaging, endourological procedures, and broad-spectrum antibiotics, the majority of such patients can be treated with minimal morbidity and mortality, even with the salvaging of the renal units (10, 11).

The disease usually occurs in female patients with diabetes with poor glycemic control, with or without urinary tract obstruction (12). *E. coli* is the most common pathogen (13). Almost 70% of patients extract *E. coli* from urine or pus cultures. Our case combines in-hospital multidisciplinary consultation methods, including urologists, critical care physicians, and microbiologists, to manage patients with EPN and develop strategies that may produce the best survival results. The first step includes full fluid resuscitation, broad-spectrum parenteral antibiotics against gram-negative bacteria, correction of electrolyte and acid-base disorders, and strict blood glucose control. We dynamically evaluated the function of each organ, such as the heart, the lung, and the kidney and provided emergency support treatment when necessary, including percutaneous drainage, positive muscle strength, mechanical ventilation, continuous hemodialysis, and so on. In cases of intractable shock or persistent bacteremia, nephrectomy should be considered.

4. Conclusion

Emphysematous pyelonephritis is an uncommon, acute, and severe necrotizing infection. Due to the rarity and variability of the clinical symptoms of EPN, diagnosing EPN proves to be a challenge. EPN can be reliably diagnosed by non-contrast CT abdominal imaging. The case study we report prove that surgical treatment of EPN is inappropriate in patients with serious complications, and the prognosis of patients may be improved by an early and regular course of antibacterial treatment.

Data availability statement

The original contributions presented in the study are included in the article/supplementary material, further inquiries can be directed to the corresponding author.

Ethics statement

The studies involving human participants were reviewed and approved by Medical Ethics Committee of Hangzhou Red Cross Hospital. The patients/participants provided their written informed consent to participate in this study.

Author contributions

ZY: data curation, funding acquisition, and writing—original draft. ZY and ZL: investigation. ZL: resources and writing—review and editing. Both authors contributed to the article and approved the submitted version.

Funding

This work was supported by Hong Hui Qing Nian (No. HHQN2020005).

Acknowledgments

We are grateful to the patient and her family for their invaluable contributions to this study. We thank the members of the Department of Critical Medicine at Hangzhou Red Cross Hospital for their contributions.

Conflict of interest

The authors declare that the research was conducted in the absence of any commercial or financial relationships that could be construed as a potential conflict of interest.

Publisher's note

References

1. Arrambide-Herrera JG, Robles-Torres JI, Ocaña-Munguía MA, Romero-Mata R, Gutiérrez-González A, Gómez-Guerra LS. Predictive factors for mortality and intensive care unit admission in patients with emphysematous pyelonephritis: 5-year experience in a tertiary care hospital. *Actas Urol Esp (Engl Ed).* (2022) 46:98–105. doi: 10.1016/j.acuroe.2021.01.010

2. Kellum JA, Lameire N, Aspelin P, Barsoum RS, Burdmann EA, Goldstein SL, et al. Kidney disease: improving global outcomes (KDIGO) acute kidney injury work group. KDIGO clinical practice guideline for acute kidney injury. *Kidney Int.* (2012) 2:1–138. doi: 10.1038/kisup.2012.1

3. Craig WD, Wagner BJ, Travis MD. Pyelonephritis: radiologic-pathologic review. *Radiographics.* (2008) 28:255–277. doi: 10.1148/rg.281075171

4. Huang J J, Tseng C C. Emphysematous pyelonephritis: clinicoradiological classification, management, prognosis, and pathogenesis. *Arch Intern Med.* (2000) 160:797–805. doi: 10.1001/archinte.160.6.797

5. Ngo XT, Nguyen TT, Dobbs RW, Thai MS, Vu DH, Van Dinh LQ, et al. Prevalence and risk factors of mortality in emphysematous pyelonephritis patients: a meta-analysis. *World J Surg.* (2022) 46:2377–88. doi: 10.1007/s00268-022-06647-1

6. Schultz EJ, Klorfein EH. Emphysematous pyelonephritis. *J Urol.* (1962) 87:762–6. doi: 10.1016/S0022-5347(17)65043-2

7. Rosenberg JW, Quader A, Brown JS. Renal emphysema. *Urology.* (1973) 1:237–9. doi: 10.1016/0090-4295(73)90743-7

8. Shah HN. Is there still a role of nephrectomy in management of emphysematous pyelonephritis in today's era? *J Postgrad Med.* (2021) 67:130–1. doi: 10.4103/jpgm.JPGM_337_21

9. Chen MT, Huang CN, Chou YH, Huang CH, Chiang CP, Liu GC. Percutaneous drainage in the treatment of emphysematous pyelonephritis: 10-year experience. *J Urol.* (1997) 157:1569–73. doi: 10.1016/S0022-5347(01)64797-9

10. Barua SK, Bora SJ, Bagchi PK, Sarma D, Phukan M, Baruah SJ, et al. Emphysematous infections of the urinary tract - an audit of 20 patients with review of literature. *Int J Adolesc Med Health.* (2017) 31:45. doi: 10.1515/ijamh-2017-0045

11. Irfaan AM, Shaikh NA, Jamshaid A, Qureshi AH. Emphysematous Pyelonephritis: A single center review. *Pak J Med Sci.* (2020) 36:S83–6. doi: 10.12669/pjms.36.ICON-Suppl.1728

12. Kangjam SM, Irom KS, Khumallambam IS, Sinam RS. Role of conservative management in emphysematous pyelonephritis - a retrospective study. *J Clin Diagn Res.* (2015) 9:C9–C11. doi: 10.7860/JCDR/2015/16763.6795

13. Zhang Y, Zang GQ, Tang ZH Yu YS. Emphysematous pyelonephritis. *Rev Inst Med Trop São Paulo.* (2015) 57:368. doi: 10.1590/S0036-46652015000400019

frontiers | Frontiers in Medicine

TYPE Case Report
PUBLISHED 26 January 2023
DOI 10.3389/fmed.2022.1089863

OPEN ACCESS

EDITED BY
Yuetian Yu,
Shanghai Jiao Tong University, China

REVIEWED BY
Georg Conrads,
RWTH Aachen University, Germany
Beena Antony,
Father Muller Medical College, India

*CORRESPONDENCE
Huijuan Wan
✉ 442636583@qq.com
Youfeng Zhu
✉ 151276953@qq.com

SPECIALTY SECTION
This article was submitted to Intensive Care Medicine and Anesthesiology, a section of the journal Frontiers in Medicine

RECEIVED 04 November 2022
ACCEPTED 29 December 2022
PUBLISHED 26 January 2023

CITATION
Zhang Y, Zhu Y and Wan H (2023) Case report:Multiple abscesses caused by *Porphyromonas gingivalis* diagnosed by metagenomic next-generation sequencing. *Front. Med.* 9:1089863.
doi: 10.3389/fmed.2022.1089863

Case report:Multiple abscesses caused by *Porphyromonas gingivalis* diagnosed by metagenomic next-generation sequencing

Yichen Zhang[1], Youfeng Zhu[1]* and Huijuan Wan[2]*

[1]Department of Intensive Care Unit, Guangzhou Red Cross Hospital, Guangzhou, China, [2]Department of Otorhinolaryngology Head and Neck Surgery, The First Affiliated Hospital, Sun Yat-sen University, Guangzhou, China

Background: Extraoral infection by *Porphyromonas gingivalis* (*P. gingivalis*) is extremely rare and challenging to diagnose because the fastidious pathogen is difficult to culture by traditional methods. We report the first case of a patient with multiple abscesses in muscles and the brain with dura empyema due to *P. gingivalis*, which was diagnosed by metagenomic next-generation sequencing (mNGS).

Case presentation: A 65-year-old male patient was admitted to our hospital for multiple lumps in his body. Brain magnetic resonance imaging (MRI) and lower-limb computed tomography (CT) revealed multiple abscesses in the brain and muscles. A diagnosis of *P. gingivalis* infection was made based on mNGS tests of blood, cerebrospinal fluid (CSF), and pus samples, as the traditional bacterial culture of these samples showed negative results. Target antibiotic therapy with meropenem and metronidazole was administered, and CT-guided percutaneous catheter drainage of abscesses in both thighs was performed. The size of muscle abscesses reduced significantly and neurological function improved. The patient was followed up for 4 months. No abscesses re-appeared, and the remaining abscesses in his backside and both legs were completely absorbed. He can speak fluently and walk around freely without any neurological deficits.

Conclusion: Metagenomic next-generation sequencing is helpful for early diagnosis and subsequent treatment of *P. gingivalis*-associated multiple abscesses.

KEYWORDS

***Porphyromonas gingivalis*, next generation sequencing (NGS), multiple abscesses, metronidazole, percutaneous catheter drainage**

Introduction

Porphyromonas gingivalis (*P. gingivalis*) is a highly adapted non-motile gram-negative, and oral anaerobe. The bacterium is strongly associated with periodontitis, which can destroy the tissues supporting the tooth and eventually lead to tooth loss (1). It can produce various virulence factors such as proteolytic enzymes, capsules, fimbriae, and lipopolysaccharides that can cause tissue destruction, severe inflammation, and sometimes abscess formation (2). Apart from oral infection, *P. gingivalis* can also cause extraoral infections (3–9), such as brain abscesses, chest wall abscesses, subdural empyema, and gas gangrene.

The diagnosis of *P. gingivalis* using conventional methods, such as blood, cerebrospinal fluid, or pus culture is difficult and time-consuming. *P. gingivalis* is a fastidious pathogen that is difficult to culture and requires samples to be transported to the appropriate laboratory immediately under strict anaerobic conditions. The culture time of *P. gingivalis* is approximately 7–10 days, which can lead to delayed diagnosis and therefore inappropriate treatment. Currently, metagenomic next-generation sequencing (mNGS) is being used to identify pathogens with high sensitivity and specificity; it can also lead to an etiological diagnosis in comparatively lesser time (10). Herein, we present the first case of multiple abscesses in a patient's muscles and the brain with dura empyema due to *P. gingivalis*, which was diagnosed by mNGS.

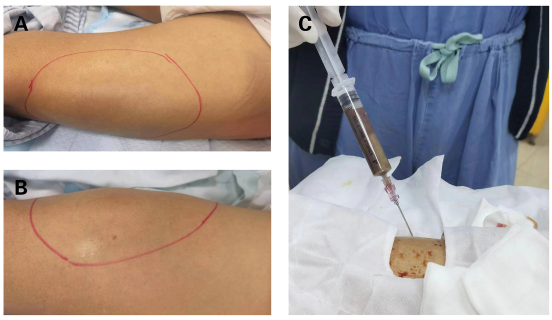

FIGURE 1
Clinical manifestation of bilateral thighs abscesses. **(A)** Bulging mass on the right thigh. **(B)** Bulging mass on the left thigh. **(C)** Brown fetid pus was aspirated by computed tomography (CT)-guided percutaneous puncture in right thigh abscess.

Case presentation

A 65-year-old male patient was admitted to our hospital for multiple abscesses. Two weeks before admission to our hospital, the patient presented with an abscess in his left palm. Four days later, three more bumps were found on his right and left thighs and his backside with mild distending pain. Five days prior to admission, as his palm abscess enlarged, he presented to the outpatient department of our hospital. He was treated with levofloxacin (100 mg, intravenous [iv], qd), and his palm abscess was removed by surgical drainage. However, his symptom worsened quickly. He developed fever, headache, gait instability, and dysarthria. The bumps in his thighs and his backside became larger, with severe distending pain in these places.

On admission, the initial physical examination showed a body temperature of 38.5°C, respiratory rate of 19/min, pulse rate of 85/min, and blood pressure of 120/73 mmHg. The cardiovascular and respiratory systems were normal. Abdomen examination did not show tenderness or hepatosplenomegaly. In addition, bumps were found on his left thigh (21 cm × 13 cm) (Figure 1A), right thigh (22 cm × 12 cm) (Figure 1B), and backside (7 cm × 3 cm) with tenderness and fluctuation. The local skin temperature was higher than that of the surrounding skin. Motor weakness of the left upper limb (muscle strength grade 4) and right lower limb (muscle strength grade 2) with bilateral hypotonicity of the upper extremities was observed. There were no signs of hyperreflexia or meningeal irritation. Both sides of the Babinski sign were negative. The patient denied any disease that can influence the immune system, such as tumors, acquired immunodeficiency syndrome (AIDS), hematological diseases, autoimmune diseases, or diabetes mellitus. He also denied the administration of any immunosuppressive agents or steroid drugs. His lymphocyte count was 1.31×10^9 cells/L, the percentage of CD3+ and CD4+ lymphocytes was 31% (normal range 27–51%), and the percentage of CD3+ and CD8+ lymphocytes was 35% (normal range 15–44%). The presence of antibodies of the human immunodeficiency virus was also negative.

Computed tomography (CT) of both lower extremities showed the presence of multiple hypodense lesions, which indicated multiple muscle abscesses in the right vastus intermedius, left vastus lateralis muscle, and left adductor magnus (Figures 2A–C). Brain magnetic resonance imaging (MRI) showed rim-enhancing lesions with perilesional edema that indicated bilateral brain abscesses in the frontoparietal lobe, right temporal occipital lobe, and right cerebellar hemisphere (Figure 3). Brain MRI also showed heterogeneously thickened dura with peripheral rim enhancement, which indicated dura empyema on the right frontoparietal lobe (Figure 3). Diffusion-weighted MRI shows a hyperintense signal within these lesions (Figure 3). A lumbar puncture was performed, which showed an intracranial pressure of >300 mmH_2O (normal range: 80–180 mmH_2O). The cerebrospinal fluid (CSF) was clear and colorless. The CSF analysis showed the following results: leukocyte count, 99,000 cells/mL; glucose levels, 3.6 mmol/L (normal range: 2.5–4.5 mmol/L); and protein levels, 1,113.9 mg/L (normal range 150–450 mg/L). Based on these findings, a diagnosis of multiple abscesses in muscles and the brain with dura empyema was made, and empirical antibiotic treatment of meropenem (1.0 g, iv drip, q8h) and linezolid (600 mg, iv drip, q12) was started. Anaerobic and aerobic cultures of blood samples and aerobic culture of CSF samples were both performed. CT-guided percutaneous catheter drainage of abscesses was performed in both thighs, and brown fetid pus was aspirated (Figure 1C). The pus sample was used to find the etiological agent using methods of traditional aerobic culture and mNGS test. Stereotactic puncture drainage of brain abscesses was proposed but not performed because the patient refused any type of intracerebral surgery.

PACEseq mNGS test (Hugobiotech, Beijing, China) using a pus sample from the right thigh abscess was performed to identify the causative pathogens. A QIAamp DNA Micro Kit (QIAGEN, Hilden, Germany) was used for DNA extraction, and a library of total DNA was built with QIAseqTM Ultralow Input Library Kit for Illumina (QIAGEN, Hilden, Germany). Qubit (Thermo Fisher Scientific, MA, USA) and Agilent 2100 Bioanalyzer (Agilent Technologies, Santa Clara, CA, USA) were used to access the quality of the DNA library. The qualified library was finally sequenced on a Nextseq 550 platform (Illumina, San Diego, CA, USA). After sequencing, adapters and short, low-quality, and low-complexity reads were removed from the raw data. Human DNA was also filtered out by mapping to the human reference database. The remaining reads were finally aligned to the Microbial Genome Database.[1] *Porphyromonas gingivalis* (60,853 specific reads), *Bacteroides heparinolyticus* (892 specific reads), and *Tannerella forsythia* (317 specific reads) were detected on day 3 (Figure 4). Blood and CSF samples were also used

1 https://www.ncbi.nlm.nih.gov/genome

FIGURE 2
Computed tomography (CT) scan result of bilateral lower extremities and timeline of treatment. **(A)** CT scan shows multiple muscle abscesses in bilateral thighs. **(B)** Right thigh abscess. **(C)** Left thigh abscess. **(D)** Timeline of treatment.

to detect pathogens using the method of the PMseq mNGS test (BGI-Shenzhen, Shenzhen, China). *Porphyromonas gingivalis* was detected both in the blood (489 specific reads) and CSF (587 specific reads) samples on day 2 and day 4 as negative results were obtained with the traditional culture of these samples. The blood, pus, and CSF samples were incubated in BACTECTM FX BC systems (Becton Dickinson, Heidelberg, Germany) for 5 days, but no positive signal appeared. As a result, the anaerobic and aerobic cultures of the blood sample and the aerobic cultures of pus and CSF samples were negative.

As *P. gingivalis* was detected, the antibiotic regimen was changed to meropenem (1.0 g, iv drip, q8h) and metronidazole (1 g, iv drip, q8h) on day 3. Chest and abdominal CT and cardiac ultrasonography were performed to identify the source of infection, but no positive result was found in either examination. A dental examination was performed, which revealed moderate oral hygiene with loss of all teeth and chronic gingivitis. We did not find any periodontal abscess. The antibiotic regimen of meropenem and metronidazole was continued until he was discharged from the ICU. The pigtail catheters were left in both legs to allow for continuous drainage with

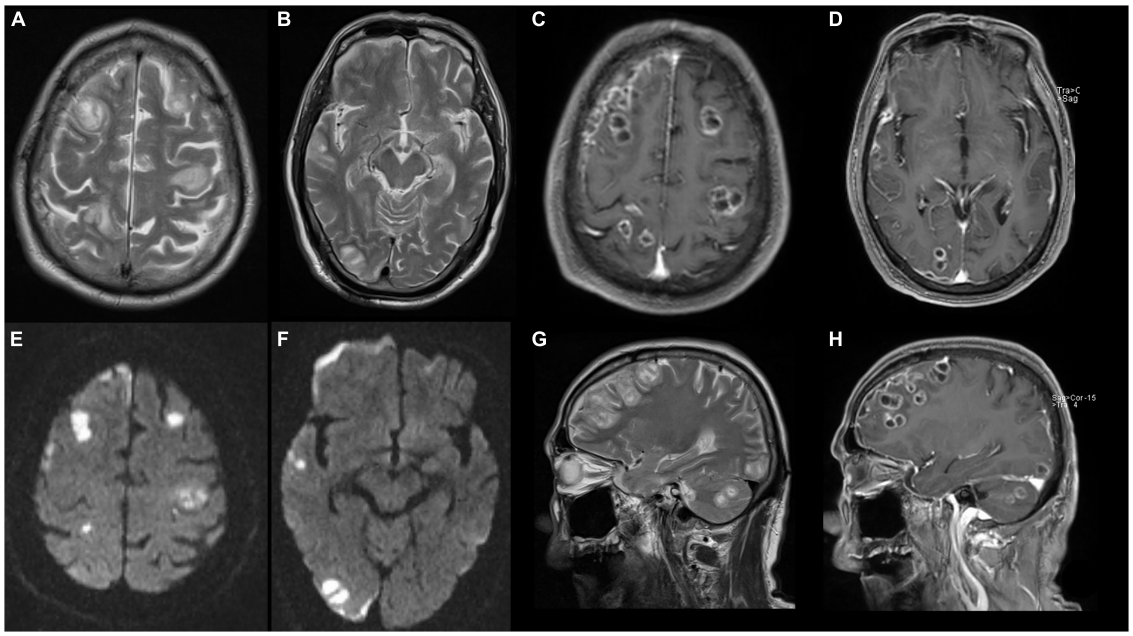

FIGURE 3
Magnetic resonance image (MRI) of brain shows abscesses in bilateral frontal lobe, right temporo-parieto-occipital lobe, and right cerebellar hemisphere with ring contrast enhancement and perilesional edema. **(A,B,G)** T2-weighted imaging. **(C,D,H)** T2 contrast-enhancement imaging. **(E,F)** Diffusion-weighted MRI.

daily flushing by metronidazole. On day 9, the drainage volume was <10 ml of serous-like liquid, and the patient's white blood cell count was back to normal levels. CT of both legs revealed a remarkable reduction in the size of the abscesses in the right vastus intermedius, left vastus lateralis muscle, and left adductor magnus. The drainage tube was removed on day 18. The size of the bump in his backside was reduced to 3 cm × 2 cm. His neurological function was improved partially. He could speak fluently, but the muscle strength of his right lower limb was still weak (muscle strength: grade 2). As his symptoms improved and his vital signs stabilized, he was discharged from the ICU on day 23 to a rehabilitation medical center. The patient was followed up for 4 months. No abscesses re-appeared, and the remaining abscesses in his backside and both legs were completely absorbed. His muscle strength improved significantly. He returned to normal health. At the time of generating this report, the patient could speak and walk around freely and had no evident neurological deficits. The timeline of the treatment is shown in **Figure 2D**.

Discussion

Porphyromonas gingivalis is a gram-negative oral anaerobe and is considered a major pathogenic agent causing periodontitis. However, *P. gingivalis* can be disseminated from the oral cavity to other body sites and cause extraoral infections, such as brain abscess, subdural empyema, chest wall abscesses, otitis media, appendicitis, and gas gangrene (3–9). Brain abscesses caused by *P. gingivalis* have been reported in several studies (3–6). Recently, Tanaka et al. (8) reported the first case of chest subcutaneous abscess caused by *P. gingivalis*. To the best of our knowledge, muscle abscesses and brain abscesses in the same patient caused by *P. gingivalis* have not been reported. Here, we reported the first case of multiple abscesses in muscles and the brain with dura empyema caused by *P. gingivalis*.

The diagnosis of brain abscess by *P. gingivalis* mainly depended on bacterial culture because of the lack of characteristic imaging and clinical features. However, the positive rate of culture for *P. gingivalis* is very low. In our case, traditional bacterial cultures of blood, CSF, and pus samples all revealed negative results. Indeed, many oral bacteria, such as *P. gingivalis*, are fastidious pathogens that are difficult to culture and must be transported to the appropriate laboratory immediately under strict anaerobic conditions. Moreover, it takes weeks or more to identify pathogens by traditional culture. Currently, mNGS can simultaneously detect various types of pathogens such as bacteria, viruses, fungi, and parasites in virtually any body fluid type, ranging from low-cellularity spinal fluid to purulent fluids, with high sensitivity and specificity and in far less time than traditional culture tests (10). In our case, *P. gingivalis* was detected within 2 days by mNGS, much earlier than by traditional culture tests, which detected no pathogens, given that the samples were sent to the laboratory at the same time. This proves that mNGS can be more beneficial than traditional testing methods in identifying potential pathogens such as *P. gingivalis*.

In a pus sample from the right thigh, 60,853 (47.84%) specific sequences of *P. gingivalis* were detected in the mNGS test. Other sequences (n = 65,133, 51.21%) included non-specific microbial sequences (n = 64,713, 50.88%) that did not indicate any specific microbe and relatively fewer environmental bacterial sequences (n = 420, 0.33%). Sequences specific for *P. gingivalis* accounted for 97.39% of all specific sequences detected by mNGS. Thus, *P. gingivalis* was the major microbe identified in the pus sample. The non-specific microbial sequences could be unspecified genome regions of *P. gingivalis* and the minor accompanying flora as no specific sequences of other species were found. As specific sequences of *P. gingivalis* were also detected in blood and CSF samples, we confirmed that *P. gingivalis* was the pathogenic bacterial species of multiple abscesses.

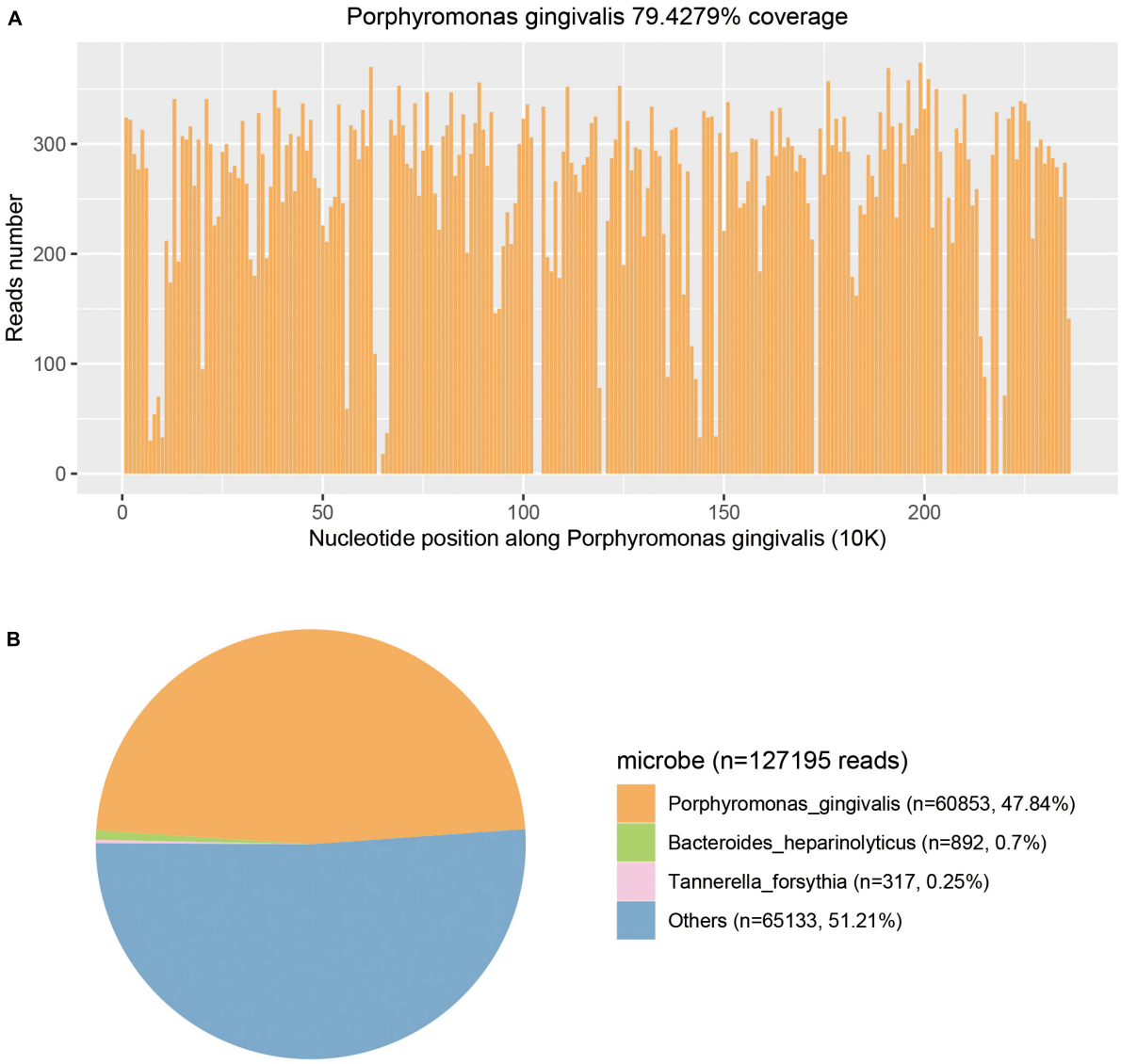

FIGURE 4
Metagenomic next-generation sequencing (mNGS) results of this case. **(A)** Courage of *Porphyromonas gingivalis* detected by mNGS was 79.4279%. **(B)** A total of 60853 specific reads of *P. gingivalis* were detected by mNGS in this case.

In our case, percutaneous puncture of bilateral femoral abscesses was performed and brown fetid pus was aspirated. Unfortunately, only aerobic culture of the pus sample was performed. As *P. gingivalis* is an anaerobic species that cannot live with oxygen, the results of aerobic cultures of pus and CSF samples were negative. However, we did confirm that there were few if any aerobes in these samples. Tanaka et al. (8) reported a case of empyema necessitans that presented as a subcutaneous chest wall abscess caused by *P. gingivalis*. In this case, percutaneous puncture of the subcutaneous abscess was performed, and foul-smelling chocolate-colored pus was aspirated. Gram smears of the pus revealed gram-negative rods, but aerobic culture showed a negative result, similar to our case. Indeed, foul-smelling pus always suggests an anaerobic infection; thus, anaerobic culture is needed.

Some previous studies have also reported brain abscesses caused by *P. gingivalis*. In these cases, patients either had a chronic odontogenic disease or had recently undergone dental surgery before brain abscesses were found. As no other sources of infection were found, they concluded that *P. gingivalis* was derived from the oral.

Targeted antibiotic therapy of meropenem and metronidazole was administrated after pathogens were detected. *Porphyromonas* spp. shows high susceptibility to penicillin, amoxicillin, amoxicillin–clavulanate, metronidazole, tetracycline, and clindamycin (11). In our case, metronidazole was also used to flush the abscess cavities *via* pigtail catheters. The size of muscle abscesses declined significantly, and neurological function improved. Some case reports have revealed that early absorption of brain abscesses leads to a good neurological prognosis (3, 5, 12, 13). In our case, stereotactic puncture drainage of brain abscesses was proposed by our neurosurgical colleagues, but the patient did not agree to the procedure. This may be why the neurological deficit did not improve as significantly as the size of muscle abscesses before discharge.

In our case, the patient denied any diseases that can decrease immune function and denied the administration of any immunosuppressive agents or steroid drugs. His lymphocyte

counts and CD4+ and CD8+ percentages were in the normal range. As a result, the immune function of the patient was accessed as normal. In most case reports concerning abscesses caused by *P. gingivalis*, the patients' immunologic functions were normal, which indicates that anyone can be infected by this microbe. The patient in our case ultimately recovered fully. No abscesses re-appeared, and the remaining abscesses were all completely absorbed without any neurological deficits. The mortality rate and morbidity rate of extraoral *P. gingivalis* infections have never been reported. However, most case reports indicate that with proper treatment, the patient should experience a good recovery.

Conclusion

We report here the first case of multiple abscesses in muscles and the brain with dura empyema caused by *P. gingivalis*. The mNGS test is helpful in the detection and identification of these pathogens, especially when traditional culture tests show negative results. With antibiotic therapy of metronidazole and meropenem combined with percutaneous catheter drainage of abscesses in both thighs, the size of the muscle abscesses declined significantly, and neurological function improved.

Data availability statement

The datasets presented in this article are not readily available to protect patient confidentiality and privacy. Requests to access the datasets should be directed to the corresponding author.

Ethics statement

The studies involving human participants were reviewed and approved by the Ethics Committee of Guangzhou Red Cross Hospital. The patients/participants provided their written informed consent to participate in this study. Written informed consent was obtained from the individual(s) for the publication of any potentially identifiable images or data included in this article.

Author contributions

All authors listed have made a substantial, direct, and intellectual contribution to the work, and approved it for publication.

Funding

This study was supported by the Guangzhou Science, Technology and Innovation Commission (201904010258) and Guangzhou Municipal Health Commission (20201A011022).

Conflict of interest

The authors declare that the research was conducted in the absence of any commercial or financial relationships that could be construed as a potential conflict of interest.

Publisher's note

All claims expressed in this article are solely those of the authors and do not necessarily represent those of their affiliated organizations, or those of the publisher, the editors and the reviewers. Any product that may be evaluated in this article, or claim that may be made by its manufacturer, is not guaranteed or endorsed by the publisher.

References

1. Mysak J, Podzimek S, Sommerova P, Lyuya-Mi Y, Bartova J, Janatova T, et al. Porphyromonas gingivalis: major periodontopathic pathogen overview. *J Immunol Res.* (2014) 2014:1–8. doi: 10.1155/2014/476068

2. Xu W, Zhou W, Wang H, Liang S. Roles of porphyromonas gingivalis and its virulence factors in periodontitis. *Adv Protein Chem Struct Biol.* (2020) 120:45–84. doi: 10.1016/bs.apcsb.2019.12.001

3. Rae Yoo J, Taek Heo S, Kim M, Lee C, Kim Y. Porphyromonas gingivalis causing brain abscess in patient with recurrent periodontitis. *Anaerobe.* (2016) 39:165–7. doi: 10.1016/j.anaerobe.2016.04.009

4. Ribeiro B, Marchiori E. Porphyromonas gingivalis as an uncommon cause of intracranial abscesses. *Rev Soc Bras Med Trop.* (2021) 54:2020. doi: 10.1590/0037-8682-0370-2020

5. Wisutep P, Kamolvit W, Chongtrakool P, Jitmuang A. Brain abscess mimicking acute stroke syndrome caused by dual filifactor alocis and porphyromonas gingivalis infections: a case report. *Anaerobe.* (2022) 75:102535. doi: 10.1016/j.anaerobe.2022.102535

6. Iida Y, Honda K, Suzuki T, Matsukawa S, Kawai T, Shimahara T, et al. Brain abscess in which porphyromonas gingivalis was detected in cerebrospinal fluid. *Br J Oral Maxillof Surg.* (2004) 42:180. doi: 10.1016/S0266-435600190-6

7. Muengtaweepongsa S, Suebnukarn S, Rasheed A, Khawchareonporn T. An unusual presentation of subdural empyema caused by porphyromonas gingivalis. *Ann Indian Acad Neurol.* (2013) 16:723. doi: 10.4103/0972-2327.120447

8. Tanaka A, Kogami M, Nagatomo Y, Takeda Y, Kanzawa H, Kawaguchi Y, et al. Subcutaneous abscess due to empyema necessitans caused by porphyromonas gingivalis in a patient with periodontitis. *Idcases.* (2022) 27:e1458. doi: 10.1016/j.idcr.2022.e01458

9. van Winkelhoff A, Slots J. Actinobacillus actinomycetemcomitans and porphyromonas gingivalis in nonoral infections. *Periodontology.* (1999) 20:122–35. doi: 10.1111/j.1600-0757.1999.tb00160.x

10. Gu W, Deng X, Lee M, Sucu Y, Arevalo S, Stryke D, et al. Rapid pathogen detection by metagenomic next-generation sequencing of infected body fluids. *Nat Med.* (2021) 27:115–24. doi: 10.1038/s41591-020-1105-z

11. Dahlen G, Preus H. Low antibiotic resistance among anaerobic gram-negative bacteria in periodontitis 5 years following metronidazole therapy. *Anaerobe.* (2017) 43:94–8. doi: 10.1016/j.anaerobe.2016.12.009

12. Akashi M, Tanaka K, Kusumoto J, Furudoi S, Hosoda K, Komori T. Brain abscess potentially resulting from odontogenic focus: report of three cases and a literature review. *J Maxillof Oral Surg.* (2017) 16:58–64. doi: 10.1007/s12663-016-0915-5

13. Van der Cruyssen F, Grisar K, Maes H, Politis C. Case of a cerebral abscess caused byporphyromonas gingivalis in a subject with periodontitis. *BMJ Case Rep.* (2017) 2017:r2016218845. doi: 10.1136/bcr-2016-218845

Frontiers in Medicine

Translating medical research and innovation into improved patient care

A multidisciplinary journal which advances our medical knowledge. It supports the translation of scientific advances into new therapies and diagnostic tools that will improve patient care.

Discover the latest Research Topics

See more →

Frontiers

Avenue du Tribunal-Fédéral 34
1005 Lausanne, Switzerland
frontiersin.org

Contact us

+41 (0)21 510 17 00
frontiersin.org/about/contact